Palaeoecology and Palaeoenvironments of the Late Permian Zechstein Sea and its Hinterlands

Martha Elizabeth Gibson

A thesis submitted in partial fulfilment of the requirements for the degree of Doctor of Philosophy

The University of Sheffield
Faculty of Science
Department of Animal and Plant Sciences

22/09/2020

Declaration

I, the author, confirm that the Thesis is my own work. I am aware of the University's Guidance on the Use of Unfair Means (www.sheffield.ac.uk/ssid/unfair-means). This work has not been previously been presented for an award at this, or any other, university.

The following chapters are intended for publication or have already been published at the time of thesis submission. Asher Haynes and David Warburton of Anglo American Plc have approved all manuscripts for publication which have used York Potash Ltd boreholes SM4 Gough, SM7 Mortar Hall, SM11 Dove's Nest and SM14b Woodsmith Mine North Shaft.

Gibson, M.E., Taylor, W.A., Wellman, C.H. 2020. Wall ultrastructure of the Permian pollen grain Lueckisporites virkkiae Potonié et Klaus 1954 emend. Clarke 1965: evidence for botanical affinity. Review of Palaeobotany and Palynology, 104169.

Gibson, M.E., Wellman, C.H. 2020. The Use of Spore-Pollen Assemblages to Reconstruct Vegetation Changes in the Permian (Lopingian) Zechstein Deposits of Northeast England. *Review of Palaeobotany and Palynology.* Accepted subject to minor revision.

Gibson, M.E., Bodman, D.B. 2020. Evaporite Palynology: a case study on the Permian (Lopingian) Zechstein Sea. *Journal of the Geological Society.* In review.

Gibson, M.E., Wellman, C.H. 2020. Zechstein forests thrived up to the Permian-Triassic mass extinction event. In prep.

Gibson, M.E. 2020. Exceptional preservation of possible endobiotic fungus inside late Permian pollen grains from the British Zechstein Group. In prep.

Table of Contents

Acknowledgements **8**

Abstract **9**

Chapter 1. Introduction & Literature Review **10**

1.1 The Permian Timescale 10

1.1.1 Overview and History *10*

1.1.2 Permian Biostratigraphy *11*

1.1.3 Terrestrial Biostratigraphy *12*

1.1.4 Zechstein Timescales *13*

1.1.5 Zechstein Biozonation *17*

1.2 Palaeocontinental Reconstruction: Pangaea 18

1.3 The Permian Atmosphere 19

1.3.1 Atmospheric O_2 ..... *19*

1.3.2 Atmospheric CO_2 ..... *20*

1.4 Sea Level 21

1.4.1 Overview *21*

1.4.3 The Zechstein Water Column *22*

1.5 Permian Climate 25

1.5.1 Icehouse-Hothouse transition *25*

1.5.2 Regional Climates *25*

1.5.3 Zechstein Climate *27*

1.6 Palaeophytogeography 29

1.6.1 Macroflora Provincialism *29*

1.6.2 Permian Palynology *30*

1.6.3 Euramerican Palynology Highlight *32*

1.7 Review of the Zechstein Fossil Record 33

1.7.1 Marine Biota *33*

1.7.2 Terrestrial Biota *36*

1.7.3 Review of Zechstein Palaeobotany *37*

1.7.4 A Review of Zechstein Palynology *38*

1.7.5 Early Research on the Zechstein Palynology *40*

1.7.6 British Zechstein Palaeobotany and Palynology *41*

Thesis outline 43

Chapter 2. Geological Setting **44**

2.1 Permian Rocks in the U.K. 44

2.1.1 Marine Permian Rocks *44*

2.1.2 Non-Zechstein Marine Permian *44*

2.2 The Zechstein Sea 46
2.2.1 Overview *46*
2.2.2 Pre-Zechstein/Rotliegend *49*
2.2.3 Cycle 1 (EZ1) *49*
2.2.4 Cycle 2 (EZ2) *57*
2.2.5 Cycle 3 (EZ3) *60*
2.2.6 Cycle 4 (EZ4) *62*
2.2.7 Cycle 5 (EZ5) *64*
2.3 Sequence Stratigraphy 64
2.3.1 ZS1 (Marl Slate, Wetherby Member/Raisby Formation) *66*
2.3.2 ZS2 (Ford Formation/Sprotbrough Member) *66*
2.3.3 ZS3 (Hartlepool/Hayton Anhydrite, Edlington Fm/Roker Dolomite) *67*
2.3.4 ZS4 (Fordon Evaporite Fm, Illitic Shale/Grauer Salzton, Brotherton/Seaham Fm) *68*
2.3.5 ZS 5,6 and 7 ..... *69*
Chapter 3. Materials and Methods **71**
3.1 Brief description of Fieldwork Sites and Sampling 71
3.2 Lithology 72
3.3 Sample Preparation 72
3.4 Carbonate Digestion in HCl 72
3.5 Silicate Digestion in HF 72
3.6 Heavy Liquid Separation 72
3.7 Storage 73
3.8 *Lycopodium* Spiking 73
3.9 Oxidisation 73
3.10 Halite Samples 74
3.11 Mounting and Imaging (light microscopy) 74
3.12 Counts 74
3.13 Quantitative Calculations 75
3.14 StrataBugs (2.1) 76
3.15 Cluster Analysis (Morisita) in PAST 76
3.16 Transmission Electron Microscopy (TEM) 76
3.17 Curation 76
Chapter 4. Plant Life Cycles **77**
4.1 Reproductive life cycles of land plants 77
4.1.1 The life cycle of a moss in which the sporophyte is attached to the gametophyte *77*
4.1.2 The life cycle of a homosporous fern or lycopod *77*
4.1.3 The life cycle of a heterosporous fern or lycopod *77*

4.1.4 The life cycle of a gymnosperm e.g. conifer ... *78*
4.1.5 The life cycle of an angiosperm ... *78*
4.1.6 A brief outline of the macroevolutionary history of these reproductive grades ... *78*
4.2.2 Pollen and spore dispersal and taphonomy ... 80
Chapter 5. Taxonomy ... **82**
5.1 Glossary ... 83
5.2 Taxonomic descriptions ... 84
Chapter 6. ... **100**
6.1 Abstract ... 100
6.2 Introduction ... 100
6.3 Geological Setting ... 102
6.3 Previous palaeobotanical and palynological studies ... 104
6.4 Materials and Methods ... 107
6.5 Palynological results ... 109
6.5.1. General description of the spore/pollen assemblages ... *110*
6.5.2. Description of palynomorph distribution by locality ... *111*
6.5.3. Summary of the distribution of taxa within the stratigraphical sequence ... *121*
6.5.4 Comparison of the Durham and Yorkshire Sub-basins ... *125*
6.6. Reconstructing the Zechstein flora ... 127
6.6.1. General comments: palaeoecology ... *127*
6.6.2. Vegetation change through time ... *128*
6.7 Palynofacies and the Zechstein palaeoenvironments ... 132
6.8 Conclusions ... 135
Acknowledgements ... 136
Supporting Information ... 136
Plate Descriptions ... 137
Chapter 7. ... **142**
Abstract ... 142
Introduction ... 142
The previous view of the Zechstein vegetation ... 144
Materials and methods ... 145
Results ... 146
Conclusion ... 147
Acknowledgements ... 147
Chapter 8. ... **149**
8.1 Abstract ... 149
2.3 Geological Setting ... 151

8.4 Materials and Methods 154
8.5 Borehole Descriptions 156
8.5.1 SM4 Gough [NZ 94613 00188] *156*
8.5.2 SM7 Mortar Hall [NZ 89989 06831] *157*
8.5.3 SM11 Dove's Nest [NZ 89429 05322] *157*
8.5.4 SM14b Woodsmith Mine North Shaft [NZ 89297 05435] *158*
8.6 Results 158
8.6.1 General comments on the palynology *158*
8.6.2 SM4 Gough *159*
8.6.3 SM7 Mortar Hall *159*
8.6.4 SM11 Dove's Nest *159*
8.6.5 SM14b Woodsmith Mine North Shaft *160*
8.6.6 Additional comments *160*
8.7 Discussion 161
8.7.1 Preservation potential of the Zechstein Group evaporites *161*
8.7.2 Taxonomic Composition *163*
8.7.3 Depositional setting and mode of transport *164*
8.7.4 Palynomorph Darkening and the Thermal Conductivity of Salt *165*
8.8 Conclusion 168
Acknowledgements 169
Plate Descriptions 169
Chapter 9. ..... **173**
9.1 Abstract 173
9.2 Full text 174
Chapter 10. ..... **184**
10.1 Abstract 184
10.2 Introduction 184
10.3 Materials and methods 187
10.3.1 Locality and geology *187*
10.3.2 Preparation and techniques *189*
10.4 Results 190
10.4.1 General Results *190*
10.4.2 SM11 Dove's Nest *192*
10.4.3 Salterford Farm *194*
10.4.4 Additional Evidence of Fungal Activity *194*
10.5 Discussion 195
10.5.1 Rarity of inclusions *195*

10.5.2 Potential host preference *196*
10.5.3 Discounting a non-fungal affinity *197*
10.5.4 Effects of processing *198*
10.5.5 The PTB "fungal-spike" *199*
10.5.6 Implications for the Zechstein environment *200*
10.6 Conclusions 201
MEG was funded by a NERC studentship through the ACCE (Adapting to the Challenges of a Changing Environment) Doctoral Training Partnership [Award Reference 1807541]. 202
Plate Descriptions 202
Chapter 11. Conclusion **209**
Chapter 5: Palynological results 209
Chapter 6: Environmental interpretation 210
Chapter 7: Evaporite palynology 211
Chapter 8: Wall-ultrastructure and development in *Lueckisporites virkkiae* 211
Chapter 9: Endobiotic fungus 212
Bibliography **214**

Acknowledgements

A Song of Salt and Acid

"All we have to decide is what to do with the time that is given us …" J.R.R. Tolkien

… and I am very glad I chose to spend 4 years at the Centre for Palynology exploring the weird and wonderful Zechstein biota. First and foremost, thank you to Charles Wellman for being an irreplaceable supervisor, for giving unparalleled support and advice and for spinning my straw-like words into publishable gold. Thank you to Alex Ball for being the best paly pal a paly gal could ask for and supplying many hours of hiking, coffee-drinking, and geological company. Thank you Enter Shikari and Knife Party for helping me push through the final six Covid-infested months. Finally, thank you to my friends for the laughs, food and support, and my family for their invaluable help proofreading hundreds of pages each of words they did not understand.

Funding for this PhD project was provided by the NERC studentship ACCE (Adapting to the Challenges of a Changing Environment) Doctoral Training Partnership [grant number 1807541]. Asher Haynes and Tristan Pottas of York Potash Ltd were pivotal in enabling this research for providing access to the fresh borehole material that was necessary for this research.

And now, at the end of it all, I think I am ready for another adventure…

Abstract

Vegetation reconstructions for the Late Permian of Europe have previously been hampered due to the lack of suitable exposures. However, the limited evidence suggests a conifer-dominated vegetation that gradually declined as environmental conditions deteriorated approaching the Permian-Triassic boundary.

The Zechstein Sea was a semi-isolated inland sea that dates from the late Wuchiapingian-early Changhsingian (~258 Ma) to the Permian-Triassic boundary (~252 Ma). It underwent 5-7 evaporation-replenishment cycles leaving behind a sequence of stacked carbonates and evaporites. The macrofossil record shows that a conifer-dominated gymnospermous flora inhabited the seas hinterlands.

New boreholes have enabled the first extensive palynological sampling of the entire Zechstein sequence of northeast England. Palynomorph assemblages have been recovered from all five of the evaporation-replenishment cycles (EZ1-EZ5). These assemblages are dominated by pollen grains, with rare trilete spores, and even rarer marine forms such as acritarchs and foraminifera test linings. Pollen grain assemblages are of low diversity (35 species) and dominated by taeniate and non-taeniate bisaccates. The assemblages vary to only a limited extent both within and between cycles EZ1-EZ5, although some minor variations and trends are documented that reflect taphonomic effects.

Based on the composition of the dispersed spore-pollen assemblages, and previous work on the Zechstein megaflora, the hinterland vegetation is interpreted as being dominated by conifers, inhabiting a semi-arid to arid landscape. The new pollen data indicate that the vegetation was little changed, both within cycles and between cycles, and persisted until the demise of the Zechstein Sea in the latest Permian-earliest Triassic, perhaps in fragmented upland refugia. At this time desert sedimentation commenced, which yields no evidence for terrestrial vegetation until the early Triassic (Induan) when evidence for a radically different flora appears. These observations suggest that vegetation loss at the Permian-Triassic boundary was rapid and catastrophic rather than representing the culmination of a slow decline.

Chapter 1. Introduction & Literature Review

1.1 The Permian Timescale

1.1.1 Overview and History

The Permian period (298.9±0.15 - 251.902±0.024 Ma) (Ramezani & Bowring 2017) is composed of three series (Cisilurian, Guadalupian and Lopingian) and nine stages (Figure 1). The system name was proposed by Murchison (1841) in collaboration with Russian geologists to describe an area of the Russian Platform that stretched from the Volga eastwards to the Urals, and from the Sea of Archangel to the southern steppes of Orrenburg (Gradstein & Kerp 2012). Permian strata were soon recognised outside of Russia and in Central Europe, but it was almost a century before the Permian was accepted as a geological system (Lucas & Shen 2018). The name originally only applied to the upper part of the sequence (Kungurian, Kazanian and Tatarian), but in 1889 the system was expanded down to include the Artinskian (Gradstein & Kerp 2012). In 1936 the Artinskian was divided to include the Sakmarian (Dunbar 1940), which was itself later split to include the Asselian as the basal stage of the Permian in 1954 (Gradstein & Kerp 2012).

The succession of the Urals geosyncline is the type area for the Permian, but Permian rocks are found worldwide (Warrington 1996). The Permian timescale used here is taken from the latest revision of the Permian timescale (Lucas & Shen 2018). For a complete description of the updates see Lucas & Shen (2018) and references within. At present the global timescale for the Permian is still in development with only six GSSPs being formally ratified and many substage bases still lacking formal definition (Lucan & Shen 2018). Correlations for the non-marine Permian (Figure 2) have

System	Series	Stage	Age of Base (Ma)
Triassic	Lower (part)	Induan	251.902±0.024
Permian	Lopingian (Upper)	Changhsingian	254.14±0.07
		Wuchiapingian	259.1±0.5
	Guadalupian (Middle)	Capitanian	265.1±0.4
		Wordian	268.0±0.5
		Roadian	272.95±0.11
	Cisilurian (Lower)	Kungurian	283.5±0.6
		Artinskian	290.1±0.26
		Sakmarian	293.52±0.17
		Asselian	298±0.15
Carboniferous	Upper (part)	Gzhelian	

Figure 1. Nomenclature and geochronology of Permian series and stages, with ages from Lucas & Shen (2018).

been based on palynomorphs, conchostracans and tetrapods, however there are problems cross-correlating with marine chronologies. Dating is difficult as the late Cisilurian-Guadalupian does not yield many low-level datable volcanic ash beds associated with fossiliferous lithologies (Lucas & Shen 2018).

1.1.2 Permian Biostratigraphy

Marine biostratigraphy forms the basis of the chronostratigraphic scale for the Permian based primarily on conodonts (Henderson 2016), fusilinids (Zhang & Wang 2017), non-fusilinid foraminifera (Vachard 2016), and ammonoids (Leonova 2016). Brachiopods, rugose corals, and radiolarians (Zhang *et al.* 2017), conchostracans (Schneider & Scholze 2016) are used to a lesser extent but only in certain strata. A common theme among marine invertebrates is how their biostratigraphic utility is hampered by high degrees of provincialism.

During the Permian marine organisms were restricted by regional glaciation during the Asselian, major sea-level lowstands during the Kungurian and Capitanian-Wuchiapingian boundary interval, a high degree of morphological plasticity in certain key taxa, and high degrees of provincialism during the early Kungurian. Provincialism in particular effects conodonts (Henderson 2016), radiolarians (Zhang *et al.* 2017) and although foraminifera underwent high rates of diversification in the Permian meaning they can be used to distinguish twelve stages their provinciality also hinders their utility (Vachard 2016; Zhang & Wang 2017). Rugose corals experience the almost complete disappearance from the Guadalupian through to the Lopingian and are not robust enough for biostratigraphy (Lucas & Shen 2018). In contrast, ammonoids form the basis for almost all Permian stages, with nine stages almost completely characterised by ammonoids (Leonova 2016) and can be successfully correlated between regions. Despite their rarity and poor stratigraphic distribution in certain regions they are valuable secondary signals for GSSP correlation. Brachiopods are the common Permian shelly benthic fauna (Wignall & Hallam 1992), and Permian brachiopods are characterised by their small size, thin shells, and dwarf morphotypes due to the prevalence of extreme environments at the end of the Permian. Their utility is hindered by their provincialism.

Other marine fauna such as non-cephalopod molluscs (bivalves, gastropods) have only been used in a limited fashion and suffer the same issues as brachiopods during the Lopingian. However, bivalves did become increasingly important constituents of marine ecosystems throughout the Permian as they experienced increases in generic richness and ecological diversity (Clapham & Bottjer 2007; Mondal & Harries 2016; Lucas & Shen 2018).

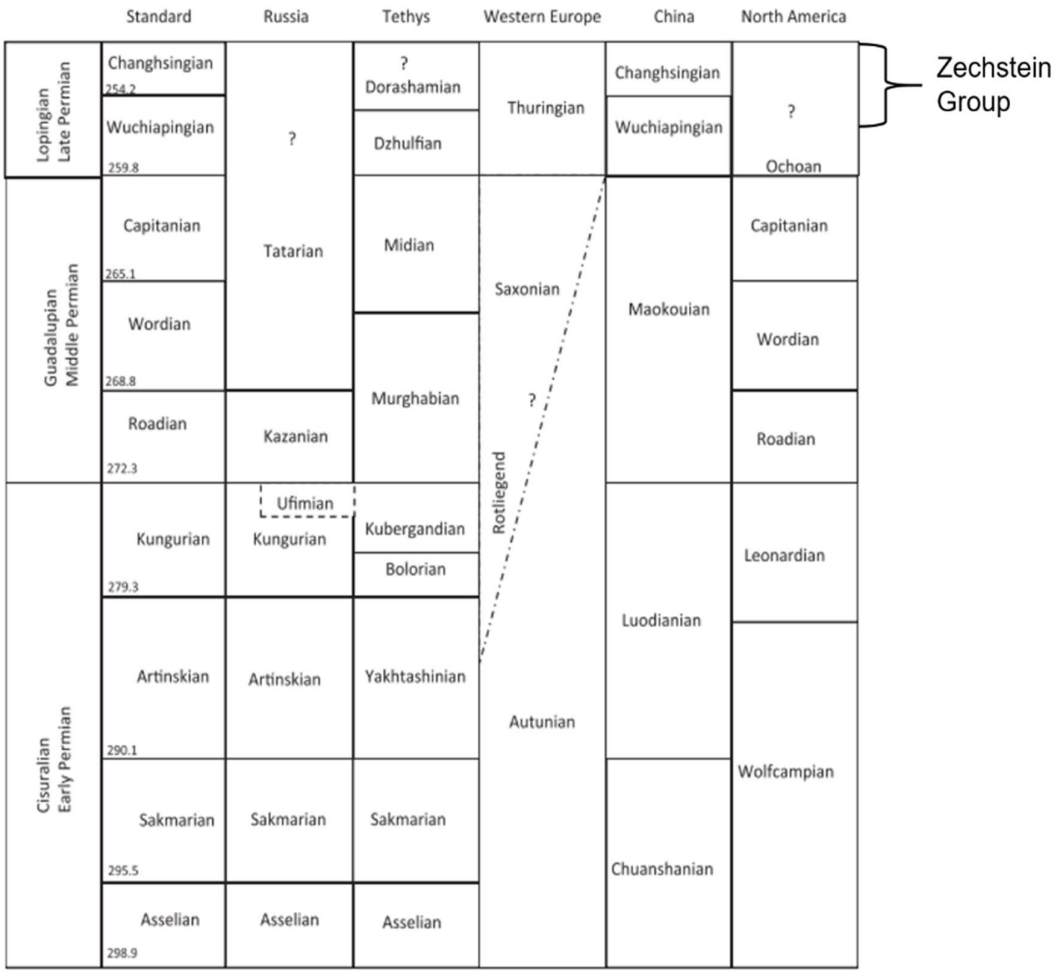

Figure 2. Chronostratigraphy of the Permian showing correlation between the Standard, the type area, the Tethys, Western Europe, China and North America, covering the Angaran and Euramerican provinces. The approximate stratigraphic position of the Zechstein Group is noted (modified from Stephenson (2018) Figure 1).

1.1.3 Terrestrial Biostratigraphy

Non-marine biostratigraphy is based on dispersed palynomorphs, plant macrofossils, tetrapod footprints and tetrapod body fossils and suffer some of the same restrictions imposed by provincialism.

Palynomorphs are useful biostratigraphic indicators because their highly recalcitrant sporopollenin walls are resistant to pressure, desiccation, and microbial decay. Palynomorphs are found in both marine and non-marine strata making them useful for cross-correlating marine and non-marine strata. However, because they only disperse tens of kilometres away from their producing plants provincialism can impede the use of palynomorphs in broad scale correlations (Traverse 2007). Plants can be incredibly sensitive to their environment, therefore the palaeoenvironmental and facies

restrictions of extinct plants effects the distribution of their palynomorphs. While neither data sets are independent regional schemes can be strong. Local scale palynostratigraphic schemes have high resolutions but a lack of schemes outside the basins, coalfields, and hydrocarbon fields where they occur means correlation with the Permian standard global chronostratigraphic scale is not always possible. Radioisotopic dating, magnetostratigraphy, independent faunal correlations and strontium isotope stratigraphy are vital supplements to palynostratigraphic schemes.

The most recent comprehensive review of Permian palynostratigraphy is Stephenson (2018) and the uppermost Zechstein-lowermost Buntsandstein palynoflora was most recently reviewed by Backhaus *et al.* (2013). Although phytogeographical provinciality from the Guadalupian onwards impedes regional correlation high resolution local schemes do exist, based on the abundance or relative proportion of well-described taxa e.g., *Scutasporites* spp., *Vittatina* spp., *Weylandites* spp., *Lueckisporites virkkiae*, *Otynisporites eotriassicus*, and *Converrucosisporites confluens*. The only pattern discernible in the Lopingian rocks of western Europe is a gradual trend towards impoverishment (Pattison *et al.* 1973) otherwise the palynology is reported as relatively homogenous (Grebe & Schweitzer 1962; Schaarschmidt 1963; Clarke 1965a; Smith *et al.* 1974). The cause of the impoverishment was assumed to be an unspecified effect of the impending PTME but not necessarily reflective of complete deforestation as taphonomic effects have not been fully explored.

Permian plant macrofossils have recently been reviewed (Cleal 2016). They are highly provincialized due the complex topography of Pangaea and resulting climatic stratification and provide a lower stratigraphic resolution than palynomorphs. However they display the overall floristic change through the Permian at all palaeolatitudes driven by climate change, large-scale volcanism and tectonically-driven landscape changes, making them good palaeoenvironmental indicators.

The tetrapod footprint and body fossil record also have biostratigraphic value, yet the tetrapod body fossil record is more useful (Lucas & Shen 2018). The Permian faunochrons are reviewed by Lucas (2006) yet there are problems with incompleteness, endemism, and taxonomy, and there is a relative lack of age control which impedes refinement of a tetrapod-based biochronology. Otherwise, tetrapods are a robust tool for global and regional age correlation. Other organisms used in non-marine biostratigraphy are charophytes, ostracods, bivalves, and fish but they are not robust enough for global correlation or provincial biostratigraphy.

1.1.4 Zechstein Timescales

The Zechstein Group (Figure 3) is an evaporite dominated unit of considerable thickness (>2.5 km) deposited by the Zechstein Sea (~258-252 Ma). A detailed geological setting can be found in Chapter

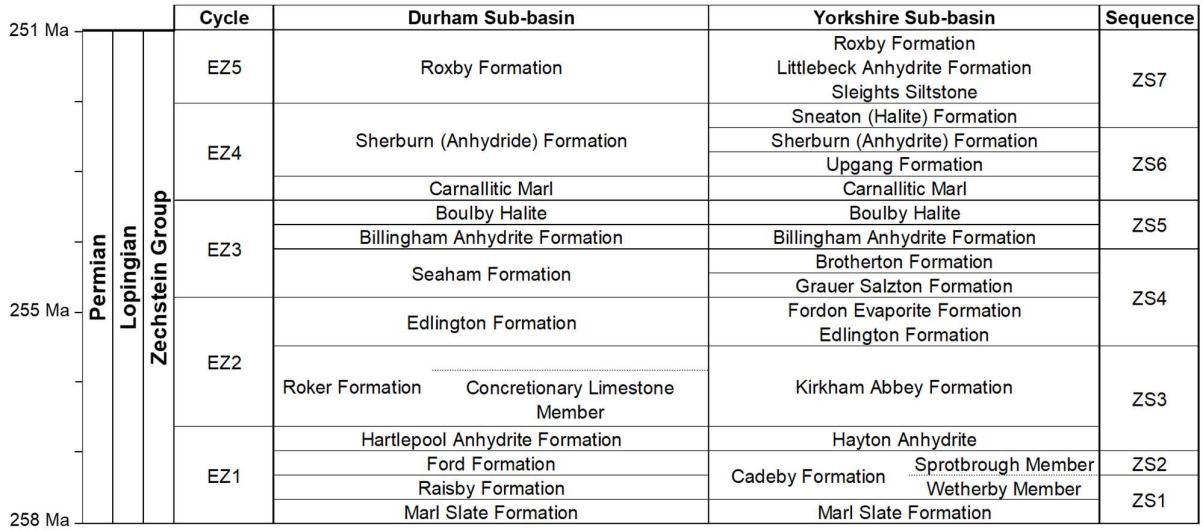

Figure 3. Stratigraphy of the British Zechstein. Dates for transgression and termination (Szurlies *et al.* 2013) and date of the EZ2 evaporites (Kemp *et al.* 2016).

2. Dating the Zechstein is difficult due to the lack of age-diagnostic definitive fauna in the underlying Rotliegend Group (Cisilurian) and typically barren overlying Triassic sediments.

Correlating the Zechstein with the global timescale is generally difficult due to the lack of index fossils with the only biostratigraphically important group being the conodonts *Mesogondolella britannica* (Legler *et al.* 2005) of the Kupferschiefer and Marl Slate and *Merrillina divergens* (Szaniawski 1969, 2001). Conodont-calibrated stages are under continuous debate (Menning *et al.* 2006; Słowakiewicz *et al.* 2009; Doornenbal & Stevenson 2010) however as there have been several incorrect age interpretations within older literature (e.g., Wardlaw & Collinson 1979, 1886). Correlation with Permian Basins in North America may be possible based on $\delta^{13}C$ anomalies at the Guadalupian-Lopingian boundary which have also been discovered in the Zechstein Basin (Słowakiewicz *et al.* 2016).

Palynology is the major biostratigraphical tool used for the Zechstein supplemented by the scarce conodonts in the lowermost Zechstein (Kozur 1994; Legler *et al.* 2005), and conchostrachans in the uppermost Zechstein and overlying Buntsandstein (Kozur 1999; Bachmann & Kozur 2004; Kozur & Weems 2011). This is due to a lack of global biostratigraphic index forms even when faunas are at their most diversified, such as during the Kupferschiefer/Marl Slate.

Estimates of the duration of the Zechstein Sea vary (Table 2). The base has been isotopically dated to 257.3±1.7Ma (Re-Os) (*Brauns et al.* 2003) for the Kupferschiefer in Germany, or to ~258Ma (Menning *et al.* 2006). This is supported by Menning *et al.* (2005) and Słowakiewicz *et al.* (2009),

however these authors combined data from shales, sulphides and conglomerates therefore the isochron may represent a mixing of components and may be less robust (Alderton *et al.* 2016).

Magnestostratigraphy has been used to date primarily the Zechstein of western and central Europe over the past twenty years in Poland (Nawrocki 1997, 2004; Nawrocki *et al.* 2003), Germany (Soffel & Wippern 1998; Szurlies *et al.* 2003; Szurlies 2004, 2007), and in the Netherlands (Szurlies *et al.* 2012). A magnetostratigraphic composite for the from the base of the Zechstein through to the lowermost Buntsandstein has been created (Szurlies 2013), allowing for a better correlation with the Permian geomagnetic polarity timescale (Hounslaw & Balabanov 2016) and the global timescale. The Zechstein interval is of dominantly normal polarity with a few reversed magnetozones which facilitate correlation throughout the Central European Basin. Based on the composite the basal Zechstein is likely equivalent to the uppermost lower-upper Wuchiapingian and overlying upper Zechstein and lowermost Buntsandstein are equivalent to the entire Changhsingian. Magnetostratigraphy places the duration of the Zechstein at only 2.8-3.5 Myr (Szurlies *et al.* 2013) which differs from the classical interpretation of the overlying Buntsandstein as Early Triassic (Harland *et al.* 1990). However, due to the normal polarity of the underlying Upper Rotliegend in Germany (Soffel & Wippern 1998) and Poland (Nawrocki 1996), which may be equivalent to the upper Wuchiapingian (Langereis *et al.* 2010), the Zechstein may in fact have a longer minimum duration of 3.4 Myr. This is close to the suggestion of 2.8 Myr by Menning *et al.* (2005).

Extrapolating the magnetostratigraphy, Szurlies (2013) suggests Z1 to lower Z3, correlated by biostratigraphy and magnetostratigraphy to the upper Wuchiapingian, have a combined duration of approximately 1.9 and 5.1 Myr. The long duration of the lower Zechstein is consistent with the the three predominantly marine lower Zechstein cycles being of a different magnitude to the subsequent four younger cycles (Peryt *et al.* 2010) when salt deposition was driven by short-term climate fluctuations (Wagner 1994). Further correlations match Z3-Z7 to the lowermost Buntsandstein, lasting approximately 1.5 Myr, with Z7 assumed to be an approximately 100 Kyr Milankovitch eccentricity cycle. Szurlies study was published in 2013 and needs updating to correlate with the latest release of the Permian timescale (Lucas & Shen 2018).

Other estimates include a total duration of 5 Myr (Menning *et al.* 2005), and of 9 Myr (Słowakiewicz *et al.* 2009). The latter is based on carbon isotope data from the base of the continuous Lopingian in the U.S.A. and central Europe. A transition from a short reversed to long normal magnetozone located in the uppermost Zechstein, which predates the PTME and conodont-calibrated Permian-Triassic boundary, has been identified and represents an important time marker for global correlation (Szurlies *et al.* 2013). There is also a debated temporal hiatus in Zechstein deposition of ~4 Myr between the Zechstein and the Lower Triassic (Henderson *et al.* 2012), but there is no strong

evidence of this (Menning *et al.* 2005, 2006). In the U.K. Zechstein deposition terminates with the Roxby Formation and the Bröckelschiefer being assigned to the Triassic. In Germany and The Netherlands, the Bröckelschiefer marks the end of Zechstein deposition (Kozur 1998) as it is time equivalent to the Zechstein in the centre of the basin (Kozur 1989, 1994).

No attempts have been made to formalise a timescale for the British Zechstein. Due to the suggested contemporaneity of the Kupferschiefer and Marl Slate, which has been debated by Stoneley (1958), the timescale for the rest of the basin provides the most appropriate framework for the British Zechstein. There have been two attempted datings of Cycle 2. North Sea strontium isotope data suggest the evaporites (polyhalite, anhydrite and kalistronite) of the EZ2 evaporites formed at 255 ± 2 Ma (late Wuchiapingian) (Kemp *et al.* 2016) and an $^{87}Sr/^{86}Sr$ curve has been create for the EZ2 evaporites (Kemp *et al.* 2018). However, an error margin of 2 Myr is unhelpful considering the entire

Age	Method	Reference
9 Myrs (251.0±0.4-260.0±0.4 Ma)	Stratigraphic correlation	Bowring et al. (1998), Slowakiewicz et al. (2009)
7 Myr (251.0±0.4-258.0±0.4 Ma) Werra = PZ1 duration ca. 1 Myr	Magnetostratigraphy	Menning et al. (2005)
5.5 to ca. 7.5 (to 10.5) Myrs (252.6±0.3 – 260.4±0.4 Ma) (263 Ma)	*Ogg et al. (2008) extended the lower boundary of the Zechstein to 263 Ma without giving an explanation for it	Mundil et al. (2004), Ogg et al. (2008)*
257.3±1.7 Ma	Re-Os radiometric ages for sulphides within the Kupferschiefer	Brauns et al. (2003)
Major deposits of the lower Zechstein may have been deposition in ca. 2 Myrs	87Sr/86Sr ratio	Denison & Peryt (2009)
Zechstein Limestone time interval of ca. 1 Myr	Stratigraphic correlation	Peryt (1992)
2.8-3.5 Myr 2.8 Myr Ca. 260.4-258 Ma	Magnetostratigraphy Stratigraphic, palaeomagnetic, micropalaeontological, and C-isotopic correlations	Szurlies et al. (2013) Menning et al. (2006), Slowakiewicz et al. (2016), Wagner (2009)
EZ2 evaporites formed 255±2 Ma (late Wuchiapingian)	87Sr/86Sr isotope from North Yorkshire polyhalite, anhydrite, and kalistronite	Kemp et al. (2016)
0.3 Myr, Roker Formation	Milankovitch cyclicity based off turbidite bed thicknesses in Marsden Bay	Mawson & Tucker (2009)
Ca1 (Zechstein Limestone) deposition duration ca. 400 Kyr	Relative thickness of strata in the Wolsztyn area	Peryt (1984)

Table 1. A summary of the different attempts to date the Zechstein Group and the methods used.

Zechstein may have been deposited in as little as 2.8 Myr (Menning *et al.* 2006). Mawson and Tucker (2009) have suggested that the Roker Formation (EZ2Ca) had a duration of 0.3 Myr, based of turbidite bed thickness at Marsden Bay, Tyne and Wear, which they correlated with Milankovitch cyclicity. Several kinds of Milankovitch cycles were identified in the laminated mudstone, correlating to ca. 100 Kyr short-eccentricity, ca. 20 Kyr precision and ca. 10 Kyr semi-precision cycles, as well as sub-Milankovitch millennial-scale cycles of 0.7-4.3 Kyr duration.

1.1.5 Zechstein Biozonation

Few biozones have been erected for the entire Zechstein, yet there are two notable attempts for macro- and microfossil biozonation. Macrofossil biozonation of the Zechstein in northern Poland was attempted by Korwowski & Klapcinski (1986). The lower three cycles PZ1, PZ2, and PZ3 show considerable variation in their macrofauna which is variable both in terms of taxonomic composition but also the frequency with which the taxa occur. This is thought to be controlled primarily by palaeogeographical zonation within the basin. However, attempts to use this scheme quantitatively

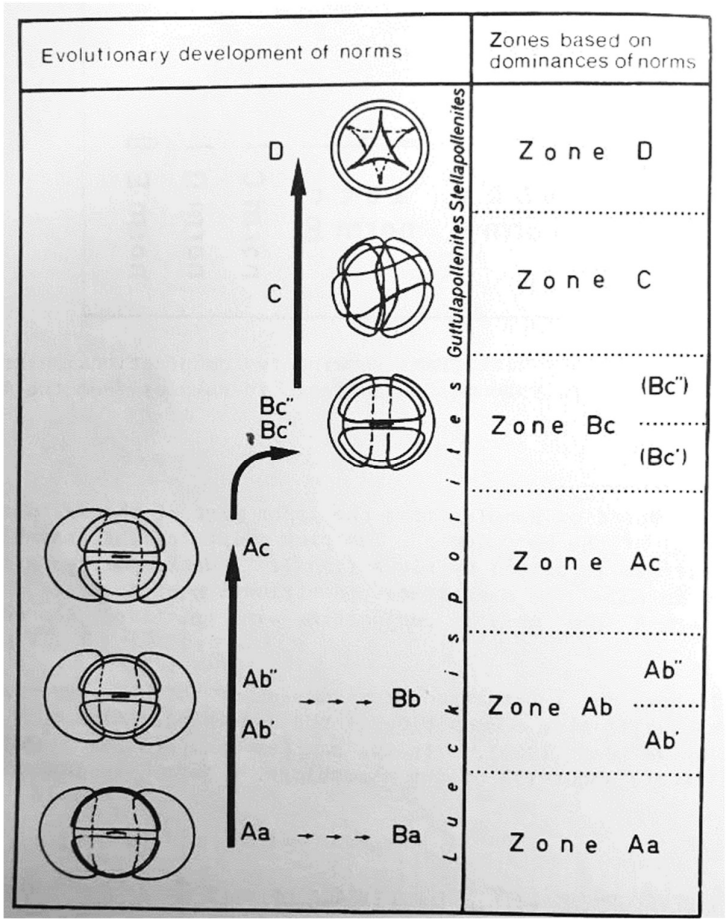

Figure 4. The proposed development of *Lueckisporites virkkiae* palynodemes and their inferred zonation (from Visscher 1971).

should be treated with caution as assemblages can be significantly modified and obscured by later redeposition with differential species reactions to these factors.

Visscher (1971) constructed palynodemes of the bitaeniate bisaccate pollen grain *Lueckisporites virkkiae* Potonié et Klaus 1954 (emend. Clarke 1965) (Figure 4). Visscher suggested the subdivision of the taxon into eleven forms (Norm A: Aa, Ab', Ab'', Ac; Norm B: Ba, Bb, Bc', Bc''; Norm C; Norm D; Norm E), based on variation within four features: (i) the structure of the sexine of the cappa; (ii) the shape of the sacci; (iii) the structure of the exine of the sacci; (iv) the presence of teratological variations. A zonation based on the relative proportions of norms Ac, Bc, C and D was suggested.

1.2 Palaeocontinental Reconstruction: Pangaea

The late Palaeozoic was a period of major continental reconfiguration. During the Permian, the continents came together to form the single landmass Pangaea which drifted steadily northwards (Figure 5). The tropical equatorial Palaeo-Tethys Ocean opened into the Panthalassic Ocean to the east, which covered most of the Earth's surface. Laurasia occupied the northern hemisphere, and Gondwana occupied the southern hemisphere. The Chinese microcontinents to the east of the Paleo-

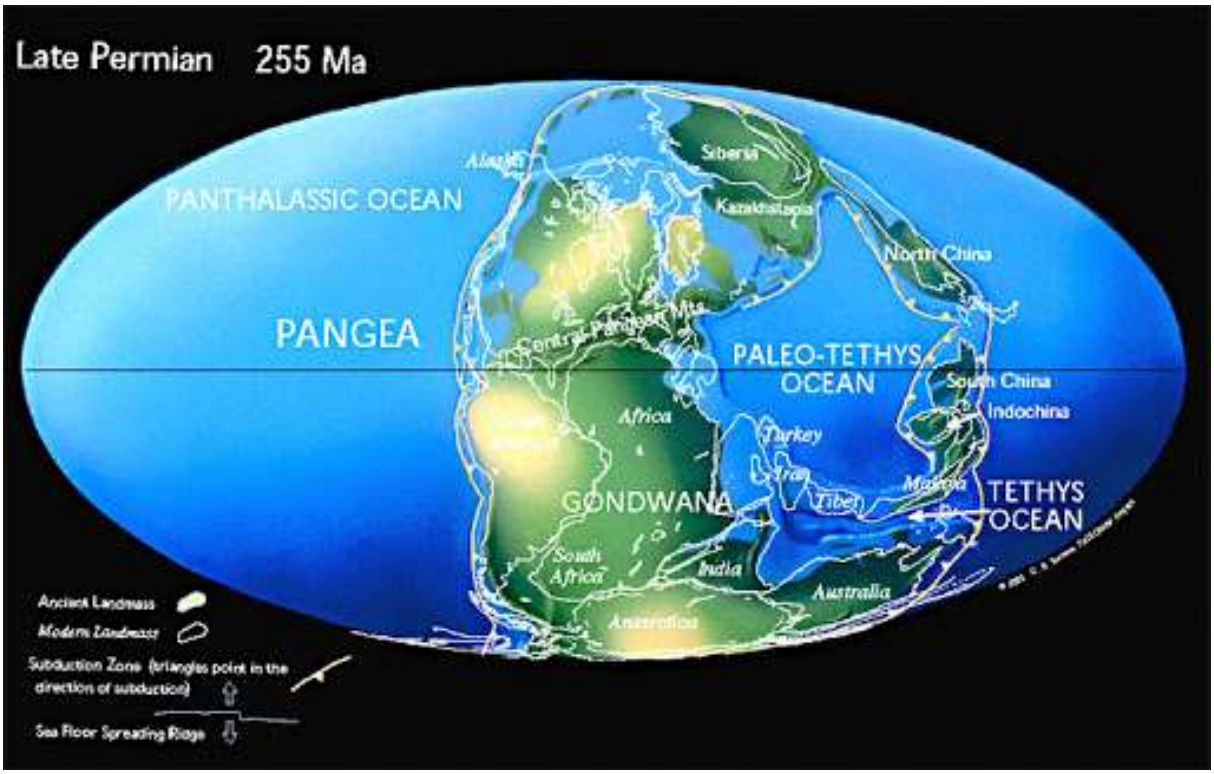

Figure 5. Palaeocontinental reconfiguration of Pangaea during the Lopingian ca. 255 Ma with the area of the Southern and Northern Permian basins is circled in red (modified from the Scotese Palaeomap Project).

Tethys spanned the equator but were separated from Pangaea until the Late Triassic (Rees 2002). The Permian also saw opening of the Neotethys Ocean with the rifting of the Cimmerian Plates (Golonka & Ford 2000).

Pangaea characterises Permian geography, spanning the tropics reaching high northern and southern latitudes (Ziegler *et al.* 2003). The super continent was divided by the Central Pangaean Mountains that formed during the Variscan Orogeny (Rees 2002), creating a substantial rain shadow at low and mid latitudes in both the northern and southern hemispheres (Beauchamp 1994). Pangaea had relatively little coastline and a large interior ringed by subduction zones called the Pangaean Ring of Fire (Scotese & Lanford 1995). This arrangement altered atmospheric and oceanic currents, changing climate and habitat distribution.

1.3 The Permian Atmosphere

Pronounced changes in atmospheric composition occurred during the Permian. General atmospheric trends show declines in atmospheric oxygen (O_2) and increases in atmospheric CO_2 concentration, contributing to global warming and aridisation at the end of the Palaeozoic (Royer 2006). Typically, high levels of carbon dioxide (CO_2) and hydrogen sulphide (H_2S) were a result of volcanic activity, causing levels of H_2S and methane many times greater than the present (Kump *et al.* 2005).

1.3.1 Atmospheric O_2

Figure 6 illustrates the trends in atmospheric O_2 concentration throughout the Phanerozoic. Atmospheric O_2 levels rose throughout the Carboniferous, reached a peak in the Cisilurian, then fell dramatically through the Lopingian, eventually restabilising in the Early Triassic (Berner 2006). High concentrations of atmospheric O_2 during the Cisilurian and Carboniferous are attributed to increased burial of organic carbon in vast swamps and the rise and spread of large vascular plants (Berner 2006). During the Asselian (298.9-295.0 Ma) increases in atmospheric O_2 led to warmer global mean surface temperatures and reduced carbon storage on land. It is possible that the high oxygen content of the atmosphere contributed to the cessation of the Asselian glaciation (Wade *et al.* 2019).

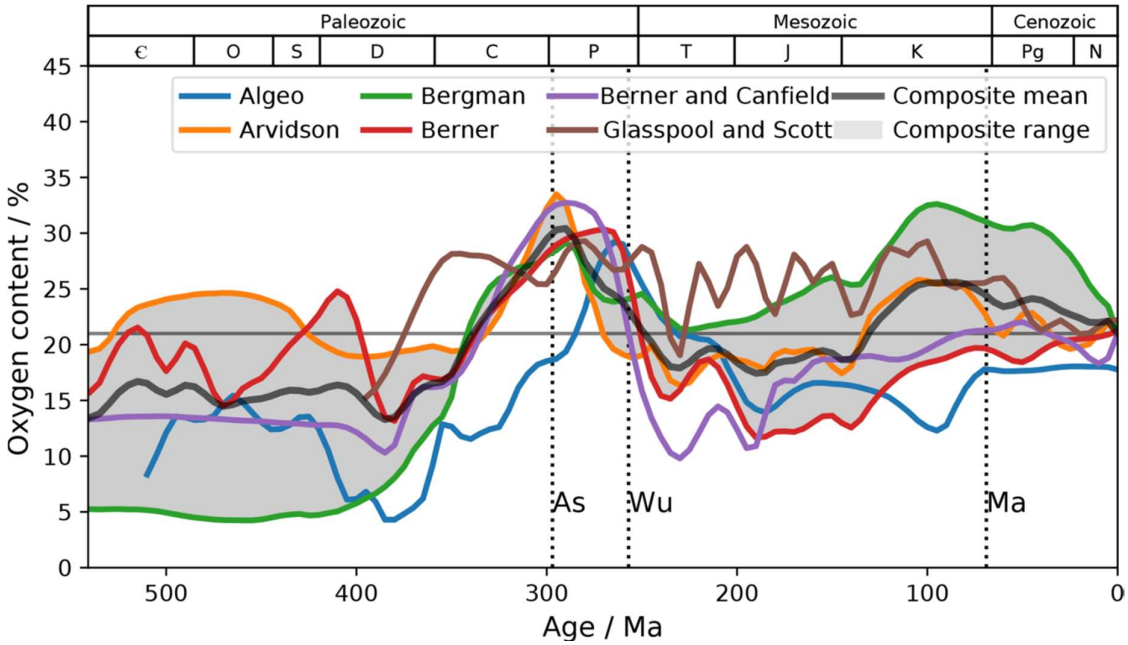

Figure 6. Reconstruction of atmospheric oxygen concentrations during the Phanerozoic. As = Asselian, Wu = Wuchiapingian, Ma = Maastrichtian (figure and references from Wade *et al.* (2019) Figure 1).

1.3.2 Atmospheric CO_2

During the Carboniferous, atmospheric CO_2 levels were similar to present-day but by the Triassic they had almost quadrupled (Berner 2006). Increased atmospheric CO_2 concentrations can be linked to vegetation change and tectonic activity (Came *et al.*, 2007). Figure 7 illustrates the trends in atmospheric CO_2 concentration throughout the Phanerozoic. Large increases in CO_2 during the Permian are reflected in the plant stomatal index (SI) (Botha & Smith 2007; Retallack 2013), and pedogenic $\delta^{13}C$ (Royer *et al.* 2001). Sharp increases in atmospheric CO_2 may have proven lethal to land plants (Benton & Newell 2014)

The massive release of greenhouses gases into the atmosphere during eruptions of the Siberian Traps Large Igneous Province caused severe heat stress for many organisms, both terrestrial and marine (Joachimski *et al.* 2012; Benton & Newell 2014). Increases in equatorial sea surface temperatures of 5-10 °C have been modelled as a result of CO_2-forced warming during the Permian (Joachimski *et al.* 2012; Sun *et al.* 2012; Cui *et al.* 2013; Chen *et al.* 2015). Increased CO_2 emissions would also have led to an intensification of the hydrological cycle due to the positive Clausius-Clapeyron slope of water vapour (Ramanathan *et al.* 2001; Allen & Ingram 2002). This may have affected the humid climate and depositional regime in the upper Zechstein (Słowakiewicz *et al.* 2009).

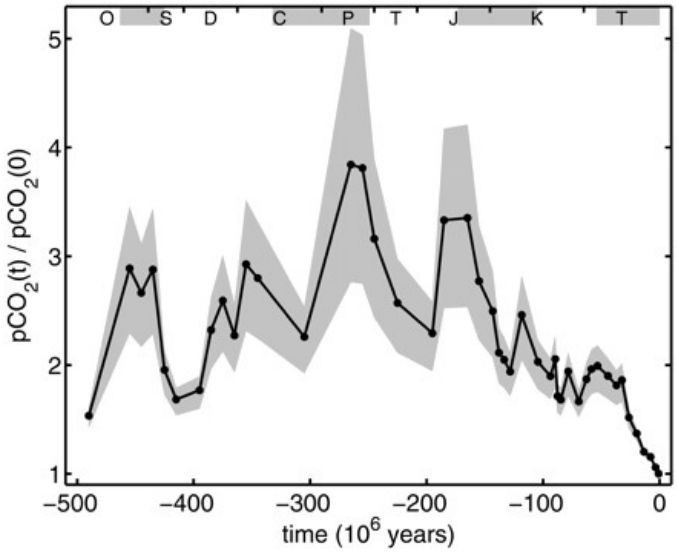

Figure 7. Reconstruction of atmospheric carbon dioxide concentrations during the Phanerozoic (adapted from Rothman (2002)).

1.4 Sea Level

1.4.1 Overview

Throughout the late Palaeozoic there was a global trend of falling sea level (Haq & Schutter 2008), thought to be a result of the formation of Pangaea leading to a volumetric increase in the size of ocean basins (Conrad 2013; Guillaume *et al.* 2016). The most widely accepted sea level curve for the Palaeozoic is Figure 8 of Haq & Schutter (2008). This model shows a slight fall in sea level from the Pennsylvanian (Gzhelian) to the early Cisilurian (Asselian). Sea level remained stable throughout the Cisilurian until the Guadalupian (Roadian) when a sharp trend in declining sea levels occurred coincident with a known period of glaciation (Glennie 1989). This trajectory of sea level fall culminated at the early Lopingian (Wuchiapingian) when the absolute minimum of sea level for the Palaeozoic was reached. Recovery began during the latest Permian (Changhsingian) with a global rise in sea levels but generally low sea levels persisted into the Early Triassic. The Guadalupian eustatic low is coincident with a fall in $\delta^{13}C$, caused by major uplift and fragmentation of Pangaea and Chinese basalt eruptions which may have resulted in ocean warming and destabilisation of clathrate reservoirs (Lo *et al.* 2002), confirmed by a negative carbon-isotope shift (Kaiho *et al.* 2005; Słowakiewicz *et al.* 2009) and coincides with a Phanerozoic minimum of the water $^{87}Sr/^{86}Sr$ curve (Korte *et al.* 2003, 2006). The rise in sea levels during the Lopingian may be a result of considerable dynamic subsidence of the continents (Cao *et al.* 2019).

1.4.2 Zechstein Sea Level

Normal marine eustatic models do not apply to the Zechstein Sea as it conforms to neither normal icehouse nor hothouse world models (Warren 2006). Under normal marine conditions in an icehouse world eustatic amplitude is in the magnitude of hundreds of meters of change, relative to tens of meters in a hothouse world. And under normal conditions the focus of sedimentation is near the shoreline, either on the shelf or basinward of the shelf. The Zechstein Sea is reconstructed as a tideless tropical inland sea (Smith 1989) with depths ranging from tens to hundreds of meters and perhaps deep marginal waters too suggested by the deep polygonal structured observed in Boulby Mine (Fordon Evaporite Formation, Cycle 2) (C. Cockell pers. comm.) Different magnitudes of sea level rise and fall with each Zechstein cycle are expected, with the magnitude decreasing as the basin shallowed with each successive cycle. The Zechstein Sea does not conform to normal eustatic models because of the initial isolation of the basin, the subsequent rapid fall in sea level of 500-1000m following widespread evaporite precipitation, then the migration of the coastline hundreds of kilometres basinward due to continued evaporation. The magnitude of sea level fall and rise in the sea was in part controlled by strait-blocking reefs (Mulholland *et al.* 2018).

1.4.3 The Zechstein Water Column

The Zechstein Sea had an intermittent connection with the open ocean Boreal Ocean to the North and perhaps to the Tethys to the southeast (Legler & Schneider 2008) (Figure 9). The sea is characterised by a stratified water column affected by basin topography and the repeated transgression-regressions. There is a misconception that anoxic and euxinic conditions were widespread throughout the basin, however these conditions are now known to have been heterogeneous (Słowakiewicz *et al.* 2016).

The deposition of the Kupferschiefer/Marl Slate took place under photic zone euxinic conditions (Paul 2006). The remaining deposition of the Cycle 1 carbonates took place under varied oxic-suboxic to anoxic bottom water conditions (Kluska *et al.* 2013; Peryt *et al.* 2015; Słowakiewicz *et al.* 2015). Following Cycle 1 it is unclear how spatially and temporally heterogenous these conditions were. Słowakiewicz *et al.* (2016) reviewed the distribution of euxinic and anoxic

co lagoonal

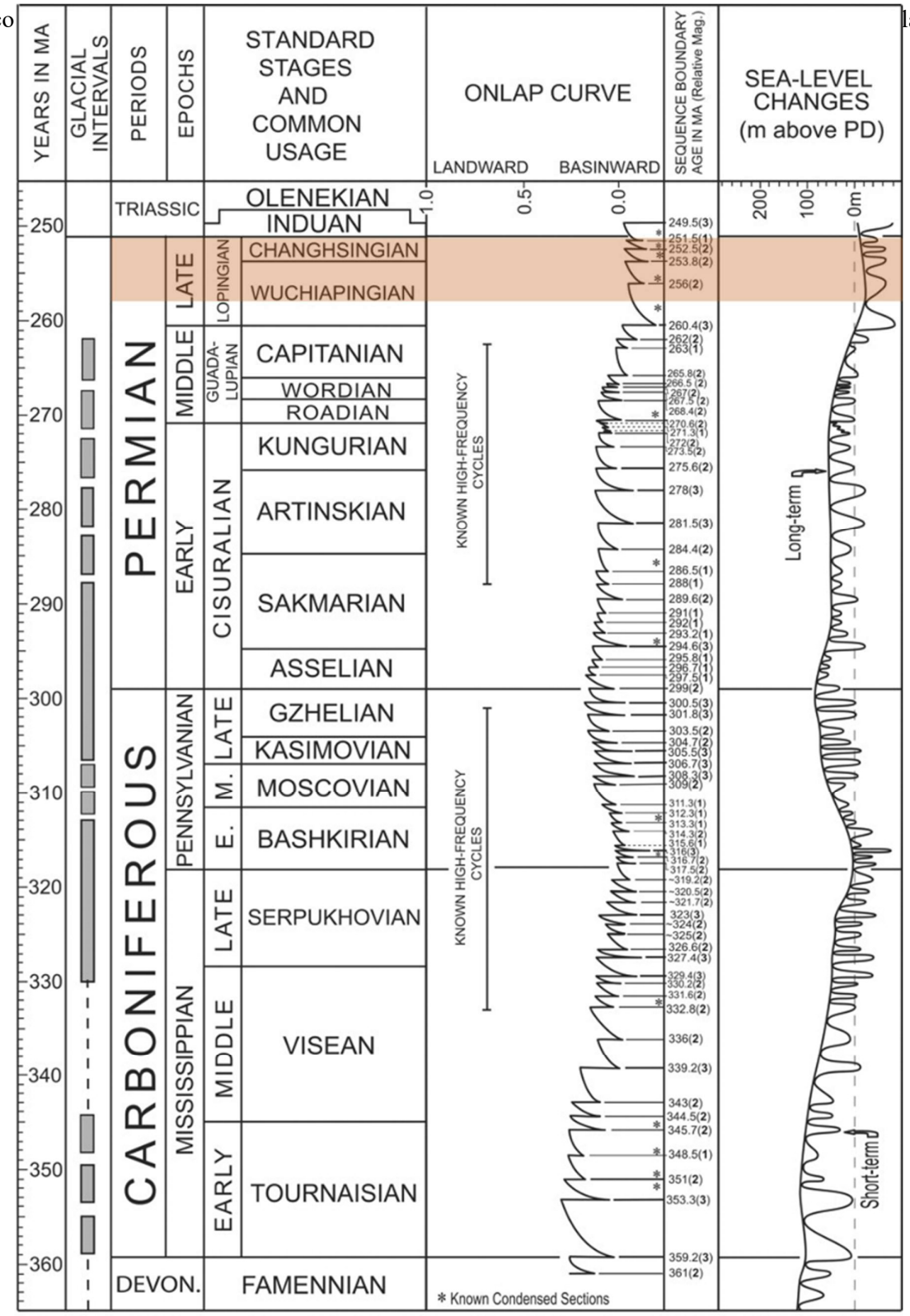

Figure 8. Tournasian to Induan sea-level changes with the approximate stratigraphic range of the Zechstein Group highlighted (modified from Haq & Schutter 2008).

facies along the northern and southern margin of the basin and were associated with localised conditions or benthic production in association with microbioalites. Elevated salinities in southeastern Germany and eastern Poland support the interpretation of a restricted basin during Z2 without a connection to the Tethys Ocean. Salinity signatures (e.g., gammericin) are absent in basinal settings of the eastern SPB and indicate that strong reducing conditions were restricted to the lower slope, shallow-basin locations, restricted lagoons, and did not develop in the basin centre.

Anoxic and euxinic marginal settings were restricted to north-east parts of the SPB as the southeastern Polish Zechstein does not display evidence of photic zone euxinia. The southern margin of the SPB is characterised by generally oxic-suboxic conditions, with local pockets of anoxia limited to restricted embayments, and higher salinities limited to restricted oxic-anoxic lagoons. In the western SPB (e.g., northeast England and adjacent offshore areas) and the NPB (Outer Moray Firth, offshore Scotland) the water columns were oxic-suboxic. Euxinic conditions were likely caused by high episodic primary productivity of organic matter on the lower slopes and in restricted lagoons.

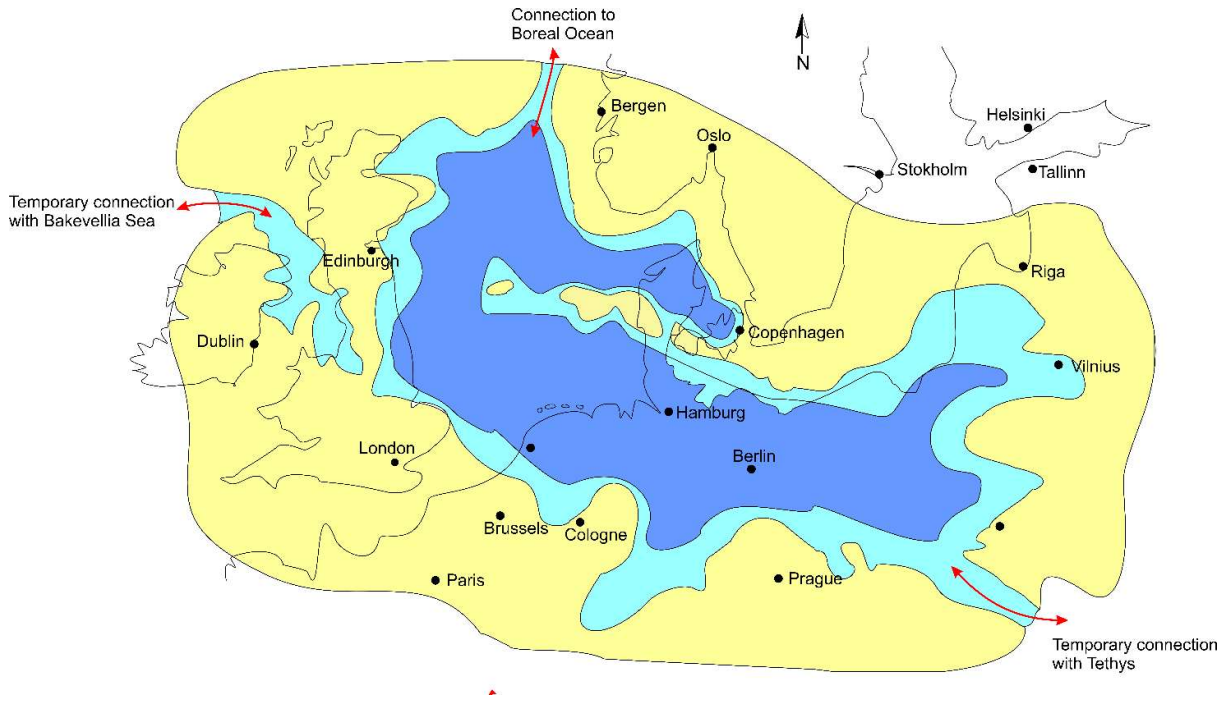

Figure 9. Palaeogeographical map of the Zechstein Sea basin, showing the location of flood pathways to the Boreal Sea and potential connection to the Palaeo-Tethys Ocean (after Słowakiewicz *et al.* 2016).

1.5 Permian Climate

1.5.1 Icehouse-Hothouse transition

The Permian period underwent a major climate evolution from the icehouse conditions of the Permo-Carboniferous to the full greenhouse conditions of the Permo-Triassic, the only transition of this kind in the geological record (Joachimski *et al.* 2012; Sun *et al.* 2012). This transition was most acute across the Permian-Triassic boundary. Therefore the climate of the Lopingian was significantly affected by the release of greenhouse gas (Winguth *et al.* 2015), causing significant disruption to global biogeochemical cycles (Grasby *et al.* 2015). There is currently no evidence for glaciation persisting into the Lopingian (Cocks & Torsvik 2006; Yeh & Shellnutt 2016). During the Asselian Gondwana was characterized by its large continental and alpine glaciers in polar regions (Fielding 2008). Global cooling has been invoked as a mechanism for climate perturbation during the Lopingian (Roscher *et al.* 2011), and the more popular warming theory is thought to have acted as a catalyst for the rate of extinction rather than the initial cause of PTME (Chen *et al.* 2015).

The Pangaean configuration created a well-differentiated climate with steep pole-to-pole gradients comparable to the modern interglacial climate (Rees *et al.* 2002) (Figure 10). Many of the Permian successions in Europe consist of 'red beds' which are sediments laid down in hot and arid conditions in either deserts or in rivers and lakes, with their red colouration due to the highly oxidising environment in which they were deposited (Benton *et al.* 2002). Widespread arid conditions are represented by the distribution of evaporite deposits in Figure 10. More pronounced CO_2-radiative forcing changed ocean circulation and stratification leading to weakened Hadley Cells, decreased magnitude of trade winds, and declines in equatorial primary productivity. Monsoonal circulation patterns arose caused by altered oceanic and atmospheric currents (Roscher 2009), the topography of the land, and the late Carboniferous glaciation (Cocks & Torsvik 2006).

1.5.2 Regional Climates

Climate along the Tethys coastline in the southern hemisphere was driven by summer moisture advection related to a low-pressure cell over Gondwana (Fluteau *et al.* 2001) and a monsoonal climate with significant summer precipitation. This established of a savannah climate that was warm and seasonally humid (Fluteau *et al.* 2001). To the east a band of warm climate stretched along the Tethys, with local dry climate conditions evidenced by the presence of evaporite deposits. This transitioned poleward into a cold climate belt (Fluteau *et al.* 2001).

In northern Gondwana, the climate was arid (Cuneo 1996). Higher latitude areas were subjected to a cold, humid, climate that would have experienced freezing periods and polar light

conditions (McLoughlin *et al.* 1997). Despite cold growing conditions, extensive coal deposits in eastern Australia, India, and Antarctica suggest year-round precipitation at high latitudes and a relatively short dry season (Retallack 1995). Winter snow cover would also have prevented the soil from drying out in winter (Fluteau *et al.* 2001).

Cathaysian had a tropical climate indicated by widespread Upper Permian coal deposits (Shouxin & Yongyi 1991; Enos 1995). The distribution of coal-bearing beds in North China suggests a longer season of rainfall in its southern part, while northern parts experienced drier climates (Poort & Kerp 1990; Shouxin & Yongyi 1991). Angara is characterised by a warm, temperate, and humid climate. In northern regions cooler conditions and high latitude year-round precipitation favoured coal production (Ziegler *et al.* 1997). To the south evaporite layers are found along a west-east gradient (Chuvasov 1995), indicating a more arid climate. In Laurussia there was a massive arid belt occupying the subtropics, yet to the there was a warm climate with continuous year-round precipitation (Utting 1994; Fluteau *et al.* 2001). The impacts of Appalachian and "Variscan" fold belt altitudes at low latitudes in Laurussia are important to Laurussian climate reconstructions, greatly altering atmospheric circulation patterns and climate via precipitation advection.

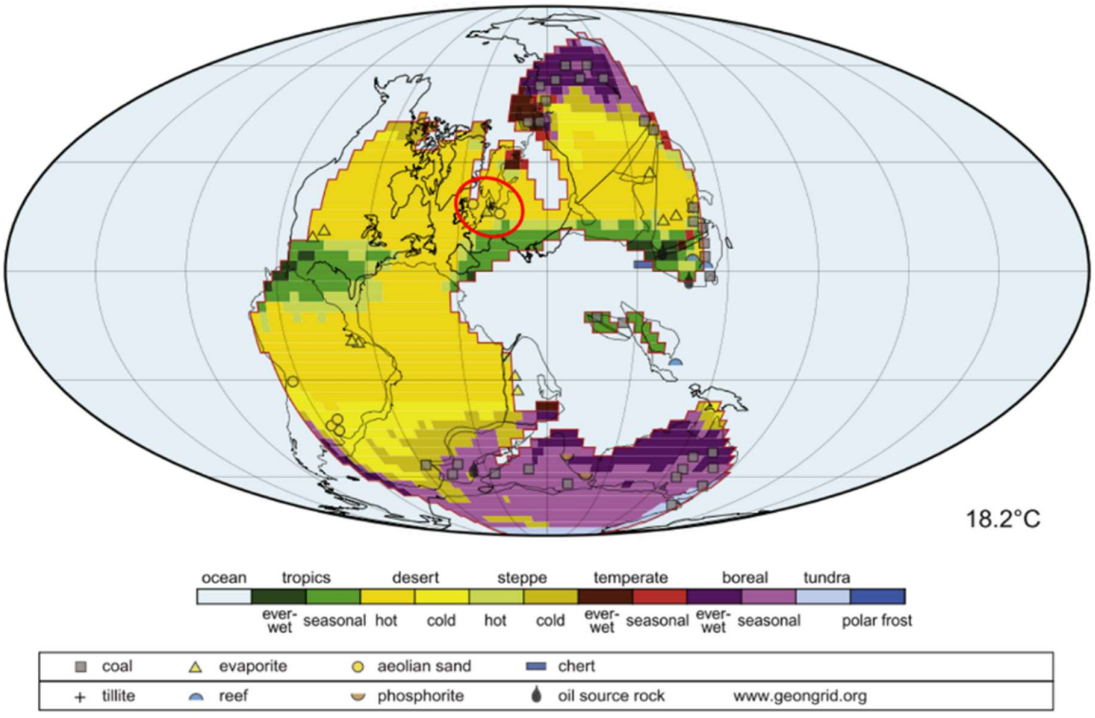

Figure 10. Simplified climate zones during the Lopingian and associated phytogeographical provinces, stars represent well-known Lopingian terrestrial systems. The location of the Zechstein Sea is circled in red (modified from Roscher *et al.* 2011).

1.5.3 Zechstein Climate

The Lopingian climate classifies as post-glacial (Hallam & Wignall 1997) following the extensive glaciation over Gondwana during the Asselian. The early Wuchiapingian experienced a warm period (Mertmann 2003) followed by a cooling trend which continued into the Changhsingian (Kidder & Worsley 2004).

The desert conditions of the Rotliegend are a prominent feature of the early Lopingian Zechstein environment. The subsequent transgression from the Boreal Ocean into the Southern Permian Basin which created the Zechstein Sea initiated climatic influence in the region. The initial Zechstein transgression is known to have occurred during a 'wet phase' referred to as the 'Upper Rotliegend–Zechstein wet phase' (Roscher & Schneider 2006). Zechstein deposition is though to have ended coincident with a strong increase in humidity and freshwater discharge at the onset of the Buntsandstein marked by a significant increase in fluvial input into the basin (Bachman & Kozur 2004; Hug & Gaupp 2006). Periodic glacio-eustatic sea-level change, may have controlled the marine incursions from the Barents Sea into the Zechstein Basin (Ziegler 1990). High evaporation rates and the mega-monsoons typical of Permian times may have facilitated the development of the smaller basin centre ZS4-7 Zechstein evaporites (Stollhofen *et al.* 2008; Szurlies 2013).

The early Zechstein is thought to have had a cool-temperate climate (Peryt *et al.* 2012). The thick evaporite deposits are interpreted to indicate increasing temperatures and aridity. The absence of palynomorphs from the upper Zechstein has been interpreted to indicate poor growing conditions therefore popular reconstructions depict central-western Europe as being barren and inhospitable (e.g., McKay 2019) with vegetation only being present immediately before and after the initial transgression (e.g., Kustatscher *et al.* 2014).

This interpretation is based on an incomplete fossil record due to 1) a lack of palynological exploration of the upper Zechstein 2) assumptions of extreme climate models that do not account for the effect of repeated wet-dry cycles on vegetation 3) not accounting for the wet-phase/fluvial phase during the uppermost Zechstein-Buntsandstein, and 4) the assumption that terrestrial environments underwent deforestation during the Lopingian (Looy *et al.* 2001; Visscher *et al.* 2004). Finally, the presence of the massive Zechstein evaporites (Figure 11) and a reliance on climate-sensitive lithologies have severely biased reconstructions.

The climate for the Polish Zechstein Basin has been interpreted by Słowakiewicz *et al.* (2009) and can be extended to the rest of the basin. The Zechstein Group was deposited under a largely arid climate (Wagner & Peryt 1997) which facilitated the deposition of thick evaporite sequences during the oldest three cycles PZ1-3. The carbonates from the lower Zechstein were precipitated in seawater

of varying salinity i.e., normal salinity (Zechstein Limestone), or higher salinity (Main Dolomite, Platy Dolomite). The overlying evaporitic series indicates progressive evaporation (Wagner 1994).

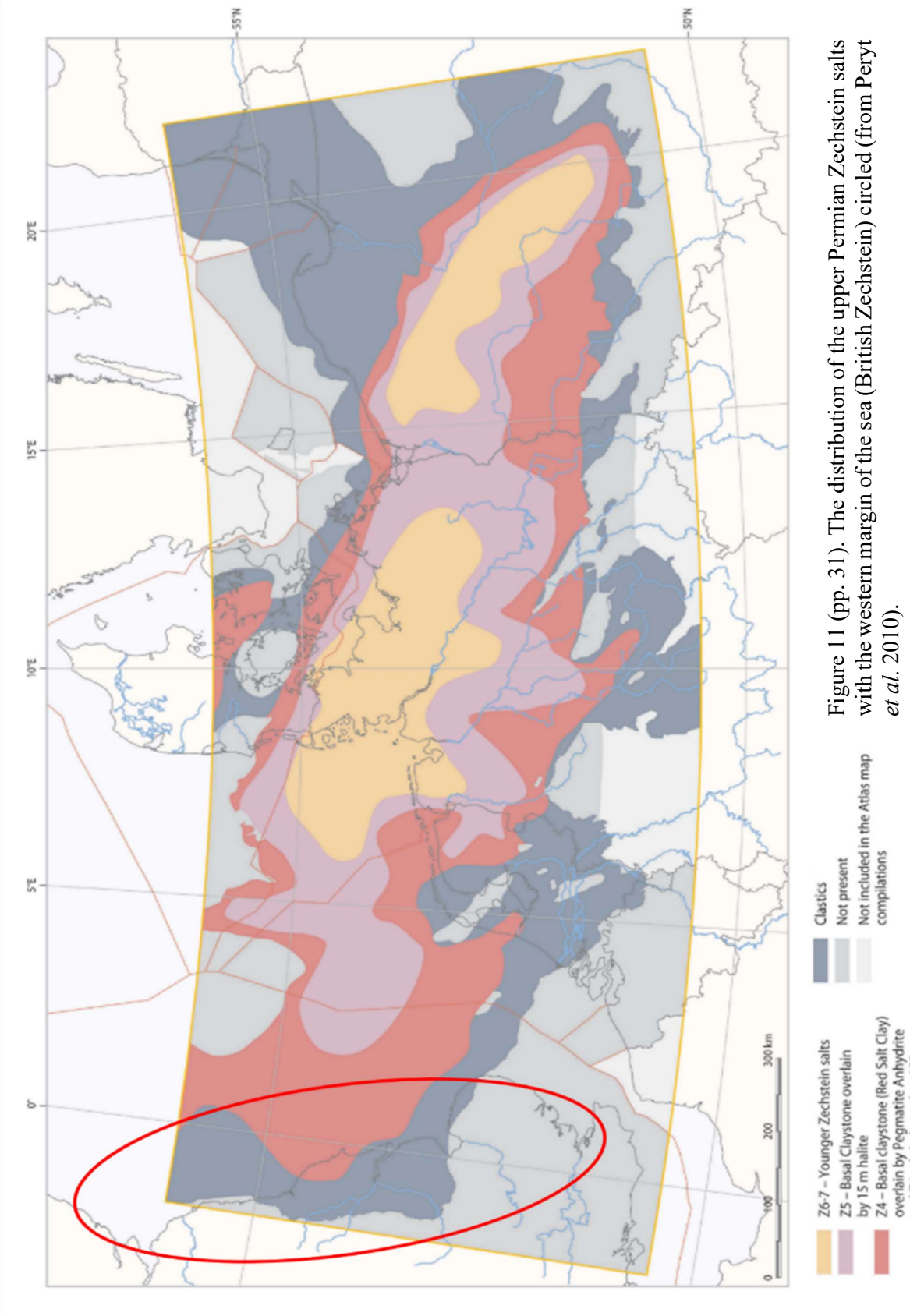

Figure 11 (pp. 31). The distribution of the upper Permian Zechstein salts with the western margin of the sea (British Zechstein) circled (from Peryt *et al.* 2010).

The cycles varied in intensity and duration. The repeated carbonate-evaporite deposition was possible under a stable and dry climate with periods of more and less intense aridity. However, at the end of Z3 there was a change to a more humid climate and the depositional setting shifted accordingly. This was caused by a global regression in sea level during. In the upper Zechstein carbonates disappear and are replaced by a new terrigenous-evaporitic cyclotherm which developed in PZ4/EZ4-5/ZS4-7. Cyclicity became tied to climatic changes of the dry-humid type, not the transgressive-regressive cycles from the lower Zechstein. In the upper Zechstein terrigenous and terrigenous-saline sediments were deposited in humid periods, while during the arid periods rock salt and minimal amounts of anhydrite formed.

The Zechstein Basin was located at mid-latitudes in the northern hemisphere and experienced minimum summer temperatures >15℃ higher than present day (22.4℃), with an average precipitation of 1-2 mm a^{-1} (Kiehl & Shields 2005). Summer temperatures may have averaged <45℃ (Roscher *et al.* 2011). The Pangaean configuration limited environmental moisture flow between humid coastal areas and the continental interiors further driving the hot arid climate (Roscher & Schneider 2006; Roscher *et al.* 2008).

1.6 Palaeophytogeography

1.6.1 Macroflora Provincialism

Phytogeographical provincialism in the Palaeozoic began with the relatively uniform phytogeography of the Devonian and ended with the distinct provinciality of the Permian (Cleal & Thomas 1991). Four phytogeographical provinces demarked Pangaea: Gondwana, Euramerica, Angara and Cathaysia (Figure 12). The provinces are defined by their plant macrofossils and are latitudinally symmetrical (Warrington 1996), with Gondwanan floras occupying southern middle and high latitudes, Angaran floras occupying northern middle and high latitudes, and Euramerican and Cathaysian floras occupying low tropical latitudes.

Cathaysiam tropical rainforests contained arborescent lycopods and sphenophytes, and vine-like gigantopterids (Ziegler 1990). The seasonally wet arid Euramerican province to the west was characterised by a less diverse flora of conifers and pteridosperms. The warm temperate belts of the Angaran and Gondwanan provinces were occupied by high-diversity floras and abundant glossopterid swamps. Diverse communities of herbaceous sphenophytes and deciduous trees occupied cool temperate regions closer to the poles. Colder regions supported a less diverse flora. Tropical forests and equatorial coals existed only in the tropical ever-wet biome of the Chinese (Rees *et al.*, 2002).

In Euramerica during the Cisilurian and Guadalupian, the coal forests declined due to increasing temperatures and aridity (DiMichele & Hook 1992; Rees *et al.* 2002). Gigantopterids, pteridosperms and sphenopsids decreased in abundance while ginkgophytes and conifers increased. Many conifers became extinct at the end of the Permian, such as the glossopterids and cordaites but the extent of global deforestation is unclear (Novak *et al.* 2019).

Throughout the Permian there was a major replacement of arborescent lycopods by arborescent tree ferns, with arborescent lycopods only remaining into the Guadalupian in China. By the beginning of the Permian the arborescent sphenophytes (horsetails) had already declined but during the Permian many new groups of seed plants emerged, such as the cycads, ginkgophytes, voltzialean conifers and glossopterids - important biomarkers for the Gondwana floral province. By the Lopingian approximately 60% of all land plants were seed plants (Gradstein & Kerp 2012). The PTME played an important role in setting the stage for the later dominance of a lycopsid flora during the Triassic (Galfetti *et al.* 2007; Ware *et al.* 2015).

1.6.2 Permian Palynology

The palynology reflects the large-scale evolutionary changes in land plants during the Permian. Palynomorph assemblages broadly correlate with their floral provinces (Hart 1970), but contemporary air circulation patterns led to 'mixed' floras in transitional zones between provinces.

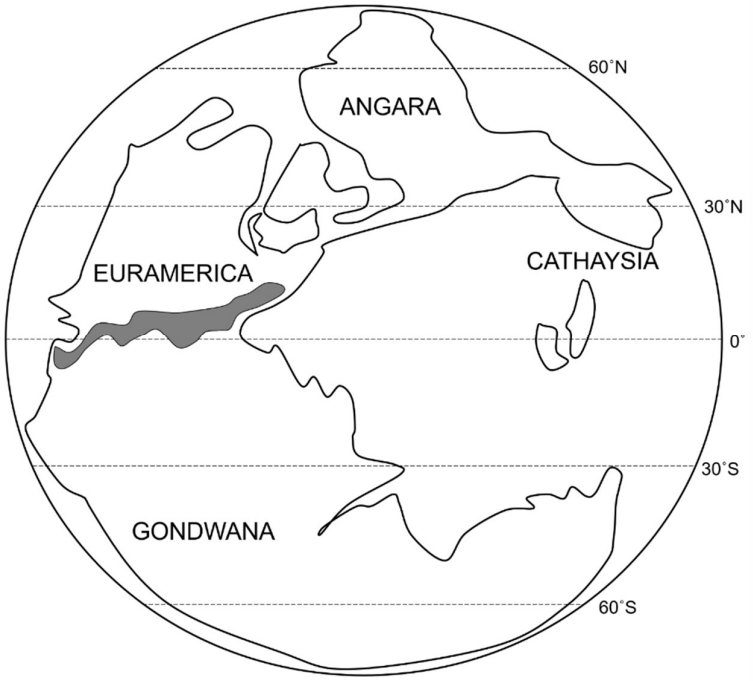

Figure 12. The palaeogeographical provinces of the Permian (redrawn from Rees *et al.* 2002).

These zones contain 'bridging taxa' which are palynological features shared between neighbouring provinces (Stephenson 2016). *Scutasporites* sp., *Vittatina* spp., *Weylandites* spp. and *Lueckisporites virkkiae* are used for Euramerican-Angaran correlations and *Vittatina* spp., *Weylandites* spp. and *Lueckisporites virkkiae* are used for Euramerican-Gondwanan correlations (Stephenson 2016). The PTME is marked by two widespread palynological events that signal extinction: an 'algal-fungal event' which is a bloom of *Reduviasporonites* spp. and acritarchs in marine environments (Eshet *et al.* 1995; Looy *et al.* 2001; Kar & Ghosh 2018; Rampino & Eshet 2018), and a 'spore-spike' (Schneebeli-Hermann *et al.* 2015).

Correlation between plant macrofossils and palynomorphs is expected as they are biologically linked (Hart 1970). However, this is not necessarily the case as 1) polymorphs are distributed much more widely than their parent plant macrofossils 2) different plant groups have different reproductive outputs 3) palynomorphs with similar morphology may be produced by multiple unrelated plants groups 4) or the same plant group may produce a variety of pollen morphologies as a result of ontogeny, or mutation, yet have been classified separately (Chaloner 2013) and 5) taphonomic factors effect plant macrofossils and palynomorphs differently (Utting & Piasecki 1995). How representative a palynomorph assemblage is of its parent flora is further complicated by many unknown Palaeozoic pollen-parent plant affinities (Chaloner 2013) meaning botanical and palynological taxonomies are largely independent. However, the broad characteristics of a palynological assemblage can be taken to represent the palaeobotanical characteristics of a parent vegetation (Stephenson 2016).

Euramerican palynology is relatively understudied compared to Gondwanan palynology, which has received more attention (Bharadwaj & Tiwari 1964; Dijkstra 1972; Pant & Mishra 1986), in part due to the rich coal deposits in Gondwana (e.g., Götz *et al.* 2018). Gondwana is the most unique of the provinces with its glossopterid *Glossopteris* flora (Cleal & Thomas 1991). Its palynology is similarly distinct and dominated by taeniate bisaccate, monosaccate pollen, and the endemic genera e.g., *Guttalapollenites*, *Microbaculispora*, *Dulhuntyispora* and *Corisaccites* (Truswell 1980). Although there are many distinct features of the Gondwana flora, mixing occurred along the province boundaries with Euramerica and Cathaysia (Kar & Jain 1975; Kaiser 1976; Archangelsky & Wagner 1983; Eshet 1990; Nader *et al.* 1993*a*, *b*). Following continental de-glaciation, the Gondwanan flora came to dominate peat and non-peat accumulating wetlands (Prevec *et al.* 2010), persisting through to the earliest Triassic (Lindström & McLoughlin 2007).

Angaran palynology reflects its cool-temperate flora composed of diverse herbaceous sphenophytes and cordaites (Utting & Piasecki 1995). It is characterised by abundant trilete spores rather than bisaccates (Hart 1970). Monosaccate pollen e.g., *Cordaitina* is common in the Cisilurian while monocolpate pollen e.g., *Cycadopites* is common in the Lopingian (Stephenson 2016).

Cathaysian flora is distinguished by its gigantopterids, neoggerathialean-like progymnosperms and cycad-like plants. Lycopsids, sphenophytes and pteridosperms were also present (Cleal & Thomas 1991). The Cisilurian floras of Cathaysia are similar to the Pennsylvanian floras of Euramerica (Kaiser 1976) so it is possible that Cathaysia acted as a refuge for Euramerican Pennsylvanian swamp vegetation. There are endemic species of *Nixispora* and *Patellisporites* found only in Cathaysia (Utting & Piasecki 1995). This flora disappeared during the PTME (Yu *et al.* 2015) with the rapid disappearance of *Gigantopteris* recorded in various Permian-Triassic transitional beds. The gymnospermous flora was replaced by a rapidly growing lycopsids and ferns (Chu *et al.* 2016).

1.6.3 Euramerican Palynology Highlight

There has been a distinct lack of palynostratigraphic work on the Permian in the type area of the southern Urals since the 1980s. Hart (1970) and Warrington (1996) have summarised prior publications previously published in Russian, but this work was based regionally and not composed into a palynostratigraphic scheme because other ammonoids and fusulinacean foraminifera already provided sufficient resolution for stratigraphic subdivision (Stephenson 2016).

Asselian palynology of the Urals has been studied by Inosova *et al.* (1975) and Faddeeva (1980), the Sakmarian, Kungurian and Kazanian (Roadian) by Hart (1970) and Faddeeva (1980). Utting *et al.* (1997) compared the Ufimian (Kungurian) and Kazanian of the Russian Platform with the sub-Angaran biozones of the Canadian Arctic. No Tatarian palynomorphs were recovered. The lower Tatarian was studied by Gomankov (1992) and the Tatarian (Capitanian, Wuchiapingian, Changhsingian) and Kazanian by Gomankov *et al.* (1998).

Areas west of the Urals from the Cisilurian onwards were deposited in restricted basins therefore correlating them with similarly aged beds in Europe is difficult. Guadalupian European assemblages are rare, but Lopingian rocks in western Europe have been more heavily studied (Grebe & Schweitzer 1962; Schaarschmidt 1963; Clarke 1965; Smith *et al.* 1974). A trend towards impoverishment in the upper parts of the Lopingian has been reported (Pattison *et al.* 1973) but this may be a taphonomic or sampling bias, or an effect of the PTME.

While there have been several noteworthy studies of the European Lopingian, e.g., Klaus (1963), Schaarschmidt (1963) and Clarke (1965), those covering possible palynostratigraphic subdivision are less common. Recent studies of European Thuringian sedimentary rocks have focused on environmental reconstructions e.g., Bercovici *et al.* (2009) or the nature of palynological responses to the PTME (Looy *et al.* 2001; Twitchett *et al.* 2001; Spina *et al* 2015). There are only a small number of publications from North America on taxonomy from the Guadalupian and Lopingian

published during the 1960s and 1970s e.g., Wilson (1962 *a, b*), Jizba (1962), Tschudy & Kosanke (1966) and Clapham (1970).

1.7 Review of the Zechstein Fossil Record

The Zechstein sequence yields a variety of flora and fauna from both marine and terrestrial environments of which a full list can be found in Appendix A.

1.7.1 Marine Biota

The Zechstein Sea provided an extreme and unusual habitat. The marine biota of Cycle 1 is well described both in terms of trace fossils and macrofossils e.g., the ichnological remains in the bioturbated carbonates of Cycle 1 in the U.K. (Cadeby Formation, Sprotbrough Member) (Kaldi 1986), the stromatolite reefs of the Cycle 1 Trow Point Bed (Smith 1986) and the various accounts of the diverse reef fauna described from across the basin especially in County Durham (e.g., Hollingworth & Pettigrew 1988).

Early observations of the biota of Cycle 1 in northeast England were made by Winch (1817) and Sedgwick (1829), followed by the more comprehensive works of Howse (1848, 1858), King (1848, 1850), and Geinitz (1861). Other early studies include Kirkby (1857-1866) and Trechmann (1945). More recently, the marine fauna of Durham was studied by Logan (1962, 1967), bryozoans by Southwood (1985), their palaeoecology by Hollingworth (1987) and gastropods by Hollingworth & Baker (1991). The microfauna has been studied, with ostracods by Robinson (1978) and Pettigrew *et al.* (1980), conodonts from Yorkshire by Swift (1986), and foraminifera by Pattison (1981).

1.7.1.1 Reef Fauna

The Zechstein reefs were an important habitat for marine organisms during Zechstein Cycle 1 and Cycle 2 with barrier reefs located at the platform edge or on the many intervening highs located within the basin. The reef biota appears to be similar across the basin, composed of the same reef-building organisms e.g., stromatolite and bryozoan (Peryt *et al.* 2012). Well-described reef complexes of the Raisby Formation in County Durham provide an insight into the reef biota from Cycle 1 (Hollingworth & Pettigrew 1988). Other reef sites in the region have been preserved but are less diverse and rich in marine life such as the stromatolite reefs in Sunderland.

The Cycle 1 reef biota was dominated by brachiopods, gastropods and bivalves (Hollingworth & Pettigrew 1987). Coquinas are composed of the brachiopod species *Strophalosia morrisiana*,

Horridina horrida and *Pterospirifer alatus* but most basinal rocks contain no benthic fauna, and instead contain sparse remains of nektonic fauna (Smith 1989). Little is known about the marine biota of evaporative phases, but the diminished dwarf biota in the upper part of the Raisby Formation and the smaller size gastropods of later cycles (Smith *et al.* 1986) suggest that these are the effects of increasingly poor marine conditions, and it is likely that these effects became more pronounced throughout the Zechstein. The biota likely became increasingly impoverished, with smaller population sizes and a higher proportion of dwarf forms, until conditions became too harsh for organisms to persist. Once normal marine conditions returned the reefs would be recolonised, perhaps with organisms migrating in from the Northern Permian Basin or from further north in the Boreal Ocean (Sørensen *et al.* 2007). Eventually the fauna disappeared.

Foraminifera are common and are represented by five groups: Ammodiscids, Nodosariids, Taxulariids, Astohizids and Disherinids (Pattison *et al.* 1973). The foraminiferal diversity in the contemporary Palaeo-Tethys was significantly higher (Lei *et al.* 2013) reinforcing a picture of a relatively impoverished Zechstein foraminiferal population. Foraminifera are rare in the British Zechstein with only a few documented examples (Pattison 1981).

The bryozoan species *Fenestrella retiformis* and *Syocladia vergulaceae* are common within the Raisby Formation (Hollingworth & Pettigrew 1987) of Cycle 1 and echinoid fragments are widespread. Crinoids are represented by the single species *Cyathocrintes ramosus*; polychaetes by *Vermilia obscuria*; and scaphopods by the genus *Dentalium*. All are reported from the northeast of England (Eden *et al.* 1957; Donovan *et al.* 1986). The northwestern European conodont genera *Ellisonia* and *Merrillina*, and one nautiloid species *Peripetoceras freislebenii* (endemic to the Raisby Formation) have also been reported from the lower Zechstein reefs of County Durham (Hollingworth & Pettigrew 1987).

1.7.1.2 Fish

Fish are relatively rare in the British Zechstein yet are widespread and varied in the Marl Slate despite the heterogenic inhospitable anoxic and euxinic conditions during deposition. Most are freshwater species which likely lived in a thin freshwater surface layer in nearshore lagoons (Legler *et al.* 2005). These include fusiform palaeoniscoids, coelocanths, and the shark *Wodnika striatula* (Smith *et al.* 1973; Pattison *et al.* 1973; Diedrich 2009).

The same fish species are recovered from the Kupferschiefer in Germany e.g., *Acrolepidae* (Schaumberg 1996; Diedrich 2009). In the U.K., Zechstein fossil fish have been found in the Marl Slate of Durham from Middridge Quarry, Eppleton Quarry and Quarrington Quarry (Dineley &

Metcalf 2007). Fish were diverse and abundant, preserved in fine-grained, flaggy rock where the specimens are well-preserved and flattened on individual laminae. The fish from Middridge Quarry appear to have been nearshore species that fed on soft aquatic vegetation, such as *Doryopteris hoffmani*, or shellfish, such as members of the *Platysomus* group based on their dentition.

However, the most common Marl Slate fish are the 'palaeoniscoid' early actinopterygians belonging to the family Palaeoniscoidae (Figure 14). These fish may have lived among masses of shoreline vegetation in the water to shelter from predators (Westoll 1934). Larger predators would have been rare, but *Coelocanthus granulatus* with its wide gape would have been a powerful predator. Similarly, *Pygopterus humboldti* was relatively large and predatory. The chondrycthians were relatively small. *Wodnika striatula* likely predated upon arthropods, while *Janassa bituminous* was a benthic durophagous petalodont (Malzahn 1986). Based on analysis of the Kupferschiefer fossil fish assemblages from Germany (Schaumberg 1978) it is likely that the actinopterygians and coelacanth were apex predators.

1.7.1.3 Lopingian Phytoplankton

Lopingian acritarchs were reviewed by Lei *et al.* (2013) and have a higher taxonomic diversity than Guadalupian assemblages as Lopingian acritarchs are more thoroughly studied. Changhsingian and Permian-Triassic boundary acritarchs have been studied in China (Ouyang 1982, 1986; Ouyang & Utting 1990), Europe and Africa (Jekhowsky 1961), Pakistan (Sarjeant *et al.* 1970), the Canadian

Figure 14. A palaeoniscoid fish cf. *Palaeoniscus freislebenii* Blainville from the Marl Slate of Crime Rigg Quarry County Durham (specimen collected 1976 and donated by P. Gibson).

Arctic Islands (Utting 1978), Kenya (Hankel 1992), and Antarctica (McLoughlin *et al.* 1997). Acritarchs have also been studied in Lopingian rocks lacking precise stratigraphical assignment in e.g., Antarctica (Farabee *et al.* 1991; Lindström 1996), Germany (Schaarschmidt 1963), Israel (Horowitz 1973; 1974), the Karoo region (Horowitz 1990; Dypvik 2001), Australia (Balme & Segroves 1966; McMinn 1982; Fielding & McLoughlin 1992), India (Tripathi 2001), and Pakistan (Hermann *et al.* 2012).

British Lopingian acritarchs have been recovered from the Lower Permian Marls of Ashfield Brick Pit, Conisbrough, Yorkshire (Wall & Downie 1963). Both globose, subpolygonal, and polygonical forms were described. Those with spherical tests resemble Jurassic *Michystridium stellatum* forms (Valensi 1953; Sarjeant 1962), Devonian and Silurian specimens (Stockmans & Willière 1960) and Mesozoic specimens of *Michystridium*. Polygonal forms are attributable to *Veryhachium.* These assemblages are composed of long-ranging species which only differ slightly form counterparts from earlier and later horizons. Larger, more distinctive, forms from the Lower Palaeozoic and Mesozoic are notably absent (Wall & Downie 1963).

1.7.2 Terrestrial Biota

1.7.2.1 Terrestrial Vertebrates

Tetrapods are well known from the Lopingian of Europe and the tetrapod *Lepidotosaurus duffi* is characteristic of the Zechstein sequence (Pattison *et al.* 1973) but it is unclear whether it is a reptile or amphibian. Small to medium sized reptiles and amphibians are found in the Marl Slate and Kupferschiefer including *Coelurosauravus* and *Protorosaurus speneri,* and possibly the diapsid *Adelosaurus huxleyi* (Evans & King 1993). The dicynodonts *Geikia* and *Gordonia* along with the cynodont *Procynosuchus* (Evans & King 1993) are found. Tetrapod footprints are preserved in the Cadeby Formation of Nottingham and belong to a small reptile or amphibian, possibly *Celichnus hicklingi* or *Rhynchosauroides* sp. (Benton *et al.* 2002).

1.7.2.2 Terrestrial Invertebrates

There are no records of terrestrial invertebrates from the British Zechstein barring reports of rare arthropod cuticle recovered from strew mounted palynological preparations from the Cadeby Formation (A. Askew unpublished MBiolSci dissertation) which further suggests the vegetation was substantial enough to support arthropod communities.

1.7.3 Review of Zechstein Palaeobotany

Early descriptions of the Zechstein flora were based on gross morphology (e.g., Waldin 1778; Sclotheim 1820; Bronn 1828; Göppert 1850; Geinitz 1861). Solms-Laubach (1884) was the first to describe the details of any internal anatomy, and the first to combine anatomical observations with gross-morphological data. Gothan & Nagalhard (1922) were the first to include cuticle as a source of anatomical information, while Schweitzer (1962, 1963) was the first to combine morphological and cuticular studies with the anatomical analysis of permineralized specimens from the Lower Rhine area. These contributions significantly enlarged the understanding of the Zechstein vegetation, but the differential preservation of specimens means their conspecificity cannot be proven. Therefore, the biological significance of many of these findings cannot been fully accepted.

British Zechstein palaeobotany was first described by Stoneley (1958) and Schweitzer (1986), with limited study since. Zechstein plant macrofossils are found in multiple preservation modes reviewed by Uhl & Kerp (2002) from German Zechstein plant localities. These include permineralizations (pyrite (chalcopyrite), calcite), compressions (coalified compressions, cuticles, "mummified" leaves, impressions), authigenic preservation, and charcoal.

The current accepted view is that vegetation was restricted to the earliest Zechstein cycle, primarily Cycle 1. Flora across the basin shows the same basic composition (Schweitzer 1986; Haubold & Schaumberg 1985; Uhl & Kerp 2003; Kutstatcher *et al.* 2014). This results from the variation caused by local factors at basin margins being overridden by the main structural controls on marine sedimentation which were approximately the same and shared throughout the basin. Therefore, patterns of sedimentation and the biotas occupying many of the sub-basins created near-uniform conditions. Similarities in geometry, lithology, sedimentology, and biota of the various separate Zechstein sequences has allowed for reasonable correlation between the first three cycles in England with northern Germany and the Netherlands (Smith 1989).

The assumption of a vegetation confined to the earliest Zechstein is flawed and based on an incomplete fossil record. Both the macro- (Weigelt 1928, 1930; Stoneley 1958; Ullrich 1964; Schweitzer 1960, 1986; Uhl & Kerp 2002; Bödige 2007; Bauer *et al.* 2013) and microfossil records (e.g., Clarke 1965; Visscher 1971, 1972; Warrington & Scrivener 1988; Legler *et al.* 2005; Legler & Schneider 2008; Warrington 2005, 2008) are essentially restricted to the earliest Zechstein with only rare reports from Cycle 2 (Pattison *et al.* 1973). Vegetation is assumed to thrive during and after the initial transgression but disappear shortly after as the environment becomes harsher.

Early studies of the German and British Zechstein have demonstrated the similarity between palynological and macrofossil assemblages across the basin. Zechstein plant macrofossils were

heavily studied during the latter half of the nineteenth century, with more recent studies (Madler 1957; Schweitzer 1960, 1968; Ullrich 1964; Tyroff 1966) corroborating these findings. Macrofossils from England (Stoneley 1958; Schweitzer 1986), Poland (Czarnocki 1965), Belgium (Florin 1954) and the Netherlands (Jongmans 1954) have also been described.

The Zechstein flora is known to be composed of the following plant macrofossil species which have been described from the Zechstein and reviewed by Schweitzer (1986): *Neocalamites mansfeldicus* (Plate 2f), *Sphenopteris dichotoma*, *S. patens* , *S. geinitzi*, *S. kukukiana*, *Callipteris martinsi*, *Taeniopteris eckardti*, *Pseudoctenis middridgensis*, *Plagiozamites bellii*, *Sphenobaeria digitata* (Plate 2d), *Pseudovoltzia liebeana* (Plate 2a-c), *Ullmannia bronni* (Plate 1f), *Ullmannia frumentaria* (Plate 1a-e), *Culmitzschia florini*, and *Rhenania reichelti*.

Taxa worth highlighting are *Callipteris martinsii* which occurs at all Zechstein plant localities (Schweitzer 1986), *Taeniopteris eckardti* which is found only in Germany (Schuster 1933) and Middridge Quarry, England, (Stoneley 1958), and *Pseudoctenis middridgensis* and *Plagiozamites bellii* (synonym: *Durhamia belii*) (Pl. 3, e-f) which are also only known from Middridge Quarry (Stoneley 1958). *Sphenopteris geinitzi*, *Quadrocladus solmsi*, *Q. orbiformis*, *Culmitschia florini* and *Rhenania reichelti* are only known from the German Zechstein (Schweitzer 1986). Individual branches of coniferous (Plate 3d; Plate 4h), ginkgophyte (Plate 3c), and sphenophyte (Plate 2e) affinity, coniferous cones (Plate 2g), cone scales (Plate 3a-b), seeds (Plate 4a-c), and individual leaves (Plate 4d-h) have also been found. Plates can be found in Appendix B.

The British Zechstein flora was divided into two types by Schweitzer (1986): a hydrophilic *Neocalamites*-Sphenopterid association inhabiting lowland area, and a xerophytic *Callipteris*-conifer association inhabiting well-drained upland areas. However, this grouping may not actually representative of the plant's habitats. It may represent wetter-transgressive or drying-regressive phases of Zechstein cyclicity, and the degree to which communities are affected by sea level rise and the increase in taphonomic window area. This segregation of floral types represents extremes, but intermediary floras are expected.

1.7.4 A Review of Zechstein Palynology

Euramerican palynology changed in response to Permian climate trends. The Guadalupian palynoflora is similar to that of the Cisilurian with some minor differences. For example, in the Urals only the presence of *Vittatina* distinguishes the Guadalupian from the Cisilurian (Warrington 1996). Palynofloras are relatively more abundant in the upper Guadalupian with taeniate bisaccate pollen, monocolpate pollen, and monosaccate pollen forming a larger proportion of assemblages. Spores are

more common and occur in slightly higher abundances during the Cisilurian and *Lueckisporites virkkiae*, *Taeniaesporites* and *Vesicaspora* appear. In the Perm region numerous representatives of *Cordaitina, Vittatina*, *Protohaploxypinus*, and *Striatopodocarpites* have been recorded alongside an increasing number of non-taeniate bisaccate pollen (Hart 1969). This pattern can be seen in the Urals, however monosaccate pollen and monocolpate pollen are scarcer (Hart 1970). Assemblages from the Pechora region are dominated by bisaccate pollen and taeniate bisaccates such as *Protohaploxypinus*, but *Vittatina* is rare (Variakhuna 1971).

A shift in the dominance of plant groups is reflected in palynological changes within the Guadalupian. In the Urals, bisaccate pollen such as *Striatopodocarpites* and non-taeniate forms increase in abundance. *Vittatina* increases in abundance and *Lueckisporites* appears. *Lueckisporites virkkiae* is a typical Zechstein palynomorph (Stephenson 2016*)*.

Lopingian assemblages resemble Guadalupian assemblages in that they also contain *Striatopodocarpites*, *Protohaploxypinus* and *Vittatina* as well as other taeniate bisaccate pollen. These taxa dominate lower parts of Lopingian sequences but monocolpate pollen achieves similar abundances in upper parts (Hart 1969, 1970). Assemblages in the Pechora region are dominated by bisaccate pollen but *Vittatina* is absent (Variakhuna 1971). Forms similar to *Lueckisporites virkkiae* have also been documented (Kiuntzel 1965).

Lopingian miospores from western Europe, Israel and the U.S.A., being at lower latitudes, are only slightly comparable to those from the type area. Bisaccate pollen is much more dominant. *Lueckisporites virkkiae* is characteristic of these assemblages and occurs in association with *Lunatisporites*, *Protohaploxypinus*, *Striatopodocarpites*, and rare *Vittatina*. Non-taeniate taxa assemblages include *Alisporites*, *Falcisporites*, *Klausipollenites* and *Jugasporites*. However, these are scarce and spores and monosulcate pollen are rare (Warrington 1996).

Evidence of wildfires can be found in the charcoal content of Upper Permian sediments collected from the Frankenberg-Geismar locality in northwest Hesse, Germany (Uhl & Kerp 2003), important for its largely pyritised plant remains (Waldin 1778; Bronn 1828; Göppert 1850; Solms-Laubach 1884; Poort & Kerp 1990; Uhl & Kerp 2002). Since the Zechstein flora grew under mesic to xeric conditions wildfires may have been a semi-regular occurrence, more regular than in comparable modern ecosystems (Paysen *et al.* 2000). Due to the allochthonous nature of the charcoalified material it is not possible to determine the frequency of wildfire events nor is it possible to determine their cause. Decomposition of leaf litter and wood under the Zechstein arid climates would have led to the accumulation of a substantial amount of potential fuel (Harrington & Sackett 1992). There is no evidence of wildfires in the form of inertinite in British Zechstein material.

Palynological studies reveal a uniform palynoflora suggesting the vegetation was also uniform. Minor differences between regions are likely due to chronostratigraphically significant regional vegetation development (Visscher 1967). Thirty-three different pollen and spore species have previously been described accompanying twenty-five plant macrofossil species (Clarke 1965a). Assemblages are composed of taeniate bisaccates, non-taeniate bisaccates, rare multisaccates, monocolpates and spores.

The palynology of the Zechstein in western Europe is well-described. Assemblages have been described by Klaus (1954, 1955, 1963), Leschik (1956), Grebe (1956), Orłowska-Zwolinska (1962), Grebe & Schweitzer (1962), and Schaarschmidt (1963). Publications authored and co-authored between the 1980s and early 2000s by G. Warrington (Edwards *et al.* 1997; Warrington & Scrivener 1988, 1990; Warrington 2005, 2008) form the basis of recent palynological study of the British Zechstein.

There have been limited attempts to investigate the palynoflora of the evaporative phases. Permian salts are known to have a high preservation potential for organic matter (e.g., works by K. Benison, Cockell *et al.*, 2020) and fossil material including the recovery of cellulose microfibres from the Salado Formation in New Mexico (Griffith *et al.* 2008).

1.7.5 Early Research on the Zechstein Palynology

The first palynological studies on the Zechstein were performed on German material (Klaus 1955; Leschik 1956; Grebe 1957). These were followed by more general studies from across Germany (Grebe & Schweitzer 1962; Loffler & Schulze 1962; Malzahn & Rabitz 1962; Schaarschmidt 1963; Sauer 1964; Trusheim 1964; Ullrich 1964; Mosler 1966; Schulz 1966). Polish Zechstein palynology was recorded by Orłowska-Zwolinska (1962), Kłosowska & Dowgiałło (1964) and Kotanska & Krason (1966). British Zechstein assemblages and their equivalents, the Irish and Bakevellia seas, were described by (Hughes *et al.* 1964; Clarke 1965a; Visscher 1971; Smith *et al.* 1986) and there is limited information from the Netherlands (Visscher 1967)**.** These early studies show that Zechstein assemblages are dominated by bisaccate pollen grains belonging to the species *Lueckisporites virkkiae*, *Klausipollenites schaubergeri*, *Limitisporites rectus*, *Labiisporites granulatus* and *Falcisporites zapfei* and *Nuskoisporites dulhuntyi* (Visscher 1967).

1.7.6 British Zechstein Palaeobotany and Palynology

The first major review of British Zechstein flora was undertaken by Stoneley (1958) in her review of the British Upper Permian flora. This publication summarised the then current knowledge on the scarce flora of the Upper Permian beds of northern England from specimens found previously in the literature. Twenty-four plant species were described, the majority of which were already known from the German Zechstein. Exceptions to this are *Hiltonia rivuli* (synonym of *Ullmannia bronni*) (Schweitzer 1986) and *Pseudoctenis middridgensis* which are endemic to the British Zechstein. Stoneley also hypothesised that the Marl Slate and Kupferschiefer were not contemporaneous based on the *Lueckisporites* biozonation, which to her suggested that the Kupferschiefer was deposited before the Marl Slate.

To date, the most comprehensive taxonomic review of British Zechstein palynology is Clarke (1965a). He reviewed the saccate and monosulcate miospores of Permian from the Hilton Beds, Kimberley and the Haughton Hall Boring in Nottinghamshire. He reported that the assemblages were dominated by taeniate bisaccate pollen with an overwhelming dominance of two genera: the bitaeniate bisaccate pollen grain *Lueckisporites virkkiae* and two species of the multi-taeniate bisaccate pollen *Taeniaesporites labdacus* and *T. noviaulensis*. This is unsurprising as *L. virkkiae* is a biomarker species for the Zechstein and deposits of equivalent age (e.g., Italian alps (Clement-Westerhof 1987); Stephenson 2016). Clarke reported that the most common non-taeniate pollen species were *Klausipollenites schaubergeri, Falcisporites zapfei, Labiisporites granulatus* and *Illinites delasaucei*. Monosaccate pollen were rare and represented by *Perisaccus granulosus, Perisaccus lanciniatus, Potoniesporites novicus, Vestigisporites minutus* and *Nuskoisporites dulhuntyi*. Monosulcate pollen was only represented by the single species *C. rarus*. Clarke hypothesised that the observed similarity in assemblages was a consequence of a relatively uniform vegetation throughout the U.K., in accordance with the widely accepted idea of a uniform vegetation along the western margin of the basin. However, it was impossible at the time of publication for Clarke to determine the exact nature of the vegetation cover due to many unknown botanical affinities within the palynological record.

In a companion paper (Clarke 1965b), some of these issues were addressed for the palynology of the British Keuper, but many affinities remain unknown. Schweitzer (1986) also addressed some of the botanical affinities. Of great significance is his description of an *Ullmannia frumentaria* cone, from which approximately ten morphologies of *Illinites*-type pollen were recovered, attributed to different stages of ontogeny of the developing pollen grains within the cone. This emphasises the care that must be taken when reviewing the taxonomy of Lopingian Euramerican pollen grains.

Visscher (1971) also reviewed the Permian and Triassic palynology of the U.K., focusing on the Kingscourt Outlier, Ireland, which was contemporary to both the Bakevellia and Zechstein seas. Of the multiple assemblages described Assemblage 1 was found to closely correlate with the Zechstein basin. It was dominated by *Lueckisporites virkkiae*, *Jugasporites delasaucei, Klausipollenites schaubergeri* and *Limitisporites moerensis*. *Perisaccus granulosus* and *Striatoabieites* spp. were minor components. However, typical Zechstein forms such as *Falcisporites zapfei*, *Labiisporites granulatus* and *Striatopodocarpites richteri* were absent.

1.7.6.1 Summary of Recent Work

The most recent work on the British Zechstein (Warrington & Scrivener 1988; Legler *et al.* 2005; Legler & Schneider 2008; Warrington 2005, 2008) has focused on the deposits themselves or those that are correlatable with the Zechstein. For example, the Lopingian of Devon yields poorly preserved gymnospermous pollen grains (Warrington & Scrivener 1988). *Lueckisporites virkkiae, Perisaccus granulosus, Klausipollenites schaubergeri, Jugasporites delasaucei, Protohaploxypinus microcorpus* and *Lunatisporites* spp. are found and are compatible with a Lopingian age. Palynomorphs recovered from the Hilton Borehole, on the Valley of Eden in Cumbria are also equivalent in age to the EZ1 of northeastern England (Jackson & Johnson 1996). It yields the longest continuous section of Permian rocks in the U.K. and it is dominated by miospores. *Crucisaccates* cf. *variosulcatus* and possibly *Proprisporites pococki* were recovered here for the first time, and algal remains may also be present (Warrington 2008).

Thesis outline

Chapter 1-5 of this thesis provide background information for the following 5 research chapters. In Chapter 2 the geological setting of the British Permian and detailed descriptions of each Zechstein cycle are provided. In Chapter 3 the sampling, processing, logging and quantitative methods used are outlined, and details of fieldwork excursions can be found in the appendix. Chapter 4 outlines the different reproductive strategies of plant group and their evolutionary significance alongside transport pathways of different terrestrial palynomorph types. Chapter 5 presents the taxonomy of the palynomorphs recovered from the British Zechstein.

Chapters 6-10 are the main research chapters of this thesis and are written in manuscript format intended for publication. Chapter 6 presents the palynological results from all field locations. A succinct interpretation of the results presented in Chapter 6 can be found in Chapter 7. The novel technique developed for extracting palynomorphs from evaporites is outlined in Chapter 8. Chapter 9 shows how transmission electron microscopy (TEM) can be used to draw conclusions on the botanical affinity of dispersed pollen grains without an affinity based *in situ* evidence. Chapter 10 deals with the first report of unusual spheroidal inclusions of a possible endobiotic fungal nature and is intended for publication. Chapter 11 forms the main conclusion of this thesis, summarising the conclusions of all previous chapters.

Chapter 2. Geological Setting

The geological descriptions used in this chapter are drawn from Smith (1989) and Peryt *et al.* (2010).

2.1 Permian Rocks in the U.K.

2.1.1 Marine Permian Rocks

Marine Permian rocks are distributed across the north of mainland U.K. They occur in two parts, with scattered occurrences in northwest England, but they are more common in northeast England with an almost continuous outcrop that extends from Tynemouth southwards to Nottingham. It is composed of a sequence of mostly dolomitised limestones that thicken progressively eastwards. These limestones are from the basal part of the first three evaporitic cycles of the Zechstein Sea (EZ1-3). To the east they are separated by evaporites and in marginal settings in Yorkshire along the western margin of the sea, and in the North Sea Basin, evaporites dominate the sequence. However, at outcrop the majority of evaporites are absent due to dissolution and the carbonate units are instead separated by erosion or emersion surfaces, often combined with siliciclastic beds or the evaporite dissolution residues. In some instances, the carbonates are affected by large-scale dissolution foundering. The carbonates of EZ2 do not crop out in Yorkshire but can be found in County Durham and Tyne and Wear i.e. the Roker Dolomite.

The British Zechstein Group was deposited in two Sub-basins, one in County Durham in the north and the other in Yorkshire in the south. Correlation of the Durham and Yorkshire Sub-basins (Figure 1) is possible with the Marl Slate and Seaham/Brotherton formations, is also possible for the early EZ1 carbonate formations, and between the EZ2 carbonate formations. However, correlation of the upper EZ1 carbonate units (Ford Formation/Sprotbrough Member of the Cadeby Formation), and the strata that lie between the EZ1 Ford Formation and EZ2 Roker Dolomite Formation in the Durham Sub-basin uncertain.

The rocks exposed in the Durham Sub-basin generally lie farther from the basin margin than those in the Yorkshire Sub-basin. Together, the sequences from the two Sub-basins provide an almost complete transect from a marginal depositional setting near the shoreline, to a more basinal depositional setting below the middle of the basin-margin slope.

2.1.2 Non-Zechstein Marine Permian

There are strata contemporaneous with the Zechstein Group underneath the eastern Irish Sea, and inland in the Solway Firth and south Lancashire/north Cheshire. These represent the eastern portions

of the Bakevellia Sea. This sequence is up to 350m thick at the basin centre (Ebburn 1981; Jackson *et al.* 1987), yet it thins sharply at the basin margins where sequences become condensed and incomplete. Onshore exposures are almost exclusively found in these marginal areas and include intercalations of continental strata that indicate the cyclical migration of shorelines. More detail on the Permian of Cumbria can be found in Arthurton *et al.* (1978), and for a review of the whole Bakevellia basin see Smith (1992).

The Zechstein and Bakevellia seas can be correlated to some degree. Three main cycles and an additional possible fourth cycle have been recognised in West Cumbria by Arthurton and Hemingway (1972), and four possibly equivalent cycles (BS1-4) have been identified in the East Irish Sea Basin (Jackson *et al.* 1987). Cycles BS1-3 of the Bakevellia Sea may correlate with EZ1-2 of the

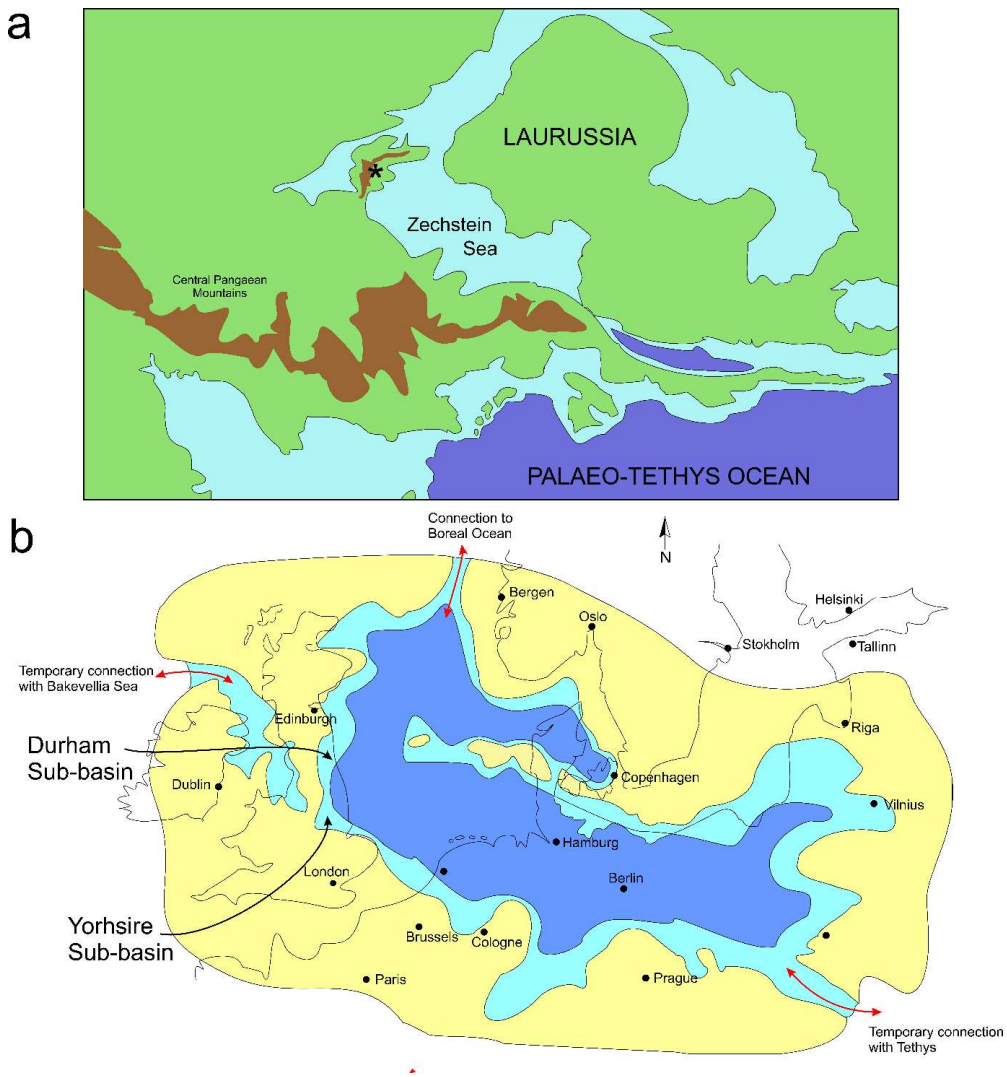

Figure 1. Palaeogeography of the Zechstein Sea a) location of the Zechstein Sea in relation the Central Pangaean Mountains and the Palaeo-Tethys Ocean. The star indicates the study area b) the boundary of the Zechstein depositional area superimposed on the outline of present-day Europe illustrating the location of the Durham and Yorkshire Sub-basins.

English Zechstein Basin (Smith *et al.* 1974; Arthurton *et al.* 1978), and it is possible that cycles EZ3-4 may correlate with the red-beds and basin-centre evaporites deposited by the Bakevellia Sea (Jackson *et al.* 1987; Smith & Taylor 1992).

2.2 The Zechstein Sea

2.2.1 Overview

During the Lopingian and early Triassic of western and central Europe a marine-continental transition accumulated in the intracontinental Southern Permian Basin (SPB) (Figure 1a). The SPB evolved on the former Variscan Foreland during the latest Carboniferous-Cisilurian (Ziegler 1990), with a depositional width of ca. 600km and trends ca. 2,500km WNW-ESE from northeast England, across the southern North Sea, and into northern Germany and Poland (Figure 1b). The SPB itself is delineated by several Variscan Highs including the London–Brabant, Rhenish and Bohemian massifs in the south, and the Mid North Sea, and Ringkøbing–Fyn highs in the north (Ziegler 1990; Geluk 2005; Peryt *et al.* 2010).

Consequently, the Zechstein Group characterises the Permian of central-western Europe. It is dominated by evaporites, is of substantial thickness (>2km) and is encountered and studied in Germany, Poland, the Netherlands, Denmark, Norway and the U.K. (Figure 2) (Glennie *et al.* 2003). The lithostratigraphical relationships between the different Zechstein successions can be found in Figure 2 The Zechstein overlies the non-marine deposits of the Rotliegend Group (Cisilurian) and underlies the Triassic, and in the U.K. is mostly composed of marginal marine deposits. The Zechstein Group extends far to the west on-shore and has been penetrated in mines in Northumberland, Lincolnshire, and Yorkshire (Talbot *et al.* 1982). In the north the Zechstein is delineated by the northern end of the South Viking Graben, and in the south by the northern flank of the London Brabant Massif (Figure 3). From the present-day distribution of the Zechstein salts is interpreted as representing the original depositional extent of the Zechstein; the Northern Permian Basin (NPB) and Southern Permian Basin (SPB). It should be noted that the western margin of the NPB (Fort Approaches Basin) is an exception, where comparatively recent erosion has truncated an extension of the basin in the present-day Scottish mainland.

Stratigraphic correlation between different Zechstein successions is complex, as local lithostratigraphic names are assigned to broadly age-equivalent and compositionally similar units across the basin (Figure 2). This issue is further complicated by the general lack of correlation studies between certain parts of the basin e.g., the U.K. and Norwegian Zechstein, the disturbance of the original stratigraphy by salt tectonics, and the lack of biostratigraphical data throughout the Zechstein.

Despite being dominated by evaporites, the Zechstein Group deposits are quite heterogenous and are also composed of clastics and carbonates (Tucker 1991). The present-day Zechstein salt can create a misleading picture due to how secondary processes can affect their primary depositional composition. Firstly, post-depositional flow is common which makes determining the original stratigraphic structure of the Zechstein Group difficult. Diapirs and pillows have formed because of the mobile nature of halite and potash salts. Secondly, the dissolution of soluble components of the original evaporites has led to the relative enrichment of halite and related non-evaporite lithologies

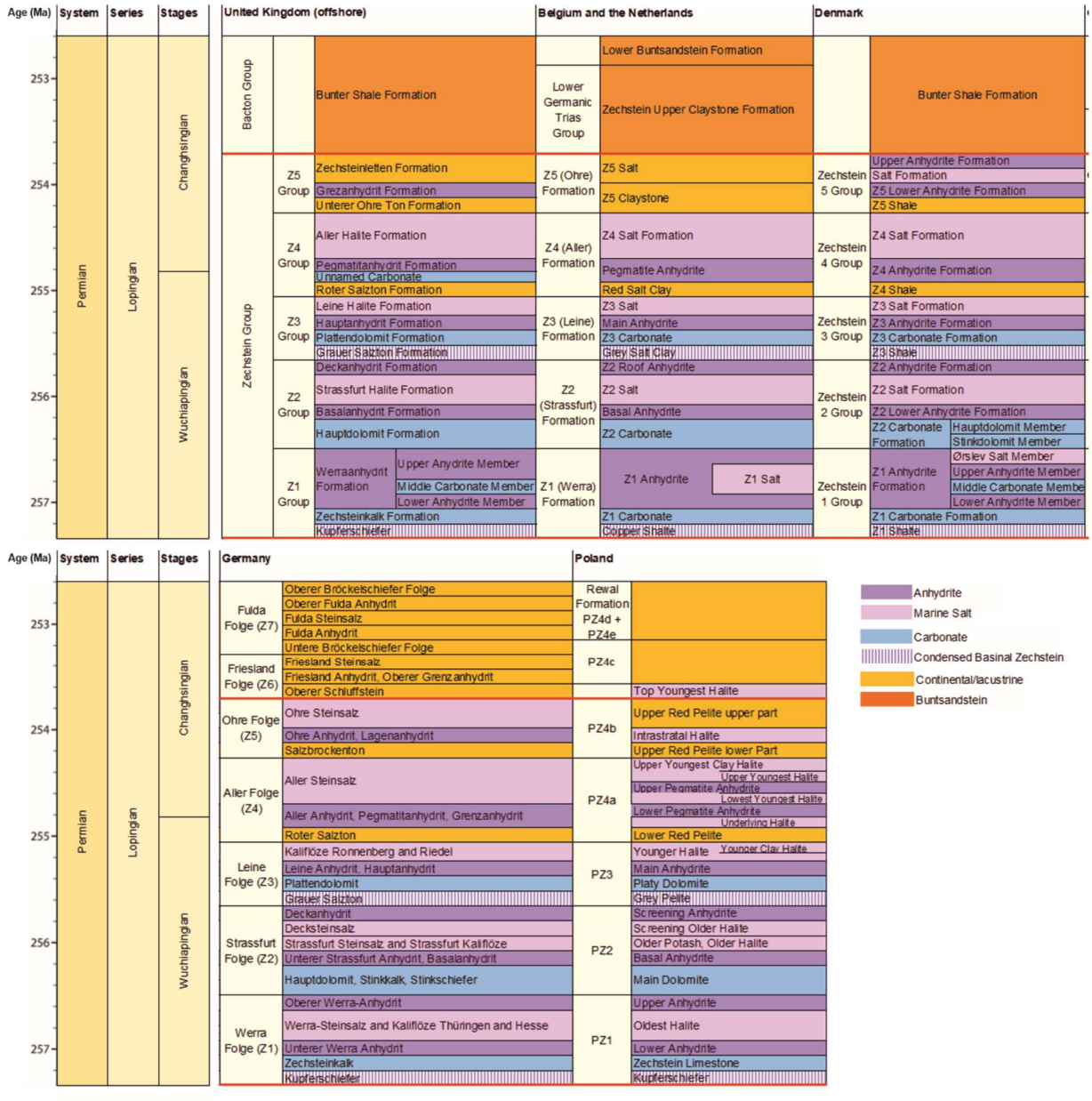

Figure 2. Lithostratigraphic correlation chart for the Zechstein Group, comparing the successions in the U.K. with Belgium and The Netherlands, Denmark, Germany, and Poland. The red lines indicate the base and top of the Zechstein Group (after Peryt *et al.* 2010).

including the carbonates and clastics. Thirdly, the array of well penetrations through the Zechstein is biased towards prospective areas such as the flanks of large diapirs and intra-basin or fault-bounded structural highs due to the preferential accumulation of hydrocarbons against these features. Lastly, the effects of salt tectonics mean there is a disparity in the response of the evaporites at the basin margin and basin centre. The Zechstein Group is relatively immobile at the basin margins as its lithologies are largely non-evaporitic meaning diapiric structures do not develop. However, in central locations where successions are dominated by thick halites the Zechstein is highly mobile.

In the U.K., the Zechstein Group is most developed on the continental shelf. During the Lopingian the SPB was located within desert belt of the northern hemisphere of Pangaea at 10-30°N (Glennie 1983) (Figure 1 a, b; Figure 3). In the U.K. the Zechstein succession is divided into five evaporation-replenishment cycles represented by the now decommissioned group names, the Don Group (EZ1a, b), Aislaby Group (EZ2), Teeside Group (EZ3), Staintondale Group (EZ4) and Eskdale Group (EZ5) (Figure 4). The spatial relationships of these units are illustrated in Figure 5.

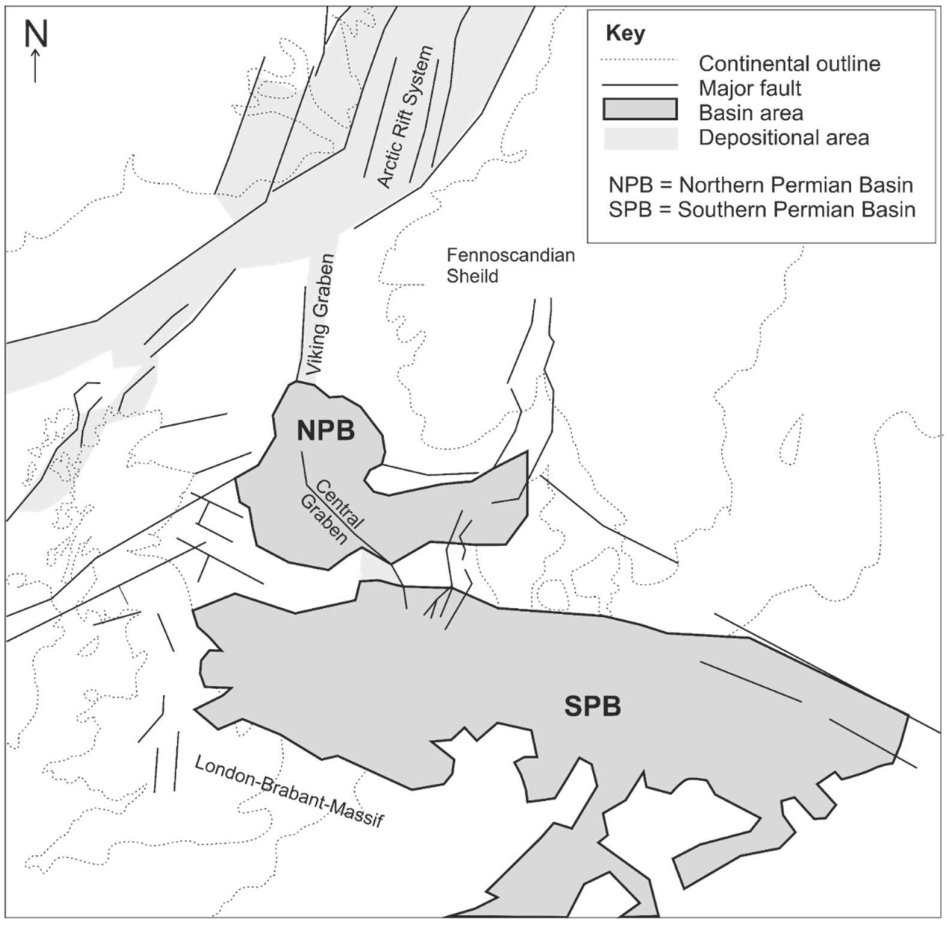

Figure 3. The location of the faults and rift systems that delineate the Northern and Southern Permian basins (modified and adapted from Legler & Schneider (2008)).

2.2.2 Pre-Zechstein/Rotliegend

During the Permian the U.K. lay near the western margin of a large inland drainage basin (SPB), the floor of which lay approximately 250m below world sea level (Smith 1970a, b; 1979; Glennie & Buller 1983; Glennie 1972, 1983). Across the Southern North Sea Basin, and in the U.K., the Rotliegend Group is well-described, and is represented by continental siltstones, and sandstones intercalated with volcanic rocks e.g. the Rotliegend volcanics from the Cisilurian of Germany (Geluk 1999, 2007). The various lithologies are divided up by space and time, influenced by distance from the margin; evaporite-rich successions are thicker in the centre of Sub-basins while non-evaporite lithologies are proportionately more voluminous where successions are overall thinner towards the basin margins or on intra-basinal highs.

The Zechstein marine deposits directly overlie (1) Carboniferous strata in the U.K., which were exposed at the time of the Zechstein transgression. In these areas this breccias formed from patchy residual gravels and thin sandstone lenses that are the remains of migrating sand dunes there were submerged during the transgression. Here the pediment surface is generally smooth and flat to gently rolling but in places is rounded tabular hills up to 150m high e.g., beneath Teeside and northernmost Yorkshire (Taylor 1974); (2) firmly cemented grey and multi-coloured sandy breccia of a uniform thickness of <2m with local thickenings of up to 10m. The breccia is composed of granular pebble clasts of more resistant Carboniferous rock. These breccias are interpreted as residual piedmont gravels, similar to those seen in modern deserts. They were originally water borne but have since stabilised for form desert pavements covered by abrasive windswept sands. Additional sand and rock debris were introduced via flash flooding events. Thicker breccias formed in a similar manner but on more distal parts of alluvial fans, similar to the Rotliegend breccias (Glennie 1972, 1974, 1984; Marie 1975); or (3) yellow, grey, and red sandstones which either directly overlay the piedmont or are separated from the piedmont by thin patchy breccias. This sandstone is the youngest of the early Permian deposits in the UK and is generally interpreted as aeolian in origin (Smith 1989). In the Durham Sub-basin, the sandstones form WSW-ENE ridges up to 60m high which have been interpreted as dunes that formed by east-north-easterly prevailing winds (Steele 1981, 1983; Yardley 1984). While in Yorkshire the sandstone forms WNW-ESE ridges (Versey 1925) but lack distinctive large-scale trough cross-bedding which can be seen in the County Durham sandstones as it is thought that during or directly after the Zechstein transgression it was redistributed (Pryor 1971).

2.2.3 Cycle 1 (EZ1)

The Zechstein sequence is thought to have been deposited between ~258-252.3 Ma (Menning *et al.* 2005; 2006), however it is debated whether sedimentation was continuous during this time. This has

led to uncertainties about the length and duration of each cycle. It has been suggested that there is a gap of ~4 Ma between the Zechstein and the Lower Triassic (Henderson *et al.* 2012), however Menning *et al.* (2005, 2006) conclude there is no evidence of a significant hiatus. Based on a combination of magnetic polarity records from The Netherlands, Germany, and Poland, a well-documented magnetostratigraphical scheme exists for the Zechstein-lowermost Bundsandstein transition (Szurlies 2013). The interval is mostly of normal polarity with a few reversed magnetozones enabling reliable correlation throughout the Central European Basin. The magnetostratigraphy has been correlated with biostratigraphical data which has improved links with the marine realm. Szurlies (2013) concludes that the basal Zechstein is likely equivalent to the uppermost lower-upper Wuchiapingian, and the lowermost Bundsandstein being equivalent to the entire Changhsingian. The study further concluded that the bio- and magnetostratigraphic data indicate a possible Zechstein duration of only 2.8-3.5 Myr. There is a transition from a short reversed to a longer normal magnetozone within the uppermost Zechstein, which predates both the end-Permian extinction and the conodont-calibrated biostratigraphical Permian-Triassic boundary.

The Zechstein deposits can be divided into 5 or 7 distinct sedimentary cycles that reflect the nature of deposition within the basin, depending on a marginal or basin centre perspective. Deposition can be correlated across the basin (Peryt *et al.* 2010) (Figure 2). Divergence within the uppermost part of the Zechstein Group makes correlations problematic, and separate schematics are used for the British, Dutch, Polish and north German successions. Stratigraphic nomenclature for the central basin is derived from their German counterparts (Van Adrichem Boogaert & Kouwe 1994), while stratigraphic nomenclature for the marginal strata of the British Zechstein is derived from Smith

Figure 4. Classification and correlation of Zechstein lithostratigraphic units in the U.K., both onshore and offshore.

(1986, 1989). This disparity is a result of different parts of the basin experiencing variable amounts of both extension and contraction (Rowan 2017).

The Zechstein transgression was caused by tectonic activity of the Greenland-Norwegian Sea rift (East Greenland-Fennoscandian Shield) and a strong thermal subsidence pulse (Legler & Schneider 2008). The transgression itself had a strong loading effect on the lithosphere causing continued regional differential subsidence throughout the basin throughout the seas duration and overstepped the margins of the proceeding Rotliegend basin (Ziegler 1990; McCann *et al.* 2008). In the region of the marine sill between the Boreal Ocean and Zechstein Sea there appears to have been two sets of rift structures defined by the Atlantic and Viking Graben rift trends, reflecting discrete extension vectors that must have alternated in their movement due to the lack of evidence for oblique slip or transtension. These interacting rift trends likely provided a complex pathway of fault blocks for the penetration of marine brines allowing for balanced inflow and evaporation for long periods of time. This would have allowed for massive volumes of halite to precipitate and would have been further influenced by thermal subsidence providing an even larger receptacle for the brines which fed the massive accumulations of halite (McKie 2017).

2.2.3.1 The Marl Slate

Shortly after the transgression it is believed that spatially heterogeneous reducing conditions presided in the basin. Permanent stagnant bottom-water conditions developed as a result of nutrient-rich water leading to high organic productivity in surface waters in combination with high evaporation rates. After the initial transgression, the water column may have been between 200 and 300m deep (Ziegler 1990). Rates of depositions for the Marl Slate are estimated at 30-40cm in 17 Kyrs (Hirst & Durham 1963). The presence of green sulphur bacteria, which would have required both light and free hydrogen sulphide indicates that photic zone euxinia, at a depth of 10-30m, occurred at least intermittently during the deposition of the Marl Slate and early history of the sea (Pancost *et al.* 2002; Słowakiewicz *et al.* 2015). Primary production in the upper part of the water column was dominated by photosynthetic cyanobacteria or green algae.

The degree of methylation of 2-methyl-2-trimethyl-tridecylchromans (MTTC) suggests euhaline to mesohaline (30-40 ‰) conditions for the Marl Slate, and the high abundance of green/purple sulphur bacteria-derived biomarkers suggest hydrogen sulphide saturation of bottom waters and a maximum depositional depth of >100m (Słowakiewicz *et al.* 2015). Further, methanogenesis was most active during the early deposition of the Marl Slate, as indicated by early carbon isotope analysis (Bechtel & Püttmann 1997) of the Kupferschiefer, the results of which show

the light carbon isotopic composition of organic matter resulting from the recycling of carbon dioxide produced by methane-oxidizing bacteria in the water.

Deep-water facies have also been identified in the Kupferschiefer (Oszczepalski & Rydzewski 1987; Paul 1987) ranging between 20-60m thick consisting of alternating organic rich shale with planar laminae of clay and planar- and wavy-laminated dolomitic calcareous clays. These deep-water facies formed either within the anaerobic zone or at the boundary with the dysaerobic zone. The shallow-water facies consist of varied thicknesses of mainly planar- and wavy-laminated dolomitic calcareous marl, were deposited in dysaerobic (Poland) and aerobic (Germany) environments. The shallow-water sediments contain various plant and animal remains including reptiles, *Lingula* brachiopod remains which suggest a nearshore brackish water environment, and bivalves, echinoids and foraminifera indicating a marine environment. Fresh water and marine fish are common (Jowett *et al.* 1987; Dineley & Metcalf 2007). Slope facies contain reworked marine benthic fauna which is characterised by laminated black shales with calcareous tempestites (Paul 1982). The Kupferschiefer is only absent on intrabasinal swells and in marginal areas where normal marine fauna is found. Instead, these contemporaneous deposits formed in calcareous facies in water that was well-aerated and situated above the chemocline.

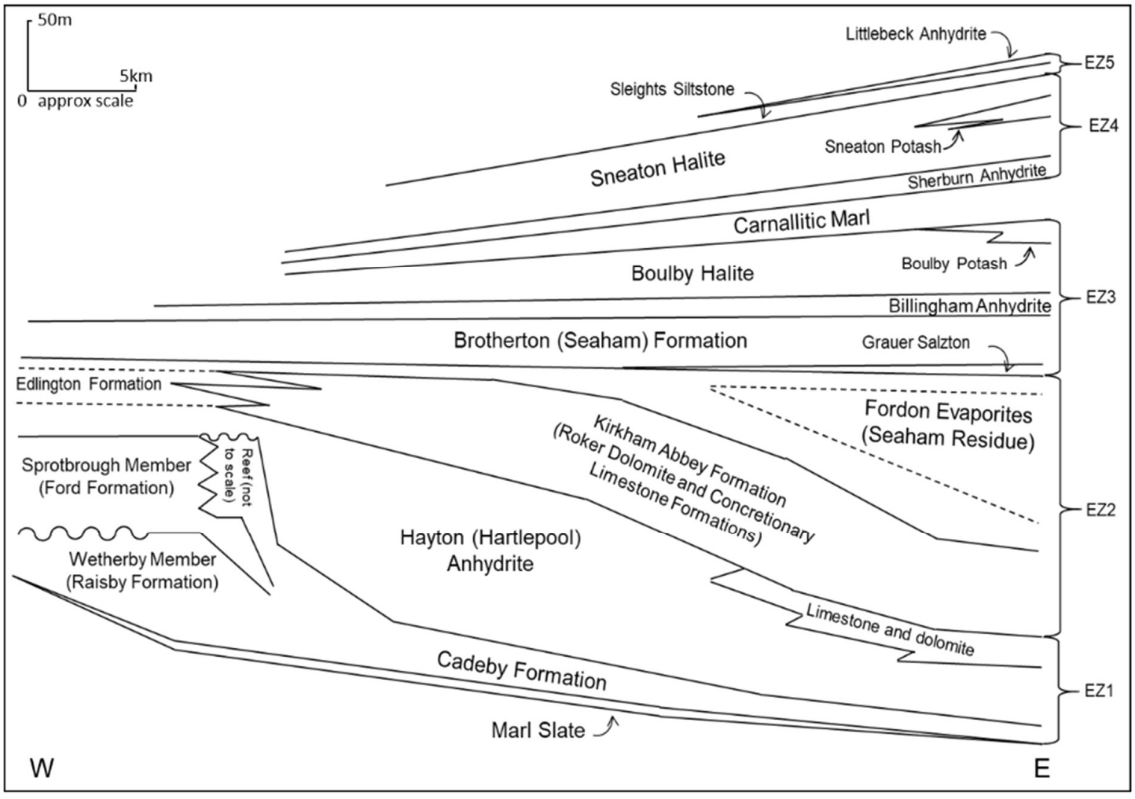

Figure 5. Spatial relationships between the Zechstein lithostratigraphical units in northeast England (redrawn from Smith 1989).

2.2.3.2 Cycle 1 Carbonates (EZ1 Ca): Cadeby/Raisby Formations

The Marl Slate is overlain by the limestone of the Cadeby and Raisby formations which were deposited in oxygenated water. These limestones can be up to 100m thick in marginal areas and intrabasinal highs. They contain a rich shallow-water fauna similar in composition to the Arctic faunal province (Hollingworth & Pettigrew 1988). However, the microfauna of Poland and Lithuania includes Tethys-related species (Peryt & Peryt 1977; Suveizdis 1975), suggesting at least a temporary connection with the Tethys Ocean at some point during Z1 in eastern regions of the basin.

In the U.K., the carbonate rocks of Cycle 1 (EZ1Ca), the Cadeby Formation, are formed of two sub–cycles A and B with the thin sapropelic Marl Slate at the base. EZ1Ca was formed on a gentle basin-margin slope, and gradually built a typical tropical carbonate shelf up to 90km wide. In north Yorkshire, the Cleveland High influenced sedimentation in the Cisilurian and continued to do so throughout EZ1, separating the Yorkshire Sub-basin from the Durham Sub-basin. It is unclear why the shelf carbonate rocks in these two Sub-basins accumulated under different conditions. It may be related to the Durham Sub-basins proximity to the connection with the boreal ocean, or the greater fluvial influence in earlier cycles in the Yorkshire Sub-basin (Smith 1989).

The carbonate wedge thins uniformly in the direction of the southern margin of the basin, and a similarly thinning is also assumed for the western margin. According to interpretations of palaeorelief a proto-Pennine land barrier separated the Zechstein Sea from the Bakevellia Sea (Smith, 1970a) to the west throughout Cycle 1 in the region of the Cleveland High. However, the strata in Cumbria (Arthurton *et al.* 1978) do not support a trans-Pennine connection during Cycle 1.

It is thought that the large hills beneath lower Teesside and at Knaresborough persisted as islands throughout the deposition of EZCa1. Although the Cleveland High is not believed to have exerted strong control on the rate of Cycle 1 deposition, elevation of the sub-Zechstein peneplain is suggested by the absence of the Marl Slate in this area (Smith 1989).

2.2.3.3 Carbonate Rocks of sub-cycle A (EZ1a Ca): Cadeby Fm, Wetherby Member

The carbonate rocks of sub-cycle A are represented by the Raisby Formation in the Durham Sub-basin and the Wetherby Member of the Cadeby Formation in the Yorkshire Sub-basin. These are mainly dolomitic limestones and dolomites, but limestone dominates to the east (Taylor & Colter 1975). They reach a maximum thickness of 75m (Smith 1989). The carbonates of the Raisby Formation formed further into the basin than then Wetherby Member equivalents, so together they form an almost complete facies transect from the shoreline to the low basin slope.

The earliest deposits of sub-cycle A are from the first marine transgression and incorporate the reworked top of the Yellow Sands in the Durham Sub-basin (Smith & Francis 1967). Reworked Yellow Sands are also present in the west of the Yorkshire Sub-basin. The initial marine deposit is the Marl Slate (0.3-1.3m) and is a dark grey to black basin floor argillaceous carbonate laminate rich in organic carbon, topped by a paler grey more coarsely laminated rock (<6m thick). The Marl Slate can be found in all deep parts of the basin below the level of an oscillating pycnocline (Dunham 1961). The succeeding carbonate environments of sub-cycle A become increasingly complex with time creating a classic shelf wedge that contains several depth-related and energy-related facies belts in the Yorkshire Sub-basin. These cannot be traced into the Durham Sub-basin across the Cleveland High. However, it is possible that they eroded post-deposition. The pycnocline eventually dissipated, perhaps due to an improvement of circulation in the basin as it progressively deepened and expanded, and anoxic sedimentation was almost entirely restricted to the basin floor.

Throughout sub-cycle A, the input of terrigenous clastic sediment was limited to small clasts along shorelines and islands derived from Carboniferous rocks, and widely distributed but small quantities (<1%) of supposedly windblown quartz silt and fine sand. There is evidence of substantial stream input (Sherlock 1911; Taylor 1968) in the carbonate rocks of the Wetherby Member around Mansfield with sand-grade clastics locally exceeding 50%. The end of sub-cycle A is marked by a relative fall in sea level of a few meters which caused the widespread emergence of shallow parts of the carbonate shelf and the formation of an erosion surface, the Hampole Discontinuity/Hampole Beds (Smith 1986). During this time peritidal and lagoonal deposits accumulated including fenestral algal-laminated oolites and multicoloured plant-bearing siliciclastic mudstones and siltstones (Smith 1986, 1974*b*; Moss 1986). This discontinuity is not seen north of the Cleveland High but there is some evidence of it at the top of the Raisby Formation in the Durham Sub-basin. In the Durham Sub-basin massive basinward sliding of slope mudstone and wackestones took place in an area eastwards of Newcastle upon Type, perhaps in response to sea level fall, sediment overloading, or earthquake even shocks, though there is little evidence for the latter (Smith 1970*c*, 1985).

2.2.3.4 Carbonate Rocks of sub-cycle B (EZ1b Ca): Cadeby Fm, Sprotbrough Member

The carbonate rocks of sub-cycle B are represented by the Ford Formation in the Durham Sub-basin and the Sprotbrough Member of the Cadeby Formation in the Yorkshire Sub-basin. They form a maximum thickness of 100m, and are composed of mainly dolomite, like their proceeding strata. The deposition of sub-cycle B ended formation of the Cycle 1 shelf wedge and took place in a setting of continuing differential subsistence involving slow basinward tilting at the margins. Salinity appears to have remained normal throughout with a minimal increase towards the end of the sub-cycle.

Deposition of sub-cycle B was initiated by a relative sea-level rise following the sea level fall that resulted in the erosional Hampole Discontinuity/Hampole Beds. Reinundation of the Hampole Beds occurred in most outcrop areas of the Yorkshire Sub-basin, although there is continuous sedimentation in areas where the first sub-cycle was not subaerially exposed (Magraw *et al.* 1963). The height of ooidal bedforms (<12m) indicates the rapid recovery in sea-level and they formed immediately above the thin transgression unit. In the Durham Sub-basin, the sea level fall is indicated by the shallow-water basal reef coquina (Tucker & Hollingworth 1986) of the Ford Formation. Recovery is indicated by a sharp upward change into carbonate rocks which formed in deeper water.

There are distinct differences between the Durham and Yorkshire Sub-basins in sub-cycle B, but the reasons why are unclear. In the Durham Sub-basin there is a major shelf-edge linear reef built upon the newly formed coquina (Smith 1958; Smith 1981), which eventually separated the westwards shelf and lagoonal environments from eastwards talus aprons and their equivalents. The ooidal grainstones that are found behind the reef indicate deposition under shallow water conditions with moderate energy levels, and the restricted fauna present may indicate a slight relative increase in salinity. In contrast, the Yorkshire Sub-basin has no shelf-edge reef, but instead displays sharp basinward thinning of the Cadeby Formation at the eastern margin of the shelf (Smith 1989). Marginally distal ooidal grainstones in this region were formed in a 10-15km wide belt, in a high energy setting with large subaqueous sandwaves which may be contradictory to shelf-edge reef formation. However, these sandwaves protected a wide lagoon or restricted shelf belt in which thinner and more uniform bedded ooid grainstones and wackestones accumulated (Smith 1974*a*; Kaldi 1980, 1986; Harwood 1981). Abundant algal stromatolites are seen to have thrived in parts of this belt during the later parts of the sub-cycle.

Almost all sub-cycle B carbonates contain <1% siliciclastic sediment, but mainly coarse silt and fine sand presumed to be aeolian in origin. Clastic sediment continued to be shed onto onlapping basal beds next to island and shorelines as in sub-cycle A. In addition, high quartz sand content east of Mansfield likely indicates the continued input of a river system there (Sherlock 1911; Taylor 1968).

At the end of sub-cycle B, the shelf-edge reef grew enough to approach sea-level partially isolating a lagoon on its western side in the Durham Sub-basin and there was a relative sea level fall of at least a few meters. The belt of sandwaves in the Yorkshire Sub-basin was active at the time and the shoreline receded eastwards by approximately 30km. The sea-level drop ended reef formation in the Durham Sub-basin and led to the formation of a strong local unconformity on the former reef flat followed by the deposition of a boulder conglomerate which is up to 17m thick. In the Yorkshire Sub-basin the recession caused subaerial exposure of some parts of the Cycle 1 onshore carbonate shelves, and altered the evolution of the coastal plane and lagoonal environments of the Edlington Formation.

The exact nature and thickness of the Cycle 1 carbonates in both Sub-basins are difficult to assess. However, sections in eastern County Durham show a dramatic thinning of the talus of the shelf-edge reef to the east (Smith & Francis 1967; Smith 1981). Exposures in South Shields suggest that sandy rocks or the oncoids and columnar stromatolites of the Trow Point Beds (0-0.6m) is all that remains of this carbonate wedge. The Trow Point Bed is widespread offshore (Smith 1970*b*; 1986), under the southern North Sea (Taylor & Colter 1975), in Germany (Richter-Bernberg 1982; Paul 1986) and in Poland (Peryt & Piathowski 1976). It likely formed under oxic conditions on the basin floor in water that was 25-100m deep.

2.2.3.5 Cycle 1 Anhydrite (EZ1 A): Hayton/Hartlepool Anhydrite

After the deposition of the Cycle 1 carbonates the Cycle 1 sulphates precipitated, mainly gypsum (now anhydrite) and secondary gypsum. The change in deposition appears to have been sharp and synchronous and is assumed to reflect basinwide increases in salinity. No major oscillations in salinity are predicted until this point.

Reconstructing the depositional environment is not straightforward yet it is suggested that the extensive anhydrite at the beginning of the Edlington Formation formed during Cycle 1, and the halite and dolomite of the Edlington Formation formed during Cycle 2. Cycle 1 sulphate rocks formed under three main facies belts (1) broad yet restricted marine shelf/lagoonal complex in the west, (2) vast marine basin plain in the east, (3) intervening basin-marginal belt.

In Cleveland, the sulphate rocks of the shelf/lagoon have been shown to have formed by both primary and secondary processes in a complex of alluvial plans, sabkhas, salt flats and lagoons that evolved in a context of continuing differential basin-wide subsistence (Goodall 1987). A similarly diverse range of environments has been proposed for the Yorkshire Sub-basin (Smith 1974*a*, *b*). In the Durham Sub-basin a discontinuous barrier contemporaneous with the shelf-edge reef from Cycle 1 has been inferred but not identified in the Yorkshire Sub-basin. In addition, the alluvial plains in the south of the Yorkshire Sub-basin were much more prominent than anywhere else and are covered by a thin layer of proximal to distal fluviatile and lacustrine sediments which include patchy gravels and scattered primary and secondary evaporites.

The Hartlepool Anhydrite of the Durham Sub-basin, and equivalent Hayton Anhydrite in the Yorkshire Sub-basin, represent the main sulphate rocks of the basin-margin belt together forming a strongly lenticular body 20-30km wide and up to 180m thick that lies immediately basinward of the edge of the Cycle 1 carbonate shelf (Peryt *et al.* 2010). There is evidence of widespread basinward foundering of the anhydrite in the equivalent Werraanhydrit in Germany (Herrmann 1964; Meier

1977; Schalnger & Bolz 1977) but this has not been identified in the Durham Sub-basin. However, there is evidence that the Hartlepool Anhydrite abutted and did not widely cover the steep seaward slope of the Cycle 1 shelf-edge reef. There is also evidence of synsedimentary slumping in the Durham Sub-basin (Smith 1989).

Basin-ward facies comprise 8-20m of interbedded halite and carbonate in which four widespread sub-cycles have been identified (Taylor & Colter 1975; Taylor 1980). They can be traced from the Yorkshire Sub-basin into the thick basin-margin anhydrite. The finely laminated anhydrite of the basin-plain facies was probably deposited 150-300m deep water (Taylor 1980). The interbedded nodular anhydrite may have formed during phases of extreme evaporative downdraw and during partial desiccation. The depositional environment of thick basin-margin anhydrite is debated and could have been a sabkha, or originally built up of 1-3cm layers of bottom-growth gypsum and selenite crystals, similar to those that characterise parts of the Werraanhydrite in Germany (Richter-Bernberg 1985).

2.2.3.6 Cycle 1 - Cycle 2 transition

The Cycle 2 carbonate passes up into the upper part of the thick marginal Cycle 1 anhydrite. This has created as of yet unresolved issues in defining the Cycle 1/Cycle 2 boundary.

2.2.4 Cycle 2 (EZ2)

Like the Cycle 1 carbonates the Cycle 2 carbonates contain three depositional cycles that reflect high amplitude sea-level fluctuations, in this case ~40-120m each (Peryt *et al.* 1989; Peryt & Dyjaczyńsky 1991). This may be a result of Milankovitch cyclicity (Strohmenger *et al.* 1998). At the end of Cycle 1 and beginning of Cycle 2 sea levels fell by 100-150m creating subaerially exposed and karstified deposits. The first sea level rise of about 70m during Cycle 2 led to the deposition of a transgressive system but only on off-platform highs (Strohmenger *et al.* 1998) and lower part of the platform slope (Peryt 1992). Another drop in sea level occurred and followed by karstification of carbonates before another sea-level rise that caused the final flooding event in Cycle 2 that effected platform carbonates.

2.2.4.1 Carbonate and associated rocks of Cycle 2 (EZ2 Ca): Edlington/Roker Fm

Deposition in Cycle 2 was initiated by a refreshening of the Zechstein waters, possibly with the additional input of water from the Tethys Ocean indicated by the evidence of spatially heterogeneous anoxia throughout the basin (Słowakiewicz *et al.* 2015). This halted gypsum precipitation and

favoured carbonate formation. What caused the refreshening is unclear though an improvement in ocean circulation as a result of a slight increase in relative sea level over the basin threshold has been suggested (Smith 1980). Differential basin subsidence and gentle tilting of the basin margin continued.

The asymmetrical shelf of Cycle 1 immediately led to the creation of shelf, slope and basin environments in Cycle 2, and resulted in the eastward shift of the main carbonate formation and deposition locus 30km eastwards. Here an outer shelf barrier complex rapidly evolved and continued the broad restricted inner shelf/lagoon mosaic that established in Cycle 1.

Correlations between the inner shelf and lagoon deposits with the barrier complex are unresolved however the middle parts of the Edlington Formation may date from the main phase of Cycle 2 carbonate formation. The Cycle 2 sediments range from eastwards-fining and thinning alluvial and lacustrine siliciclastic sands, silts and clays to extensive lenses and generally westward-thinning sheets of lagoonal carbonate, anhydrite and halite. The evaporites included both primary and reworked subaqueous types and secondary types, but much of the halite was likely dissolved in situ and during later diagenetic processes. Goodall (1987) showed how rocks of the Edlington Formation in the Durham Sub-basin were formed on a complex of alluvial plains that developed and changed quickly, sabkhas, salt flats and marine or hypersaline lagoons and salinas. The coastline could have changed repeatedly, and desiccation was likely periodic. The Yorkshire Sub-basin displays a similar range of depositional settings (Smith 1974*a*, *b*, 1980) although the northern and central parts of the Sub-basin are less thoroughly described due to how parts of Cycle 1 interdigitate and grade south-westwards into alluvial plains.

2.2.4.1 Cycle 2 Anhydrites (EZ2 A): Fordon Evaporite Fm

The basal anhydrite is composed of a thin sequence of stromatolitic anhydrites several tens of meters thick in platform areas and only a few meters thick in the basin centre. This thin sequence passes into massive anhydrite with pseudomorphs of selenite crystals which formed in shallow-water saline environments. This is followed by bedded and laminated anhydrite. Sometimes thin sporadic intercalations of halite can be seen in the anhydrite. The individual laminae of anhydrites can be correlated across the basin for up to 400km (Richter-Bernburg 1955, 1985).

Subsistence caused by the deposition of the Cycle 1 anhydrite formed a depression in which the halite and potassium-magnesium salts of Cycle 2 was deposited. This sequence is more than 1000m thick in the basin centre (Zirngast 1991) and about 100m or absent on platforms.

2.2.4.3 Cycle 2 Halite (EZ2 Na): Fordon Evaporite Fm./Seaham Residue

Cycle 2 to is notable for this thick halite deposits, which at their thickest exceed 700m in the basin centre. The upper part of the Cycle 2 evaporite deposits includes an extensive layer or potassium-magnesium salts with sylvinite and carnallite, known as the Strassfurt-Kaliflöz. Regionally the halite is overlain by the Screening Anhydrite which is interpreted as being a mixing of residual brines and new sea water from the Cycle 3 transgression (Peryt *et al.* 1996). The Cycle 2 salts have experienced extensive deformation and movement which means reconstructing their original thickness and compositions is challenging. It is these salts that the Zechstein is so renowned for their commercial value.

The Cycle 2 halite developed from a deep-water ocean salt basin with free brine exchange to a shallow-water system with closed salinas fringed by coastal salt pans at the basin borders (Peryt *et al.* 2010). At the end of the deposition of the Cycle 2 anhydrite water depths were up to tens of meters deep in a saline to salt pan environment (Czapowski *et al.* 1990). By the beginning of halite deposition water depths had increased to up to 140m at the basin periphery though by the end of deposition it returned to being in the magnitude of only tens of meters deep (Czapowski *et al.* 1990). A rapid transition between deep-water to shallow-water environments occurred as the basin filled and the salt began to encroach on the slope and finally the top of the former carbonate platform. This deposition formed accumulations of rock-salts and potassium-magnesium salts several tens of meters thick which are found mainly in the central basin where they were originally formed in salinas.

2.2.4.4 Cycle 2 – Cycle 3 Transition: Grey Salt Clay/Illitic Shale/Grauer Salzton

The transgressional stratum of Cycle 3 is the Grey Salt Clay/Illitic Shale/Grauer Salzton which is confined mostly to the east, but in the west is overlapped by the main part of the Cycle 3 carbonate unit. This transgression was likely gentle due to the exceptionally low relief surface of the inundated shelf, and there is little evidence of erosional surface or reworking of Cycle 2 deposits at exposure. Basal layers of the Grauer Salzton can be salty and/or sandy. However, the transgression relief surface may have been up to 30m in places where the Cycle 2 grainstone shoals were not covered by Cycle 2 evaporites, such as in North Yorkshire where clasts of lithified Cycle 2 oolite grainstones have been recorded in Cycle 3 basal carbonates (Smith 1989). The Cycle 3 transgressional waters likely had above average salinity based on the rare early Cycle 3 marine biota present along the coastal margin (Smith 1989). However, salinity is thought to have decreased again to slightly above normal throughout Cycle 3 (Smith 1974*b*, 1980).

2.2.5 Cycle 3 (EZ3)

Cycle 3 deposition was initiated by a marine incursion that transgressed over the extensive salt and gypsum flats of the Cycle 2 evaporites, creating a shallow inland sea which progressively deepened in central parts of the basin where sedimentation continued to be slow (Smith 1989). The Cycle 3 sea would have continued to stay shallow across the carbonate wedge at the margin where deposition kept pace with continuing subsidence.

2.2.5.1 Cycle 3 carbonates (EZ3 Ca): Brotherton Fm

There is limited lithological variation within the Cycle 3 carbonates of the Brotherton Formation, apart from some local thinning across the Cleveland High. All Cycle 3 carbonates are pelleted lime muds, that are now packstones, wackestones and carbonate mudstones. They commonly contain laminae and thin beds of grey, green, purple and occasionally red mudstones found in what were areas landward of shelf. There are local occurrences of oolite beds and grainstones. Cycle 3 carbonates contain sedimentary structures, such as low-amplitude ripples, small-to-medium scale cross lamination, broadly lenticular bedding, indicating free sediment movement and uniform sedimentary environments over most of northeast England. This was a low-to-moderate energy level system, that experienced periodic storms, evidenced by widespread sheets of *Calcinema* (probably algae) debris and the presence of larger bedforms (Smith 1989). No carbonate shelf-edge reefs or barrier shoals have been located in either Sub-basin during Cycle 3, and the prevailing low energy levels is consistent with a shallow depositional environment of 5-20m deep water along a significantly broad shelf in basically a tideless, tropical, inland sea.

The upper carbonate beds contain stromatolites lamination that also suggest a reduced energy environment. As the sediment surface built up towards the sea level the basin margins prograded. During the late Cycle 3 carbonate phase there was westwards expansion of deposition into the southern part of the Vale of Eden (Cumbria) in part due to differential subsistence along the Stainmore Trough that opened up a passage from the Zechstein Sea (Smith 1989). The continually reducing volume of the sea during Cycle 3 and onwards, saw the start of a shift to a more humidity driven depositional system, rather than one controlled by arid-humidity cycles (Słowakiewicz *et al.* 2009).

2.2.5.2 Cycle 3 Evaporites

Carbonate deposition was ended by the shallowing and increasing salinity of the Zechstein Sea and resulted in the formation of widespread and varied evaporite deposits. Subsistence was relatively slow and uniform and was accompanied by gentle basinward tilting, although the Cleveland High may

have influenced the rate of subsidence in northern North Yorkshire leading to more rapid subsidence in certain areas such as Ripon (Smith 1989). Interpretations of the Cycle 3 evaporites are complicated by extensive dissolution. The carbonates are capped by stromatolites and distorted by the rapidly increasing sulphate content on top of which are carbonate layers which are replaced by sulphate layers of increasing thickness and frequency. The carbonate layers exhibit microbialite lamination and microfossils and their direct, and indirect, activities (Gasiewicz & Peryt 1994). The alternation of microbialite-sulphate layers may be linked to seasonal changes in sea level and the rate of evaporation-water influx. This pattern is typical of extremely shallow water environments experiencing rapid changes in salinity.

2.2.5.3 Cycle 3 Anhydrite and Gypsum (EZ3 A): Billingham Anhydrite

The anhydrite deposits of Cycle 3 are represented by the Billingham Anhydrite which is a sheet deposit that thickens gradually basinward reaching a maximum thickness of 15m on land, thinning westwards and eventually disappearing westwards-south westwards due to dissolution. The Billingham Anhydrite is a varied deposit, that while mainly nodular in character it does include some sheets of laminated to thin-bedded anhydrite with breccia lenses comprised of angular flakes of anhydrite and dolomite. Deposition was at times subaqueous indicated by traces of bottom-growth gypsum, though the abundant remains of cyanophyte carbonaceous laminae suggest this was not always the case. The depositional surface was vast and flat and close to sea level and was subjected to periodic flooding. It is on this surface that gypsum formed partly within brine-soaked sabkhas as well as in a complex of lagoons and very shallow seas. The shallow open sea lay to the east, while a gently rolling rocky desert lay to the west and south.

2.2.5.4 Cycle 3 Halite (EZ3 Na) and Potash (EZ3 K): Boulby Halite

The halite phase of Cycle 3 is represented by the Boulby Halite Formation which encompasses the Boulby Potash Member. In total, they form a 90m thick deposit of evaporites in coastal areas, but thin gradually westwards, and to the east they reach a thickness of 120m in parts of the Southern North Sea Basin (Taylor & Colter 1975; Smith & Crosby 1979). The Boulby Halite comprises four lithological units (Units A-D) which evolved in response to increasing salinity. Unit A is 15m of halite interbedded with anhydrite, including layers of halite containing pseudomorphs of bottom-growth gypsum and indicates phases of subaqueous deposition and is the transitional unit from the deposition of the underlying anhydrite. Unit B also contains pseudomorphs of bottom-growth gypsum which have been interpreted to have been produced in extensive salt flats that were subaerially

exposed but occasionally flooded by a hypersaline sea (Smith 1989). Unit C is a potash unit, also deposited in a salt flat environment which extended far offshore and passes laterally into the upper part of Unit B possibly due to early diagenetic modification. The final unit, Unit D, is only a few meters thick and composed of almost pure halite, and formed under similar salt flat conditions as for unit B.

2.2.5.5 Cycle 3 – Cycle 4 Transition: Carnallitic/Rotten Marl

At the boundary between Cycle 3 and Cycle 4 the sea drew down far into the basin and was replaced by a coastal plain upon which up to 25m of siliclastic silts, clays and subordinate sands were deposited by wind and water in a range of deposition environments including continental, lagoonal, and near marine settings likely all within 1-2m of the contemporary sea level. This resulted in the sediments that form the mainly red, and hygroscopic, Rotten Marl/Carnallitic Marl. Parts of the Carnallitic Marl contain abundant halite, others abundant carnallite, which result from nucleations and displacive growth of halite from saturated ground waters shortly after deposition and burial.

2.2.6 Cycle 4 (EZ4)

During Cycle 4 the Zechstein Sea would have resembled a large salt lake, that expanded yet again to inundate the extensive coastal plains of Cycle 3. Continuing differential subsidence accompanied and possibly resulted from a water level rise of a few meters.

2.2.6.1 Cycle 4 Carbonates (EZ4 Ca): Upgang Formation

The carbonates of Cycle 4 are thin and represented by the Upgang Formation which is widespread and up to 1m thick in marginal parts of the Yorkshire Sub-basin. It is a sandy ooidal dolomite but in coastal areas it is a poorly-defined argillaceous magnesitic deposit less than 70m thick. No marine fossils have been recorded from it and it may have been a limnic chemical precipitation (Smith 1989).

2.2.6.2 Cycle 4 Evaporites (EZ4 A, EZ4 Na and EZ4 K): Sherburn Anhydrite, Sneaton Halite, Sneaton Potash

The sulphate rocks of Cycle 4 are the Sherburn Anhydrite Formation which is one of the most lithologically distinctive and extensive Zechstein units and can be all that remains of Cycle 4. It contains pseudomorphs of bottom-growth gypsum and is cross laminated and contains current-rippled

anhydrite in places, indicating mainly subaqueous deposition under shallow water conditions in a sea or lake.

The Cycle 4 chloride phase is represented by the Sneaton Halite Formation which includes the Sneaton Potash Member. It is 60m thick and slightly less extensive than the Boulby Halite of Cycle 3 (Smith & Crosby 1979). The Cycle 4 chlorides have been less effected by dissolution than the Cycle 3 ones as they have been encased in relatively impermeable mudstone and siltstone. As in Cycle 3, the Cycle 4 chlorides are divided into lithological units, though there are five (Units A-E) for Cycle 4 (Stewart 1951; Raymond 1953; Smith 1973, 1974*b*).

Unit A is a 5-7m thick, slightly anhydritic rhythmically layered halite containing traces of halite pseudomorphs of bottom-growth gypsum. Deposition was subaqueous occurring in shallow extensive brine pans, possibly with periodically complete desiccation. Unit B is 8-12m thick and was deposited under similar conditions, though possibly in even shallower water with more frequent or longer periods of subaerial exposure. Unit C is the Sneaton Potash, where potassium and magnesium ions gradually accumulated in groundwaters, marginal playas and basin centre brines before being preserved as a multi-layered potash unit. Deposition occurred in salt flats that extended tens of kilometres around a central playa that would have expanded and contracted seasonally, with minor climatic variations, and sometimes expanded almost the basin margins. There is debate over whether there was a connection to the open ocean at this time to supply the extensive salts that precipitated out during this phase. Unit D is a haslgebirge salt. Halite is intercalated with red siltstone and mudstone and is regarded as a coastal plain deposit (Smith 1971) that was formed by secondary displace growth of halite within a siliciclastic host during a phase when the basin centre playa and surrounding salt flats drew even further into the east. Unit E is a relatively thin pure halite, like Unit D of Cycle 3, and is interpreted as a final brief expansion of the waning Cycle 4 sea or lake.

2.2.6.3 Cycle 4 – Cycle 5 Interval: Sleights Siltstone

Cycles 4 and 5 are separated by a phase during which the Zechstein Sea drew to the east yet again and its margins prograded. The Sleights Siltstone is 2-4m thick and lithologically similar to the Carnallitic Marl at the Cycle 3 – Cycle 4 boundary. It is comprised of a sheet deposit that formed under a range of environments within 1-2m of the contemporary sea level. It is generally inseparable from the Roxby Formation where the Cycle 5 evaporites are absent, and commonly contains idiomorphic halite crystals that formed in brine-soaked coastal and lake marginal plains.

2.2.7 Cycle 5 (EZ5)

2.2.7.1 Zechstein 5 (EZ5): Littlebeck Anhydrite

Cycle 5 is an incomplete evaporite cycle represented on land only by the Littlebeck Anhydrite, a uniform layer of slightly haematitic anhydrite, a partly laminated shallow-subaqueous deposit only found in a 0-30km belt in North Yorkshire, North Humberside and Lincolnshire (Smith 1974; Taylor & Colter 1975). Its thickness increases by a few meters to the east, where it splits to contain a median halite layer (Taylor & Colter 1975). Cycle 5 marks the final short-lived expansion of the thoroughly reduced Zechstein Sea, filling spaces left by the differential basin-centre subsidence of previous cycles.

Withdrawal of the sea ended Zechstein sedimentation in northeast England, although evidence of 2-3 later expansions is represented by smaller thin lenses of anhydrite offshore (EZ6-7) (Smith & Crosby 1979). The final expansion led to great marginal plains, tongues and sheets of siliclastic water-laid silts, clays and subordinate sands that extend far into the basin centre, becoming the Roxby Formation – a finely cyclic sediment formed on distal extremities of an enormous network of alluvial fans and tidal flats, which pass up into the formal basinal areas for the Sherwood Sandstone (Triassic).

Z5 and younger cycles are deposited in an ever-shrinking evaporite basin and the progradation of terrigenous deposits towards the basin centre. The halite deposited in Z5 has a high bromine content indicating they formed under marine conditions (Peryt *et al.* 2010). But the rapid decrease in bromine concentration in Z6 halite indicates a change to a salt-lake environment with salt recycling but without a connection to the sea (Kühn & Schwerdtner 1959; Smith 1971, 1974; Czapowski 1990). Z5 does not have a consistent deposition across the basin. In the Netherlands Z5 is limited to the north-east, and offshore to the north-west. This arrangement outlines depocentres that existed towards the end of Zechstein Sedimentation. Z5 is composed of several meters of basal claystone overlain by up to 15m of halite. Younger Zechstein salts from Z6 and Z7 are found in north-western Germany (Best 1989), Poland (Wagner 1994) but not in the Netherlands.

2.3 Sequence Stratigraphy

Alternatively, the British Zechstein strata can be divided into seven evaporite-carbonate sequences that have been described in detail by Tucker (1991). This is opposed to the classic Zechstein cycle organisation of five carbonate-evaporite cycles. Figure 5 compares these two organisations. A sequence stratigraphic approach is particularly valuable for marginal locations around the Zechstein basin, as the standard carbonate-evaporite cycle concept is based on events occurring in the basin centre. In a sequence stratigraphic approach, the sequence boundaries are produced by major and

minor sea-level falls. Consequently, evaporites occur within the lower parts of sequences as they are precipitated in the lowstand systems tracts (LST) as well as in early stages of transgressive system tracts (TST), largely within the basin, and against the shelf foreslope as a result of "Type 1" relative sea-level falls - where the sea level drops below the shelf break. A "Type 2" boundary is where sea level drops, but not below the level of the shelf break. Shallow water carbonate occurs in upper parts of the sequences because they are principally deposited the deposits of the transgressive and highstand systems tracts (HST) following flooding of the basin. Carbonates are deposited during TST and HST while evaporites are precipitated in shallow marginal areas during the early TST as salinity is continually reduced in the basin. Evaporites can also form during the late highstand, especially on more landward parts of the carbonate platform.

A sequence stratigraphic interpretation is based off the characteristic 5-cycle interpretation of the Zechstein. 7 cycles are defined as opposed to the 5-cycle interpretation in Figure 5. The first carbonate-evaporite cycle (EZ1) is composed of two and a half sequences, the Marl Slate-Raisby Formation/Wetherby Member form ZS1, and the Ford Formation/Sprotbrough Member forms ZS2. The evaporites of EZ1, the Hartlepool/Hayton Anhydrite, form the lower part of ZS3 with the upper part being the carbonates Roker-Concretionary/Kirkham Abbey Formations of the second carbonate-evaporite cycle (EZ2). The fourth sequence (ZS4) consists of the Fordon Evaporite Formation of the upper part of the second cycle and the carbonate of EZ3 (Seaham/Brotherton Formation). The fifth sequence (ZS5) is composed of the Billingham Anhydrite (middle EZ3) and the Boulby Halite (upper

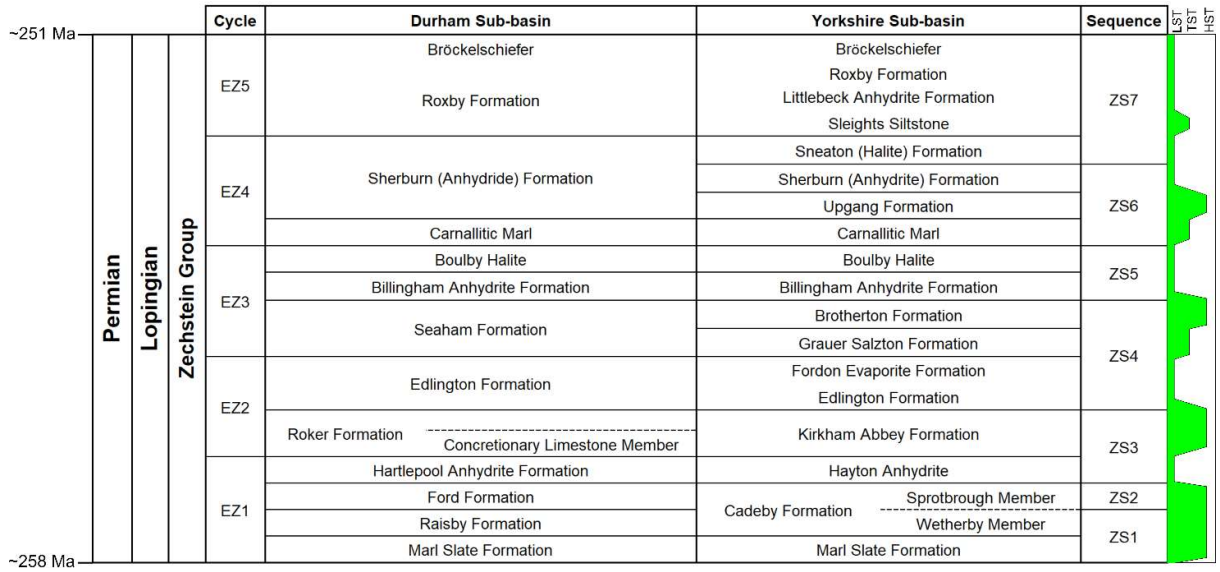

Figure 5. Evaporite-carbonate sequence stratigraphy of the Permian strata in the Yorkshire and Durham Sub-basins in relation to carbonate-evaporite cycles in Germany and the Netherlands. EZ = carbonate-evaporite cycles, ZS = evaporite-carbonate sequences, LST = lowstand systems tract, TST = transgressive systems tract, HST = highstand systems tract (adapted from Tucker 1991).

ZS3). The sixth sequence (ZS6) comprises the Carnallitic Marl Formation, Upgang Formation and Sherburn Anhydrite of EZ4. And the final sequence (ZS7) is composed of the Sneaton Halite (uppermost EZ4), Sleights Siltstone, Littlebeck Anhydrite, and Roxby Formation of EZ5.

2.3.1 ZS1 (Marl Slate, Wetherby Member/Raisby Formation)

The transgressive systems tract of ZS1 is the Marl Slate, deposited during the flooding of the basin. The late TST and HST is represented by the Raisby Formation. The maximum flooding surface (MFS) cannot be distinguished here. ZS1 ended with a relatively minor sea-level fall: in the Durham Sub-basin this is represented by a downward shift in facies, where the mid-ramp wackestones of the uppermost Raisby Formation are overlain by the shallow-water oolites of the Fordon Formation. The sequence boundary is therefore between the Raisby and Ford Formations. In the Yorkshire Sub-basin the upper sequence boundary is marked by the discontinuity at the base of the Hampole Beds, near to top of the Wetherby Member. As in the Raisby Formation, there is also a downward facies shift across this boundary in Yorkshire. Megabreccia in Durham is interpreted as the LST of ZS2, therefore the boundary is drawn at the base of the megabreccia.

2.3.2 ZS2 (Ford Formation/Sprotbrough Member)

ZS2 represents a relatively minor fall in sea. This is because there is no evidence of sub-aerial exposure of the outer Raisby ramp. In the Yorkshire Sub-basin, the facies do not change significantly across the boundary however there is a basinward shift of facies with oolites below topped by the tidal flat laminites of the Hampole Beds. In Durham ZS2 beings with the slope wedge of the slide megabreccia. More proximal positions of the Durham and Yorkshire Sub-basins are equivalent to shelf margin wedge systems tracts. They are very shallow water deposits that precede the deeper water facies of the TST.

In the Durham Sub-basin, the shelf margin wedge is represented by coquina on which the Ford Formation reef developed. The TST and HST in the Yorkshire Sub-basin is the shelf margin wedge of the peritidal Hampole Beds which are topped by the oolitic Sprotbrough Member. The late HST and basinward progradation is represented by the local peritidal facies of the uppermost Sprotbrough Member. The ZS2 in the Durham Sub-basin is a “Type 2” sequence. The shelf margin wedge is the basal coquina. The TST and HST is the reef, which shows vertical growth for over half of its thickness (TST) and shows that reef growth kept pace with the rising sea level; in the back reef area oolite and lime mud production also kept pace so there is no detectable topography between the reef and back reef lagoon.

The HST in the Ford Formation is indicated by progradation of the reef over its debris, as well as some onlapping of back-reef facies on to the reef itself. The downlap surface is not exposed at outcrop but clinoforms are well displayed at outcrop. The basinal equivalent of the 100m thick Ford Formation reef TST and HST may be the extremely condensed Trow Point Bed (South Shields), which in some toe-of-slope areas rests on the slide breccia.

During the period of reef growth sediment was not being transported any significant distance into the basin from the shelf margin, with the exception of the talus immediately adjacent to the reef, comprising the clinoforms. This may be indicative of intense cementation of the reef front which was located in a windward location (prevailing winds being north-westerly). Reef growth ceased with a relative fall in sea level, creating the upper sequence boundary on top of the Ford Formation.

2.3.3 ZS3 (Hartlepool/Hayton Anhydrite, Edlington Fm/Roker Dolomite)

A "Type 1" sequence boundaries at the base and top of ZS3 were caused by relative sea level falls which would have entirely exposed the carbonate platforms at the basin margins. The Hartlepool/Hayton Anhydrite precipitated as a lowstand wedge of gypsum adjacent to the foreslope of the shelf, in shallow water during a period of sea-level fall, the low stand and subsequent slow rise. The basin at this time was undergoing incomplete downdraw, with evaporation that was sufficient enough to drive the basin into a sulphate precipitating phase but not into a halite precipitating phase. Massive gypsum precipitation took place in the shallow water around the basin margins below the shelf. Water was deep over much of the basin floor resulting in a condensed section of gypsum and carbonate/organic matter continuing to be deposited there. Water balance-salinity estimates suggest that seawater influxes into the basin were common alongside brine reflux out of the basin to account for the volume of anhydrite and absence of halite (Taylor 1980). Atmospheric relative humidity likely controlled evaporite mineralogy too.

When the basin began to fill again the marginal platforms flooded. During the early TST evaporites continued to be deposited, evidenced by residue and gypsum upon the Sprotbrough member in the Yorkshire Province. A transitional phase in evaporites to carbonate sedimentation with marginal shallow-water evaporites but basinal carbonates is represented by upper Werra Anhydrite (equivalent to the Hayton/Hartlepool Anhydrites) which onlaps the Zechsteinkalk (equivalent to Cadeby Formation) shelf margin, and organic-rich carbonates.

During the mid-late TST and HST the basin became more open marine, and shallow water carbonates formed on the marginal platforms, the Roker-Concretionary/Kirkham Abbey Formations. Aggradation and progradation of these carbonates during the HST can be seen in Durham Sub-basin

with the basinward progression of the facies belts, and of the shelf deposits of the Roker Dolomite over the slope sediments of the Concretionary Limestone.

During the TST and HST, the clays and evaporites of the Edlington Formation were deposited in hypersaline lagoons and salt plans landwards of the carbonates. A condensed section, of mostly carbonates, continued to be deposited in the sediment-starved basin centre. When the Roker carbonate platform was exposed and during the development of the sequence boundary, meteoric leaching likely took place, but no karsts have been described.

2.3.4 ZS4 (Fordon Evaporite Fm, Illitic Shale/Grauer Salzton, Brotherton/Seaham Fm)

ZS4 is also a "Type 1" sequence with well-developed lowstand facies (the Fordon Evaporite Formation) deposited primarily in the basin after a sea level fall. The following TST and HST occur within the carbonates.

The fall in sea level created the sequence boundary on top of the Edlington Roker-Concretionary/Kirkham Abbey Formations, and a lowstand wedge of gypsum was precipitated against the foreslope of the shelf and gypsum was deposited on the basin floor where the water was sufficiently deep. A folded anhydrite bed beneath the finely-laminated Basal Anhydrite and on top of the basinal laminated carbonates of the Concretionary Limestone, indicates downslope movement of sulphate from the marginal wedge. This may be due to further sea level fall before the water in the basin was hypersaline enough for sulphate to precipitate.

Deposition of the gypsum-halite wedge and basinal sulphate laminite was succeeded by continued downdraw during which the Fordon Evaporite Formation halite precipitated. The Fordon Evaporite halite is a basin-fill halite. It is possible that higher frequency water-level changes may have occurred in the basin during this LST, which could account for the interbedding of sulphate and chloride in the lower part of fills prior to the main phase of halite precipitation during which several 100 meters of halite accumulated.

Some balance was achieved through periodic seepage into the basin which was enough to maintain halite precipitation but not sufficient to support massive gypsum precipitation. Thin anhydrite laminate within the halite suggests frequent replenishment and or seasonal variations in evaporation. Since halite is a lowstand basin fill much of the basin topography was removed at this point. During the TST the basin and surrounding platform were flooded reflooding which led to the precipitation of anhydrite while the waters were still at a hypersaline stage. Following this the thin

but extensive Illitic Shale/Grauer Salzton was deposited, and then the mid-late TST and HST carbonates of the Seaham/Brotherton Formations.

The gypsum and evaporite dissolution residue between the Roker and Seaham carbonates can be attributed to the Fordon Evaporites and could be the initial deposits of the TST on the flooding of the platforms, instead of the upper part of the Edlington Formation which prograded over the Roker Dolomite.

Salinity was likely slightly higher than normal during the deposition of the Seaham/Brotherton carbonates on the wide low-energy aggraded shelf. At this point the shelf was surrounded by a shallow halite-filled basin. The late HST of the Seaham Formation is indicated by peritidal carbonates and sabkha evaporites.

2.3.5 ZS 5,6 and 7

These are relatively thin compared to ZS 1-4. They could be taken as one whole sequence consisting of several parasequences, or ZS6-7 could be taken together. ZS5-7 are only known from subsurface data, the data from which is itself limited. The depositional environments and original extents and geometries of the evaporites beds are particularly poorly understood.

2.3.5.1 ZS5 (Billingham Anhydrite, Boulby Halite)

The Billingham Anhydrite displays an increase in thickness towards the centre of the basin which may suggest preferential deposition within the basin centre and the aggradation and onlap of the Seaham shelf. This may indicate a hiatus below the Billingham Anhydrite for the basin in the chronostratigraphy shown in Tucker (1991, Fig. 7). Alternatively, the anhydrite was deposited as an extensive gypsum platform with the basinward thickness increase resulting from differential subsistence. Another interpretation is that the Billingham Anhydrite is a late HST of ZS4, but this there is no evidence of basinward progradation, so this is unlikely. The Boulby Halite is also first and foremost a lowstand deposits, formed when the basin was undergoing near-complete desiccation and drawdown, the Boulby Halite has a basin-filling geometry, and likely has a LST to TST interpretation.

2.3.5.2 ZS6 (Carnallitic Marl, Upgang Formation, Sherburn Anhydrite)

ZS6 begins with the Carnallitic Marl Formation which represents the first real siliciclastic input into the basin. An environment with floodplains, coastal plains, salt pans and lagoons, it is more proximal than the underlying Boulby Halite, supporting the suggestion of the sequence boundary being located

between the two. The TST is the Upgang Formation which reflects marine reflooding of the basin, but these waters would have been hypersaline still. The HST may be the Sherburn Anhydrite, however it is only 9m thick.

2.3.5.6 ZS7 (Sneaton Halite, Littlebeck Anhydrite, Roxby Formation)

The LST of ZS7 is the basin centre Sneaton Halite as well as the silts and marls of the Sleights Siltstone at the basin margin maybe as well. The TST is the Littlebeck Anhydrite and the HST and final filling of the Zechstein Basin is the dominantly siliciclastic Roxby Formation.

Chapter 3. Materials and Methods

3.1 Brief description of Fieldwork Sites and Sampling

For a full stratigraphical and lithological description of the fieldwork sites and boreholes used. Included in this Appendix are the total number of samples taken at each locality.

Multiple excursions to acquire samples were undertaken.

- 9th December 2016: Sampling of core material from SM11 Dove's Nest at the Sirius Mineral Plc (York Potash Ltd), Scarborough.
- 5th July 2017: An exploration of Ashfield Brick Pit and Cadeby Quarry. These sites are described by Downie (1967) in his field guide 'Geological Excursions in the Area around Sheffield and the Peak District National Park'
- 2nd January 2018: An excursion to Marsden Bay and Claxheugh Rock accompanied by Paul Gibson (North East Geological Society) to sample the Marl Slate and Roker Dolomite formation exposures. Sites are described in Scrutton (1995) in 'Northumbrian Rocks and Landscape: A Field Guide', specifically from Chapter 13 'The Magnesian Limestone between South Shields and Seaham'
- 25th March 2018: An excursion to the British Geological Survey core store, accompanied by Geoffrey Warrington, to sample the Cadeby Formation from Salterford Farm (Oxton) Borehole from (BGS Memoir Nottingham 126 pp89) and Woolsthorpe Bridge Borehole (BGS Memoir Melton Mowbray 127 pp21)
- 6th December 2018: A second excursion to Sirius Minerals Plc (York Potash Ltd) core store in Scarborough to resample parts of SM11 Dove's Nest, and to carry out sampling of SM4 Gough, SM7 Mortar Hall, and SM14b Woodsmith Mine North Shaft, with an emphasis on evaporative lithologies
- 15th April 2020: Excursion to Pot Riding, Levitt Hagg Hole and Sandal House EZ1 exposures, accompanied by Rick Ramsdale of the Sheffield Area Geology Trust
- Crime Rigg Quarry sample was donated by Paul Gibson (North East Geological Society)
- Little Scar, Seaton Carew, samples were donated by Brian Spencer (Consultant Geologist, formally at FWS Consultants for Sirius Minerals)

All sampling consisted of using a 20oz Estwing chisel head hammer to obtain approximately 50g of material per sample, 50g being enough to allow for multiple maceration attempts. See Appendix C for the field work reports.

3.2 Lithology

The rocks sampled from the borehole and outcrop samples are of a variety of lithologies including anoxic shales, mudstones, evaporites and pure salts including polyhalite, halite, halitic polyhalite, polyhalitic halite, polyhalitic anhydrite, anhydrite, carnallite, sylvinite, as well as argillaceous limestone, dolomitic limestone, dolomitic mudstone, red mudstones. Full details of the methodology used for processing the evaporites can be found in Chapter 8.

3.3 Sample Preparation

Each sample was thoroughly washed and dried, and its lithology examined. 40g was weighed and crushed using a mortar and pestle until a gravel approximately 0.5cm^3 in dimension was achieved. Where possible 20g of the gravel was selected for acid maceration with the remainder being stored for repeated maceration if necessary, and for lithological reference. In instances where insufficient material was present, as much processable material as possible was measured to the nearest whole gram.

3.4 Carbonate Digestion in HCl

The samples underwent a two-stage acid maceration treatment. Samples first underwent an overnight carbonate digestion in 50ml 35% HCl. The samples were then neutralised over a minimum sequence of 3 dilutions each by 50%. Sediment was allowed to settle overnight between each dilution before pouring off any excess liquid to ensure a minimal loss of palynomorphs.

3.5 Silicate Digestion in HF

A minimum of 24 hours after the final HCl dilution, samples were placed in 20ml 40% HF to undergo silicate digestion. After 24 hours 20ml 35% HCl followed by an additional 10ml of 40% HF was added to complete the reaction. The samples remained in HF for a minimum of 3 weeks to ensure sufficient breakdown of the inorganic material. Samples were then neutralised over a minimum 8 dilutions each by 50% following the same method as for HCl dilution, again to ensure a minimal loss of palynomorphs.

3.6 Heavy Liquid Separation

Neutralised samples were sieved using both a 10 µm and 20 µm nylon mesh sieve with the resultant material decanted into centrifuge tubes. Samples were first top-sieved through a 10 µm mesh. A spot

sample was taken to determine the presence of acritarchs. If no acritarchs were found the residue from a 20 µm was used. Samples were centrifuged for 10 minutes at 2000rpm in 35ml of distilled water to settle all residue. The distilled water in each sample was decanted and replaced with 35ml of zinc chloride ($ZnCl_2$) and centrifuged for another 10 minutes at 2000 rpm to thoroughly separate the organic matter from any sediment debris remaining after maceration.

3.7 Storage

Following heavy liquid centrifugation samples were washed and sieved with 2-3 drops of 10% HCl to remove traces of the zinc chloride and protect the nylon mesh of the sieve from damage caused by exposure to the zinc chloride. Samples were stored in water with 1-2 drops of 10% HCl to prevent fungal growth.

3.8 *Lycopodium* Spiking

Samples were spiked with *Lycopodium clavatum* Linnaeus (Stag's-horn Clubmoss) spores prior to oxidisation. *Lycopodium* was added before the oxidisation treatment to accommodate for any palynomorph losses that may occur during subsequent treatments because they behave in the same way during processing as palynomorphs (Lignum *et al.* 2008). *Lycopodium* tablets (density of x=9666, s = ± 2123, V = ± 2.2%) were dissolved in 10% HCl before being added to palynomorphs samples at a ratio of 2 tablets per 5ml of organic yield to enable quantitative counting of the palynomorph assemblage. This residue was placed in permanent storage under water with 1-2 drops of 10% HCl to prevent fungal growth. Some samples i.e., evaporite samples, were not spiked with *Lycopodium* due to the risk of further sieving and washing samples threatening the resulting palynomorph yield.

3.9 Oxidisation

Schulze's Solution (60% nitric acid saturated with potassium chlorate) was used to oxidise samples containing a suitable density of palynomorphs, gauged by preliminary light microscope investigation of a <1ml spot sample. Samples containing enough organic material were oxidised for various lengths of time depending on the colour and condition of the palynomorphs in each sample, and the amount of amorphous organic matter (AOM) obscuring the palynomorphs. Some samples required only a quick oxidisation of 5 minutes, while the darkest samples required longer exposure to the Schulze's Solution, being oxidised overnight for up to 30 hours.

3.10 Halite Samples

Full details of the methodology used for processing evaporites can be found in Chapter 8. Rock salt samples weighing 30-200 g were dissolved in 1 L of boiling water until full dissolution was reached. The solution was then filtered through a (15µm) sieve. The residue was treated with a boiling 40% conc. hydrofluoric acid (HF) treatment for 15 minutes. The residue was neutralized and separated from any remaining clastic particles with zinc chloride solution ($ZnCl_2$ (S.G. 1.95)). In cases where pollen grain morphology was not distinct enough for further analysis, a portion of the sample was treated with Schulze's reagent, a supersaturated solution of 70% conc. nitric acid (HNO_3) and potassium chlorate ($KClO_3$) in order to oxidize and lighten the pollen grains to facilitate analysis. The resulting organic residue (typically <1 ml) was strew mounted onto glass slides for light microscope (LM) analysis. Where possible pollen counts to 200 were conducted per sample. Specimens were photographed using a QImaging (Model No. 01-MP3.3-RTV-R-CLR-10) camera mounted on an Olympus BH-2 transmitted light microscope in conjunction with QCapture Pro software. Individual images were viewed and resized using the GIMP 2.0 software package. Materials are curated in the Centre for Palynology, The University of Sheffield (rock salt, remaining organic residue, LM slides).

3.11 Mounting and Imaging (light microscopy)

Following oxidisation and *Lycopodium* spiking all samples were strew mounted onto glass slides and cured with Petropoxy 154 at 150°C for 30 minutes. A transmitted light microscope was used to assess the condition and colour of palynomorphs and perform 200 minimum counts per sample. Light micrographs were taken using a QImaging (Model No. 01-MP3.3-RTV-R-CLR-10) camera mounted on an Olympus BH-2 transmitted light microscope in conjunction with QCapture Pro software. Images were taken 50x or 100x magnification objective depending on the size of the palynomorphs. Immersion oil was used with the 100x lens to create images of superior clarity.

3.12 Counts

Counts of abundance were taken for all samples, even when they did not contain a typically sufficient density of palynomorphs. Counts were carried out by traversing a slide lengthways from bottom right to upper left-hand corner. The incidence of every palynomorph species was recorded along with the number of *Lycopodium* spores. Counting ceased when the number of palynomorphs reached 200. Damaged but identifiable palynomorphs > c. 50% were counted however any smaller portions (<25%) were disregarded (Riding & Kyffin-Hughes 2010). The location of well-preserved specimens for photography were noted using the England Finder coordinate system. Occurrences of spheroidal

inclusions within the corpus and sacci of pollen grains was also recorded. After completing the 200 count the rest of the slide was covered in the same fashion and any species not occurring in the 200 count were recorded as 'rare'. In slides containing fewer than 200 palynomorphs, counts were still recorded, and while valid have reduced statistical power (Traverse 2007). All counts were rarefied to 200 in 'R' using the rarefy function in the package 'vegan'. See Appendix E for the R-code.

3.13 Quantitative Calculations

Quantitative palynomorph counts were calculated as the number of a given species per unit of rock processed. The abundance of each taxon was calculated as a proportion of overall palynomorph concentration. This method is derived from a combination of Stockmarr's equation (Stockmarr 1971) and Benninghoff's absolute pollen determination method (Benninghoff 1962). These counts will be used to produce pollen diagrams. Draft pollen diagrams were created in R using the 'latticeExtra' and 'analogue' packages and the function stratiplot(). However, due to the inefficiency of these packages the industry standard program Stratabugs will be used to produce the final figures.

The absolute abundances of palynomorphs were calculated using the equation after Benninghoff (1962), which is:

$$c = \frac{m_c \times L_t \times t}{L_c \times w}$$

This is where:

- c the number of indigenous palynomorphs per gram of dry rock (= concentration)
- m_c the number of indigenous palynomorphs counted
- L_t the number of *Lycopodium* spores in each tablet (i.e., 9666)
- t the number of tablets added to the sample
- L_c the number of *Lycopodium* spores counted
- w the weight of dry sediment processed in grams

See Appendix J for a list of *Lycopodium* counts per sample.

3.14 StrataBugs (2.1)

The program StrataBugs was used to create pollen diagrams. All counts, excluding those below 200, were rarefied to 200 in 'R' before being uploaded to StrataBugs. A template displaying depth (m), lithostratigraphy, sequence stratigraphy (where appropriate), analyst, sample depth, palynomorph and microfossils species was created. A lithostratigraphic scheme for the British Zechstein was used to facilitate the drawing of charts. All data from boreholes and outcrops was plotted against this template. These charts can be found in Chapter 6.

3.15 Cluster Analysis (Morisita) in PAST

Clustering analysis (Morisita; after Schneebeli-Hermann *et al.* (2017)) was performed on the composite dataset to identify similar assemblages. Analyses were performed in PAST using a Classical, Paired-Group, Stratigraphic arrangement. See Appendix K for the graphical and numerical outputs of the analysis.

3.16 Transmission Electron Microscopy (TEM)

Some of the residue strew mounted for LM analysis was reserved for picking. Three specimens of each of the three variants of Clarke (1965a) were individually picked for TEM analysis. Picking was achieved by transferring the palynological residue into ethanol and strew mounting this onto glass slides. The ethanol was left to evaporate naturally before slides were examined under a light microscope attached to a micromanipulator. Select pollen grains were individually picked. Picked specimens were encased in agar and dehydrated in 100% ethanol, impregnated with Spurr resin, and cut into ultrathin sections using a diamond knife. Two perpendicular sections were put according to the planes in seen in Chapter 10, Figure 2. Sections were examined and photographed under a FEI Tecnai Spirit TEM at 80kV. Staining with uranyl acetate followed by Reynold's lead citrate (Venable & Coggeshall 1965) did not reveal any additional ultrastructural features. Composite TEM images made from individual micrographs were compiled using the GIMP 2.0 software package.

3.17 Curation

Materials including rock, maceration residue, and slides are housed in the collections belonging to the Centre for Palynology at the University of Sheffield, Dainton Building, Western Bank, S10 2TN, Sheffield, South Yorkshire, U.K.. TEM blocks and sections are help at the Department of Biology at the University of Wisconsin Eau-Claire, Wisconsin, U.S.A.

Chapter 4. Plant Life Cycles

4.1 Reproductive life cycles of land plants

Reproduction in land plants follows the alternation of generations between a distinct haploid sexual stage (sporophyte) and a diploid asexual stage (gametophyte). The relationship between the sporophyte and gametophyte varies among plant groups. The following summaries are based on Bell & Hemsley (2011) and Qui *et al.* (2012).

4.1.1 The life cycle of a moss in which the sporophyte is attached to the gametophyte

In mosses the gametophyte generation dominated over the sporophyte generation and reproduction is reliant on free water. Gametophytes produce haploid gametes, the female part being the archegonium and the male part the antheridium. Antheridia release numerous male gametes (sperm) which swim using their flagella towards the archegonium which contains the female gametes. The haploid gametes merge via fertilization to form a diploid zygote which grows into a diploid sporophyte. The sporophyte produces haploid spores which disperse to give rise to a haploid gametophyte.

4.1.2 The life cycle of a homosporous fern or lycopod

Homosporous ferns produce only one kind of spore which germinates to produce a gametophyte. The manifestations of the two generations are more extreme. Spores are produced by meiosis and they germinate and divide mitotically to form multicellular gametes that are photosynthetically and nutritionally independent. Mature gametophytes bear archegonia and antheridia which produce gametes by mitosis. Gametes are ejected onto damp ground which allow sperm to swim to the egg for fertilization for form a diploid zygote. The zygote divides mitotically, developing into a mature sporophyte.

4.1.3 The life cycle of a heterosporous fern or lycopod

Heterosporous ferns have sporophytes which produce two different kinds of spore. Megasporangia on the sporophyte produce megaspores and microsporangia produce microscopes. The megaspores grow in to megagametophytes while microspores grow into microgametophytes. The megagametophytes produce only eggs while the microgametophytes produce only sperm. Following release, the gametes merge via fertilization to produce a zygote which grows into the next generation of the sporophyte.

4.1.4 The life cycle of a gymnosperm e.g. conifer

Gymnosperms produce seeds and carry both male and female sporophylls on the same sporophyte. The sporophyte is typically arborescent and is the dominant generation, producing haploid male microscopes and female megaspores. The gametophytes are very small and strictly heterosporous with the male being the pollen grain and the female being found in the ovule. Inside male (staminate) cones the microspores form and undergo meiosis to produce a tetrad. Pollen is released and carried by wind to the ovule where the sperm is delivered via a pollen tube to the ovule where fertilization occurs. The ovule is released from the female cone once it has matured into a seed. The sporophyte grows from this seed using the stored food as an energy reserve.

4.1.5 The life cycle of an angiosperm

Angiosperms have incredible reproductive diversity due to their wide variety of pollinators. As in gymnosperms the sporophyte is the dominant phase, they heterosporous, and microspores develop into pollen grains while the megaspore forms the ovule. Male microsporocytes divide to form pollen grains inside the anthers' microsporangia. The female megasporocyte undergoes meiosis to produce four megaspores which further divide via mitosis. The largest form the female gametophyte and the other produce additional cells. Pollen is dispersed from the anthers and once it reaches the stigma of the flower a pollen tube extends down the style and enters the ovule through an opening in the integuments of the ovule, delivering the pollen. A double fertilization event occurs where one sperm and egg combine for form a diploid zygote and the other fuses with one of the additional cells to form a triploid cell which develops into the endosperm (food source). The zygote develops into the embryo and seed forms consisting of toughened layers of integument, the endosperm, and the embryo. Seeds are dispersed and grow into the next generation of the sporophyte.

4.1.6 A brief outline of the macroevolutionary history of these reproductive grades

Transitioning from an aquatic to terrestrial environment required adaptive innovation. The terrestrial dominance of plants was facilitated by the alternation of generations which allows different generations to occupy different niches, enabling plants to sequentially adapt to terrestrial environments, a sporangium in which spores form, a gametophyte which produces haploid cells, and apical meristem tissue in roots and shoots in vascular plants.

Plant reproductive evolution followed a shift from homomorphy to heteromorphy and all land plants (embryophytes) are diplobiontic with both haploid and diploid generations being multicellular (Stewart & Rothwell 1993). Either the gametophyte is the dominant phase of the life cycle as in

bryophytes (liverworts, hornworts, mosses) upon which the sporophyte is highly dependent, or the sporophyte is the dominant phase with a highly reduced gametophyte (seed plants).

In early land plants fluid was still required for reproduction to allow the movement of motile gametes towards stationary female gametes in e.g., the bryophytes. These plants were homosporous and dominated by the haploid sporophyte generation. Haploid populations adapt to environmental change faster allowing the rapid colonization of new niches.

During the transition to vascular plans the major change was the establishment of a free-living sporophyte that gained nutritional independence with the aid of a rooting system. Homosporous ferns have an intermediate position in the continuum of land plant cycles as they have persistent photosynthetic gametophytes as in bryophytes but have elaborate dominant sporophytes like seed plants. The emergency of the diploid phase (sporophyte) as the dominant stage in vascular plant reproduction is advantageous because diploidy allowed the masking of deleterious mutations through genetic complementation.

The Early to Middle Devonian fossil record provides evidence for the origin of heterospory (e.g., Steemans *et al.* 2011) which appears to have evolved several times within land plants making the switch from homospory to heterospory vital for plant macroevolution. The first seed plants appeared in the Late Devonian (e.g., Wang *et al.* 2015). Heterosporous reproduction is coupled with a reduction of the gametophyte phase, shortening the life cycle of the plant and increasing the rate at which new forms appeared, promoting evolution.

The appearance of the seed habit drove the rise and dominance of the first progymnosperms and then the gymnosperms during the late Palaeozoic. Seeds contain a nutrient reserve and can lay dormant for extended periods of time before germinating providing a significant advantage for proliferation and enormous evolutionary implications. The end Permian mass extinction caused a reduction in species diversity of gymnosperm genera (Novak *et al.* 2019) setting the stage for the rise of the angiosperms. Yet seed plants continued to undergo a significant expansion of morphological diversity during the Early-Middle Jurassic with regards to their seed cones (Leslie 2011). Angiosperms arose from the gymnosperms during the Mesozoic (Bell & Hemsley 2007) and they inhabited the seed habit with strengthened tissues with stems and branches acquiring pliancy, and vessels developed from tracheids. Their reproductive regions which became highly specialized, coevolving with their pollinating organisms.

4.2.2 Pollen and spore dispersal and taphonomy

Plants differ in their reproductive output which effects their abundance in the pollen record. Wind-pollinated seed plants (e.g., conifers) as well as some spore-producing plants such as Lycopodium (club moss) Pteridium (eagle fern) and Sphagnum (peat moss) produce large amounts of pollen or spores. In fact, wind-pollinated trees are the major producers of pollen. Partly or wholly insect pollinate (entomophilous) genera produce much less pollen than strictly wind-pollinate (anemophilous) genera. Zoophilous plants, such as many angiosperms, produce parge pollen that can often be clumped.

Following release pollen or spore dispersion has a composite nature, particularly in forests. The transportation pathways of pollen are summarized by Tauber (1965). Pollen and spores can take several pathways including high-level airborne, low-level airborne and water-borne from run off and streams. Pollen dispersal into the atmosphere is affected by the turbulence of the atmosphere, wind speed and direction, the terminal velocity of the falling pollen (related to pollen morphology) (e.g., Theuerkauf *et al.* 2012), and the height and strength of the pollen source (vegetation height, vegetation habitat and the volume produced). However, the majority of pollen falls onto the ground near the parent plant unless the air is turbulent (Prentice 1985).

Pollen source areas are the distance from a pollen deposition point beyond which the relationship between vegetation composition and pollen assemblage does not improve (Sugita 1994). This assumes that distant plants contribute less to pollen deposition at a site. The source area of pollen and spores is related to their dispersal potential and their mode of reproduction and transport, meaning a means that a pollen sample dominated by anemophilous pollen or spores will represent a greater area than one dominated by obligate entomophilous or zoophilous taxa.

The space represented by a sample of pollen and spores is dependent on the taxonomic composition of the flora, its reproductive capacity, and the dispersal method of the pollen grain or spore (Hjelle & Sugita 2012). Recent studies show that modern pollen-assemblage richness does generally reflect the contemporary floristic richness at both local and regional scales (e.g., Birks *et al.* 2016). More modern models show that the Prentice (1985) model for dispersal in neutral and unstable conditions strongly underestimates pollen deposition arriving from distances of 10-100km which underlies approaches that translate pollen percentages into past plant abundances (e.g., Sugita 2007a, b).

It can be possible to distinguish local, regional, and extra-regional pollen within assemblages, depending on the depositional setting and dimensions of the catchment area. In small basins or under a closed canopy pollen produced by local vegetation is well-represented but in large basins where is

pollen produced by trees growing further away the regional signal can overshadow the local signal. Deltaic, fluvial, large lake and marine settings will provide a more regional than local view of the vegetation. The smaller the source area the higher the chance rarer vegetation can be inflated as it concentrates their presence. The dark diversity of pollen richness (e.g., Lewis *et al.* 2016) must also be considered, which is the unseen proportion of species richness in assemblages.

Ultimately, the preservation potential of a pollen or spore depends on the amount of sporopollenin in their exine, which is related to the thickness of the exine and the ratio of endexine to ektexine, with more ektexine meaning more sporopollenin). Sporopollenin content varies between and within broader taxonomic groupings e.g., Equisetum (horsetail) spores (and pollen in the Palaeozoic) have a low preservation potential because of their low sporopollenin content. Horsetail pollen also possess fragile elaters which make them even more susceptible to poor preservability. On the other hand, certain bisaccate producing genera such as Pinus (conifer) has a thick sporopollenin-rich exine and therefore has a high preservation potential.

The substrate pollen and spores land on also exerts strong control over their preservation potential. Acidic environments preserve better than alkaline ones, oxidising environments are notoriously bad at preserving, and low energy sedimentary situations are better than high energy ones.

Chapter 5. Taxonomy

Pollen grain measurements are given in minimum (mean) maximum µm. Measurements were taken using the eyepiece graticule on a BH-2 transmitted light microscope at x40 or x100 magnification. Measurements from Hart (1964) and Clarke (1965a) are included for palynomorphs that were rare (n=1-10).

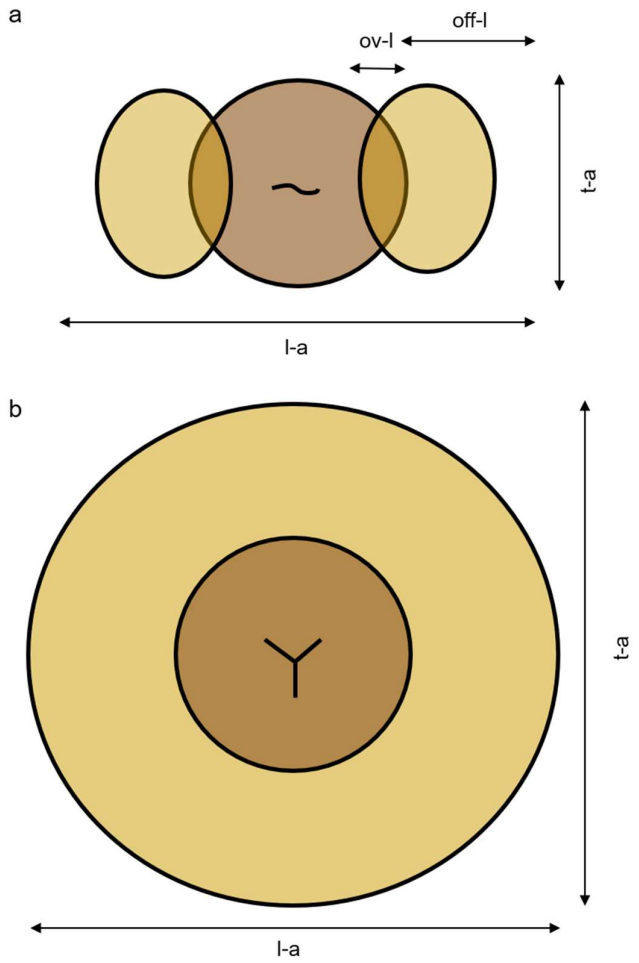

Figure 1. Diagram of a) bisaccate (modelled on *Illinites tectus* and b) monosaccate (modelled on *Nuskoisporites dulhuntyi*) pollen grains illustrating the orientation of the basic measurements used in taxonomic descriptions. t-a=transverse axis, l-a=longitudinal axis, ov-l=saccus overlap, off-l=saccus offlap.

5.1 Glossary

Terminology derived from Halbritter *et al.* (2018)

Alete Describing a spore or pollen grain without a laesura

Bisaccate Describing a pollen grain with two sacci

Diploxylonoid Used to describe the sihlouette of a bisaccate pollen grain where the outline of the sacci in polar view is discontinuous with the outline of the corpus making the grain seem as if it is made of three distinct units

Distal root/zone The distance between the saccin on the distal side of the corpus

Colpus An elongated aperture with a length:breadth ration greater than 2

Corpus The body of a saccate pollen grain. Synonymous with central body.

Exine The outer layer of the wall of a palynomorphs composed of resistant sporopollenin

Haploxylonoid Used to describe sihlouette of a bisaccate pollen grain where the outline of the sacci in polar view is more or less continuous with the outline fo the corpus making the grain seem smooth and elipsoidal

l-a maximum length of the longitudinal axis (vertical axis)

Laesura The mark at the proximal pole of a spore or pollen grain, it is the 'aperture' in the exine

Leptoma The thin-walled fistal side of the corpus in saccate pollen grains (sysnonym of cappula) Limbus

Saccus/sacci air bladder(s)

t-a maximum length of the transverse (horizontal) axis

Taeniae Parallel strips of exine on the proximal side of the corpus, common in gymnospermous pollen grains

Tetrad scar/mark The monolete or trilete mark on the proximal face of spores or pollen grains

Trilete Describing a spore or pollen grain with three laesurae

Triradiate mark a Y-shaped mark on the proximal surface of pre-pollen through which the grain germinated

Trisaccate Describing a pollen grain with three sacci

Monolete Describing a spore or pollen grain with a single laesura

Muri A form of saccus ornamentation made up of interconnected ridges

5.2 Taxonomic descriptions

Plates can be found in the electronic supplement to this chapter.

Potonieisporites Bhardwaj 1954

Synonyms

Hoffmeisterites Wilson

Description Monosaccate. *P. novicus* exhibits 2 sets of folds. The first is located along the inner margin of the spore body and the second set is located closer to the polar region with an orientation perpendicular to the long axis of the grain.

Comparison *Vestigisporites* Hart 1960 appears similar to *Potonieisporites* in polar view however *V. minutus* has a less well-developed saccus laterally. *Florenites* Schopf *et al.* 1944 has a distally attached saccus which is free proximally and has a triradiate mark. *Sahnisporites* Bhardwaj 1954 has a characteristic thickened sulcus.

Potoniesporites novicus Bhardwaj 1954

(Plate I Figure 1, 2)

Remarks Differs from *P. neglectus* Potonié and Lele 1961 in the polygonal or trapezoid shape of the spore body and the smaller lateral width of the saccus. *P. simplex* Wilson 1962 is overall smaller in size and has lips around the laesura. *P. bhardwaji* Remy and Remy 1961 is larger in size and does not have a rim separating the saccus edge and the spore body and has a longer monolete mark.

Dimensions l-a: 40(68)83µm; t-a: 45(64)83µm (n=7)

Perisaccus Naumova 1953 emend. Klaus 1963

Synonym *Simplicesporites* Leschik

Description Monosaccate. In British material *Perisaccus* has secondary folds which cross the central body margin, without displacing it, and two sets of secondary folds which can be seen within the area of the aperture. *Perisaccus* differs from *Florinites* in the position of the saccus attachment which is distal in *Florinites*. *Endosporites* Wilson & Coe has a larger Y-mark which *Perisaccus* does not have and *Remysporites* Butterworth & Williams 1958 has a larger Y-mark. *Nuskoisporites* Potonié & Klaus has a saccus that is attached both proximally and distally. *Accinctisporites*, *Patinasporites*, *Zonalisporites*, and *Succinctisporites* are monosaccates but are alete.

Perisaccus granulosus Leschik 1955 emend. Clarke 1965

(Plate I Figure 2, 3)

Synonym

Simplicesporites granulosus Leschik

Perisaccus granulatus Klaus

Remarks Circular or oval central body. Central body is smooth with a small triradiate mark in the centre. This Y-mark is one-third the radius of the central body and often open. The saccus is proximally attached to the central body while the distal surface remains free. The saccus transverse-axis is less than half the central body transverse-axis. The saccus is covered in closely packed isodiametric granules with a diameter of 1µm.

Dimensions l-a: 83(94)113µm; t-a: 60(80)105µm (n=7)

Perisaccus laciniatus Leschik 1955 emend. Clarke 1965

(Plate I Figure 5, 6)

Remarks *P. laciniatus* as emended by Clarke (1965) is different from *P. virgatus* comb. nov. in that it lacks spines attached to the granules. It differs from *P. granulosus* comb. nov. only in its considerably larger saccus and larger saccus offlap diameter. Overall size is within the range of *P. granulosus*.

Dimensions l-a: 55(74)100µm; t-a: 50(70)88µm (n=10)

Vestigisporites Balme and Hennelly 1955 emend. Hart 1960

Synonym *Sahnites* Pant 1955 partim

Description Monosaccate with a haploxylonoid outline. The central body is circular or oval with an elongation of the longitudinal-axis. The proximal surface has a centrally placed monolete aperture. The terminal sacci are laterally united into a bladder that forms a continuous equatorial air chamber with terminal swellings. *Vestigsporites* differs from *Illintes* in the shape of the proximal aperture and the monosaccate condition.

Vestigisporites minutus Clarke 1965

(Plate I Figure 7-9)

Remarks Small, bilateral, monolete monosaccate. The central body is circular (rarely oval) with a thin exine. The small terminal saccus swellings are connected laterally by the exoexinal strip. The sacci are covered in infra-reticulate sculpture. The distal saccus attachment leaves an elongated oval free where the exine is thin. The central body is smaller and darker spore than *V. hennellyi* Hart 1960.

V. hennellyi also has a reduction of the lateral saccus extension creating a bisaccate condition.

Dimensions 53(62)70µm; l-a: 33(40)53µm (n=20)

Nuskoisporites Potonié & Klaus 1954

Synonyms *Zonotriletes partim*

Description Monosaccate. Essentially circular in outline. The central body can be circular, oval, or even slightly triangular. The proximal root is intra-marginally attached meaning the proximal zone is normally less than three-quarters of the radius of the central body. The central body bears a distinct trilete aperture which is rarely absent. The saccus sculpture is infra-reticulate. There is a distinct equatorial limbus. *Nuskoisporites* differs from *Cordaitina* in that it has a distinct trilete aperture, a strong limbus, and an intra-marginally attached proximal root.

Nuskoisporites dulhuntyi Potonié & Klaus 1954

(Plate I Figure 10)

Synonyms

Zonotriletes sarcostemmus Luber & Valts 1941 *partim*

Nuskoisporites klausi Grebe 1961

Remarks Circular outline and central body with a distinct trilete aperture. The sutures of the aperture are less than half the radius of the central body. The saccus offlap is less than half the central body radius and the saccus offlap:overlap is 1.5:1 or 2:1. The limbus is distinct.

Dimensions l-a: 108µm; t-a: 90µm (n=2) (maximum diameter is 80-200 µm (Hart, 1964))

Nuskoisporites cf. *rotatus* Balme & Hennelly 1965

(Plate I Figure 11)

Synonym

Cordaitina rotatus Balme and Hennelly 1955

Remarks Circular outline. The circular central body has a trilete aperture that can extend the complete radius of the central body. The sacci offlap is distinctly greater than the overlap. The outline of the central body is very regular and the structure is infra-reticulate so that it appears to be infra-punctate. *N.* cf. *rotatus* is distinguished by its trilete aperture, the central body to maximum diameter ratio, and the saccus infra-structure.

Dimensions l-a**:** 90µm; t-a: 78µm (n=1) (maximum diameter: 79-219µm (Hart, 1964))

Crustaesporites Leschik 1956

Description Polysaccate. Typically with three simple sacci and a circular, sub-circular, or triangular central body. The proximal cap has striations and ribs similar to the striate bisaccates. *Crustaesporites* is different from *Alatisporites* Ibrahim in its ribs and striations on the proximal cap.

Crustaesporites globosus Leschik 1956

(Plate I Figure 12)

Remarks Sub-circular to roundly triangular central body. The sacci are distinctly smaller than the central body. The sacci are reniform in shape, unite laterally, and the saccus offlap is greater than the overlap and attachment lines can be present. There are six to eight ribs on the proximal cap which often anastomose.

Dimensions l-a: 88µm t-a: 88µm (n=1) (maximum diameter: 95µm (Hart, 1964))

Lueckisporites (Potonié & Klaus 1954) Jansonius 1962

Synonym

Striatites Pant 1955 *partim*

Description Bisaccate. Diploxylonoid. The central body is circular or elongated along the longitudinal-axis. The proximal cap has two longitudinal ribs in polar view. Sacci are more or less semi-circular in shape and their structure is infra-reticulate. The distal root is less than the transverse-axis of the sacci. The distal zone is approximately one-third or less than the longitudinal-axis of the central body in dimension. Differs from *Protohaploxypinus*, *Striatopodocarpites*, and *Striatoabietites* in the number of longitudinal ribs on the proximal cap.

Lueckisporites virkkiae Potonié & Klaus 1954 emend. Clarke 1965

(Plate II Figure 1-5)

Remarks Slightly diploxylonoid. The central body is circular or has a slight elongation of the longitudinal-axis. The proximal surface has two ribs separated by a wide central striae. The sacci are less than semi-circular in shape and the transverse-axis of the sacci is slightly greater than the transverse-axis of the central body. Distal roots are convex meaning the distal zone is centrally more than half the transverse-axis of the central body in dimension. In the British Zechstein, *L. virkkiae* is divided into three morphological variants. Variant A possesses well-developed proximal thickenings, which are distinctly separate, and well-developed sacci, being most similar to *L. microgranulatus* Klaus 1963. Variant B is most similar to *L. parvus* Klaus 1963 and has a smaller body, smaller saccus and a small saccus offlap. Variant C has a weakly-developed proximal cap with incomplete separation

of the proximal ribs, is generally smaller in size than Variant A, and is most similar to *L. microgranulatus* "kleinere variante" Klaus 1963.

Dimensions *L. virkkiae* Variant A t-a: 55(75)95µm and l-a: 30(43)53µm (n=20), *L. virkkiae* Variant B t-a: 38(48)70µm and l-a: 30(43)62µm (n=22), *L. virkkiae* Variant C t-a: 55(60)70µm and l-a: 25(39)58µm (n=20)

Taeniaesporites (Leschik 1956) Jansonius 1962

Synonyms

Lueckisporites Potonié & Klaus 1954 *partim*

Lunatisporites Leschik 1955

Succinctisporites Leschik 1955

Striatites Pant 1955

Jugasporites Leschik 1956 (pars.)

Pollenites Pautsch 1958

Lueckisporites Potonié & Klaus, Grebe & Schweitzer 1958 (pars.)

Striatites Pant 1963; Schaarschmidt (pars.)

Striatites Pant 1963

Descriptions Diploxylonoid to haploxylonoid striate bisaccate. The central body is circular or elongated along the longitudinal axes. The proximal cap has three to five ribs in polar view. The length of the distal root is equal to or slightly less than the transverse-axis of the central body. The distal zone is greater or equal to one-third of the longitudinal-axis of the central body in dimension. *Taeniaesporites* differs from other taeniate bisaccates in the number of ribs it has in polar view. For this genus the shape of the sacci and the comparative size of the central body and sacci are not used as diagnostic features.

Taeniaesporites albertae Jansonius 1962

(Plate II Figure 6)

Remarks Slightly diploxylonoid. The central body is elongated along the longitudinal-axis. The proximal cap has four longitudinal ribs in polar view. The sacci are semi-circular or less in shape. The transverse-axis of the sacci is less than or equal to the transverse-axis of the central body. The distal zone varies from one-quarter to one-half the longitudinal-axis of the central body in dimension. *T. albertae* differs from the rest of the genus by the distal lateral separation of its sacci (*T. kraeuseli*) and small sacci (*T. noviaulensis* and *T. sulcatus*)

Dimensions t-a: 30(58)73µm; l-a: 33(42)53µm (n=8)

Taeniaesporites angulistriatus (Klaus 1963) emend. Clarke 1965

(Plate II Figure 7)

Synonyms

Striatites angulistriatus Klaus 1963

Striatites ovalis Schaarschmidt 1963

Remarks *T. angulistriatus* is distinctive for its small size. The distal root area is narrow. The longitudinal ribs and sacci are both covered in scabrate sculpture. *T. angulistriatus* differs from *T. kraeuseli* Leschik in the shape and sculpture of the sacci, and from other species in its rib and saccus sculpture.

Size t-a: 45(66)75µm; l-a: 38(41)45µm (n=6)

Taeniaesporites bilobus Clarke 1965

(Plate II Figure 8)

Remarks Diploxylonoid outline. Small, dark coloured, circular central body. The proximal cap has up to five parallel longitudinal ribs. The sacci are relatively larger than the central body and have a medium infra-reticulum with a radial alignment from the saccus roots. *T. bilobus* is distinguished by its comparatively larger sacci and the circular central body.

Dimensions t-a: 65(78)88µm; l-a: 30(45)55µm (n=3) (t-a: 28-33µm; l-a: 60-79µm (Clarke, 1965))

Taeniaesporites labdacus Klaus 1963

(Plate II Figure 9-10)

Synonyms

Lueckisporites sp. Potonié & Klaus 1954 *partim*

Lueckisporites noviaulensis Grebe & Schweitzer

Remarks Haploxylonoid outline. The proximal cap has four longitudinal ribs of which the central pair are more developed than the lateral ones. The ribs may join terminally to form an elevated rectangular area around the proximal pole. The sacci are covered in thick muri which form a coarse infra-reticulum.

Dimensions t-a: 70(84)100µm and l-a: 38(46)55µm (n=23)

Taeniaesporites noviaulensis Leschik 1956

(Plate II Figure 11)

Synonyms

Taeniaesporites novimundi Jansonius 1962 *partim*

Lueckisporites noviaulensis Grebe & Schweitzer 1962

Striatites noviaulensis Schaarschmidt 1963

Taeniaesproites ortisei Klaus 1963

Remarks Diploxylonoid outline. The central body is circular or has an elongation of the longitudinal-axis. The proximal cap has four longitudinal ribs in polar view. The sacci are semi-circular or greater and distinctly separate laterally. The transverse-axis of the sacci is greater than the transverse-axis of the central body. The distal zone is one-half or more than the longitudinal-axis of the central body in dimension. *T. noviaulensis* differs in its wider distal zone and sacci which are more than semi-circular. *T. noviaulensis* differs from *T. novimundi* in the shape of the central body, the form of the taeniae, and the shape and sculpture of the sacci.

Size l-a: 55(90)112µm; t-a: 45(50)68µm (n=20)

Taeniaesporites novimundi Jansonius 1962

(Plate II Figure 12)

Synonym *Taeniaesporites noviaulensis* Jansonius 1962 *partim*

Remarks Diploxylonoid outline. The central body is circular or with a distinct elongation of the longitudinal axis. The central body has four ribs on the proximal surface. The sacci are greater than or approximately semi-circular in shape and are distinctly separate laterally. The transverse-axis of the sacci is greater than the transverse-axis of the central body. The distal zone is half or more of the longitudinal-axis of the central body in dimension. *T. novimundi* differs from *T. noviaulensis* in having a slightly more round, and less elongated longitudinal-axis of the central body.

Dimensions l-a: 78(87)100µm; t-a: 30(50)70µm (n=20)

Protohaploxypinus (Samoilovich 1953) emend. Hart 1964

Synonyms

Striatopinites Sedova 1956

Striatopiceites Sedova 1965

Lueckisporites Potonié & Klaus 1954 *partim*

Lunatisporites Leschik 1956

Protosacculina Malyavkina 1953 *partim*

Striatites Pant 1965

Taeniaesporites Leschik 1965 *partim*

Faunipollenites Bhardwaj 1963

Rhytisaccus Naµmova 1939 *partim*

Striatocordaites ex Abramova & Marchenko 1960

Striatoconiferites ex Abramova & Marchenko 1960

Striatohaploxypinites ex Abramova & Marchenko 1960

Pemphygalates Luber & Valts 1941 *partim*

Coniferalates Andreyeva 1956 *partim*

Description Striate bisaccate. Haploxylonoid to slightly diploxylonoid. Circular or oval central body with a slight transverse-axis or lateral-axis elongation. The proximal cap is divided into four or more longitudinal ribs. The sacci shape varies from semi-circular, less than semi-circular, or slightly greater than semi-circular in shape. The sacci sculpture is infra-reticulate. The distal root length is equal to or slightly less than the transverse-axis of the central body. The distal zone is less than or equal to two-thirds of the lateral-axis of the central body.

Protohaploxypinus chaloneri Clarke 1965

(Plate III Figure 1, 2)

Remarks Circular or subcircular central body. The proximal cap has ten to twelve longititudinal ribs which are interrupted and anastomose. The sacci are semi-circular in outline. The sacci infrasculpture is a well-defined microreticulum without a radial pattern. *P. microcorpus* is most similar to *P. minor* (Klaus 1963) comb nov. but differs in the shape of the sacci and presence of distal attachment thickenings.

Dimensions t-a: 55(75)98µm and l-a: 40(52)73µm (n=22)

Protohaploxypinus jacobii (Jansonius 1962) Hart 1964

(Plate III Figure 3, 4)

Synonym

Striatities jacobii Jansonius 1962

Remarks Slightly diploxylonoid. Circular, or more or less circular, central body. The proximal cap has ten to twelve ribs. The sacci are semi-circular or less than semi-circular in shape. The sacci can unite laterally but do not form bladders. The distal zone is one-third to two-thirds the lateral-axis of the central body in dimension. *P. jacobii* differs from *P. latissimus* in its slight diploxyponoid outline, from *P. dvinensis* which has a flattened lateral margin of the central body, and from *P. amplus* which has a narrower distal zone and relatively larger sacci. The number of longitudinal ribs are a distinguishing feature.

Dimensions l-a: 75(95)103µm; t-a: 40(52)78µm (n=20)

Protohaploxypinus microcorpus (Schaarschmidt 1963) emend. Clarke 1965

(Plate III Figure 5)

Synonyms

Striatites jacobii Jansonius 1963

S. microcorpus Schaarschmidt 1963

Remarks Haploxylonoid to slightly diploxylonoid. The central body is circular to sub-circular with a slight elongation along the transverse-axis. The proximal cap has between ten and twenty crowded and interrupted longitudinal ribs.

Size l-a: 45(61)75µm; t-a: 33(47)70µm (n=12)

Protohaploxypinus cf. samoilovichii (Jansonius 1962) Hart 1964

(Plate III Figure 6)

Synonym

Striatites samoilovichii Jansonius 1962

Remarks Slightly diploxylonoid. Circular central body. The proximal cap has six to ten longitudinal ribs visible in polar view. The sacci are roughly semi-circular or slightly greater than semi-circular and are slightly smaller than the central body in size. The distal zone is one-third or less than the longitudinal-axis of the central body in dimension. The distal roots have attachment lines. *P*. cf. *samoilovichii* from other *Protohaploxypinus* species in its distal root attachment lines.

Dimensions l-a: 75(94)113µm; l-a: 40(60)90µm (n=5) (t-a: 60(66)70µm (Clarke, 1965))

Striatopodocarpites Sedova 1956 emend. Hart 1964

Synonyms

Striatites Pant 1955 *partim*

Taeniaesporites Leschik 1956 *partim*

Lueckisporites Potonié & Klaus 1954 *partim*

Phytisaccus Naµmova partim

Strotersporites Wilson 1963

Rhizomaspora Wilson 1963

Verticipollenites Bhardwaj 1963

Lahirites Bhardwaj 1963

Hindipollenites Bhardwaj 1963

Description Striate bisaccate. Strongly to moderately diploxylonoid. The length of the distal roots of the sacci is less than the diameter of the central body in transverse direction. The central body is circular to slightly oval in outline and has a proximal cap that is divided into four or more longitudinal ribs. The sacci are noticeably larger than the central body and are semi-circular in shape. Sometimes the terminal sacci can become fused to form slight lateral bladders. *Striatopodocarpites* (Sedova

1956) emended differs from *Protohaploxypinus* (Samoilovich 1953) in its strong diploxylonoid outline, greater than semi-circular sacci, and relatively small central body size.

Striatopodocarpites fusus (Balme and Hennelly) Potonié 1958

(Plate III Figure 7)

Synonyms

S. globosus Leschik 1959

Lueckisporites fusus Balme and Hennelly 1955

Remarks Strong diploxylonoid. Central body more or less circular. The sacci are large and covered in a fine radial reticulate sculpture. The proximal cap is covered in six to ten faint ribs that anastomose, and is divided into irregular blocks by small splits perpendicular to the long axis of the grain. The distal zone is narrow, typically less than one quarter longitudinal-axis of the central body in dimension. *S. fusus* differs from the type species by the absence of sacci, the narrower distal zone, and the faint nature of the ribs.

Dimensions l-a: 80(110)148µm; t-a: 50(73)8µm (n=5) (l-a: 81(112)146 µm; t-a (central body): 28(38)48µm (Hart, 1964))

Striatopodocarpites antiquus (Leschik) Potonié 1958

(Plate III Figure 8)

Remarks The sacci can sometimes fuse laterally making the pollen monosaccate. *S. antiquus* differs from *S. phaleratus* (Balme and Hennelly) Hart 1964 in the lack of a distal groove bordering the lips, and from *S. balmei* Sukh Dev 1959 in its narrower ribs and smoother saccus reticulum.

Dimensions t-a: 58(103)123µm; l-a: 55(70)83µm (n=6)

Striatoabietites Sedova 1956 emend. Hart 1964

Synonyms

Lueckisporites Potonié & Klaus 1954 *partim*

Pemphygalates Luber and Valts 1941

Protodiploxypinus Samoilovich 1953 *partim*

Description Striate bisaccate. Diploxylonoid. The central body is circular or elongated longitudinally. The proximal cap has six or more longitudinal ribs in polar view. The distal root length is equal to or less than the transverse-axis of the central body. The sacci are smaller than the central body and the transverse-axis of the sacci is more or less equal to the transverse-axis of the central body. The distal zone is usually more than half the longitudinal axis of the central body in dimension.

Striatoabietites (Sedova 1956) emend. Hart 1964 differs from *Striatopodocarpites* (Sedova 1956) emend. Hart 1964 in how the sacci are smaller than the central body, its wider distal zone and is less diploxylonoid. *Protohaploxypinus* (Samoilovich 1953) emend. Hart 1964 is more haploxylonoid and has a narrower distal zone.

Striatoabietites richteri (Klaus 1955) Hart 1964

(Plate III Figure 9)

Synonyms

Lueckisporites richteri Klaus 1955

Taeniaesporites richteri Leschik 1956

Striatites richteri Potonié 1958

Illintes Stratus Orlowska-Zwolinska 1962

Striatities richteri Potonié 1963; Schaarschmidt

Stroterosporites jansonii Klaus 1963

Stroterosporites richteri Klaus 1963

Remarks Central body is circular or has an elongation of the longitudinal-axis. The proximal cap has twelve to sixteen longitudinal ribs in polar view. The distal zone is one-half or three-quarters the longitudinal-axis of the central body in dimension. The sacci are semi-circular or slightly greater than semi-circular in shape. *S. richteri* is distinguished by the shape of its sacci and how its transverse-axis is slightly greater than that of the central body and differs from *Striatopodocarpites* in its wide distal zone and a more elongate body.

Dimensions l-a: 88(101)115µm; t-a: 55(71)90µm (n=3) (l-a: 108µm; t-a: 59µm (Hart, 1964))

Vittatina Luber ex Jansonius 1962

Synonym

Striatoluberae Hart 1963

Description Striate bisaccate with highly reduced sacci. Bisaccate forms have minute, barely noticeable, terminally attached sacci. In species where sacci are developed *Vittitina* is more diploxylonoid. The proximal cap is divided into longitudinal ribs which meet terminally and can anastomose or they can crowd together terminally. Distally the body can be granular, laevigate, or transversely striated. Terminally the longitudinal ribs may pass onto the distal surface. When they meet in a regular pattern they give the effect of terminal transverse striations on the distal surface. This genus differs from other striate bisaccates in its reduced or absent sacci.

Vittatina hiltonensis Chaloner and Clarke 1962

(Plate III Figure 10, 11)

Remarks Strictly asaccate. The entire proximal face is covered in thick exinous longitudinal ribs that run parallel with the long equatorial axis. They are separated by relatively narrow striae. The ribs do not appear to anastomose but can be displaced or twisted locally.

Dimensions t-a: 38(49)62µm and l-a: 30(46)65µm (n=11)

Illintes (Kosanke) emend. Potonié & Kremp 1954

Synonyms

Limitisporites Leschik 1963 emend. Schaarschmidt

Jugasporites Leschik 1963 emend. Klaus

Limitisporites Leshick 1963; Klaus

Description Bisaccate. Haploxylonoid to diploxylonoid. The central body is circular or oval with a slight longitudinal-axis or transverse-axis elongation. The proximal surface of the central body has a central trilete aperture. The surface of the central body is either finely granulate, laevigate or punctate. The sutures of the trilete mark are either equal or of unequal lengths.

Illintes delasaucei (Potonié and Klaus) Grebe & Schweitzer 1962

(Plate IV Figure 1)

Synonyms

Limitisporites delasaucei Schaarschmidt

Jugasporites delasaucei Leschik

Remarks The central body is circular with a slight elongation along the longitudinal axis of the central body. The sacci can be laterally connected by an exoexinal strip up to 9µm wide. The sacci have an infra-reticulate sculpture. The arms of the trilete mark are of unequal lengths.

Dimensions t-a: 50(58)73µm and l-a: 38(44)63µm (n=20)

Illintes klausi Clarke 1965

(Plate IV Figure 2)

Remarks The large circular central body has a small triradiate mark. The sacci are small and crescent shaped in polar view and semi-circular or less in shape. The proximal cap has a large triangular area where the exine is thin which contains the Y-mark. The saccus sculpture is a fine reticulum. *I. klausi* differs from *I. parvus* Klaus 1963 in the structure of the proximal face. It differs from other members of the genus in the shape of the saccus offlap.

Dimensions l-a: 40(50)70µm; t-a: 38(41)48µm (n=6) (l-a: 41(47)50µm; t-a: 27(32)39µm (Clarke, 1965))

Illintes tectus Leschik 1956 emend. Clarke 1965

(Plate IV Figure 3, 4)

Remarks Circular to slightly elongate central body with a slight elongation along the longitudinal-axis. The sacci are semi-circular or crescent-shaped. The tetrad scar is less variable than that of *I. delasaucei*. *I. tectus* has two roughened areas, or thickenings, on either side of the tetrad scar.

Dimensions t-a: 55(65)75µm and l-a: 30(40)48µm (n=20)

Labiisporites Leschik emend. Klaus 1963

Description Bisaccate. *Labiisporites* differs from *Illintes* in that it has no Y-mark and no distal sulcus. It is different from *Alisporites* emend. Nilson 1958 in how it has a distinct central body, a coarser infra-reticulum on the sacci, and is overall larger in size with a triangular outline.

Labiisporites granulatus Leschik 1956

(Plate IV Figure 5, 6)

Synonym

Limitisporites granulatus Leschik 1956

Remarks Haploxylonoid. The central body has a distinct transverse-axis elongation and a granulate sculpture. The sacci are semi-circular or less in outline and smaller than the central body. The distal zone is one-third or less than the transverse axis of the central body. *L. granulatus* differs from *Limitisporites granulatus*, *L. lepidus* and *L. monstruosus* in its outline, shape of the central body and with of the distal zone, as well as the granulate sculpture.

Dimensions l-a: 33(45)58µm; t-a: 35(43)53µm (n=22)

Klausipollenites Jansonius 1962

Synonym

Falcisporites Leschik emend. Schaarschmidt

Piceapollenites Potonié 1931

Remarks Bisaccate. Haploxylonoid. The longitudinal-axis of the central body is elongated. A monosaccate condition is sometimes possible if the sacci unite laterally. Sacci are smaller than the central body. Differs from *Falcisporites* emend. Klaus 1963 in its elongated outline and lack of a distal furrow. Differs from *Alisporites* Nilsson 1958 in the oblate outline and absence of clear saccus attachments.

Klausipollenites schaubergeri Potonié & Klaus emend. Jansonius 1962

(Plate IV Figure 7, 8)

Synonym

Falcisporites schaubergeri Schaarschmidt

Remarks An ubiquitously Zechstein bisaccate. The longitudinal-axis is elongated and the sacci are smaller than to the central body. The sacci may unite laterally to form a monosaccate. *K. schaubergeri* is distinguished from *Vestigisporites minutus* by the emphasised longitudinal-axis, more elongate outline, larger size, and bisaccate condition.

Dimensions l-a: 60(72)95µm; t-a: 30(42)53µm (n=24)

Falcisporites Leschik emend. Klaus 1963

Description Bisaccate. Haploxyponoid with a circular central body. Different from *Klausipollenites* as it has sacci are not laterally connected. *Paravesicaspora* Klaus 1963 differs in its rhombic-shaped central body and sacci that connect laterally.

Falcisporites zapfei (Potonié & Klaus) Leschik 1956

(Plate IV Figure 9, 10)

Synonym *Pityosporites zapfei* (Potonié & Klaus) Leschik 1956

Remarks The circular central body has a transverse narrow sulcus. The sacci are similar in size to the central body and approximately semi-circular in shape. The distal zone is distinct.

Dimensions l-a: 85(95)106µm; t-a: 55(66)73µm (n=24)

Alisporites Daugherty emend. Nilsson 1958

Description Haploxylonoid to slightly diploxylonoid. Transverse distal sulcus runs centrally across the central body. The central body is circular to oval with an elongation along the lateral-axis or longitudinal-axis. The sacci are equal or less than the size of the central body and less than or approximately semi-circular in shape. The transverse-axis of the central body is greater than or equal to the transverse-axis of the sacci. The distal zone varies in length, being distinct to obscure. *Alisporites* has a distinct centrally placed distal transverse sulcus. *Alisporites* differs from *Falcisporites* emend. Klaus in the more distinct prolate central body.

Alisporites nuthallensis Clarke 1965

(Plate IV Figure 11)

Remarks Elliptical-shaped central body where the transverse-axis exceeds the longitudinal-axis. The

central body is dark in colour with a reticulate sculpture. The sacci are well-developed and joined laterally by a very thin exoexinal strip. The sacci are covered in a medium infra-reticulate sculpture. Close resemblance with some *Caytonanthus* Harris pollen.

Dimensions l-a: 63(75)108µm; t-a: 30(43)58µm (n=20)

Platysaccus (Naumova) ex Potonié & Klaus 1954

Synonyms

Lueckisporites Potonié & Klaus 1955, Balme and Hennelly

Cuneatisporites Leschik 1955

Cuneatisporites Leschik 1962, Bhardwaj

Description This genus is distinguishable by its distinctive diploxylonoid outline and non-striate body.

Platysaccus radialis (Leschik 1955) emend. Clarke 1965

(Plate IV Figure 12)

Synonym

Cuneatisporites radialis Leschik 1955

Remarks The central body is oval with the width exceeding the length. The proximal face is granular or scabrate. The sacci are discrete and three-quarters circular in outline and the offlap is greater than the overlap. One edge of the saccus is attached equatorially while the other is attached near the distal pole. The distal attachments come with crescent shaped thickenings which may be folds which usually extend to the equator. A leptoma is present but no colpus is seen within this area. The saccus sculpture is medium reticulate and a radial pattern is observed starting at the saccus roots. Different from *P. papilionis* in the shape of the spore body. *P. umbrosus* Leschik 1956 has an irregular enveloping saccus. *P. leschicki* Hart 1960 is much larger than *P. radialis*.

Dimensions l-a: 60(76)95µm; t-a: 33(39)45µm (n=5) (l-a: 41(45)40µm; t-a: 56(64)77µm (Clarke, 1965))

C*ycadopites* (Wodehouse 1935) Wilson and Webster 1946

Description Monocolpate. *Cycadopites* has an elliptical outline with a thin exine, a well-defined irregular sulcus that extends to the equatorial margin and the sculpture is finely granular.

Cycadopites rarus Clarke 1965

(Plate IV Figure 13)

Remarks The elliptical outline is 'squared off' where the irregular sulcus is open. *C. rarus* is large. It is most similar to *Ginkgocycadophytus* sp. Samoilovich 1953.

Dimensions l-a: 100µm; t-a: 75µm (n=1) (l-a: 66-108µm; t-a: 28-40µm (Clarke, 1965))

Non-Pollen Taxonomical Descriptions

Reduviasporonites Wilson 1962 emend. Foster *et al.* 2002

Synonyms

Reduviasporonites Wilson 1962

Chordecystia Foster 1979

Tympanicysta Balme 1980

Description Microfossil of fungal or algal affinity that usually forms chains but is also present as pairs of cells or singular cells. Most cells contain an inner body of the same shape and can be adpressed to the inner surface of the cell. Two species: *R. catenulatus* and *R. chalastus*. *R. catenulatus* is subcircular or oval in outline suggesting an original spherical or ovoid shape. *R. chalastus* is subrectangular suggesting an original cylindrical shape.

Reduviasporonites cf. *catenulatus* Wilson 1962

(Plate V Figure 1)

Remarks *R.* cf. *catenulatus* is found as either chains or dispersed pairs and single cells. The cells are sub-circular or sub-rectangular suggesting the original cells were sub-spherical in shape. The inner body is adpressed to the outer wall and is similar in shape to the outer wall.

Dimensions l-a: 14µm; t-a: 15µm (Foster *et al.*, 2002)

Additional findings

Cingulate trilete spore ?*Densoisporites* spp. (Plate IV Figure 14) and cavate trilete spores (Plate IV Figure 15), Acanthomorph acritarchs (Plate V Figure 2) have also been recovered but not at significant abundance alongside foraminiferal test linings (Plate V Figures 3-4), tetrads (Plate V Figure 5-7) and possible aberrant trisaccate morphs of bisaccates (Plate V Figures 8-12).

Chapter 6.

The use of spore-pollen assemblages to reconstruct vegetation changes in the Permian (Lopingian) Zechstein deposits of northeast England

Martha E. Gibson[a*] and Charles H. Wellman[a]

[a]Department of Animal & Plant Sciences, University of Sheffield, Alfred Denny Building, Western Bank, Sheffield S10 2TN, UK.

[*]marthae.gibson@gmail.com

Status as of 11th November 2020: manuscript under review in Review of Palaeobotany and Palynology. I undertook the fieldwork, sample processing, data collecting and data interpretation for this paper.

6.1 Abstract

New boreholes have enabled, for the first time, extensive palynological sampling through the entire Lopingian Zechstein sequence of northeast England. Palynomorph assemblages have been recovered from throughout the sequence from all five of the evaporation-replenishment cycles (EZ1-EZ5). These assemblages are dominated by pollen grains, with rare trilete spores, and even rarer marine forms such as acritarchs and foraminiferal test linings. The assemblage of pollen grains is of low diversity (35 species) and dominated by taeniate and non-taeniate bisaccate pollen. The assemblage varies to only a limited extent both within and between cycles, although some minor variations and trends are documented. Based on the composition of the dispersed spore-pollen assemblages, and previous work on the Zechstein megaflora, the hinterland vegetation is interpreted as being dominated by conifers that inhabited a semi-arid to arid landscape. This flora is shown to have persisted throughout the entire Zechstein sequence, despite previous assertions that it disappeared as conditions became increasingly drier over the course of the latest Permian.

Key words: palaeobotany, palynology, pollen, spores, vegetation change, Permian.

6.2 Introduction

The Lopingian Zechstein Sea was a large intercontinental sea located in Pangaea just north of the equatorial Central Pangaean Mountain Range. A remarkable stratigraphical sequence deposited in the sea is dominated by carbonate/evaporite cycles. The sequence can be divided into seven cycles at the centre of the basin, although this is reduced to five cycles towards the margins (EZ1-5) (Figure 1).

These cycles essentially represent a sequence of large-scale evaporation-replenishment events. The biota of the Zechstein Sea and surrounding hinterlands is also remarkable. Marine biotas are impoverished due to high salinities. Although reefs developed during the early cycles, these diminished and then vanished as conditions became more saline and harsher during the later cycles. Palaeobotanical and palynological studies reveal that a typical Euramerican flora occupied the hinterlands, low lying areas and riparian environments around the Zechstein Sea during the early cycles (EZ1-2). However, hitherto there has been little floral evidence in later cycles (EZ3-5) and it is often assumed that vegetation diminished as harsher desert conditions prevailed as the climate became warmer and drier. It is of particular interest that the sequence accumulated during the build up to the end-Permian mass extinction (Erwin, 1993; Benton and Twitchett, 2003; Erwin, 2006; Hallam and Wignall, 1997) and there is some evidence that the event may itself be reflected in the highest cycle toward the centre of the basin (e.g., García-Veigas et al., 2011).

Recently, new boreholes have become available that penetrate the younger cycles (EZ3-5) at the margins of the Zechstein Sea in northeast England. These have yielded, for the first time, rich palynomorph assemblages from these younger cycles. This paper reports on a quantitative analysis of these palynomorph assemblages, in addition to those from older cycles (EZ1-2) collected at outcrop. The new data provides evidence for the nature of the hinterland vegetation from throughout all five cycles developed at the margins of the basin. This has enabled reconstruction of the vegetation changes that accompanied the evaporation-replenishment cycles observed in the sedimentary sequences.

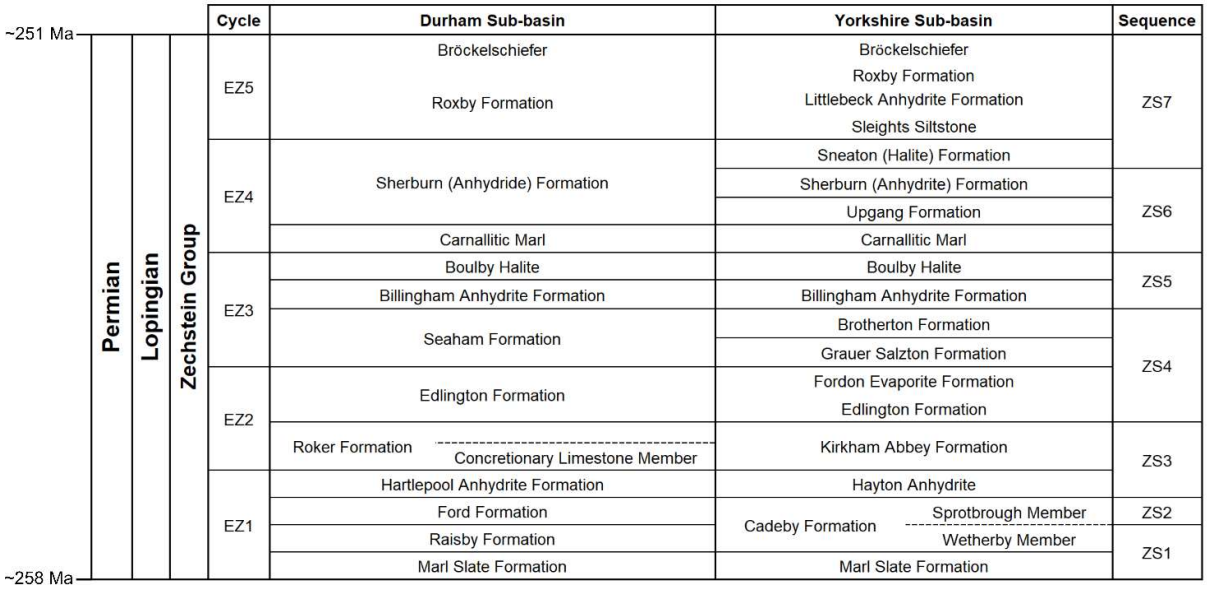

Figure 1. Stratigraphy and correlation of the UK Zechstein deposits between the Durham Sub-basin and Yorkshire Sub-basin. Approximate Zechstein Group dates taken from Menning et al. (2005, 2006).

6.3 Geological Setting

In western and central Europe, a Lopingian to early Triassic marine-continental transition accumulated in the intracontinental Southern Permian Basin (SPB). The SPB evolved on the former Variscan foreland in the latest Carboniferous-early Permian (Ziegler, 1990). The depositional area has a width of ca. 600 km and trends ca. 2,500 km WNW-ESE from northeast England, stretching across the southern North Sea, and into northern Germany and Poland. The SPB is delineated by several Variscan Highs including the London–Brabant, Rhenish, and Bohemian massifs in the south, and the Mid North Sea, and Ringkøbing–Fyn highs in the north (Ziegler, 1990; Geluk, 2005; Peryt et al., 2010).

Within the SPB tectonism initially had a relatively minor influence on the deposition of the Lopingian-early Triassic deposits. Rather, evolution of the SPB is considered to have been influenced by thermal relaxation of the lithosphere (van Wees et al., 2000) causing differential subsidence across the basin. However, the role of tectonism increased in importance in the latest Permian-earliest Triassic (uppermost Zechstein-Buntsandstein) when tectonic pulses began to affect sedimentary successions.

The initial transgression of the Zechstein Sea was a consequence of rifting in the Arctic-North Atlantic, accompanied by a contemporaneous rise in global sea levels. This resulted in flooding of the SPB via the Viking Graben System (Ziegler, 1990). Although this flooding pathway had existed previously and was responsible for minor and short-lived marine incursions during the middle Permian Upper Rotliegend (Legler and Schneider, 2008), the initial Zechstein transgression was a much more catastrophic flooding event. It is represented by the deposition of the 'Kupferschiefer' (copper shale), or Marl Slate in the UK, which indicates permanent flooding of the sub-sea-level SPB (Glennie and Buller, 1983; van Wees et al., 2000).

The Kupferschiefer/Marl Slate was deposited under basin-wide euxinic conditions (Pancost et al., 2002; Paul, 2006) and is a 0.5 m thick layer of black shale across the basin that provides an excellent marker horizon utilised in regional correlation (Geluk, 2005; Doornenbal and Stevenson, 2010). A Re-Os age of 257.3 ± 1.6 Ma for the Kupferschiefer in central Germany (Brauns et al., 2003) indicates a Lopingian (early Wuchiapingian) age for the basal Zechstein. However, this Re-Os age has been challenged (Słowakiewicz et al., 2009). Dating of the Zechstein in central Germany places the Zechstein Transgression at 258 Ma (Menning et al., 2005, 2006) (Figure 1).

During the Lopingian, the SPB was located within the supercontinent Pangaea in the northern hemisphere desert belt at 10-30°N (Glennie, 1983). Zechstein deposition took place under arid and semi-arid climate conditions, the influence of which is documented by up to seven cycles of

sedimentation and stacked evaporation cycles (Figure 1). These provide a framework for lithostratigraphical subdivision and facilitate basin-wide correlation (Richter-Bernburg, 1955). While the Zechstein Sea existed, the SPB was filled with approximately 2000m of siliciclastics, carbonates and evaporites (Peryt et al., 2010) following the classic model of cyclical chemical precipitation in a giant saline basin of Richter-Bernburg (1955). At its maximum extent, towards the centre of the Zechstein Sea, the Zechstein Group consists of seven evaporation cycles, the Werra (Z1), Staßfurt (Z2), Leine (Z3), Aller (Z4), Ohre (Z5), Friesland (Z6) and Fulda (Z7) cycles.

The entire Zechstein sequence is considered to be of Lopingian age and accumulated within a period of 2.8-3.5 Myr (Szurlies, 2013; Menning et al., 2005), 5 Myr (Menning et al., 2006), or up to 9 Myr (Słowakiewicz et al., 2009) (Figure 1). There is no consensus yet for one timescale for all of the Zechstein sequence and it is likely that different regions of the basin were deposited at different times. The British Zechstein is yet to be dated and, so far, attempts to match the Zechstein in the UK to the global chronostratigraphic timescale have been unsuccessful (D. Grocke pers. comm.). Consequently, the dates presented here are based on the latest magnetostratigraphical dating from the German/Dutch Zechstein successions (i.e., Szurlies, 2013) and carbon isotope studies (e.g. Słowakiewicz et al., 2009).

The UK Zechstein crops out over northeast England from Country Durham south to Nottinghamshire (Figure 2). These deposits accumulated in two sub-basins, separated by the Cleveland High, which ran along the western margin of the sea: the Yorkshire Sub-basin to the south and the Durham Sub-basin to the north (Smith, 1989). The sequence is divided into five evaporation cycles represented by EZ1-5 (Figure 1). The Zechstein Group is separated from the deposits of the Bakevellia Sea to the west by the low-lying, gently undulating topography of the Protopennines (Stone et al., 2010).

The Zechstein displays an overall regressive and hypersaline trend, with the thickness of strata thinning towards the margins of the SPB. As such, only the first three cycles display a full cycle of lithologies including marine clastics, carbonates and evaporites. The upper cycles are dominated by clay and siltstones and generally contain fewer evaporites. These evaporites formed in more localised depressions and do not extend basin-wide (Smith, 1989).

The Kupferschiefer (Marl Slate) represents one of three regionally extensive marker horizons used in correlation of the Zechstein (Geluk, 2005), the others being the ‘Grauer Salzton’ (Grey Salt Clay/Illitic Shale) at the base of Z3, and the ‘Roter Salzton’ (Red Salt Clay/Carnallitic Marl Formation) at the base of Z4. All three markers are assumed to represent nearly synchronous flooding events (Doornenbal and Stevenson, 2010).

Zechstein lithostratigraphy is well-defined and correlated throughout the interior of the SPB for cycles Z1 to Z3. However, correlation of the upper Zechstein is more difficult with disagreement regarding correlation of the Z4 of Poland (PZ4a-e) with Z5-lower Z7 in Germany (Wagner and Peryt, 1997; Käding, 2000; Peryt et al., 2010). In Germany, the Zechstein-Buntsandstein boundary is placed at the base of the first prominent sandstone directly above the Z7 Formation (Röhling, 1993 and references therein).

Zechstein deposition terminated when the connection with the Boreal Ocean was interrupted by major clastic influx into the SPB (Ziegler, 1990). The SPB initially transitioned into an extensive sabkha environment with isolated salinas, later becoming an extensive inland playa lake in which the Lower Buntsandstein Subgroup was deposited (Hug, 2004; Hug and Gaupp, 2006). Salt precipitation progressively retreated further into the basin centre during the uppermost Zechstein. Tectonism resulted in downwarping of the central parts of the basin with uplift creating minor unconformities at its margins (Geluk, 1999). Zechstein sedimentation finally ended with the progradation of the uppermost part of EZ5/Z7, a sequence of fine-grained clastic facies formerly named the 'Bröckelschiefer' (Peryt et al., 2010).

Figure 1 illustrates the general stratigraphical sequence of the Zechstein of northeast England. Figure 2 illustrates the location of the Zechstein sequences analysed in this study and Figure 3 illustrates the stratigraphy and correlation of the Zechstein sequences. Full lithostratigraphical and facies descriptions are provided in Appendix A of the online supplementary information. It is important to note that in northeast England only Cycles 1-3 are exposed. Later cycles (Cycles 4-5) and the Permian-Triassic boundary can only be accessed by boreholes and are comparatively understudied.

6.3 Previous palaeobotanical and palynological studies

The palaeobotany of the British Zechstein sequence is well documented and comprises a typical Euramerican flora dominated by gymnosperms (Stoneley, 1958; Schweitzer, 1986; Cleal and Thomas, 1995). Rich palynomorph assemblages have previously been described from the Zechstein of northeastern England (Wall and Downie, 1963; Clarke, 1965) as well as equivalent deposits from the Bakevellia Sea of northwest England (Clarke, 1965; Warrington, 2008) and the Kings Court outlier in Ireland (Visscher, 1971, 1972). The palynology of other Permian strata in the UK has been reviewed by Warrington and Scrivener (1988) and Warrington (2005). All of these studies report mainly pollen assemblages (with subsidiary spores) but include rare evidence for marine elements such as acritarchs and foraminiferal test linings.

Wall and Downie (1963) reported the presence of marine acritarchs in Zechstein deposits from Ashfield Brick Pit, Conisborough, Yorkshire. They were rare, with the assemblages dominated by pollen, and included relatively simple forms such as *Veryhachium* and *Micrystridium*.

The most comprehensive review of British Zechstein palynology is Clarke (1965). Spore-pollen assemblages from the Hilton Plant Beds, Kimberley Railway Cutting and Haughton Hall Boring in Nottinghamshire were reviewed. Thirty-three taxa were reported, with assemblages containing an overwhelming dominance of *Lueckisporites virkkiae*, with *Taeniaesporites noviaulensis* and *T. labdacus* also being very abundant. Clarke reported that the most common non-taeniate taxa were *Klausipollenites schaubergeri*, *Falcisporites zapfei*, *Labiisporites granulatus* and *Illinites delasaucei*. Monosaccate pollen were represented by *Perisaccus granulosus*, *P. laciniatus*, *Potonieisporites novicus*, *Vestigisporites minutus* and *Nuskoisporites dulhuntyi*, although none of these species are common. Monosulcates are only represented by the genus *Cycadopites*. Clarke suggested that the similarity seen between Zechstein assemblages and other co-eval assemblages from the UK indicated that the Lopingian vegetation was fairly uniform throughout this region. Due to the palynological assemblages being derived from a very limited stratigraphical range it was not possible for Clarke to comment on any temporal variation. Clarke also erected three variants of *L. virkkiae* based on gross morphological differences. According to Clarke (1965) Variant A is the largest and is described as having well-developed, distinctly separate proximal thickenings and well-developed sacci, being most similar to the holotype and *L. microgranulatus* Klaus 1963. Variant B has sacci that are less well-developed and a small saccus offlap, being most similar to *L. parvus* Klaus 1963. Variant C has a weakly developed proximal cap that is not completely separated into two halves and is generally smaller with a more elongate corpus, being most similar to *L. microgranulatus* "kleinere variante" Klaus 1963.

Visscher (1971) reviewed the Permian and Triassic palynology of the Kingscourt Outlier, Ireland, which is a correlative of the Bakevellia and Zechstein seas. The oldest assemblage described (Assemblage 1) was found to closely correlate with Lopingian Zechstein assemblages from western Europe. This assemblage is dominated by *Lueckisporites virkkiae*, *Jugasporites delasaucei*, *Klausipollenites schaubergeri* and *Limitisporites moerensis*. *Perisaccus granulatus* and *Striatisaccus* sp. are minor components. However, typical Zechstein forms *Falcisporites zapfei* (Potonié and Klaus, 1954), *Labiisporites granulatus* and *Striatopodocarpites richteri* were notably absent, presumably due to the semi-isolated nature of deposits of the Kingscourt Outlier to the west of the Zechstein Basin. Visscher proposed a zonation, based on 'palynodemes' of *L. virkkiae*, which represents a rare attempt to apply a palynology-based biostratigraphy to the Zechstein Group.

More recent work on the Permian palynology of the UK has tended to focus on equivalents of the Zechstein deposits (Warrington and Scrivener, 1988; Legler et al., 2005; Legler and Schneider, 2008; Warrington, 2005, 2008). For example, the Lopingian of Devon yields poorly preserved bisaccate gymnosperm pollen (Warrington and Scrivener, 1988). *Lueckisporites virkkiae*, *Perisaccus granulosus*, *Klausipollenites schaubergeri*, *Jugasporites delasaucei*, *Protohaploxypinus microcorpus* and *Lunatisporites* spp. are found and are all compatible with a Lopingian age. The Hilton Borehole, in the Valley of Eden in Cumbria, yields the longest continuous section of Permian rocks in Britain and includes strata equivalent to the Zechstein succession (EZ1) of eastern England (Jackson and

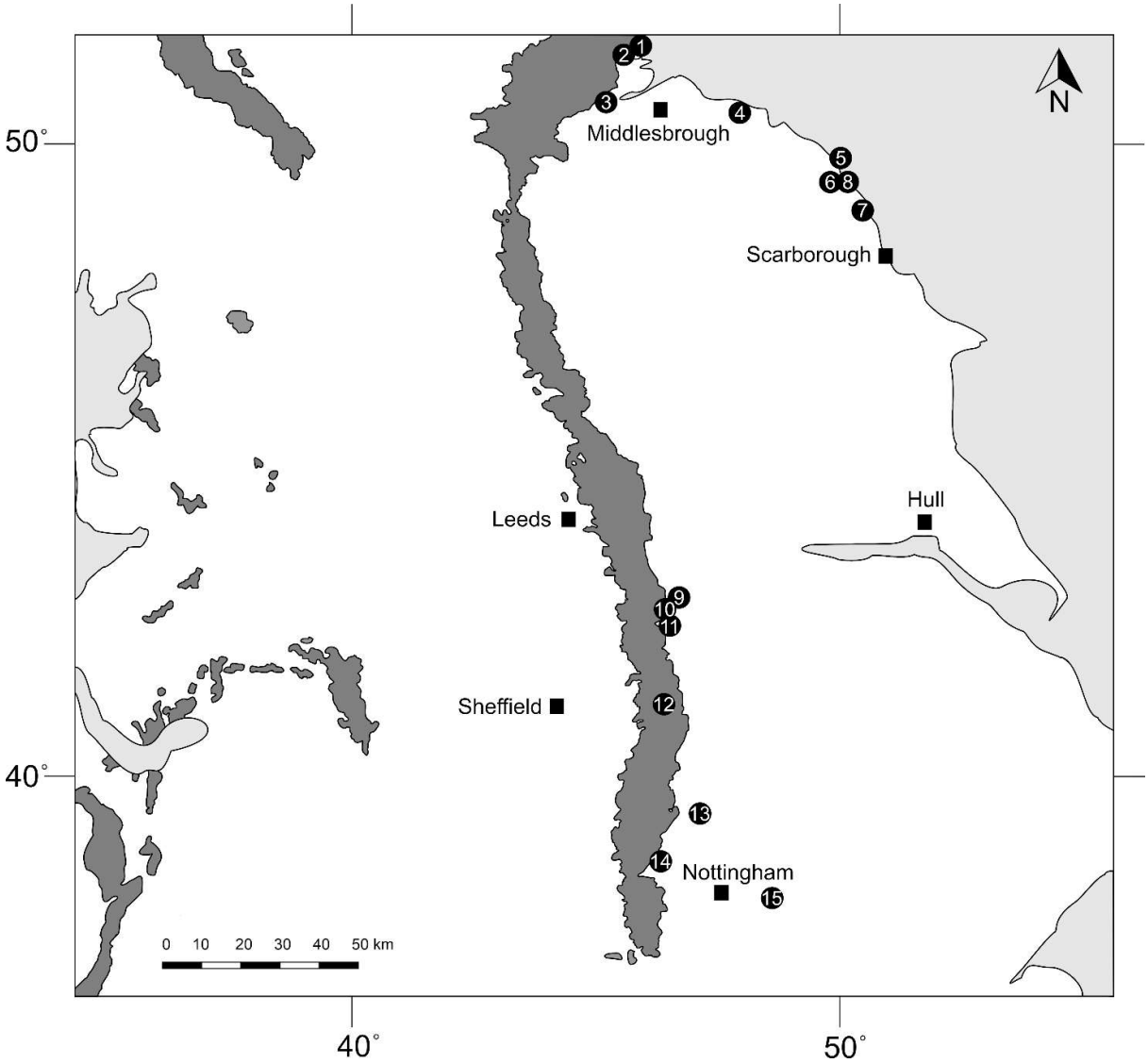

Figure 2. Outcrop map of the UK Zechstein deposits showing the location of the boreholes and outcrop exposures considered in this paper. 1) Marsden Bay, 2) Claxheugh Rock, 3) Crime Rigg Quarry, 4) Little Scar, 5) SM7 Mortar Hall, 6) SM11 Dove's Nest, 7) SM4 Gough, 8) SM14b Woodsmith Mine, 9) Pot Riding, 10) Levitt Hagg Hole, 11) Sandal House, 12) Ashfield Brick Pit, 13) Salterford Farm, 14) Woolsthorpe Bridge, 15) Kimberley. Permian outcrops are shaded in grey.

Johnson, 1996). Warrington (2008) described palynomorph assemblages, dominated by pollen, but also containing algal remains. *Crucisaccates* cf. *variosulcatus* and possibly *Proprisporites pococki* were reported for the first time from the Upper Permian of the UK.

6.4 Materials and Methods

The Zechstein sequence of northeastern England was extensively collected from both outcrop and boreholes to gather a set of samples for palynological analysis from throughout the sequence. A total of 192 samples were collected from six boreholes (SM4 Gough, SM7 Mortar Hall, SM11 Dove's Nest, SM14b Woodsmith Mine North Shaft, Salterford Farm, Woolsthorpe Bridge) and outcrop samples from the Yorkshire Sub-basin (Kimberley Railway Cutting, Levitt Hagg Hole and Little Scar beach) and from the Durham Sub-basin (Claxheugh Rock, Crime Rigg Quarry and Marsden Bay). Figure 1 shows the location of the boreholes and outcrops discussed in this study. See Appendix B of the online supplementary information for a list of the borehole samples and their lithology, and Appendix C for a list of the outcrop samples. Appendix D provides more details of the stratigraphic range of the sampled localities/boreholes. The sampling resolution was determined by the frequency of lithologies suitable for palynomorph preservation and by the extent of exposed sections/borehole material available for sampling.

The samples were palynologically processed using different techniques depending on whether the lithology was clastic-carbonate or evaporite. For clastic-carbonate lithologies 20g of sample was prepared using standard palynological HCl-HF-HCl acid maceration techniques. The residue was first top sieved at 10µm to detect the presence of acritarchs, then at 20µm, and subjected to heavy liquid separation using zinc chloride to extract and concentrate the organic residues. Evaporite lithologies were processed according to the method outlined in Gibson and Bodman (2020), whereby samples are dissolved in hot water, boiled in concentrated 40% HF for 15 minutes to remove any remaining clastics, then subjected to heavy liquid separation using zinc chloride to extract and further concentrate any organic residue.

For productive samples, the residues varied considerably in palynomorph colour/opacity. In most samples the palynomorphs were beautifully preserved and of very low thermal maturity (translucent yellow-orange). In some samples the palynomorphs were of very low thermal maturity and appeared hyaline (e.g., Marl Slate of the Durham Sub-basin). These were stained using Bismark Brown to improve contrast and visibility of palynomorphs. On the other hand, samples associated with evaporites were often opaque dark brown-black (frequently 98-100% PDI) (Goodhue and

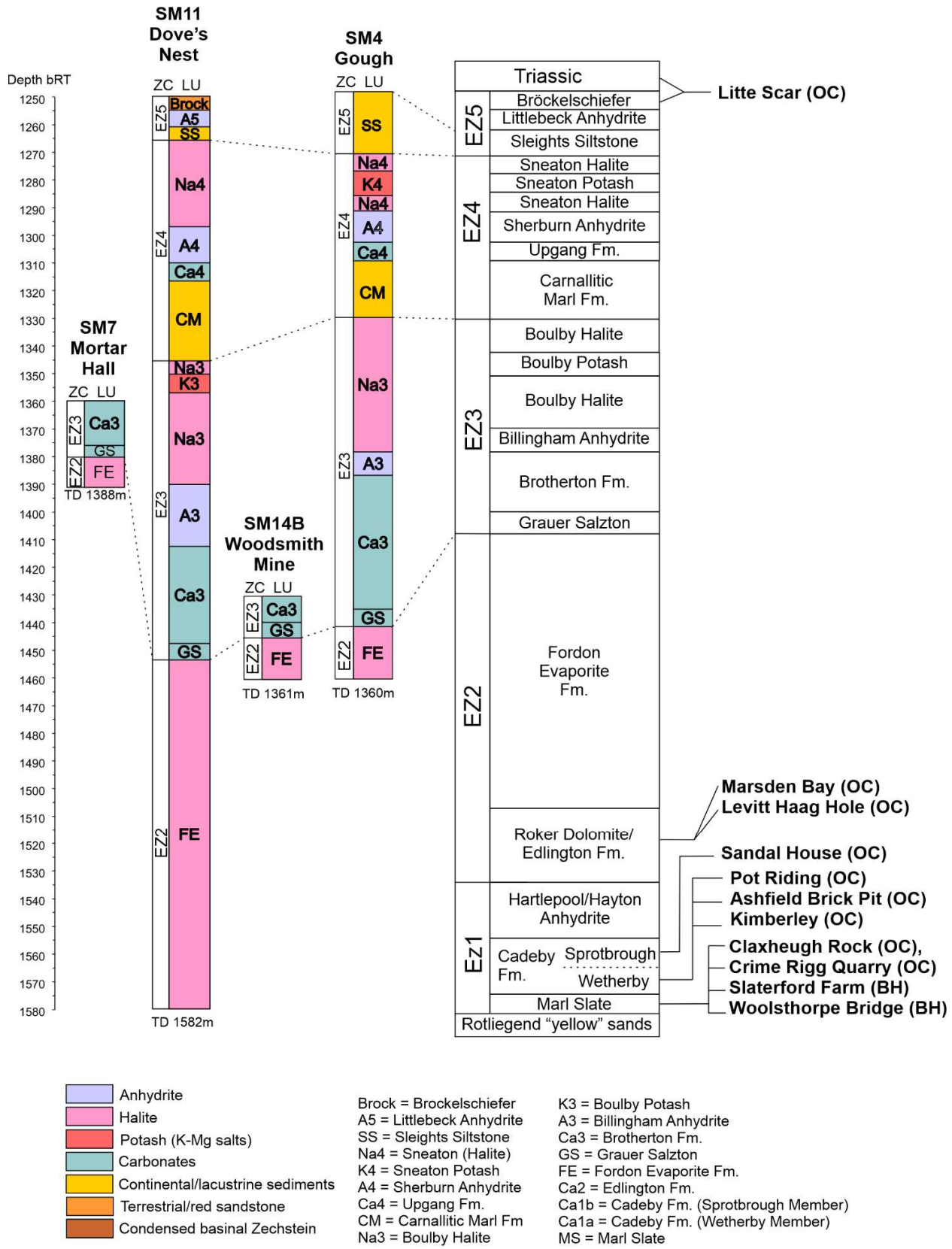

Figure 3. Stratigraphy and correlation of the sequences analysed in this study. OC = Outcrop, BH = borehole, ZC = Zechstein cycle, LU = Lithostratigraphic unit, and TD = Terminal Depth (m) of commercial boreholes. C = carbonates and E = evaporites.

the Zechstein deposits have not been subjected to deep burial and high heat flow and palynomorph assemblages above and below are of very low thermal maturity (see Gibson and Bodman (2020)). It appears to result from a diagenetic effect of preservation within evaporites. Where necessary, samples were oxidized using Schulze's reagent for up to 26 hours which cleared the palynomorphs to translucent orange. Samples containing large quantities of amorphous organic matter (AOM) were treated with pulsed ultrasound treatment to break up the AOM and prevent it from obscuring palynomorphs during analysis. The organic residue was strew mounted onto glass slides for light-microscopic (LM) analysis.

Once a taxonomy had been established (at least one slide was logged for each sample recording all taxa present) a minimum count was made for each sample. If sufficient palynomorphs were present a minimum count of 200 was undertaken. When there were insufficient palynomorphs the entire palynomorph population was counted. To accommodate for differences in quantitative approach, samples containing a yield greater than 200 were rarefied to 200. Damaged grains (>50%) identifiable as bisaccate or monosaccate pollen grains were logged as Unidentifiable to avoid misclassification of samples as barren. The count data was recorded and manipulated using the packages StrataBugs 2.1 and R.mSpecimens were analysed and photographed using a QImaging (Model No. 01-MP3.3-RTV-R-CLR-10) camera mounted on an Olympus BH-2 transmitted light microscope in conjunction with QCapture Pro software. All samples, residues, and LM slides are curated in the Centre for Palynology at the University of Sheffield, UK.

6.5 Palynological results

Recovery was highly variable from the different lithologies sampled. Many of the clastic deposits yield abundant organic residue containing rich and diverse assemblages of well-preserved palynomorphs of low thermal maturity. Most of the evaporite deposits produced very low yields of organic residue, although these often contained palynomorphs. However, palynomorphs from the evaporites were variable in preservation, varying both in quality of preservation (excellent to poor) and colour (translucent pale yellow to opaque black). All of the palynological samples were dominated by pollen, with very rare spores, and only occasional marine forms (acritarchs and foraminiferal test linings). A list of the taxa encountered is provided in Table 1 and illustrations of these taxa are in Plates I-III. Figures 4-14 illustrate the palynomorph occurrence and distribution for each locality. The raw data is provided in J. Table 2 summarises the palynomorph distribution.

6.5.1. General description of the spore/pollen assemblages

The assemblages are often dominated by the taeniate bisaccate *Lueckisporites virkkiae* (Plate I, 1-5) occurring at sufficient frequencies to dominate assemblages by ~50.0%. Variant A (Plate I, 1, 2) is the most common variant, averaging 9.9-26.8% of assemblages, with Variant B (Plate I, 3) and Variant C (Plate I, 4, 5) being noticeably less abundance, 1.7-5.1% and 1.5-9.4% respectively. *L. virkkiae* maintains dominance throughout the Zechstein sequence.

Taeniaesporites spp. (Plate I, 6-12), the most common species of which is *T. labdacus* (up to 14.0%, average 0.7-5.9%) (Plate I, 6, 7), is present up until the Cycle 4 carbonates but no later. Average abundance ranges between 1.3-22.5%, with maximum abundance achieved in the Marl Slate. *Protohaploxypinus* spp. (Plate I, 13-16), the most common of which are *P. chaloneri* (Plate I, 13, 14) and *P. jacobii* (Plate I, 15, 16), has a slightly greater temporal range than *Taeniaesporites*, and is present into the Cycle 4 evaporites. *Protohaploxypinus* spp. ranges in abundance from 0.6-2.2% of assemblages, but individual species can reach abundances of 3.4% (e.g. *P. jacobii* in the Cycle 3 evaporites). The presence and abundance of other taeniate species is also as expected from Lopingian assemblages. The distinct asaccate species *Vittatina hiltonensis* (Plate II, 1, 2) maintains a rare abundance throughout of 0.5-3.17%. *Striatioabietites* (Plate II, 3) and *Striatopodocarpites* (Plate II, 4, 5) occur at low abundances only, typically <0.5% of the assemblages, but up to 2.0% in the Cycle 3 evaporites. *Platysaccus radialis* (Plate II, 6) is a rare bisaccate only occurring in the Cycle 1 carbonates (1.0%) and very rare in the Cycle 4 carbonates (<0.5%).

Regarding non-taeniate bisaccate pollen, *Klausipollenites schaubergeri* (Plate II, 7, 8) is the most abundant and is present from the Marl Slate through to the Cycle 4 evaporites. It is similar in morphology to *Vestigisporites minutus* (Plate II, 9-11), but distinctly bisaccate rather than monosaccate and larger in size. *K. schaubergeri* exhibits a large range in abundance but on average represents between 5.8-20.0% of assemblages. A maximum abundance of 27.0% is achieved in the Cycle 2 carbonates, but abundances can be as low as 0.5%. *Illinites* spp. (Plate II, 12-15) is the only other pollen grain taxon to occur in the Cycle 5 evaporites alongside *Lueckisporites virkkiae*, however it is absent in the Cycle 4 evaporites and Cycle 5 carbonates. It is easily identifiable with its distinct corpus and sacci shape meaning its presence can be recorded even in poorly preserved samples. *Illinites* spp. is represented by three species, with *I. delasaucei* (Plate II, 12) being the most common (0.5-6.5%) and *I. klausi* (<0.5-3.5%) (Plate II, 13) and *I. tectus* (0.5-5.2%) (Plate II, 14, 15) being present at lower abundances. *Falcisporites zapfei* (Plate I, 12, 13) is the largest non-taeniate bisaccate recovered, occurring at low abundances from the Marl Slate through to the Cycle 4 carbonates at <0.5-1.3%. The distinctive bisaccate *Alisporites nuthallensis* (Plate II, 18) is present from the Marl Slate through to the Cycle 4 carbonates at low abundances of 0.5-2.4%. The triangular-outlined pollen

species *Labiisporites granulatus* (Plate II, 19, 20) was observed at average abundances of 0.5-5.1%, but with abundances as high as 18.0% in the Cycle 3 evaporites. This species exhibits one of the largest variations in abundance in the studied material.

Large monosaccate pollen species are, as expected, rare e.g., *Nuskoisporites dulhuntyi* (Plate III, 1), *N*. cf. *rotatus* (Plate III, 2), *Perisaccus granulosus* (Plate III, 3, 4) and *Potonieisporites novicus* (Plate III, 5, 6). *Nuskoisporites* spp. and *P. granulosus* are present in the Marl Slate through to the Cycle 4 carbonates, while *Potonieisporites novicus* has a similar range yet is not present in the Marl Slate. These large monosaccate pollen typically only represent 1.0-2.0% of assemblages or less. However, the small monosaccate *Vestigisporites minutus* is one of the most common pollen species comprising on average 5.0% of assemblages. *V. minutus* can comprise up to 17.5% of assemblages in Cycle 3 evaporites.

The possible cycad pollen, *Cycadopites rarus,* is very rare (0.5%). *C. rarus* is only recorded in the Cycle 3 evaporites. Trilete spores (Plate II, 8, 9) maintain a low abundance throughout Cycle 1-4 but reach their maximum presence of 13.6% in the assemblages of the Cycle 4 evaporites. However, assemblages from Cycle 4 and Cycle 5 were of a lower yield relative to earlier cycles. Trisaccate pollen grains are rare and may represent aberrant forms of other pollen species (Foster and Afonin, 2005; Metcalfe et al., 2009). They occur at <0.5% from Cycle 1 carbonates to Cycle 3 evaporites but are not found in assemblages beyond. Tetrads are only found in Cycle 1 carbonates at maximum abundances of 0.5%. Cuticle fragments of varying size (20-200µm) were common in assemblages, with larger fragments recovered from the evaporite preparations than standard preparations.

6.5.2. Description of palynomorph distribution by locality

6.5.2.1. Cycle 1 transgressional sediments and carbonates (EZ1 Ca) (Marl Slate and carbonates): Claxheugh Rock and Crime Rigg Quarry exposures

Palynomorph assemblages from Cycle 1 of the Durham Sub-basin were recovered from exposures of the Marl Slate at Claxheugh Rock (Figure 4) and Crime Rigg Quarry (Figure 5). Palynological preparations contain vast amounts of amorphous organic matter (AOM). Palynomorphs are present and are well-preserved and hyaline in appearance. The hyaline nature hampered identification of palynomorphs, but genus-level identifications, and some species-level identifications of distinct taxa, were possible after samples were stained with Bismarck Brown.

The assemblages recovered from the exposure at Claxheugh Rock (Figure 4) were composed of taeniate bisaccate species: *Lueckisporites virkkiae* (31.5%), *Protohaploxypinus* sp. (1.0%),

Taeniaesporites sp. (17.0%) and *Vittatina hiltonensis* (1.0%). Non-taeniate bisaccate species include *Alisporites nuthallensis* (<0.5%), *Illinites* sp. (2.0%), *Klausipollenites schaubergeri* (8.5%), rare *Labiisporites granulatus* (<1.0%) and *Falcisporites zapfei* (<0.5%). Rare multisaccate *Crustaesporites globosus* (<0.5%) (Plate III, 7) was present. Monosaccate pollen was represented by *Vestigisporites minutus* (3.5%) and rare *Perisaccus granulosus* (<0.5%) and *Nuskoisporites dulhuntyi* (0.5%). One sample (CLR) did not contain Unidentifiable palynomorphs but contains rare unidentifiable spores (<0.5%), while the other sample (CLR2) contains 93.0% Unidentifiable palynomorphs.

The assemblage from Crime Rigg Quarry (Figure 5) was composed of the taeniate bisaccate species *Lueckisporites virkkiae* (43.5%), *Protohaploxypinus* sp. (2.5%), rare *Striatopodocarpites* sp. (<0.5%%), *Taeniaesporites* sp. (28%), and *Vittatina hiltonensis* (2.0%), and the non-taniate bisaccate species *Illinites* sp. (7.0%), *Klausipollenites schaubergeri* (8.0%), *Labiisporites granulatus* (1.5%), *Falcisporites zapfei* (<0.5%), as well as the monosaccate pollen *Perisaccus granulosus* (<0.5%) and *Vestigisporites minutus* (7.5%).

6.5.2.2. Cycle 1 transgressional sediments and carbonates (EZ1 Ca) (Cadeby Fm.: Wetherby/Sprotbrough Mb.): Kimberley railway cutting exposure and the Salterford Farm and Woolsthorpe Bridge boreholes

Palynomorph assemblages from Cycle 1 of the Yorkshire Sub-basin were recovered from the Cadeby Fm. exposure in Kimberley railway cutting (Figure 6), Salterford Farm borehole (Figure 7), and Woolsthorpe Bridge borehole (Figure 8). The palynomorphs were well preserved and translucent. Both assemblages from Kimberley railway cutting, K5 and K6, contain *Lueckisporites virkkiae* (K5 39.0%, K6 50.0%), *Taeniaesporites* sp. (K5 2.5%, K6 1.0%), *T. labdacus* (K5 10.5%, K6 6.5%), *T. novimundi* (K5 2.5%, K6 2%), *T. noviaulensis* (K5 2.5%, K6 5.5%), *T. angulistriatus* (K5 2.0%, K6 2.0%), *T. albertae* (K6 7.5%), *Protohaploxypinus jacobii* (K5 2.0%), *Striatopodocarpites antiquus* (K5 1.0%, K6 0.5%), *Vittatina hiltonensis* (K5 2.5%), *Illinites* sp. (K5 5.5%), *I. delasaucei* (K5 9.5%, K6 8.5%), *I. klausi* (K6 3.5%), *I. tectus* (K5 1.0%, K6 0.5%), rare *Nuskoisporites dulhuntyi* (K5 <0.5%) and *Potonieisporites novicus* (K5 <0.5%), rare *Perisaccus granulosus* (K6 <0.5%), unidentifiable spores (K5 2%, K6 0.5%), and rare tetrads (K6 0.5%).

Assemblages from the Salterford Farm borehole samples were composed of the taeniate bisaccate species *Lueckisporites virkkiae* with Variant A (21.3%), Variant B (1.7%) and Variant C (2.5%), *Protohaploxypinus* sp. (0.5%) *P. chaloneri* (<0.5%), *P. jacobii* (0.5%), *Striatoabieites richteri* (0.5%), *Striatopodocarpites* sp. (0.5%), *Taeniaesporites* sp. (0.5%), *T. albertae* (0.8%), T.

angulistriatus (0.8%), *T. bilobus* (<0.5%), *T. labdacus* (2.8%), *T. novimundi* (1.3%), *T. noviaulensis* (0.8%). The non-taeniate bisaccate pollen *Alisporites nuthallensis* (2.5%), *Falcisporites zapfei* (0.9%), *Illinites delasaucei* (5.1%), *I. tectus* (0.5%), *Klausipollenites schaubergeri* (14.3%), *Labiisporites granulatus* (3.5%), *Platysaccus radialis* (1.0%) and *Potonieisporites novicus* (0.5%) were recovered. The multisaccate *Crustaesporites globosus* was recorded (0.5%). Monosaccate pollen were represented by *Nuskoisporites dulhuntyi* (0.5%), *Perisaccus granulosus* (0.6%) and *Vestigisporites minutus* (6.7%). *Reduviasporonites* sp. was found throughout (2.7%), trisaccate pollen were rare (0.4%) and spores were found in all samples (1.6%). A solitary tetrad in YFP6368 was recovered and a single foraminiferal test lining was recovered from SF465. The Unidentifiable palynomorph component averages at 33.0%.

The sample of Marl Slate obtained from Woolsthorpe Bridge borehole (Figure 8) was not species rich and was dominated by Unidentifiable palynomorphs (56.1%). Identifiable taeniate bisaccate pollen include *Lueckisporites virkkiae* Variant A (15.8%), Variant B (1.8%) and Variant C (3.5%), *Taeniaesporites labdacus* (1.8%), *T. albertae* (3.5%), and non-taeniate bisaccate pollen include *Klausipollenites schaubergeri* (12.3%) and *Labiisporites granulatus* (1.8%). The only monosaccate taxon present was *Vestigisporites minutus* (3.5%).

The remaining Cycle 1 carbonates, sampled at Ashfield Brick Pit, Sandal House, and Pot Riding, were essentially barren of palynomorphs, containing only a few palynomorphs of such poor preservation they lacked characters that enabled them to be identified even as Unidentifiable pollen grains. Therefore, these sites were designated as barren.

6.5.2.3. Cycle 1 evaporites (EZ1 A) (Hartlepool Anhydrite/Hayton Anhydrite)

Cycle 1 evaporites were not covered in the sampling range of this study as they are not represented by any of the borehole material and they are not exposed at outcrop as a result of dissolution.

6.5.2.4. Cycle 2 carbonates (EZ2 Ca) (Roker Dolomite/Edlington Fm. and Kirkham Abbey Fm.): Marsden Bay

A sample of red mudstone from the Edlington Fm. collected from outcrop at Levitt Hagg Hole was barren of palynomorphs. Samples of Roker Dolomite Fm. from Marsden Bay (MB1-6) (Figure 9) contained taeniate and non-taeniate bisaccate pollen, as well as rare monosaccate pollen. The assemblage of MB2 was the best preserved. The taeniate bisaccate taxa were represented by *Lueckisporites virkkiae* (53.5%), and *Taeniaesporites* sp. (1.8%) is also abundant, with *T.*

angulistriatus (<0.5%), *T. labdacus* (0.5%) and *T. novimundi* (<0.5%). *Protohaploxypinus* sp. (3.1%) was present, with *P. chaloneri* (<0.5%) and *P. jacobii* (<0.5%) present. *Striatopodocarpites* sp. (<0.5%) was rare and only found in one sample (MB2). *Vittatina hiltonensis* (0.9%) was present at rare abundance in MB1-3. Smooth bisaccate pollen was represented by abundant *Illinites* sp. (6.1%) with rare *I. delasaucei* (<0.5%) only recovered from MB2. *Klausipollenites schaubergeri* was abundant (23.3%), while *Labiisporites granulatus* (1.0%), *Alisporites nuthallensis* (0.9%) was uncommon, and *Falcisporites zapfei* (<0.5%) (MB4-6) and *Potonieisporites novicus* were rare (<0.5%). The monosaccate pollen *Nuskoisporites dulhuntyi*, and *Perisaccus granulosus* were rare (<0.5%), and *Vestigisporites minutus* (MB1-2) was found in MB1-2. The Unidentifiable component was only present in MB1 and only comprises 16% of the assemblage. Unidentifiable trisaccate pollen grains were recovered from MB1 (<0.5%).

The remaining samples from Marsden Bay (MB4-6) contained similar assemblages, but typically of lower yield. MB4 contains an exceptionally well-preserved assemblage but was of low yield (n=102), with *Lueckisporites virkkiae* composing 20.0% of the assemblage. There were no Unidentifiable palynomorphs, but *L. virkkiae* Variant A was abundant (14.0%) while Variant B was rare (<0.5%). Other taeniate genera *Taeniaesporites* sp. were present (1.8%) as well as *Protohaploxypinus* spp. which was only found in MB4 (0.5%), with rare *P. chaloneri* (<0.5%) and *P. microcorpus* (<0.5%) recovered from MB5. The non-taeniate bisaccate pollen *Illinites* sp. (10.7%), *Falcisporites zapfei* (0.5%), and *Klausipollenites schaubergeri* (16.7%) were abundant in MB4-6. The only monosaccate taxon recovered from MB4-6 was the small species *Vestigisporites minutus* that was only recovered from MB5 (2.5%). Unidentifiable pollen grains comprised on average 54.5% of the assemblages.

6.5.2.5. Cycle 2 evaporites (EZ2 A, EZ2 K, EZ2 Na) (Fordon Evaporites Fm): SM4, SM11 and SM14b boreholes

The borehole material captures both the lower (SM11) and upper (SM4, SM14b) parts of the Fordon Evaporite Fm. In borehole SM11 (Figure 10), the lower part of the Fordon Evaporite Fm. contained assemblages with a low yield. Palynomorphs were mostly of the Unidentifiable type, corroded, dark and fragmented. However, some very well-preserved specimens of *Illinites* sp., *Klausipollenites schaubergeri*, *Reduviasporonites* sp., *Lueckisporites virkkiae* Variant A and Variant B, and *Vestigisporites minutus* were recovered.

The upper part of the Fordon Evaporite Fm. in SM11 (Figure 10) contained a more varied assemblage with samples containing greater yields. Very high proportions of Unidentifiable pollen

grains persisted, as well as some very well-preserved palynomorphs originating in the evaporites. Assemblages were dominated by *Lueckisporites virkkiae* Variant A, *Klausipollenites schaubergeri*, *Vestigisporites minutus* and assorted *Illinites* sp., *Taeniaesporites* sp. and *Protohaploxypinus* sp.

On average assemblages from the Fordon Evaporite Fm. from SM11 (Figure 10) contained taeniate bisaccate species *Lueckisporites virkkiae* Variant A (13.3%), as well as Variant B (4.1%) and Variant C (3.8%), *Taeniaesporites* sp. (5.2%), rare *T. angulistriatus* (0.5%), *T. albertae* (1.3%), *T. noviaulensis* (1.0%), and *T. labdacus* (1.31%%), rare *Protohaploxypinus* sp. (1.3%) including *P. chaloneri* (0.8%), *P. jacobii* (0.5%) and *P. microcorpus* (0.5%). *Striatopodocarpites antiquus* (0.5%) and *Vittatina hiltonensis* (0.5%) were very rare. The non-taeniate bisaccate pollen were represented by *Klausipollenites schaubergeri* (6.4%), *Illinites* sp. (5.1%) including *I. delasaucei* (1.8%), and rare *Labiisporites granulatus* (1.8%), *Falcisporites zapfei* (0.5%) and *Potonieisporites novicus* (0.5%). Monosaccate pollen were rare and were represented by *Nuskoisporites dulhuntyi* (0.5%), yet *Vestigisporites minutus* was abundant (6.7%). *Reduviasporonites* sp. was present (9.6%), yet samples were dominated by Unidentifiable palynomorphs (74.52%). Some trisaccate pollen grains were recovered (6.67%), as well as rare spores (0.5%) and very rare acritarchs (<0.5%).

The Unidentifiable component appears to increase in prominence throughout the upper part of the Fordon Evaporite Fm. Species richness and abundance of palynomorphs also appears to increase throughout the Fordon Evaporite Fm. as the proportion of Unidentifiable palynomorphs progressively dominates samples.

Borehole SM4 (Figure 11) captures the top of the Fordon Evaporite Fm., where samples either had a high yield or a very low yield (<100 pollen grains) yet were still dominated by Unidentifiable palynomorphs (95.1%), which indicates pollen transport from a nearby source vegetation. In addition to the Unidentifiable palynomorphs, rare *Lueckisporites virkkiae* (1.8 %) including Variant A (0.5%) and *L. virkkiae* Variant C (1.5%), *Taeniaesporites* sp. (4.3%), *Protohaploxypinus chaloneri* (1.5%), *Klausipollenites schaubergeri* (0.5%) and *Vittatina hiltonensis* (<0.5%), and unidentifiable spores (1.0%) were recovered. Only in the lower parts of the Fordon Evaporite Fm. were the three "Variants" of *L. virkkiae* distinguishable.

In borehole SM14b (Figure 12), the Fordon Evaporite Fm. palynomorph assemblages were generally well-preserved and of a high yield. Although containing a high proportion of Unidentifiable palynomorphs (80.0%), *Lueckisporites virkkiae* Variant A (11.0%) and Variant C (5%) are present, as well as *Klausipollenites schaubergeri* (5.9%), *Potonieisporites novicus* (7.0%) and *Illinites delasaucei* (7.0%), and *Reduviasporonites* sp. (3.0%). *L. virkkiae* Variant C was the latest variant to appear in the core relative to the other two.

6.5.2.6. Cycle 2 – Cycle 3 transitional (EZ3 Ca) (grey salt clay/illitic shale/Grauer Salzton): SM4 borehole

In SM4 (Figure 11) the Grauer Salzton/Brotherton Fm. boundary assemblage was dominated by Unidentifiable palynomorphs (87.7%), but unlike the other boreholes containing palynomorphs identifiable to species level the assemblage was found to contain *Lueckisporites virkkiae* Variant A (3.8%), Variant B (0.9%), and Variant C (2.8%), *Illinites* sp. (0.9%), *Labiisporites granulatus* (1.9%), *Taeniaesporites* sp. and *T. labdacus* (0.9%). In borehole SM7 (Figure 13) a single sample captures the palynology of the Grey Salt Clay. It contains an abundant assemblage composed only of Unidentifiable palynomorphs (100.0%). In borehole SM11 (Figure 10) this transitional stratum was either barren or was composed of a very abundant sample of only 100.0% Unidentifiable palynomorphs. In SM14b (Figure 12) assemblages of the Grauer Salzton are barren.

6.5.2.7. Cycle 3 carbonates (EZ3 Ca) (Brotherton Fm.): SM7, SM11 boreholes

In borehole SM7 (Figure 13) a single assemblage from the Brotherton Fm. was recovered. Though of low yield (<200) the assemblage contains the taeniate bisaccate species *Lueckisporites virkkiae* (10.0%), including "Variants A" (2.5%), Variant B (1.0%) and very rare Variant C (0.5%). *Taeniaesporites* sp. (1.0%) was rare with *T. noviaulensis* (<0.5%) being very rare. *Protohaploxypinus* sp. was rare (<0.5%), *Illinites* sp. (1.5%) is present. *Klausipollenites schaubergeri* (8.0%) was present, *Vestigisporites minutus* was rare (0.5%) and was the only monosaccate species recovered. Well over half of the assemblage was composed of Unidentifiable palynomorphs (74.0%).

Many of the Brotherton Fm. samples from borehole SM11 (Figure 10) were barren (n=15). Recovered assemblages contain abundant palynomorphs, but were dominated by Unidentifiable palynomorphs (90.2%), presumably an effect of adverse preservational conditions during deposition. There appears to be an increase in the Unidentifiable component from the end of Cycle 2 evaporites through to the Brotherton Fm. However, not all samples were dominated by Unidentifiable palynomorphs. Some assemblages were very well-preserved.

Pollen taxa that occurred in low abundances include the taeniate bisaccate species *Lueckisporites virkkiae* (4.8%) including abundant *L. virkkiae* Variant A (10.4%), with *L. virkkiae* Variant B (3.5%) and Variant C (1.3%), *Protohaploxypinus* sp. (3.3%), *Striatopodocarpites antiquus* (0.8%), *Taeniaesporites* spp. (2.0%) including *T. angulistriatus* (0.5%), *T. noviaulensis* (0.5%), and *T. labdacus* (0.5%). Non-taeniate bisaccate pollen recovered were *Alisporites nuthallensis* (<0.5%), *Falcisporites zapfei* (<0.5%), *Illinites* sp. (3.3%) *I. klausi* (<0.5%) and *I. delasaucei* (0.5%), *Klausipollenites schaubergeri* (5.9%), *Labiisporites granulatus* (1.0%) and *Potonieisporites novicus* (<0.5%). The monosaccate pollen *Vestigisporites minutus* (7.8%), *Nuskoisporites* cf. *rotatus* (<0.5%),

and *Nuskoisporites dulhuntyi* (<0.5%) were present. Trisaccate pollen grains and spores, and *Reduviasporonites* sp. were all rare (<0.5%).

The sample of Brotherton Fm. from SM4 (Figure 11) was barren. However, the sample of Brotherton Fm. from SM14b (Figure 12) contained an abundant yield of pollen, dominated by Unidentifiable palynomorphs (99.5%), but also contained very rare occurrences of *Lueckisporites virkkiae* (1.7%), and *Taeniaesporites* sp. (0.6%)

6.5.2.8. Cycle 3 evaporites (Billingham Anhydrite (EZ3 A), Boulby Potash (EZ3 K) and Boulby Halite (EZ3 Na)): SM11 borehole

Assemblages in borehole SM11 (Figure 10) became better-preserved throughout the evaporites, especially in the Billingham Anhydrite and Boulby Halite.

6.5.2.9 Cycle 3 anhydrite (Billingham Anhydrite): SM11 borehole

There was no recovery from the Billingham Anhydrite or lower part of the Boulby Halite in SM4 (Figure 11).

In SM11 (Figure 10) the Billingham Anhydrite assemblages yielded *Lueckisporites virkkiae* (7.5%), including Variant A (16.9%), Variant B (2.8%) and Variant C (3.5%), *Protohaploxypinus* sp. (1.3%), *P. chaloneri* (1.3%), *P. jacobii* (1.4%), *P. microcorpus* (0.9%) and *P.* cf. *samoilovichii* (0.5%), *Taeniaesporites* sp. (2.8%), *T. angulistriatus* (1.2%), *T. labdacus* (2.6%) and *T. novimundi* (1.5%) and *T. noviaulensis* (1.5%), *Striatopodocarpites* sp. (0.6%), *Striatoabieites antiquus* (1.6%) and rare *Vittatina hiltonensis* (<0.5%). Non-taeniate bisaccate pollen were represented by *Alisporites nuthallensis* (1.8%), *Falcisporites zapfei* (0.9%), *Illinites sp*. (5.0%), *I. delasaucei* (4.2%), *Klausipollenites schaubergeri* (16.3%), *Labiisporites granulatus* (1.5%), *Potonieisporites novicus* (0.8%). The multisaccate *Crustaesporites globosus* was present but rare (0.5%). The monosaccate pollen were represented by *Nuskoisporites dulhuntyi* (0.8%), *Perisaccus granulosus* (0.9%) and *Vestigisporites minutus* (6.3%). *Reduviasporonites* sp. (1.7%), spores (1.8%), and acritarchs (0.5%), were rare.

6.5.2.10. Cycle 3 potassium-magnesium salts (Boulby Potash): SM11 borehole

In SM11 (Figure 10) the Boulby Potash yielded an assemblage composed of the taeniate bisaccate species *Lueckisporites virkkiae* (49.5%), *Protohaploxypinus* sp. (0.5%), *P. jacobii* (2.5%), *P. microcorpus* (1.5%), *Taeniaesporites albertae* (2%), *T. labdacus* (2.5%) and *T. noviaulensis* (2.0%),

the non-taeniate bisaccate species *Falcisporites zapfei* (1.0%), *Illinites tectus* (4.0%), *Klausipollenites schaubergeri* (4.5%), *Labiisporites granulatus* (18.0%), *Potonieisporites novicus* (0.5%), and the monosaccate species *Vestigisporites minutus* (5.0%) and *Perisaccus granulosus* (1.0%). *Reduviasporonites* sp. was present (5.0%), as well as very rare spores (<0.5%).

6.5.2.11. Cycle 3 halite (Boulby Halite): SM4, SM11 boreholes

In borehole SM11 (Figure 10) the Boulby Halite contained the taeniate bisaccate species *Lueckisporites virkkiae* (13.0%) including Variant A (21.7%), Variant B (1.4%) and Variant C (9.3%), *Protohaploxypinus* sp. (0.5%), including the species *P. chaloneri* (2.3%) and *P. jacobii* (2.5%), Taeniaesporites sp. (3.76%), *T. angulistriatus* (0.5%), *T. labdacus* (2.5%), the non-taeniate bisaccate species *Falcisporites zapfei* (1.0%), *Illinites* sp. (<0.5%), *Klausipollenites schaubergeri* (8.9%), *Labiisporites granulatus* (9.3%), *Potonieisporites novicus* (0.5%). The monosaccate pollen were represented by *Vestigisporites minutus* (6.2%) and *Perisaccus granulosus* (1.0%). *Reduviasporonites* sp. was present (2.6%) as well as very rare trisaccate species (<0.5%). The Unidentifiable component averaged at 58.7% of the assemblage.

In borehole SM4 (Figure 11) assemblages of Boulby Halite were either barren or contained assemblages of low yield, dominated on average 90.8% by Unidentifiable palynomorphs. *Klausipollenites schaubergeri* (8.7%), *Lueckisporites virkkiae* (11.0%), *Vestigisporites minutus* (2.9%), *Taeniaesporites* sp. (1.45%) including *T. novimundi* (2.9%) were recovered. It is in the Boulby Halite that *Vestigisporites minutus* makes its first appearance in borehole SM4, although earlier occurrences cannot be excluded on the basis of recovery of *V. minutus* in the Fordon Evaporite Fm. of borehole SM11.

6.5.2.12. Cycle 3 – Cycle 4 transition Carnallitic Marl Fm. (Rotten Marl): SM4, SM11 boreholes

Exceptionally well-preserved assemblages were extracted from the Carnallitic Marl Fm. in borehole SM11 (Figure 10) using standard palynological acid maceration techniques, representing the first time palynomorphs have been recorded from the formation.

In SM4 (Figure 11) an assemblage from the base of the Carnallitic Marl Fm. was not diverse or of high yield, but it was sufficiently well-preserved, relative to the underlying Boulby Halite, to recover *Lueckisporites virkkiae* (11.6%), *Klausipollenites schaubergeri* (8.7%), *Vestigisporites minutus* (9.2%), *Taeniaesporites* sp. (1.5%) including *Taeniaesporites novimundi* (2.9%), and Unidentifiable palynomorphs (72.5%)

Assemblages from the Carnallitic Marl Fm. of borehole SM11 (Figure 10) were of varying quality. Assemblages contained moderate amounts of Unidentifiable palynomorphs (15.3%) as well as distinctly well-preserved pollen grains. Taeniate bisaccate pollen were represented by the species *Lueckisporites virkkiae* (52.0%) including *L. virkkiae* Variant A (20.0%), *L. virkkiae* Variant B (4.4%), *L. virkkiae* Variant C (3.6%), *Protohaploxypinus* sp. (1.5%), *P. chaloneri* (1.7%), *P. jacobii* (0.8%), *Striatopodocarpites fusus* (<0.5%), *Taeniaesporites* sp. (3.0%), *T. albertae* (1.3%), *T. angulistriatus* (2.7%), *T. bilobus* (0.5%), *T. labdacus* (5.9%), *T. noviaulensis* (2.2%), *T. novimundi* (0.6%), and *Vittatina hiltonensis* (0.6%). Non-taeniate bisaccate pollen were represented by *Alisporites nuthallensis* (0.8%), *Falcisporites zapfei* (1.2%), *Illinites* sp. (3.0%), *I. delasaucei* (2.5%), *I. klausi* (0.5%), *I. tectus* (2.1%), *Klausipollenites schaubergeri* (11.4%), *Labiisporites granulatus* (0.8%), *Potonieisporites novicus* (0.5%). The multisaccate *Crustaesporites globosus* was present (1.0%). Monosaccate pollen were represented by *Nuskoisporites dulhuntyi* (<0.5%), *Perisaccus granulosus* (0.5%), and *Vestigisporites minutus* (5.1%). *Reduviasporonites* sp. (2.5%) and rare acritarchs (0.5%) were also present. The Carnallitic Marl Fm. in SM11 is the only recorded instance of *Taeniaesporites bilobus* in borehole SM11.

6.5.2.13. Cycle 4 carbonates (EZ4 Ca) Upgang Fm.: SM4, SM11 boreholes

In SM11 (Figure 10) the Upgang Fm. yielded assemblages composed of the taeniate species *Lueckisporites virkkiae* (52.0%), *Protohaploxypinus chaloneri* (0.5%), *P. jacobii* (<0.5%), *Taeniaesporites angulistriatus* (1.0%), *T. labdacus* (6.0%), *T. noviaulensis* (1.5%), *T. novimundi* (1.0%), *Striatoabieites richteri* (<0.5%), *Striatopodocarpites antiquus* (<0.5%), *Vittatina hiltonensis* (1.0%), and the non-taeniate bisaccate species *Falcisporites zapfei* (1%), *Illinites delasaucei* (2.0%), *Klausipollenites schaubergeri* (16.5%), *Labiisporites granulatus* (1.5%), *Potonieisporites novicus* (<0.5%). The monosaccate pollen were represented by *Perisaccus granulosus* (0.5%) and *Vestigisporites minutus* (9.0%). *Reduviasporonites* sp. (1.0%) was present but rare, and the Unidentifiable component was comparatively reduced (4.0%). The Upgang Fm. was not sampled in SM4 (Figure 11).

6.5.2.14. Cycle 4 evaporites (Sherburn Anhydrite (EZ4 A), Sneaton Halite (EZ4 Na) and Sneaton Potash (EZ4 K)): SM4, SM11 boreholes

Analysis of rock salt samples yielded palynological recovery from the Cycle 4 evaporites. Palynomorphs have not previously been recorded from either the Cycle 4 or Cycle 5 evaporites as they are not lithologies typically targeted for palynological analysis and are often missing from

borehole cores as the underlying Carboniferous and earlier Permian strata are more commercially important. Therefore, the results presented here from Cycle 4 and above provide a unique insight into the vegetation during latest Zechstein times.

In SM11 (Figure 10) two samples from the lower Sneaton Halite, were of low yield and composed mostly of Unidentifiable pollen grains, however *Lueckisporites virkkiae* Variant C, *Klausipollenites schaubergeri*, and *Reduviasporonites* sp. were recovered as well. In SM11 one sample from the upper Sneaton Halite contained only rare Unidentifiable pollen (n=3).

In SM11 the Sherburn Anhydrite assemblage was dominated by Unidentifiable pollen grains (71.4%) and contained the taeniate bisaccate pollen *Lueckisporites virkkiae* (3.2%), *L. virkkiae* Variant C (9.4%), the non-taeniate bisaccate pollen *Klausipollenites schaubergeri* (1.6%), *Labiisporites granulatus* (9.1%), *Potonieisporites novicus* (9.1%), and considerable abundance of *Reduviasporonites* sp. (22.8%).

In borehole SM4 (Figure 11), the Sneaton Halite and Sneaton Potash assemblages did not have a high yield (<200 count) and are dominated by Unidentifiable palynomorphs (88.9-100.0%), though they contained *Klausipollenites schaubergeri* (7.4%) and *Lueckisporites virkkiae* (3.7%). The upper Sneaton Halite of borehole SM11 contained a single sample of very low yield composed only of Unidentifiable palynomorphs.

The Sneaton Potash in SM4 was dominated by Unidentifiable pollen grains (91.8%), with the assemblage also containing *Lueckisporites virkkiae* (8.2%) and *Klausipollenites schaubergeri* (8.5%).

6.5.2.15. Cycle 5 carbonates (EZ5 Ca) Sleights Siltstone: SM4 borehole

The Sleights Siltstone from borehole SM4 (Figure 11) contained an assemblage composed only of Unidentifiable palynomorphs at a very low yield (<200 count) (sample SM4 1258.63 m).

6.5.2.16. Cycle 5 evaporites (Littlebeck Anhydrite and Bröckelschiefer): SM11 borehole

There was no recovery from the Littlebeck Anhydrite in any of the borehole material. However, the Bröckelschiefer in SM11 (Figure 10) yielded an assemblage composed of *Lueckisporites virkkiae* Variant C (2.0%), *Illinites* sp. (5.0%) and dominated by Unidentifiable pollen grains (93.0%)

6.5.2.17. Latest Zechstein: Little Scar Beach outcrop

Samples from Little Scar (Figure 14) were mostly barren yet those that did contain a yield had a very low abundance of palynomorphs (<50). However, *Taeniaesporites* sp. was found in LSSC 1 (2.5%), and LSSC 1-6 did contain very low abundances of Unidentifiable palynomorphs (80.0-100.0%). LSSC 1 had the highest yield of palynomorphs at 38 palynomorphs per slide. What is most interesting about these samples is that LSSC 2 and LSSC 3 contained benthic foraminiferal test linings (Plate III, 10), which are indicative of relatively normal marine conditions. Foraminiferal test linings were incredibly rare throughout the material used in this study, only otherwise found in material from Salterford Farm borehole belonging to the Marl Slate (EZ1) (Plate III, 11). Belonging to Cycle 4-5, the strata at Little Scar beach form a useful comparison the strata of a younger age from Cycle 1.

6.5.3. Summary of the distribution of taxa within the stratigraphical sequence

6.5.3.1. Cycle 1 Marl Slate: the principal Zechstein transgression

The Marl Slate assemblages are generally very well preserved as they were recovered from bituminous anoxic shale. In terms of average percentage abundance, they are dominated by *Lueckisporites virkkiae* (53.5%) and *Taeniaesporites* spp. (22.5%), but also contain *Klausipollenites schaubergeri* (8.3%), *Illinites* sp. (5.5%), *Vestigisporites minutus* (5.5%), *Vittatina hiltonensis* (2.5%), and less than 2.0% each of *Alisporites nuthallensis*, *Crustaesporites globosus*, *Nuskoisporites dulhuntyi*, *Perisaccus granulosus*, *Protohaploxypinus* spp., *Striatopodocarpites* sp. and spores. In samples where Unidentifiable pollen grains are present, they represent 93.0% of the assemblage indicating poor preservation. Many pollen grains are of a hyaline nature making species identification difficult. Recovery of benthic coiled foraminiferal test linings from Salterford Farm borehole sample SF465 corroborates marine conditions during deposition.

6.5.3.2. Cycle 1 Carbonates

The Cycle 1 carbonates assemblages are generally more speciose than those from the Marl Slate and the palynomorphs are less hyaline in nature making species differentiation and identification easier. Assemblages are still dominated by *Lueckisporites virkkiae* (44.5%), but here the three variants of Clarke (1965) are distinguishable. *Klausipollenites schaubergeri* is more abundant than in the Marl Slate (13.7%) as well as *Illinites* sp. (5.5%) but with the three species *I. delasaucei*, *I. klausi* and *I. tectus* distinguishable, of which *I. delasaucei* reached abundances of 9.5%. *Vestigisporites minutus* is of similar abundance (4.8%) while *Vittatina hiltonensis* increased in abundance (3.2%). A variety of *Taeniaesporites* spp. are present including *T. albertae* (5.5%), *T. angulistriatus* (1.7%), *T. labdacus* (4.5%), *T. noviaulensis* (3.0%) and *T. novimundi* (1.8%). *Alisporites nuthallensis* (2.4%) and

Labiisporites granulatus (2.6%) increase in abundance. *Protohaploxypinus* sp. (0.6%), *P. jacobii* (1.3%), and *Falcisporites zapfei* (1.0%) are less abundant than in the Marl Slate, becoming rare, while *Nuskoisporites dulhuntyi* (0.5%), *Perisaccus granulosus* (0.5%), and *Striatopodocarpites* sp. (0.5%) maintain a rare abundance. *Striatoabieites richteri* (0.5%) and *Reduviasporonites* sp. (3.4%) appear, along with very rare tetrads (<0.5%). *Crustaesporites globosus*, *Cycadopites rarus* and acritarchs are not present. In the Cycle 1 carbonates better preservation enables the identification of more species, giving the impression of increased species richness. According to previous literature Zechstein Cycles 1 and 2 yielded the richest palynomorph assemblages, which this data supports, but a preservational bias should not be ignored.

6.5.3.3. Cycle 2 Carbonates

The Cycle 2 carbonate assemblages are also dominated by *Lueckisporites virkkiae* (53.5%), but only Variant A is distinguishable. *Alisporites nuthallensis* becomes rare (1.0%), *Illinites* sp. increases in abundance (8.4%), *I. delasaucei* decreases dramatically (<0.5%) and *I. klausi* and *I. tectus* disappeared. *Klausipollenites schaubergeri* (20.0%) and *Taeniaesporites* spp. (4.6%) increases in abundance yet fewer species are present with *T. noviaulensis* absent, and overall the abundance of individual species decreases, suggesting *Taeniaesporites* is not well enough preserved to distinguish species in these assemblages. *Protohaploxypinus* spp. continues to be rare (2.2%) however more species are present including *P. chaloneri* (0.5%), *P. jacobii* (<0.5%), and *P. microcorpus* (1.0%). *Nuskoisporites dulhuntyi* (1.0%) and *Perisaccus granulosus* (<0.5%) maintains a rare abundance. *Vestigisporites minutus* decreases in abundance by over a half (1.9%). *Falcisporites zapfei* (1.0%), *Vittatina hiltonensis* (0.5%), spores (<0.5%), *Striatopodocarpites* sp. (<0.5%) and *Potonieisporites novicus* (<0.5%) are rare. *Striatoabieites richteri*, *Platysaccus radialis*, and *Reduviasporonites* sp. disappears and *Crustaesporites globosus*, *Cycadopites rarus*, acritarchs, and tetrads are still absent. Unidentifiable pollen grains comprise on average 44.9% of assemblages, slightly less (~4.5%) than in the Cycle 1 carbonates.

6.5.3.4. Cycle 2 Evaporites

The Cycle 2 evaporite assemblages contains *Lueckisporites virkkiae* (5.5%) at much lower abundances but with all three variants distinguishable, due to a relative increase in the abundance of Unidentifiable pollen grains (77.4%), a result of many poorly preserved assemblages. Consequently, the abundance of many species appears to decline. *Illinites* sp. experiences a slight decline in abundance (5.6%) with *I. delasaucei* increasing in abundance (2.5%), and *I. klausi* reappearing

(<0.5%) while *I. tectus* remains absent. *Klausipollenites schaubergeri* dramatically declines in abundance (6.4%), *Nuskoisporites dulhuntyi* declines (0.5%). *Protohaploxypinus* sp. is rare (1.3%), with little change in the species remaining from the Cycle 2 carbonates: *P. chaloneri* (1.5%), *P. jacobii* (0.5%), and *P. microcorpus* (0.5%). *Taeniaesporites* spp. overall experiences a slight increase in abundance (5.1%) and a reorganization of species as *T. noviaulensis* appears (1.0%) while *T. novimundi* disappears. *T. albertae* (1.3%) and *T. angulistriatus* (0.5%) maintain rare abundances. *Striatoabieites richteri* remains absent and *Striatopodocarpites* sp. disappears. *Vittatina hiltonensis* continues to be rare (<0.5%). *Alisporites nuthallensis* (1.0%) as well as *Perisaccus granulosus* (0.5%) maintain low abundances. *Falcisporites zapfei* disappears. However, some species experience increases in abundance such as *Labiisporites granulatus* (1.8%), *Nuskoisporites* cf. *rotatus* appears for the first time (<0.5%), *Platysaccus radialis* reappears but is very rare (<0.5%), *Potonieisporites novicus* increases slightly in abundance (2.6%). *Reduviasporonites* sp. reappears at considerable abundance (8.4%). *Cycadopites rarus*, acritarchs and tetrads remain absent while spores maintain a rare abundance (0.8%).

6.5.3.5. Cycle 3 Carbonates

The Cycle 3 carbonate assemblages display a continuing trend of increasingly abundant Unidentifiable pollen grains (89.1%) at the expense of identifiable species. *Lueckisporites virkkiae* is present at yet again slightly lower abundances (4.5%), however all variants are distinguishable. *Alisporites nuthallensis* becomes very rare (<0.5%). *Illinites* sp. declines again in abundance (3.1%), along with *I. delasaucei* (0.5%), while *I. tectus* maintains its very rare abundance (<0.5%). *Klausipollenites schaubergeri* continues to decline (5.9%), as does *Labiisporites granulatus* (1.5%). *Nuskoisporites* cf. *rotatus* (<0.5%), *N. dulhuntyi* (<0.5%), and *Potonieisporites novicus* (0.5%) maintain rarity. No individual species of *Protohaploxypinus* are distinguishable, and *Protohaploxypinus* sp. maintains rarity (1.0%). *Reduviasporonites* sp. dramatically decreases from 8.8% to extremely rare (<0.5%). *Taeniaesporites* spp. experiences a considerable decrease in abundance (1.6%) with *T. labdacus* (0.7%), *T. noviaulensis* (1.0%) and *T. angulistriatus* remaining rare (1.0%). *Vestigisporites minutus* decreases further in abundance (3.2%). *Striatoabieites richteri* remains absent, *Perisaccus granulosus*, *Platysaccus radialis* and *Vittatina hiltonensis* are not present. However, *Striatopodocarpites antiquus* reappears but is rare (0.5%) alongside *Falcisporites zapfei* (<0.5%). Trisaccate pollen grains are very rare (<0.5%).

6.5.3.6. Cycle 3 Evaporites

In the Cycle 3 evaporites many species experience an increase in abundance accompanied by a decline in the proportion of Unidentifiable pollen grains (60.9%). *Alisporites nuthallensis* maintains rarity (1.8%), *Crustaesporites globosus* reappears but is rare (<0.5%), *Cycadopites rarus* occurs for the only time in the Zechstein succession (0.5%), *Falcisporites zapfei* maintains rarity (0.9%). *Illinites* sp. increases (5.0%) and *I. delasaucei* (4.2%) and *I. tectus* (5.2%) experience large increases, while *I. klausi* is absent. The abundance of *Klausipollenites schaubergeri* returns to Cycle 2 levels (14.1%), and *Labiisporites granulatus* also recovers (5.1%). *Lueckisporites virkkiae* also starts to recover but does not reach early Zechstein abundances (8.9%), however all three variants are distinguishable, with Variant A notably accounting for 18.6% of assemblages. *Nuskoisporites dulhuntyi* is still rare (0.8%) as well as *Potonieisporites novicus* (0.9%), and *Perisaccus granulosus* reappears (0.9%). All species of *Protohaploxypinus* are present with undifferentiated individuals only comprising 1.1% of assemblages. *P.* cf. *samoilovichii* (0.5%), *P. chaloneri* (1.5%), *P. jacobii* (1.7%), and *P. microcorpus* (1.1%) reappear. *Reduviasporonites* sp. increases slightly (1.8%), *Striatopodocarpites antiquus* is still rare (1.2%) and *Striatopodocarpites* sp. reappears (1.1%). *Taeniaesporites* sp. increases (2.9%) and *T. alb*ertae (2.0%) and *T. novimundi* (1.7%) reappear, while *T. angulistriatus* maintains low abundance (1.1%). *T. labdacus* (2.6%) and *T. noviaulensis* (1.8%) both increase marginally in abundance. *Vestigisporites minutus* increases in abundance (5.9%), *Vittatina hiltonensis* reappears although is very rare (<0.5%). However, some species do not recover. *Nuskoisporites* cf. *rotatus* is absent. *Platysaccus radialis* and *Striatoabieites richteri* remain absent, as do tetrads. However, acritarchs (0.5%) and trisaccate pollen grains (0.5%) were recovered although no spores were recovered.

6.5.3.7. Cycle 4 Carbonates

The Cycle 4 carbonate assemblages are once again dominated by *Lueckisporites virkkiae* (52.0%), with all three variants distinguishable. The Unidentifiable component is considerably reduced (13.9%). Other species also experience increases in abundance. *Crustaesporites globosus* increases slightly (1.0%). *Nuskoisporites* cf. *rotatus* reappears (1.0%) however, *N. dulhuntyi* decreases slightly (0.5%). *Platysaccus radialis* reappears at very rare abundances (<0.5%). *Striatoabieites richteri* reappears and *Striatopodocarpites fusus* appears for the first time, both at very rare abundances (<0.5%). *Taeniaesporites* sp. increases slightly (3.0%), with increases also seen in *T. angulistriatus* (2.3%), and *T. labdacus* (5.9%). *T. bilobus* appears for the first and only time (0.5%). *T. albertae* (1.3%), *T. noviaulensis* (0.7%) and *T. novimundi* (0.7%) maintain their rarity alongside *Vittatina hiltonensis* (0.7%). *Vestigisporites minutus* more or less maintains abundance (5.6%). Other species

experience noticeable reductions. *Klausipollenites schaubergeri* declines slightly in abundance (12.1%), *Alisporites nuthallensis* maintains low abundance (0.5%), while *Illinites* sp. reduces slightly (3.0%), with slight decreases in *I. delasaucei* (2.4%) and *I. tectus* (2.0%), while *I. klausi* reappears at low abundances (0.5%). *Perisaccus granulosus* (0.5%) and *Potonieisporites novicus* (0.5%) maintain rare abundances. *Protohaploxypinus* sp. (1.5%) is present at low abundance within individual species also occurring at low abundance or being rare; *P. chaloneri* (1.4%), *P. jacobii* (0.9%) and *P. microcorpus* (0.5%). *Reduviasporonites* sp. declines slightly (1.8%), *Striatopodocarpites antiquus* disappears. *Cycadopites rarus* and *Striatopodocarpites* sp. are absent. Acritarchs maintain a rare abundance (0.5%), while tetrads and spores remain absent. No trisaccate pollen grains are recovered after the Cycle 4 carbonates.

6.5.3.8. Cycle 4 evaporites and Cycle 5

The assemblages from Cycle 5 carbonates and evaporites are comparatively impoverished with samples having low yields, a trend that appears to start in the Cycle 4 evaporites. The Cycle 4 evaporites contain an assemblage dominated by Unidentifiable pollen grains (84.2%), accompanied by the fungus/algae *Reduviasporonites* sp. (22.8%), *Lueckisporites virkkiae* (15.7%), *Protohaploxypinus* cf. *samoilovichii* (9.1%), and *Klausipollenites schaubergeri* (5.8%). In the Cycle 5 carbonates only Unidentifiable pollen grains (96.0%) were recovered from borehole material, and benthic coiled foraminiferal test linings (15.0%) from outcrop at Little Scar Beach (samples LSSC 2 and LSSC3). The Cycle 5 evaporites from borehole material only contain sparse *Illinites* sp. (5.0%), *Lueckisporites virkkiae* (2.0%) and an abundance of Unidentifiable pollen grains (93.0%).

6.5.4 Comparison of the Durham and Yorkshire Sub-basins

Comparisons between spore-pollen assemblages from the Yorkshire and Durham Sub-basins are only possible for the lower cycles as the upper cycles from the Durham Sub-basin have not yielded palynomorphs.

In terms of the lowest cycle Cycle 1 The Marl Slate/'Lower Magnesian Limestone' assemblages in Salterford Farm borehole (Yorkshire Sub-basin) contain more taxa than Claxheugh Rock and Crime Rigg Quarry (Durham Sub-basin). However, differences are likely the result of differential preservation as the proportion of Unidentifiable pollen grains is considerably lower in Salterford Farm compared to the samples from Claxheugh Rock and Crime Rigg Quarry, and in general samples from the Marl Slate of the Durham Sub-basin are more hyaline in appearance than those from the Yorkshire Sub-basin. *Illinites delasaucei*, *Klausipollenites schaubergeri*,

Lueckisporites virkkiae Variant A, *Vestigisporites minutus* are the most common species in Salterford Farm. *Lueckisporites virkkiae*, *Taeniaesporites* spp., *Illinites* spp., *Vestigisporites minutus* and *Klausipollenites schaubergeri* are most abundant taxa in Claxheugh Rock, and *Illinites* spp., *Klausipollenites schaubergeri*, *L. virkkiae*, *Taeniaesporites* spp. and *Vestigisporites minutus* are the most common species in Crime Rigg Quarry. In addition, *Taeniaesporites* spp. is more abundant in the Durham Sub-basin. It appears that *Vestigisporites minutus* is not a common component of early Zechstein palynofloras. *V. minutus* is present in low abundance at Kimberley and in Woolsthorpe Bridge borehole but maintains considerable presence through the Salterford Farm borehole. In the Durham Sub-basin *V. minutus* is only present in one sample from Claxheugh Rock yet is reasonably abundant in the single sample from Crime Rigg Quarry.

The Cadeby Formation exposed in the Kimberley railway cutting, that was palynologically analysed by Clarke (1965), was resampled. The assemblages described here correspond to samples K5 and K6 of the original study. Our findings are very similar to those of Clarke (1965), but with some minor differences that concern observations on taxa that are rare in the assemblages. Our study did not recover *Striatopodocarpites cancellatus* or *Labiisporites granulatus*. The reprocessed K5 sample revealed the presence of *Taeniaesporites angulistriatus*, *Striatopodocarpites antiquus*, *Vittatina hiltonensis*, *Illinites tectus*, *Perisaccus granulosus*, *Nuskoisporites dulhuntyi*, *Potonieisporites novicus* and *Alisporites nuthallensis*. Both the original study and this study note the absence of *Vestigisporites minutus*, a species that is abundant throughout the borehole and outcrop material. *Alisporites nuthallensis* was identified in this analysis of the Kimberley material and different *Protohaploxypinus* species were identified in Clarke's study. These two genera are both rare meaning any disparity in presence and abundance is likely due to the rarity of these two taxa and the low probability of all species occurring in all of the slides made from the same sample.

Previous work on the Cycle 1 carbonates from Woolsthorpe Bridge (Warrington, 1980; Berridge et al., 1999) recorded the presence of a characteristic Zechstein miospore assemblage composed of *Alisporites* sp., *Crustaesporites* cf. *globosus*, *Falcisporites zapfei*, *Klausipollenites schaubergeri*, *Lueckisporites virkkiae*, ?Perisaccus *granulosus*, *Protohaploxypinus* spp., *P.* cf. *chaloneri*, *P.* cf. *jacobii*, *P. microcorpus*, ?*Striatopodocarpites* sp., *Taeniaesporites* spp., *T. labdacus*, *T. noviaulensis*. *Labiisporites granulatus*, *Taeniaesporites albertae,* and *Vestigisporites minutus* were not recorded (G. Warrington pers. comm.) but have been recovered during this study.

Recovery of an assemblage from the Cadeby Formation, comparable to those from the 'Lower Marl' at Kimberley, Cinderhill, and Woolsthorpe Bridge, has previously been reported from Salterford Farm (Warrington, 1980; Berridge et al., 1999). The age of these assemblages has been interpreted as Lopingian based on the presence of *Lueckisporites virkkiae*.

6.6. Reconstructing the Zechstein flora

6.6.1. General comments: palaeoecology

The Zechstein Sea was located within the Permian Euramerican phytogeographical province with a flora dominated by abundant conifers and pteridosperms with rare ginkgophytes, sphenophytes, ferns, lycopsids and potentially cycads (Schweitzer 1986; Cleal and Thomas, 1995). Detailed descriptions of Lopingian Euramerican flora have been provided for England, Germany and Poland (e.g. Kurtze, 1839; Geinitz, 1869; Solms-Laubach, 1884; Gothan and Nagelhard, 1923; Weigelt, 1928, 1930; Stoneley, 1958; Schweitzer, 1960, 1962, 1968, 1986; Ullrich, 1964; Poort and Kerp, 1990; Brandt, 1997; Uhl and Kerp, 2002), Spain (Bercovici et al., 2009), and the southern Alps (e.g. Clement-Westerhof, 1984, 1987, 1988; Visscher, 1986; Kutstatcher et al., 2012, 2014, 2017; Labandiera et al., 2016). A Zechstein-type flora has also been reported from Belgium (Florin, 1954). The floras are generally found in deposits of marginal marine or fluvial lowstand settings (e.g., Ullrich, 1964, Weigelt, 1928; Weigelt, 1930; Schweitzer, 1968; Schweitzer, 1986; Uhl and Kerp, 2002). It appears that the vegetation was fairly uniform across the basin, low in diversity and dominated by conifers (see Table 2), suggesting an arid to semi-arid environment and with plants adapted to periodic water stress.

The British Zechstein flora has been described in detail by Stoneley (1958) and Schweitzer (1986). Due to the suggested Lopingian climate trend towards increasing aridification the Zechstein flora has been interpreted as most abundant during Cycle 1 and the principal transgression and gradually disappearing from Cycle 2 onwards (Schweitzer, 1986). A similar trend of gradual decline was also suggested based on previous interpretation of palynomorph assemblages (Pattison et al., 1973; Smith et al., 1974).

Botanically based climatic inferences can be made from anatomical structures or by comparisons with other similar Lopingian Euramerican floras. The conifers and peltasperms from the Zechstein Basin and southern Europe exhibit some xerophorphic adaptations. They have very thick papillate cuticles, deeply sunken stomata, stomatal pores covered by overarching papillae, and some conifers leaves seem to have been thick and fleshy. However, not all taxa in the plant assemblages are fully adapted to xerophytic conditions.

The British Zechstein flora was previously divided into two groups based on their palaeoecology (Schweitzer, 1986). A xerophytic *Callipteris*-conifer association, which corresponds to the *Callipteris*-*Walchia* association of Gothan and Gimm (1930), and a hygrophylic *Neocalamites*-Sphenopterid association that corresponds to the *Calamites*-pecopterid (fern) association of Gothan and Gimm (1930). However, given more recent reconstructions of Lopingian Euramerican vegetation (e.g., Bercovici et al., 2009; Kutstatcher et al., 2012, 2014; Labandiera et al., 2016; Kustatscher et al.,

2017) a different structure is proposed. It is likely that conifers (e.g., *Ullmannia*, *Pseudovoltzia*, *Ortesia*) with their more xerophytic adaptations occupied the arid to semi-arid, well-drained, inland and hinterland areas and low-lying slopes of the Protopennines. Pteridosperms (peltasperms) (e.g., *Peltaspermum*) with their thicker cuticles likely inhabited coastal areas, living in drier lowland patches, and in the hinterlands with the conifers. Horsetails (*Neocalamites*) likely occupied wet lowland riparian environments, shallow water coastal bogs and lakes, and the mouth of rivers. Pteridosperms (e.g. *Sphenopteris*) likely inhabited slightly less humid habitats while ginkgophytes (e.g. *Sphenobaieria*) and potential cycads (e.g. *Pseudoctenis*, *Taeniopteris*) inhabited more humid lowland areas near bodies of water.

The dominance of taeniate bisaccate pollen of conifer and pteridosperm affinity in this study concurs with previous investigations. While their dominance in assemblages likely reflects the general nature of the parent vegetation, it should be noted that multitaeniate pollen grains were produced by multiple plant groups (Chaloner, 2013), and there may also be a taphonomic bias towards bisaccate pollen due to their thick exines. Pollen grains of probable ginkgo and possible cycad (*Cycadopites rarus*) affinity are rare. This is expected as ginkgophytes are known to be rare components of the Zechstein flora, with some exceptions (e.g. Bauer et al. 2014), and potential cycads even rarer. However, this may also be the result of a taphonomic bias. Finally, interpreting the exact nature and habitat of the vegetation is also complicated by the lack of autochthonous plant remains beyond Cycle 1.

6.6.2. Vegetation change through time

The changing nature of spore-pollen assemblages through the Zechstein sequences of northeast England, as reported in this study, can be interpreted to document the changing nature of the flora. The affinities of many of the spore-pollen taxa are well documented. However, in some cases the lack of in situ occurrences means that some abundant bisaccate taxa, such as *Labiisporites granulatus*, and some monosaccate pollen taxa, such as *Vestigisporites minutus* and *Perisaccus granulosus*, have not yet been assigned to a parent plant group.

The palynological data spans almost the entire temporal extent of the Zechstein, allowing a reinterpretation of the flora. Plants were assumed to gradually disappear after Cycle 2 due to aridification and high rates of evaporation, with aridity being enhanced by the decreasing magnitude of successive transgressive episodes. Instead, the assemblages from the upper Zechstein Cycle 4 and Cycle 5 show that the conifer-pteridosperm dominated flora persisted through to the Permian-Triassic boundary. This was likely facilitated by increasing fluvial activity, seen in the increase in terrigenous

fluvial sediments, from the end of Cycle 3 onwards. Presumably, this provided sufficient humidity to support the flora. Thus, it appears likely that the flora had an azonal distribution that was more severely influenced by edaphic factors than larger scale climate change.

While the upper Zechstein (Cycle 4-5) assemblages suggest a decline in the flora towards the Permian-Triassic boundary this may also be a taphonomic effect. The assemblages recovered from the Carnallitic Marl Formation (Cycle 4) in SM11 (Figure 10) and SM4 (Figure 11) yield palynomorph assemblages of similar composition and abundance to those recovered from the Marl Slate (Cycle 1) (Figure 4-6), suggesting that conditions were not as inhospitable during the upper Zechstein as previously assumed.

In the British Isles the Zechstein can be divided either into the classic five carbonate-evaporites cycles or seven evaporite-carbonate sequences based on Tucker's (1991) sequence stratigraphic scheme for the basin margins. The pollen charts in Figures 4-14 have been presented against both organisations. The sequence stratigraphic approach is particularly appropriate as the locations studied here are marginal marine. Changing shorelines would have had significant impacts on the Zechstein vegetation, with highstands and lowstands effecting groundwater levels, precipitation, and therefore the distribution of suitable wetter habitats and taphonomic windows. Interpreting the data at the scale of transgression-regression cycles or sequences may reveal the responses of vegetation to the accompanying patterns of drastic climatic and environmental changes.

Long term changes across the Zechstein sequence and slow rates of change are likely a reflection of climate and environmental trends of increasing aridity and temperature that characterise the Lopingian. The Zechstein Group covers the last ~6 million years of the Permian meaning any slow changes may be indicative of floral turnover associated with the end-Permian mass extinction. While the assemblages of Cycle 5 are comparatively impoverished and composed of highly degraded Unidentifiable pollen grains, this may also be indicative of longer, water-borne transport from inland or hinterland areas via the fluvial depositional system of Cycle 5 instead of reflecting the true nature of the state of the flora. Furthermore, there is no coincident increase in spores with the reduction in Cycle 5 assemblages that typifies the floral turnover at the Permian-Triassic boundary. Yet, this may also be a taphonomic effect since assemblages are generally poorly preserved.

The cyclic transgressions into the Zechstein Basin would have forced the hydrological cycle by shifting coastlines and altering local topography. During highstands increased runoff likely caused high groundwater stages in lowland areas already characterised by more hygrophytic flora. During lowstands reduced runoff may have led to increased drainage and desiccation of lowlands with the low-lying Protopennines already characterised by more xerophytic flora. This can explain coeval

occurrences of wet and dry lowlands and intrazonal vegetation throughout the Zechstein. Palynological assemblages may be expected to reflect these changing conditions, yet this is not necessarily reflected in the results presented here.

Ginkgophytes, horsetails ferns, lycopsids and possible cycads are among the rarest elements in the Zechstein flora, living around lakes and abandoned river channels, or along streams in a distal flood plain setting. While this is supported by their relative absence in the microfossil record, and may reflect the true nature of the vegetation, it may also be a taphonomic effect. Their dependence on the vicinity of large bodies of water or elevated ground water levels would have made them more sensitive to changes in sea level accompanying the Zechstein cycles.

The magnitude of sea level change diminished with each cycle as the sea progressively shrank in volume. The hygrophytic flora would have become increasingly stressed by the restriction of its habitat and the diminishing taphonomic window resulting in their rarity in the fossil record as both micro- and macrofossils. While their absence may be explained by sparsely distributed wet habitats suitable for reproduction, e.g., bryophytes are dependent on moist substrate upon which to reproduce (Whitaker and Edwards, 2010), it may reflect the poor preservation potential of certain palynomorph morphologies relative to the thicker walled conifer and pteridosperm bisaccate pollen. For example, horsetails are known to thrive in disturbed, anoxic, and saline environments (Husby, 2013) making them ideally suited to coastal Zechstein environments. Therefore, the rarity of horsetails in the microfossil record may be explained by the poor preservation potential of their palynomorphs. Modern horsetails (*Equisetum*) produce spores that are enveloped by four flexible ribbon-like elaters that are incredibly fragile (Marmottant et al., 2013). Furthermore, horsetails have a remarkable ability to reproduce vegetatively via rhizomes, compensating for the inefficiency of reproduction via spores, allowing horsetails to rapidly colonize coastal environments (Hauke, 1963), whilst remaining under-represented in the microfossil record.

Sea level highstands may explain the preferential preservation of coastal, nearshore, and inland habitats in certain strata, for example the Marl Slate (Cycle 1 transgression) and Carnallitic Marl Fm. (Cycle 3-4 boundary). Both are known for an abundance of microfossil remains, with the Marl Slate being notable for its macrofossil remains due to favourable taphonomic conditions. Increasing energy levels during the initial Zechstein transgression caused by the middle Wuchiapingian sea level highstand (Legler et al., 2011; Legler and Schneider, 2013) led to the rapid burial of material and the movement of azonal, coastal, flora into the taphonomic window created by this marginal environment. The transgression also established a distal fluvial plain with meandering and abandoned channels (like those at Pot Riding, Cadeby Formation, Cycle 1), resulting in the impression of a richer and lusher vegetation (e.g. Kustatscher et al., 2017). The Carnallitic Marl Fm.

marks the initiation of a humid fluvial environment and therefore is also affected by a similar favourable taphonomic bias. With higher sedimentation rates the preservation potential of the Marl Slate and Carnallitic Marl Fm. was considerably higher than that of other sedimentary settings resulting in a higher local diversity relative to other palynomorphs assemblages.

Unfortunately, the scarcity of plant macrofossils from beyond Cycle 1 means it is not possible to investigate the effects of sea level change on macrofossil preservation in the upper Zechstein, when sea level changes were of a lesser magnitude relative to the lower Zechstein, e.g., 1-2 meters rather than the sea level drop of 100-150m between Cycle 1 and Cycle 2 (Smith, 1989). The absence of the Cycle 1 evaporites (Hayton Anhydrite/Hartlepool Anhydrite) means there is no palynological data for the first major regression and evaporative phase and the biotic responses of the flora cannot be reconstructed. By Cycle 2 the vegetation had already experienced a drastic environmental transition between arid and marine-buffered conditions during the evaporative phase of Cycle 1.

There are several possible trends discernible from the Zechstein palynoflora. There appears to be an overall reduction in palynomorph diversity and abundance through the Zechstein Group, punctuated by taphonomic effects. *Lueckisporites virkkiae* consistently dominates assemblages by up to ~50.0%. It is a typical Zechstein taxon recovered in the Baltic (Podoba, 1975), throughout Europe (e.g. Klaus, 1963; Clarke, 1965; Visscher, 1971; Massari et al., 1988; Warrington and Scrivener, 1988; Massari et al., 1994, 1999; Pittau, 1999; Legler et al., 2005; Pittau, 2005; Legler and Schneider, 2008; Warrington, 2005, 2008; Gibson et al., 2020) and from age equivalent deposits in the U.S.A. (Wilson, 1962; Clapham, 1970). It is an important and distinct conifer signal throughout the Zechstein.

The Marl Slate palynoflora is abundant, corroborating previous studies of taxonomic diversity and relative abundance of palynomorph taxa, mirroring previous reports of the macrofossil record (Stoneley, 1958; Schweitzer, 1986). At the top of the Cycle 2 Fordon Evaporite Fm. there appears to be an increase in pollen abundance seen in SM4 (Figure 11) and SM11 (Figure 10). In particular, Unidentifiable pollen increase in abundance approaching the Cycle 2-3 boundary. This may be in response to increasing sea level during the late regressive-early transgressive phase expanding the distribution of coastal habitats and the taphonomic window. This trend is also visible in SM14b (Figure 13) where Unidentifiable pollen grains increase over the Cycle 2-3 boundary and the number of taxa present decline across the Grauer Salzton into the Brotherton Fm. *Lueckisporites virkkiae* and *Taeniaesporites* spp. survive the boundary, and *Nuskoisporites* appears. Before the boundary, an assemblage of *Illinites delasaucei*, *Klausipollenites schaubergeri*, *Labiisporites granulatus*, *Lueckisporites virkkiae*, *Potonieisporites novicus*, *Reduviasporonites*, *Taeniaesporites* sp. and

Vestigisporites minutus is present. It would appear a strong taphonomic bias is in effect as Unidentifiable pollen grains come to utterly dominate assemblages throughout the Brotherton Fm.

Preservation within the Cycle 3 evaporites (Billingham Anhydrite) of SM11 (Figure 10) is exceptional and the intermittent recovery throughout the evaporites is related to a lower sampling resolution through the evaporites instead of barren samples. The Carnallitic Marl Fm. palynoflora provides unique inside into the Cycle 3-Cycle 4 boundary flora. There is a noticeable increase in identifiable pollen species over the boundary. The assemblages recovered from the Carnallitic Marl Fm. from SM4 and SM11 (Figures 10-11) illustrate how conifers represent the most dominant component of the vegetation in the upper Zechstein e.g., *Lueckisporites virkkiae*, *Taeniaesporites* sp., and *Illinites* sp. Pollen grains of probably pteridosperm affinity occur less frequently e.g. *Protohaploxypinus* sp., *Striatoabieites* sp., *Striatopodocarpites* sp. and *Vittatina hiltonensis*. Throughout Cycle 4 some species disappear including *Vittatina* sp. (*Vittatina hiltonensis*) (Plate II, 1, 2). It is known to be rare in Lopingian assemblages (Clarke, 1965; Variakhuna, 1971) yet it appears intermittently though boreholes SM4 (Figure 11) an SM11 (Figure 10), at abundances no greater than 1.0%, until the Cycle 4 carbonates after which it disappears.

SM11 (Figure 10) has the longest temporal range of all boreholes studied and provides the best insight into the uppermost Zechstein flora. Palynomorphs were recovered across the Carnallitic Marl Fm.-Sleights Siltstone-Littlebeck Anhydrite boundaries, but then tail off and only Unidentifiable pollen grains are recovered through the rest of the sequence. The upper Zechstein trends are heavily affected by sampling resolution and the effect of the depositional settings on the quality of preservation. The relative proportions of conifer and pteridosperm pollen does not shift with conifer pollen being consistently more abundant. This trend continues into the uppermost Zechstein, with the recovery of *Illinites* spp. from the Little Scar assemblages, confirming the dominance of conifers throughout the Zechstein.

The palynoflora does not suggest evidence of vegetation destabilisation which is associated with the end-Permian mass extinction (Looy et al., 2001; Lindström and McLoughlin, 2007; Hochuli et al., 2010; Xiong and Wang, 2011; Hochuli et al., 2016; Schneebeli-Hermann et al., 2017; Fielding et al., 2019; Novak et al., 2019). Instead, it suggests an azonal vegetation dominated by conifers and pteridosperms inhabited a semi-arid landscape up to the Permian-Triassic boundary.

6.7 Palynofacies and the Zechstein palaeoenvironments

The fossil record is a result of the complex interplay between biotic and abiotic factors, and the composition of each palynomorph association is controlled by ecological factors, the depositional

environment and taphonomic processes. Therefore, disentangling preservational biases from biological signals is vital for palaeoecological reconstructions. Zechstein spore-pollen assemblages are a case in point.

The Zechstein Group is interpreted as mostly marine in origin, albeit rather unusual due to varying and increased salinity related to the evaporation-replenishment cyclicity, with the upper Zechstein (Cycles 4-5) recognised as predominantly fluvial-terrestrial. However, the paucity of marine palynomorphs remains surprising for the lower Zechstein (Cycles 1-3). The palynomorph assemblages are entirely dominated by allochthonous forms derived from the adjacent land mass: pollen, spores, and land plant cuticles (Stoneley, 1958). Presumably, these were transported in from the land by a combination of wind and water. The latter was probably most significant during siliciclastic phases of sedimentation and surely must have been the principal transporter of large fragments of plant cuticle. The former may, however, have been important in transporting pollen into hypersaline pools from which the evaporites were deposited. Acritarchs, indicative of marine influence, are surprisingly rare. They are absent from most samples despite sieving at 10μm and, where present, constitute no more than 0.5% of assemblages. In this study we only report *Micrystridium*-type from Cycle 3 evaporites and Cycle 4 carbonates, although Wall and Downie (1963) previously reported them from Cycle 1 only. The lack of acritarchs presumably reflects the harsh hypersaline marginal conditions that were not conducive for marine phytoplankton to thrive.

The rare foraminiferal test linings from Salterford Farm and Little Scar beach are of interest both for their rarity and location in the stratigraphic column, specifically for the specimens recovered from Little Scar. These may represent the latest occurrence of Permian foraminifera recovered in the UK (B. Spencer pers. comm.). Encrusting foraminifera have been well-documented from the Polish Zechstein reef systems (Peryt et al., 2012) where they form important constituents of the limestone formations during the early Zechstein. These test linings are benthic coiled forms, but their low quality of preservation makes taxonomic identifications difficult. The foraminifera from Salterford Farm are not unexpected as the sea during Marl Slate times was representative of relatively normal shallow marine conditions. However, from Little Scar, close to the Permian-Triassic boundary, benthic foraminifera appear in sediments interpreted as accumulating in the arid and hypersaline environments of the later Zechstein cycles.

Reduviasporonites in the British Permian has been correlated with brackish environments (Warrington, 2008). This is compatible with the pattern of recovery of these palynomorphs in this study. This reconstruction suggests that pockets of wetter environment persisted throughout the Zechstein. A fungal affinity has been invoked for *Reduviasporonites* with it interpreted as a saprophytic agent responsible for the degradation of widespread abundant dead organic matter

preceding the end-Permian mass extinction (Visscher et al., 1996, 2011; Hochuli, 2016). Mass occurrences of *Reduviasporonites* have been interpreted as an end-Permian fungal spike, coincident with vegetation die-off and environmental disturbance prior to and during the extinction. However, high abundances of *Reduviasporonites* have also been attributed to 'algal blooms' (Elsik, 1999; Afonin et al., 2001; Foster et al., 2002; Spina et al., 2015). Regardless of affinity, mass occurrences of *Reduviasporonites* are an important stratigraphical marker of the Permian-Triassic boundary in terrestrial and shallow marine environments. Interestingly, *Reduviasporonites* maintains a rare to low abundance throughout the Zechstein sequence, but occurs at higher abundances at the top of the Fordon Evaporite Fm. (8.4%) (Cycle 2 (EZ3 A, K-Mg, Na) and in the Cycle 4 evaporites (Sherburn Anhydrite, Sneaton Halite) (22.8%). However, recovery at this high abundance was only recorded in one sample of <100 yield (see Table 1 Appendix B and Appendix E SM11 1478.30 m) which is not conclusive evidence of a mass occurrence. The lack of a definitive "spike" in abundance at the top of the Zechstein sequence may be viewed as further evidence that there was no significant deforestation or vegetation turnover during Zechstein times.

A variety in quality of preservation is observed in the Zechstein material: (i) assemblages dominated by beautifully preserved palynomorphs of low thermal maturity (e.g., from the Marl Slate); (ii) assemblages dominated by very well-preserved palynomorphs that are dark in colour. (e.g. from the Carnallitic Marl Fm in SM11 Dove's Nest); (iii) assemblages dominated by AOM but containing well-preserved yet hyaline palynomorphs which need to be stained with Bismarck Brown to facilitate identification (e.g. from the Marl Slate at Claxheugh Rock); (iv) assemblages of abundant Unidentifiable pollen grains of very poor quality preservation; (v) Assemblages containing a mixture of types ii-iv above (e.g. argillaceous halite samples containing well-preserved intact palynomorphs as well as highly degraded Unidentifiable grains).

The evaporite palynomorph assemblages are of particular interest because they contain a mixture of pollen preservation types, which can be explained by two preservational processes. Well-preserved, intact palynomorphs were likely blown to the site of deposition on the wind, settled on the surface of the super-saturated sea water where they were encapsulated in the rapidly growing halite crystals. Poorly preserved pollen grains originate from clayey or argillaceous layers/pockets within the salt and arrived at the site of deposition via different means, having been subjected to higher degrees of biological degradation. Some may have washed in from the land via rivers or streams. Others may have settled out from the marine water column. While reworking within individual halite units is a possibility due to the high mobility of halite, the possibility of reworking between evaporite units is discounted based on the relative immobility of anhydrite and potassium-magnesium salts

which constrain the more mobile layers of halite. The preservation potential of the Zechstein evaporites is discussed in more detail in Gibson and Bodman (2020).

The dark colour of palynomorphs in some assemblages (particularly Type (ii) above) is a curious matter. Across EZ1-5 an apparent reverse thermal maturity profile indicated by palynomorph colour is observed with older assemblages being paler and more translucent than younger ones. Instead of being a true reverse thermal maturity profile darkening may be a result of the thermal conductivity of evaporites in combination with the exposure of palynomorphs to a hypersaline environment. It is also be a taphonomic effect of palynomorphs from the Marl Slate of the Durham Sub-basin which are exceptionally hyaline in appearance, possibly due to the more basinward location of the Durham Sub-basin.

6.8 Conclusions

Euramerica during the Permian was characterised by a progressive trend towards more arid climates (Roscher and Schneider, 2006; Montañez et al., 2007). However, the semi-arid climates of the Zechstein Basin were punctuated by several periods of more humid conditions associated with marine transgressions.

Spore-pollen preservation potential is highest during transgressive phases and just before regressive phases (e.g. Kustatscher et al., 2017). Other points of cycles fall outside of this taphonomic window of preservation, resulting in a reduced recovery of palynomorph. The use of evaporite palynology helps compensate for this, providing insight into the regressive phase flora for the first time.

Pollen-dominated assemblages have been recovered from throughout the Zechstein Group. Assemblages are dominated by conifer pollen, reflecting the characteristics of the gymnospermous Euramerican parent flora. The composition of assemblages remains relatively unchanged, both within and between Zechstein cycles. This confirms the reported uniform nature of the Zechstein vegetation.

Despite the additional taphonomic window afforded by the evaporites there remains difficulties disentangling taphonomic effects from biological signals. Regardless, the gymnospermous inland and hinterland flora appears to have persisted throughout the course of Zechstein deposition at least until the sea finally disappeared at or close to the Permian-Triassic boundary.

Acknowledgements

MEG was funded by a NERC studentship through the ACCE (Adapting to the Challenges of a Changing Environment) Doctoral Training Partnership [grant number 1807541]. We thank Geoffrey Warrington for taxonomic advice; David Bodman for assistance in the preparation of evaporite palynology samples; Asher Haynes of Sirius Minerals Plc and the York Potash Ltd for coordinating access to boreholes SM4 Gough, SM7 Mortar Hall, SM11 Dove's Nest and SM14b Woodsmith Mine North Shaft; Tracey Gallagher of the British Geological Survey for coordinating access to boreholes Salterford Farm and Woolsthorpe Bridge; the Yorkshire Wildlife Trust for approving access to the Pot Riding exposure at the Sprotbrough Gorge site; Doncaster Council for approving access to the Levitt Hagg Hole site; the owners of Transgear Units for providing access to the Sandal House exposure; Geoffrey Clayton for discussions on reverse thermal maturity profiles; Brian Spencer for the donation of the Little Scar Seaton Carew samples; Rick Ramsdale of the Sheffield Area Geology Trust for fieldwork assistance at the Pot Riding, Sandal House and Levitt Hagg Hole Sites. Finally, we thank the two reviews whose comments greatly improved the manuscript.

Supporting Information

Additional Supporting Information can be found in the accompanying electronic appendices:

Appendix F. Lithostratigraphical and facies descriptions for all localities

Appendix G. Location and stratigraphic range of all localities

Appendix H. List of borehole samples, their lithology, and yield

Appendix I. List of outcrop samples, their lithology, and yield

Appendix J. Raw count data

Figure Descriptions

Figures can be found in the electronic supplement to this chapter.

Figure 11. Occurrence and distribution of palynomorphs from SM4 Gough.

Figure 13. Occurrence and distribution of palynomorphs from SM7 Mortar Hall.

Figure 10. Occurrence and distribution of palynomorphs from SM11 Dove's Nest.

Figure 12. Occurrence and distribution of palynomorphs from SM14b Woodsmith Mine North Shaft.

Figure 7. Occurrence and distribution of palynomorphs from Salterford Farm.

Figure 8 Occurrence and distribution of palynomorphs from Woolsthorpe Bridge.

Figure 6. Occurrence and distribution of palynomorphs from Kimberley, Nottinghamshire.

Figure 4. Occurrence and distribution of palynomorphs from Claxheugh Rock.

Figure 5. Occurrence and distribution of palynomorphs from Crime Rigg Quarry.

Figure 9. Occurrence and distribution of palynomorphs from Marsden Bay.

Figure 14. Occurrence and distribution of palynomorphs from Little Scar.

Tables can be found in the electronic supplement to this chapter.

Table 1. List of the taxa encountered during this study and their probable botanical affinities.

Table 2. Summary of the distribution of the taxa encountered during this study.

Plate Descriptions

Plate I. Taeniate bisaccate pollen grains. England Finder co-ordinates included. Scale bar represents 50 μm in all images. Images taken using a QImaging (Model No. 01-MP3.3-RTV-R-CLR-10) camera mounted on an Olympus BH-2 transmitted light microscope in conjunction with QCapture Pro software.

1. *Lueckisporites virkkiae* Variant A (KIM 5, P43)
2. *L. virkkiae* Variant A (SM11 1312.24 m, U42/1)
3. *L. virkkiae* Variant B (KIM 5, B33/1)
4. *L. virkkiae* Variant C (KIM 6, E36/1)
5. *L. virkkiae* Variant C (SM11 1312.24 m, K30/1)
6. *Taeniaesporites labdacus* (SM11 1312.24 m, W45/2)
7. *T. labdacus* (SM11 1312.24 m, J32/2)
8. *T. noviaulensis* (SM11 1312.24 m, R42)
9. *T. noviaulensis* (SM11 1312.24 m, M48/2)
10. *T. novimundi* (SM11 1312.24 m, S31/2)
11. *T. angulistriatus* (SM1 1312.24 m, V35/3)
12. *T. albertae* (SM11 1458.37 m, J46/3)
13. *Protohaploxypinus chaloneri* (SM11 1312.24 m, G30)
14. *P. chaloneri* (SM11 1312.24 m, R36/3)
15. *P. jacobii* (SM11 1312.24 m, S46)
16. *P. jacobii* (SM11 1312.24 m, L33/1))
17. *P. microcorpus* (SM11 1312.24 m, K33)
18. *P.* cf. *samoilovichii.* (SM11 1334.10 m, O39)

Plate II. Taeniate and non-taeniate bisaccate pollen and monosaccate pollen. England Finder co-ordinates included. Scale bar represents 50 μm for all images. Images taken using a QImaging (Model No. 01-MP3.3-RTV-R-CLR-10) camera mounted on an Olympus BH-2 transmitted light microscope in conjunction with QCapture Pro software.

1. *Vittatina hiltonensis* (SM11 1312.24 m, F31)
2. *V. hiltonensis* (M4 1438.07 m, H32/2)
3. *Striatoabieites richteri* (SM11 1312.24 m, K27/3)
4. *Striatopodocarpites antiquus* (SM11 1312.24 m, P27)
5. *S. fusus* (SM11 1312.24 m, M29)
6. *Platysaccus radialis* (SM11 1312.24 m, J33/4)
7. *Klausipollenites schaubergeri* (SM11 1312.24 m, T39/3)
8. *K. schaubergeri* (SM11 1312.24 m, D32/3)

9. *Vestigisporites minutus* (KIM 5, P41)
10. *V. minutus* (SM11 1312.24 m, L30)
11. *V. minutus* (SM11 1312.24 m, J44/2)
12. *Illinites delasaucei* (SM11 1312.24 m, V41)
13. *I. klausi* (SM11 1328.76 m, P31/4)
14. *I. tectus* (SM11 1312.24 m, K30)
15. *I. tectus* (SM11 1312.24 m, Q41)
16. *Falcisporites zapfei* (SM11 1312.24 m, H42)
17. *F. zapfei* (SM11 1312.24 m, M33/2)
18. *Alisporites nuthallensis* (SM11 1312.24 m, M45)
19. *Labiisporites granulatus* (SM11 1312.24 m, L41)
20. *L. granulatus* (SM11 1312.24 m, G48/3)
21. *Alisporites nuthallensis* (SM11 1312.24 m, M45)

Plate III. Monosaccate pollen grains, trilete spores and foraminiferal test linings. England Finder co-ordinates included. Scale bar represents 50 µm for all images. Images taken using a QImaging (Model No. 01-MP3.3-RTV-R-CLR-10) camera mounted on an Olympus BH-2 transmitted light microscope in conjunction with QCapture Pro software.

1. *Nuskoisporites* cf. *rotatus* (SM11 1328.76 m, E43)
2. *N. dulhuntyi* (SM11 1312.24 m, T35/3)
3. *Perisaccus granulosus* (SM11 1312.24 m, W35/3)
4. *P. granulosus* (SM11 1312.24 m, O43/1)
5. *Potonieisporites novicus* (SM11 1304.14 m, E31)
6. ?*Potonieisporites novicus* (1312.24 m, D32/2)
7. *Crustaesporites globosus* (SM11 1328.76 m, R40/1)
8. Trilete spore (SM11 1465.92 m, P39)
9. Trilete spore (SM11 1465.92 m, C31/4)
10. Foraminiferal test lining (LSSC3, C37/4)
11. Foraminiferal test lining (SFYFP6373, S48)

Plate I

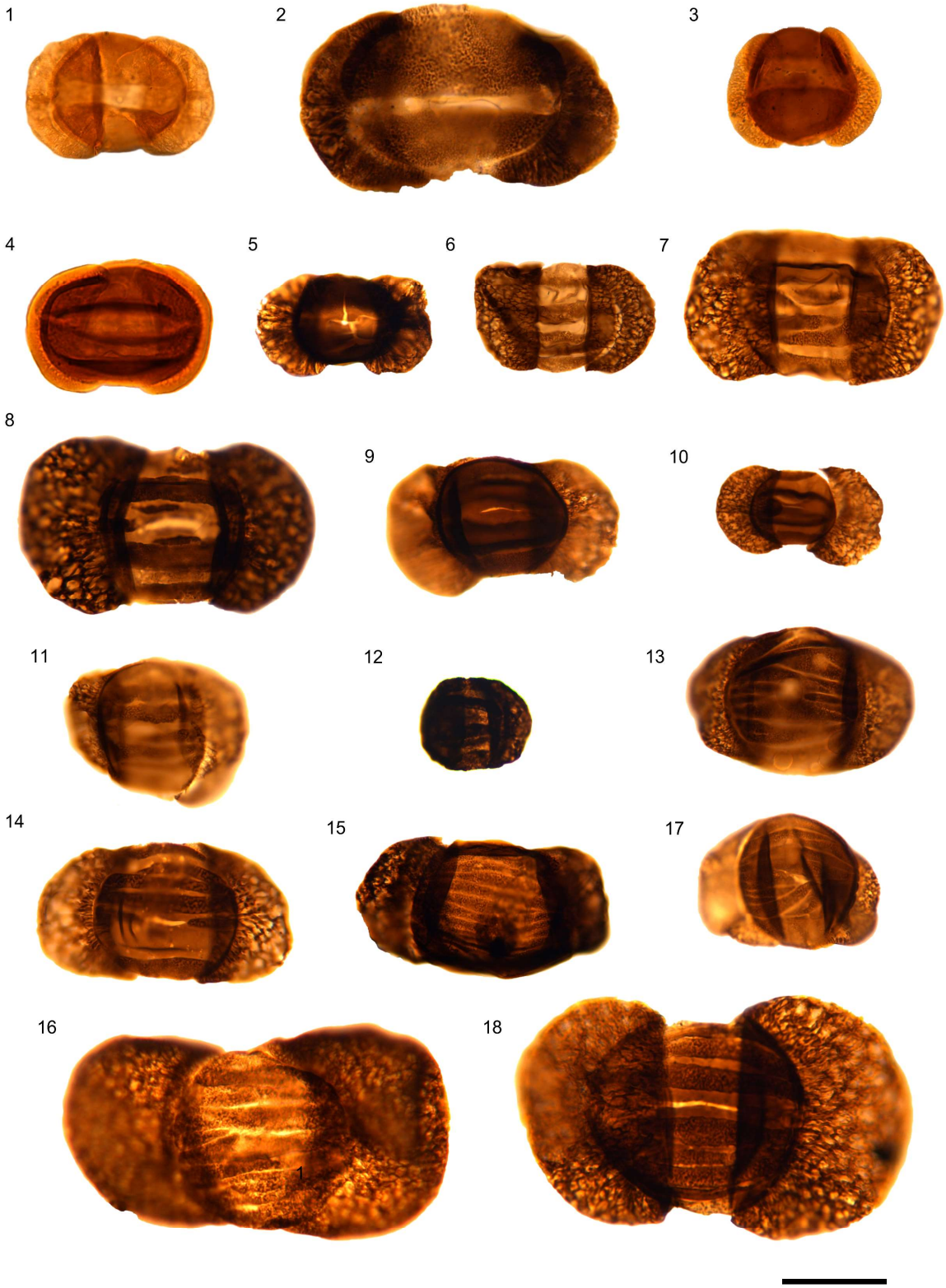

Plate II

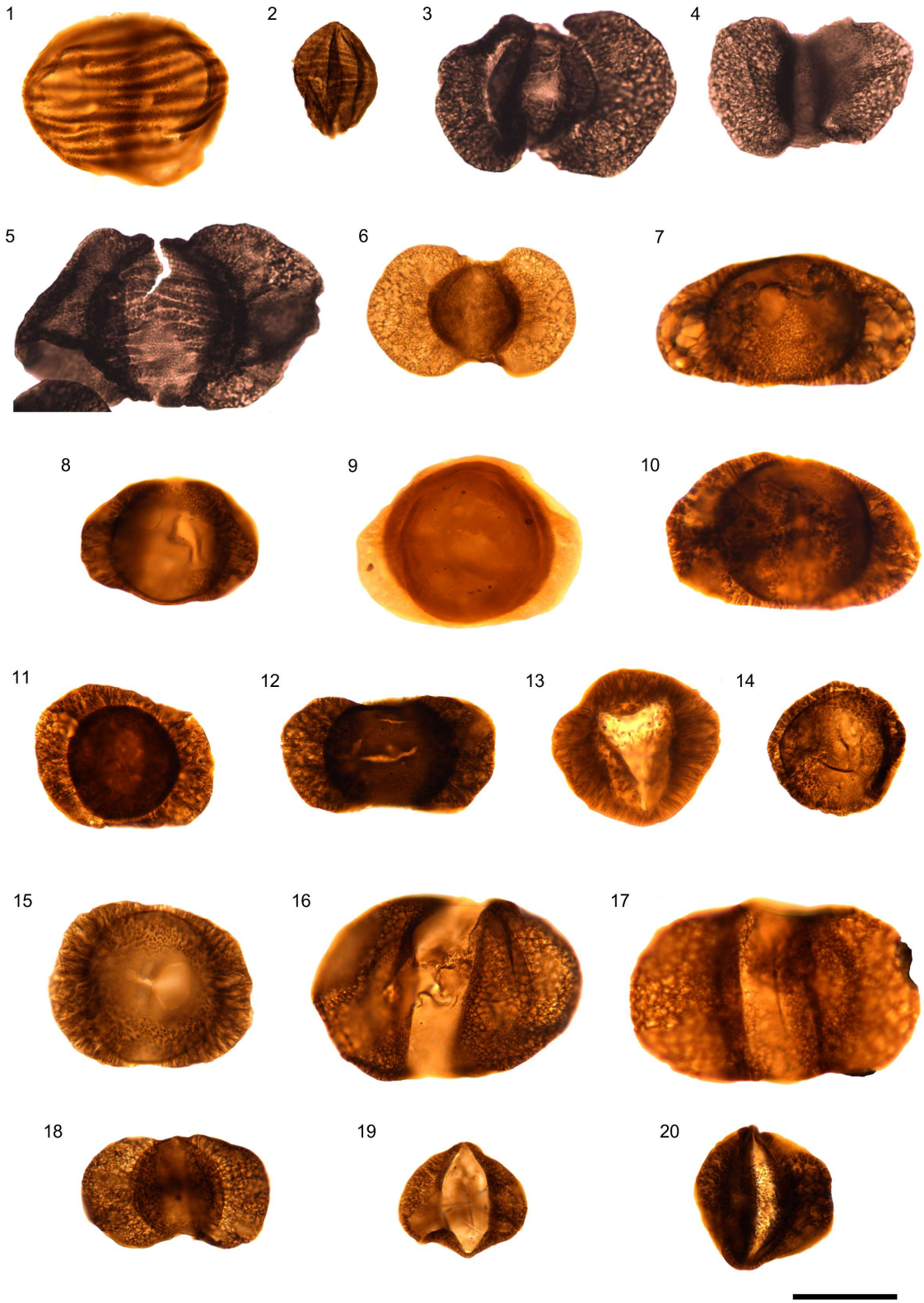

Plate III

Chapter 7.

Zechstein forests thrived up to the Permian-Triassic mass extinction event

Martha E. Gibson[1*] and Charles H. Wellman[1]

[1]*Department of Animal and Plant Sciences, Alfred Denny Building, University of Sheffield, Western Bank, S10 2TN, Sheffield, South Yorkshire, United Kingdom*

[*]*corresponding author: marthae.gibson@gmail.com*

Status as of 11th November 2020: manuscript in preparation. I wrote and undertook all interpretations in this paper.

Abstract

The Zechstein Sea was a large inland sea situated within northern Pangaea during the Lopingian. It was infilled by a remarkable carbonate-evaporite sequence consisting of up to seven evaporation-replenishment cycles. Previous palaeobotanical-palynological evidence shows that the hinterlands were vegetated with typical Euramerican gymnosperm forests during the earliest cycle. However, it is usually considered that these gradually declined and eventually disappeared as the environment became progressively hotter and drier approaching the Permian-Triassic Mass Extinction event. For the first time, pollen assemblages have been recovered from the entire Zechstein sequence, based on newly available borehole cores, and using improved techniques for recovering pollen from evaporites. The new pollen data indicate that the vegetation was little changed, both within cycles and between cycles, and persisted until the demise of the Zechstein Sea in the latest Permian-earliest Triassic. At this time desert sedimentation commenced, which yields no evidence for terrestrial vegetation until the early Triassic (Induan) when evidence for a radically different flora appears. These observations suggest that vegetation loss at the Permian-Triassic boundary was rapid and catastrophic rather than representing the culmination of a slow decline.

Keywords

Vegetation change, climate change, evaporites, spores, pollen grains, PTME, P-T boundary

Introduction

The Permian-Triassic Mass Extinction (PTME) (ca. 251myrs), the most severe biological crisis in Earth's history (Benton & Twitchett 2003; Erwin 2006), has been repeatedly associated with global

deforestation (Looy *et al.* 2001; Visscher *et al.* 2004). Recently, however, it has been suggested that there was a more gradual destruction of gymnosperm forests paving the way for the herbaceous lycopsid dominated terrestrial environments of the Early Triassic (Fielding *et al*. 2019; Gastaldo 2019; Novak *et al.* 2019). In Europe, the plant megafossil record for the Lopingian-early Middle Triassic interval is not well understood, largely because latest Lopingian strata are often eroded at outcrop and so there is limited understanding of how vegetation in Europe responded to the PTME (Kerp 2000). Previous palynological studies provide additional evidence but have suffered due to the same problem.

Lopingian vegetation reconstructions of central-western Europe are primarily based on evidence from the succession deposited in the epeiric Zechstein Sea (Clarke 1965a; Schweitzer 1986) (Fig. 1). The thick evaporite-dominated Zechstein Group was deposited during the latest Wuchiapingian (~258 Ma) to latest Changhsingian, ceasing at the Permian-Triassic boundary (PTB) (~252 Ma) (Fig. 2). Palaeobotanical and palynological evidence from the lower part of the Zechstein sequence suggests the inland sea was initially surrounded by a typical Euramerican gymnospermous vegetation (Schweitzer 1986) (Chapter 6 Table 1). However, palaeobotanical and palynological evidence has not previously been forthcoming from the middle and upper part of the Zechstein sequence, meaning the biotic responses of the vegetation during the ~6 Myrs preceding the PTME in unknown.

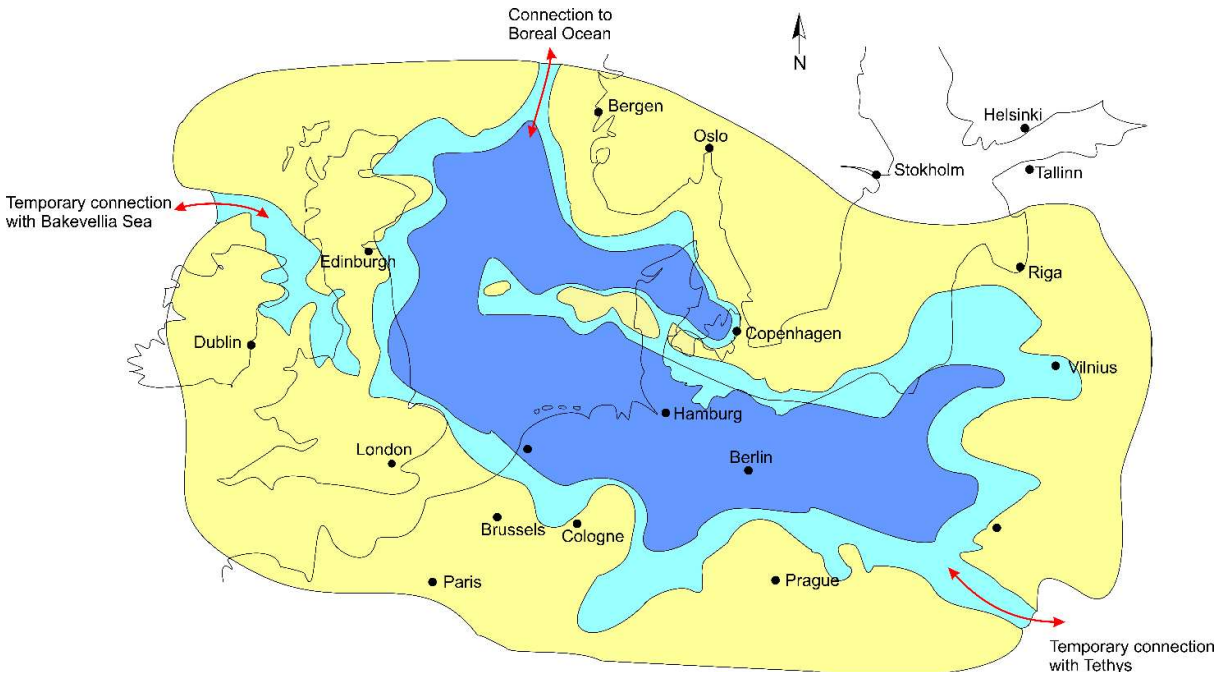

Figure 1. Palaeogeographical map of the Zechstein Sea.

Here we report on newly discovered palynological assemblages from throughout the entire Zechstein sequence. These have been recovered from fresh boreholes and by employing novel techniques to recover palynomorphs from evaporite samples.

The previous view of the Zechstein vegetation

Climate was a major vegetation control during the Permian, leading to the formation of distinct phytogeographical provinces (Ziegler 1990; Rees *et al.* 1999). The Zechstein Sea was located in the Euramerican floral province at mid-latitudes (10-30˚N) in an arid to semi-arid climate belt in the continental interior of Pangaea (Figure 1) (Montañez *et al.* 2007; Roscher *et al*. 2008, 2011).

The Lopingian fossil record of the European Zechstein is characteristically depauperate. Current vegetation reconstructions are based on both macrofossil occurrences and the dispersed fossil spores and pollen grain record (Chapter 6 Table 1) which are both almost entirely restricted to the earliest Zechstein. The vegetation is found to be composed of phylogenetically advanced gymnosperms (Stoneley 1958; Schweitzer, 1986), dominated by conifers and peltasperms, and accompanied by ginkgoes, tree ferns and rare cycads. It is likely that conifers (e.g. *Ullmannia*, *Pseudovoltzia*, *Ortesia*) with their more xerophytic adaptations occupied the arid to semi-arid, well-drained, inland and hinterland areas and low-lying slopes of the Protopennines. Pteridosperms (peltasperms) (e.g., *Peltaspermum*) with their thicker cuticles likely inhabited coastal areas, living in drier lowland patches, and in the hinterlands with the conifers. Horsetails (*Neocalamites*) likely occupied wet lowland riparian environments, shallow water coastal bogs and lakes, and the mouth of rivers. Pteridosperms (e.g., *Sphenopteris*) likely inhabited slightly less humid habitats while ginkgoes (e.g. *Sphenobaieria*) and potential cycads (e.g. *Pseudoctenis*, *Taeniopteris*) inhabited more humid lowland areas near bodies of water.

The plant macrofossil record is essentially exclusive to the Marl Slate (and equivalents) of Cycle 1 (see Figure 2) (e.g. Weigelt 1928, 1930; Stoneley 1958; Ullrich 1964; Schweitzer 1960, 1986; Uhl & Kerp 2002; Bödige 2007; Bauer *et al*. 2013). Dispersed spore-pollen assemblages are predominantly from Cycle 1 (Clark 1965a; Visscher 1971, 1972; Warrington & Scrivener 1988; Legler *et al*. 2005; Legler & Schneider 2008; Warrington 2005, 2008), with rare reports from Cycles 2 and 3 (Pattison *et al.* 1973). Based on these findings it has been suggested that vegetation thrived during and after the transgression of the Zechstein Sea into the Southern Permian Basin (SPB) (e.g. Kustatscher *et al.* 2014) but it was progressively decimated through the remaining cycles as the climate became harsher approaching the PTME.

A Zechstein vegetation extinction has been reinforced by the impression of extreme aridity during Zechstein times. Unsuitable conditions are assumed on the basis of the worsening climatic and environmental trends preceding the PTME, including increasing equatorial temperatures (Sheilds & Kiehl 2018), high atmospheric CO_2 concentrations (Black *et al.* 2019), low global sea levels providing limited ocean recharge into the SPB (Haq & Schutter 2008; Conrad 2013; Guillaume *et al.* 2016), and the widespread presence of evaporites in central Europe and the U.S.A. (e.g., Roscher *et al.* 2011).

However, it has recently been suggested that vegetation extinctions were not as devastating as previously assumed, with only minor declines in vegetation abundance following the P-T boundary (Fielding *et al.* 2019; Gastaldo 2019; Novak *et al*. 2019; Vajda *et al.* 2020). Furthermore, there was a shift in depositional environment from arid-humid cyclotherms to a predominantly humid fluvial environment after Cycle 3 (Słowakiewicz *et al.* 2009) that is not reflected in the current reconstruction.

Materials and methods

We have recovered, for the first time, spore/pollen assemblages from throughout the Zechstein sequence of eastern England. The material was recovered from a series of new borehole cores utilising both traditional palynological processing techniques and a newly developed technique for recovering palynomorphs from evaporites (Gibson & Bodman, *in review*). The study utilises the spore/pollen taxonomy outlined in Gibson & Wellman (*in review*). Stratigraphical details and palynomorph distribution are detailed in this study and in the on-line supplementary information. This new data on spore-pollen assemblages from all five of the Zechstein carbonate-evaporite cycles enables for

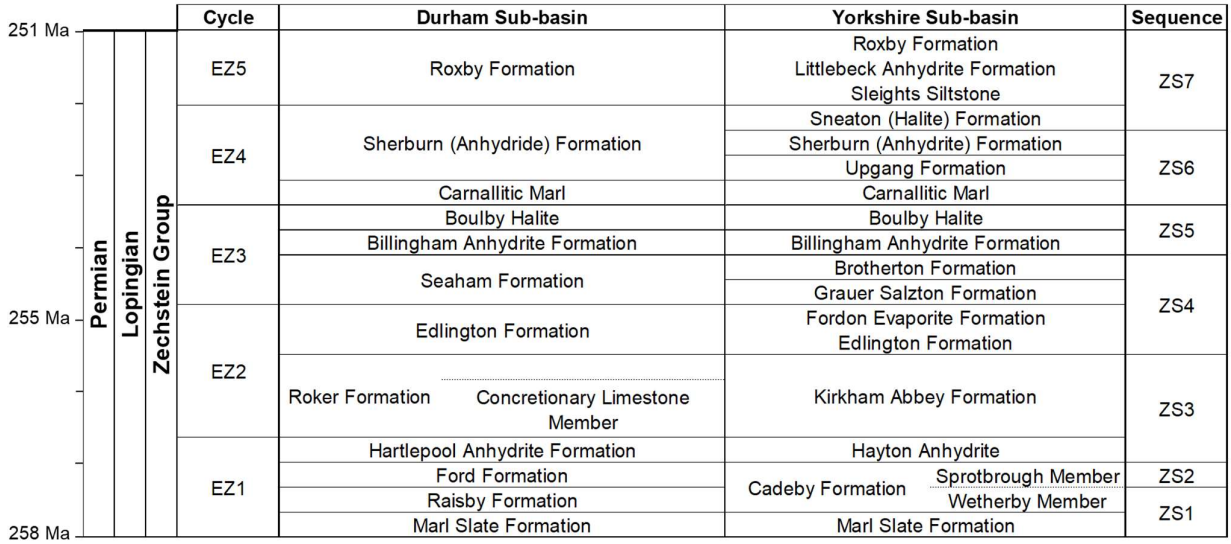

Figure. Stratigraphy of the British Zechstein. Dates for transgression and termination (Szurlies *et al.* 2013) and date of the EZ2 evaproites (Kemp *et al.* 2016).

generation of a new vegetation reconstruction. The range of the vegetation is expanded well-beyond previous estimates, by ca. 3-4myrs based on the 255 Ma date of the EZ2 evaporites (Kemp *et al.* 2016).

Results

The vegetation change through the Zechstein is illustrated in Figure 3. Throughout the sequence taeniate and non-taeniate bisaccate as well as monosaccate pollen grains of a gymnospermous affinity dominate assemblages. Through all cycles conifers and pteridosperms dominate the vegetation with ginkgoes and sphenophytes being much minor components. Lycopsids are very rare. This agrees with previously published accounts of British Zechstein palaeobotany (Stoneley 1958; Schweitzer 1986).

There are limited differences in assemblage composition throughout the sequence, with only minor variations in the presence-absence of taxa. However, the abundance of "Unidentifiable" palynomorphs can vary considerably, likely due to taphonomic effects. These are pollen grains of apparent high thermal maturity (Gibson & Bodman, *in review*), possibly a result of the high thermal conductivity of halite (Allen & Allen 2005). Exclusion of these pollen grains from the analysis may have given the impression of a barren landscape instead of a vegetated hinterland during Cycle 3 and the upper Zechstein Cycles 4-5. The abundance of this class of palynomorph during the uppermost Zechstein is a significant contribution to our understanding of PTB vegetation dynamics.

The recovery of exceptionally well-preserved pollen grains from the Carnallitic Marl Formation, a transgressive unit at the start of Cycle 4, is evidence that complex vegetation inhabited the upper Permian environment as its composition is comparable to the abundance and diverse Marl Slate assemblages. The uppermost assemblages from Cycle 5 are composed of the pollen grains of gymnosperm and known conifer affinity *Illinites* (Schweitzer 1986), suggesting conifers persisted close to the P-T boundary in Europe. These results are consistent with other recent palynological studies in which pollen and spores are observed to be relatively constant across the time frame studied with a slight drop observed only at the P-T boundary instead of a drawn-out decline (Nowak et al., 2019).

The palynology of the evaporites (Gibson & Wellman, *in review*), albeit sometimes at a lower yield, is further evidence that despite harsh environmental conditions there was likely sufficient precipitation in inland areas to sustain vegetation. This decline in yield is most likely a result of 'salting' whereby the rapid rate of precipitation of salts dilutes the abundance of palynomorphs encased within it (Gibson & Bodman, *in review*).

Conclusion

A more complex picture of the biosphere and climate during the PTME is emerging, with new evidence for significant changes in climate (Romano et al. 2013), and in the flora based on palynological analyses (Hochuli *et al.* 2010; Hermann *et al.* 2011; Hofmann *et al*. 2011; Schneebeli-Hermann *et al*. 2015; Ware *et al.* 2015; Fielding *et al.* 2019; Nowak *et al*. 2019). It is believed that the profound floral shift to lycopsid dominance happened ca. 500-kyr after the PTME (Gradstein *et al*. 2012; Ware *et al.* 2015) around the Griesbachian-Dienerian boundary (GDB) instead of during the Lopingian. The new reconstruction of the Zechstein vegetation supports this sequence of events as there is no evidence of vegetation turnover across Zechstein cycles.

This implies that land plants did not undergo a gradual decline preceding the PTME. Instead, the vegetation loss at the P-T boundary was rapid and catastrophic, eventually being replaced by the lycopsid-dominated flora of the Triassic (Grauvogel-Stamm & Ash 2005; Kustatscher *et al.* 2007). The Zechstein is not only useful for investigating the responses of plants in Europe prior to the PTME and across the PTB, but it is also a realistic model for future change especially for low-diversity gymnospermous vegetation in semi-arid climates such as the Mediterranean.

Acknowledgements

MEG was funded by a NERC studentship through the ACCE (Adapting to the Challenges of a Changing Environment) Doctoral Training Partnership [Award Reference 1807541].

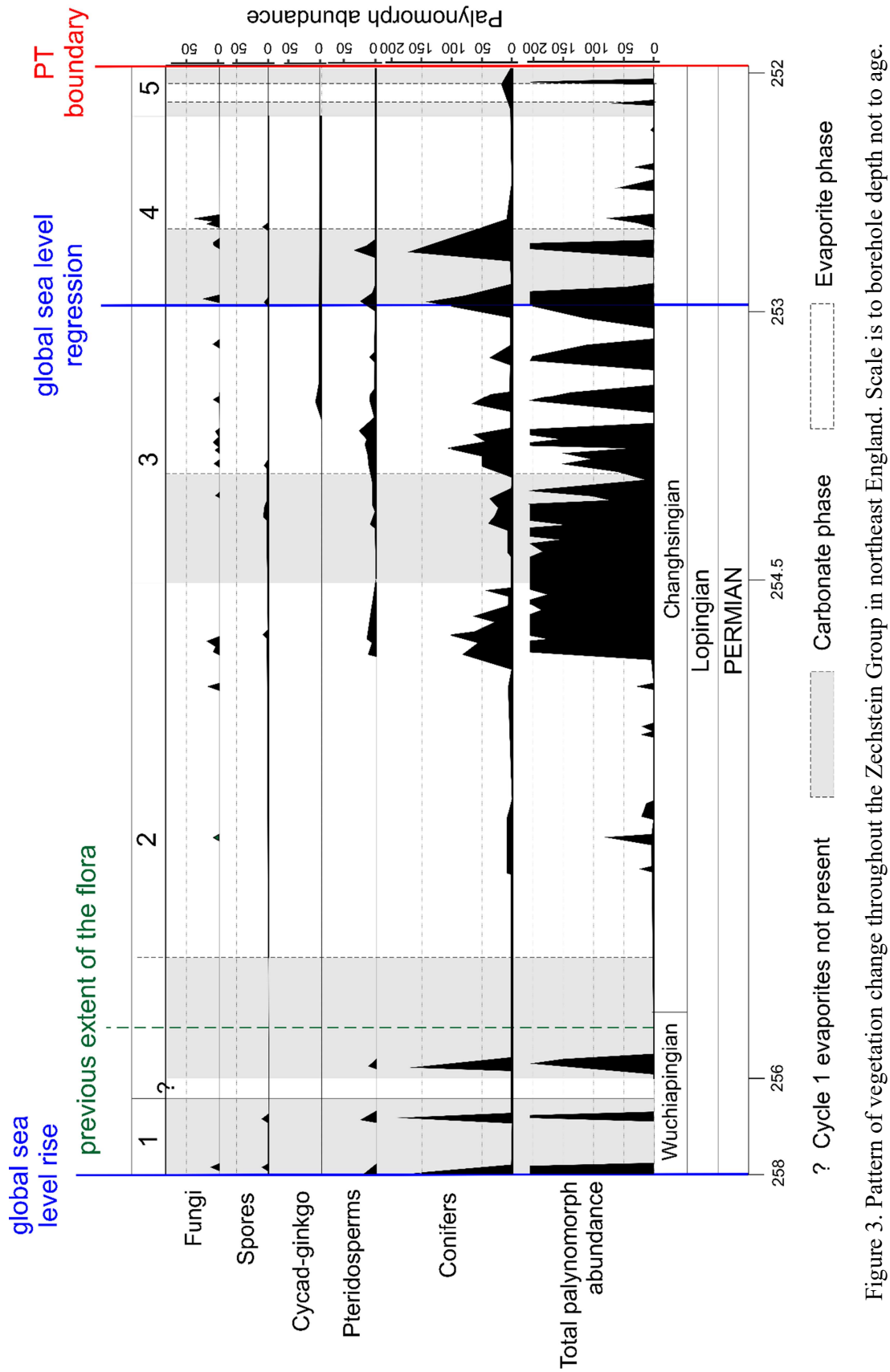

Figure 3. Pattern of vegetation change throughout the Zechstein Group in northeast England. Scale is to borehole depth not to age.

Chapter 8.

Evaporite Palynology: a case study on the Permian (Lopingian) Zechstein Sea

Martha E. Gibson[1*] and David J. Bodman[1,2]

[1]*Dept. Animal and Plant Sciences, The University of Sheffield, Alfred Denny Building, Western Bank, Sheffield, S10 2TN, United Kingdom*

[2]*MB Stratigraphy Limited, Unit 11 Clement Street, Sheffield, S9 5EA, United Kingdom*

[*]*corresponding author: marthae.gibson@gmail.com*

(<40 character title: Zechstein evaporite palynology)

Status as of 11th November 2020: manuscript under review in Journal of the Geological Society. I undertook the fieldwork, data collection and data interpretation for this paper. David. J. Bodman aided with sample processing.

8.1 Abstract

Evaporites characterize the Lopingian of Europe but present obstacles for biostratigraphic analysis. Here we present a case study for processing the Lopingian Zechstein Group evaporites of central-western Europe for the recovery of palynomorph assemblages. We demonstrate that full recovery is easily achieved with two main modes of palynomorph preservation observed; palynomorphs are either exceptionally well-preserved and orange-brown in colour, or poorly-preserved, brown-black, opaque and fragmented. The latter are reminiscent of palynomorphs of high thermal maturity. However, we propose that the intact nature of preservation is a result of the rapid growth of near-surface halite crystals, with their darkening a consequence of locally-enhanced heat flux due to the relatively high thermal conductivity of salt. This case study has enabled novel insight into an otherwise undescribed environment, and demonstrates the utility and possibility of extracting palynomorphs from a variety of rock salt types. This method should be applicable to a wide range of ancient evaporite and could also be applied to other Permian evaporite systems, which are used as analogues for extra-terrestrial environments.

Keywords: Evaporites; palynology; preservation; thermal maturity; Zechstein Sea

8.2 Introduction

Ancient salt deposits were deposited under extreme environmental conditions, representing periods of climate and environmental change. Thick sequences of evaporites can present technical challenges for palynological and biostratigraphical studies. This can be problematic for borehole material analyses and the identification of biozones. Nevertheless, with appropriate processing techniques, they represent a valuable opportunity for high resolution studies.

The palynology of evaporites was studied intensively during the 1950s and 1960s, with the initial exploration of Permian salts commencing earlier (Lück 1913; Klaus 1953; Reissinger 1938). The studies of Wilhelm Klaus were instrumental in developing an understanding of evaporite palynology with multiple published accounts on the Permian and Triassic evaporites of Austria and Germany (Klaus 1953*a*, *b*, 1955*a*, *b*, 1963, 1964), as well as the observations made on the preservation potential of palynomorphs within evaporites (Klaus 1970, 1972). The Permian (Zechstein Group) and Triassic salt deposits of Europe have also been explored by Potonié and Klaus (1954), Leschik, (1956), Grebe (1957), Déak (1959), Stuhl (1962), Freudenthal (1964), Kłowska and Dowgiałło (1964), Visscher (1966), and Dybová-Jachowicz (1974).

Palynomorphs extracted from evaporites have been used in biostratigraphical studies, for example with a late Devonian–early Carboniferous salt diapir in Kazakhstan (Varencov e*t al*. 1964) and with the palynology of the Permian (Shaffer 1964; cf. Reuger 1996; Kosanke 1995; Reuger 1996) and Jurassic (Jux 1961; Kirkland 1969; cf. Reuger 1996) in North America. The preservation potential of Upper Permian salts has further been demonstrated by the recovery of cellulose microfibres from the Salado Formation in southeastern New Mexico (USA) (Griffith *et al.* 2008). More recent palynomorphs have been extracted from Miocene evaporites (Kirchheimer 1950; Balteş 1967; Pertescu *et al*. 1999; Pertescu and Bican-Brişan 2005; Durska 2016, 2017, 2018), and from 35 kyr old selenite crystals in Mexico (Garofalo *et al.* 2010).

The Lopingian Zechstein Sea of western and central Europe is a classic example of a giant evaporite basin. The basin is filled with thick evaporites which originate from marine-derived brines, supplemented by intermittent meteoric contributions (Denison and Peryt 2009). The Zechstein Basin was partially isolated from the open ocean and underwent five cycles of climate-driven carbonate-evaporite deposition from the latest Wuchiapingian–Changhsingian (~251-258 Ma) (Menning *et al*. 2005, 2006; Szurlies *et al*. 2013; Soto *et al*. 2017; Kemp *et al.* 2018).

The Zechstein Group evaporites form a total thickness of ca. 2000 m (Peryt *et al*. 2010; Zhang *et al*. 2013) and therefore present ample opportunity for developing a method for extracting

palynomorphs from a variety of evaporative lithologies including rock salt, potassium-magnesium salts, and sulphates. Here we present a methodology for processing and extracting palynological assemblages from comparatively small samples of evaporites from borehole core material and discuss the condition of the palynomorph assemblages recovered.

2.3 Geological Setting

During the Lopingian (late Wuchiapingian; ~258 Ma) the Southern Permian Basin was flooded by a catastrophic marine transgression from the Boreal Ocean to the north, triggered by tectonic activity of the Greenland-Norwegian Sea rift (East Greenland-Fennoscandian Shield). The transgression coincided with a strong thermal subsidence pulse (Glennie *et al*. 2003; Legler and Schneider 2008) leading to the formation of the Zechstein Sea. This transgression had a loading effect on the lithosphere which led to continued regional differential subsidence (Smith 1989). At the marine sill junction between the Boreal Ocean and the Zechstein Sea, two sets of rift structures existed defined by the Atlantic and Viking Graben rift trends. These reflect discrete extension vectors, whose interactions likely provided a complex pathway of fault blocks that allowed the penetration and inflow of marine brines and evaporation for long periods of time, facilitating the precipitation of large volumes of evaporites. Isolation from the open ocean was exacerbated by the presence of barrier reefs in the region of the marine sill (Mulholland *et al*. 2018). Thermal subsidence further influenced the Zechstein Basin by creating an even larger and deeper accommodation space for brines, thus continually increasing the massive accumulations of evaporites within the basin (Peryt *et al*. 2010).

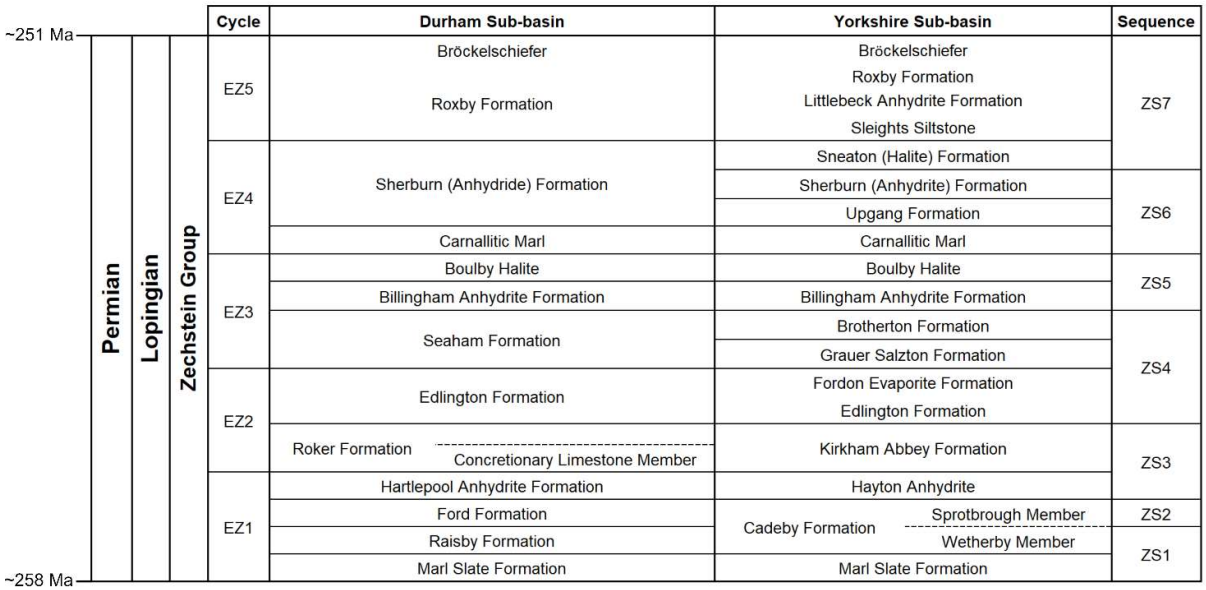

Fig. 1. Stratigraphy of the UK Zechstein Group. EZ1, Zechstein Cycle and ZS, Zechstein Sequence.

It is generally accepted that the Zechstein was fed by open-ocean waters from the Boreal Ocean, however other routes of flooding have been suggested, e.g., across the Pennines from the Bakevellia Sea to the west (Smith and Taylor 1992), or via a temporary connection to the Palaeo-Tethys Ocean to the southeast ((Peryt and Peryt 1977; Ziegler *et al.* 1997; Şengor and Atayman 2009; Słowakiewicz *et al.* 2016). The Zechstein Basin margins were relatively shallow, and evaporites formed in a sabkha-playa type depositional setting and therefore not as thick as the evaporite deposits in the centre of the basin (Tucker 1991; Zhang *et al*. 2013).

The repeated marine restriction of the basin, combined with high rates of evaporation, created stacked cycles of carbonate sedimentation and climate-driven evaporite precipitation (Smith 1980; Tucker 1991; Geluk 2005; Peryt *et al*. 2010; Jackson and Stewart 2017). These cycles can be correlated across the entire basin, which stretches ca. 2500 km WNW-ESE from the northeast coast of Great Britain eastwards across the North Sea, and northern Germany and Poland. The depositional area is ca. 600 km wide and is delineated by several Variscan topographic highs including the London-Brabant, Rhenish, and Bohemian massifs in the south, the Mid North Sea High, and Ringkøbing-Fyn highs in the north (Ziegler 1990; Geluk 2005; Peryt *et al*. 2010).

During system highstands, following basin recharge with water from the open ocean, carbonate reefs formed along basin margins and on isolated highs, while basin areas were comparatively sediment-starved and formed condensed sequences that are still largely correlatable. During lowstands caused by basin restriction, high evaporation rates would have led to supersaturated seawater conditions. The Zechstein Group sequence contains a variety of evaporite mineral types, mostly the chloride and sulphate salts, halite (NaCl), anhydrite (KCl), sylvinite (NaCl and KCl), and polyhalite ($K_2Ca_2Mg(SO_4)4{\cdot}2H_2O$). Generally, the first to precipitate were the sulphate salts (anhydrite/gypsum). Once salinity reached 10-11 times (340‰ - 360‰) that of normal seawater (35‰), halite (NaCl) began to precipitate (Warren 2006). Once seawater reached supersaline concentrations of 70-90 times normal seawater concentration, potassium-magnesium salts (potash) were precipitated. Therefore, the composition of the salts during the regressive phases reflects the progressing evaporitic conditions.

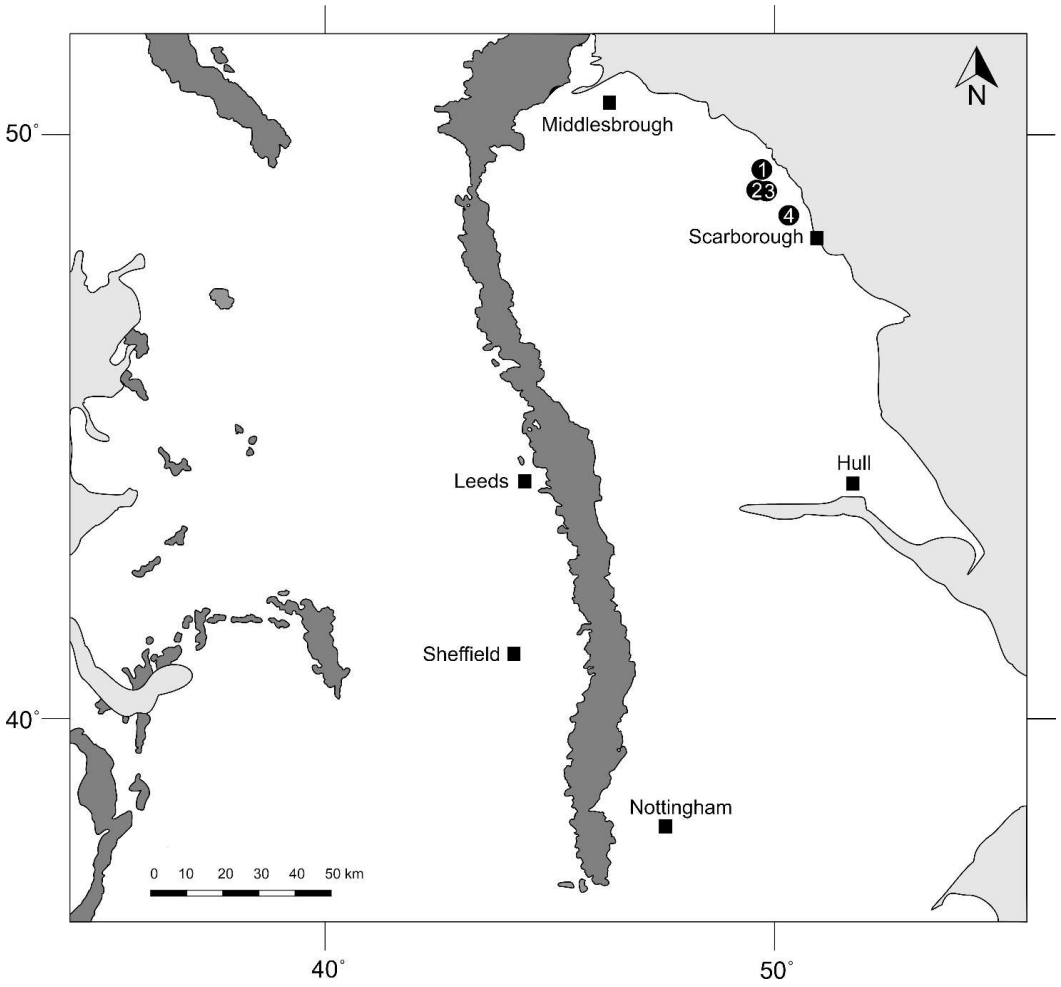

Fig. 2. Map of the boreholes SM4 Gough, SM7 Mortar Hall, SM11 Dove's Nest and SM14b Woodsmith Mine North Shaft in relation to the UK Permian outcrops.

In the UK, Permian rocks crop out over northeast England in two sub-basins (Fig. 1). In the north the Durham Sub-basin and in the south the Yorkshire Sub-basin, separated by the Cleveland High (Smith *et al*. 1989). The material used in this study was obtained from the Yorkshire Sub-basin. The end of Zechstein Group deposition is marked by a distinct change from marine deposition to continuous continental conditions during the Early Triassic, marked by the Bröckelschiefer Member that rests unconformably on the Cycle 5 deposits (Bourquin *et al*. 2007). In the UK, the Bröckelschiefer Member is assigned to the Early Triassic but is considered Lopingian in age in the Netherlands and Germany (Peryt *et al*. 2010). This facies change is a result of a shift towards more humid climatic conditions following Cycle 3. The upper Zechstein Group evaporites are correspondingly less extensive with only anhydrites being found onshore in the UK in Cycle 5.

The precise ages of the upper Permian formations in the UK are unknown but are generally considered to be Lopingian in age. However, in central Germany the base of the Zechstein Group sequence (Kupferschiefer Member) has been given a Re-Os age of 257.3 ± 1.6 Ma (Lopingian (lower Wuchiapingian)) (Brauns *et al*. 2003), and with an estimated duration of only 2.8-3.5 myr (Szurlies *et al*. 2013) between ~258-252.3 Ma (Menning *et al*. 2005, 2006) for the Zechstein Group of central Europe. It is still debated whether sedimentation was continuous during this time (Henderson *et al*., 2012). Although there is no complete timescale for the UK Zechstein Group, a duration of 0.3 myr for the Cycle 2 carbonates (Roker Formation) (Mawson and Tucker 2009), and a date of 255 ± 2 Ma (late Wuchiapingian) for the Cycle 2 evaporites (Kemp *et al*. 2016; Kemp *et al*. 2018) have been suggested.

8.4 Materials and Methods

Samples were collected from four borehole cores drilled by York Potash Ltd (SM4, SM7, SM11, SM14b) through the Zechstein Group in the vicinity of Scarborough, in North Yorkshire, UK. A total of 49 samples of rock salt were collected from across the four borehole cores (SM4 n=17, SM7 n=1, SM11 n=24, SM14b n=7). The types of rock salt sampled include various sodium chloride and potassium chloride salts: anhydrite, sylvinite, carnallite, halite, as well as halite with argillaceous inclusions of clay and organic material. Sample lithologies are displayed in Appendix H.

Rock salt samples weighing 30-200 g were dissolved in 1 L of boiling water until full dissolution was reached. The solution was then filtered through a (15 μm) sieve. The residue was treated with a boiling 40% conc. hydrofluoric acid (HF) treatment for 15 minutes. The residue was neutralized and separated from any remaining clastic particles with zinc chloride solution ($ZnCl_2$ (S.G. 1.95)). In cases where pollen grain morphology was not distinct enough for further analysis, a portion of the sample was treated with Schulze's reagent, a supersaturated solution of 70% conc. nitric acid (HNO_3) and potassium chlorate ($KClO_3$) in order to oxidize and lighten the pollen grains to facilitate analysis. The resulting organic residue (typically <1 ml) was strewn-mounted onto glass slides for light microscope (LM) analysis. Where possible pollen counts to 200 were conducted per sample. Specimens were photographed using a QImaging (Model No. 01-MP3.3-RTV-R-CLR-10) camera mounted on an Olympus BH-2 transmitted light microscope in conjunction with QCapture Pro software. Individual images were viewed and resized using the GIMP 2.0 software package. Materials are curated in the Centre for Palynology, The University of Sheffield (rock salt, remaining organic residue, LM slides).

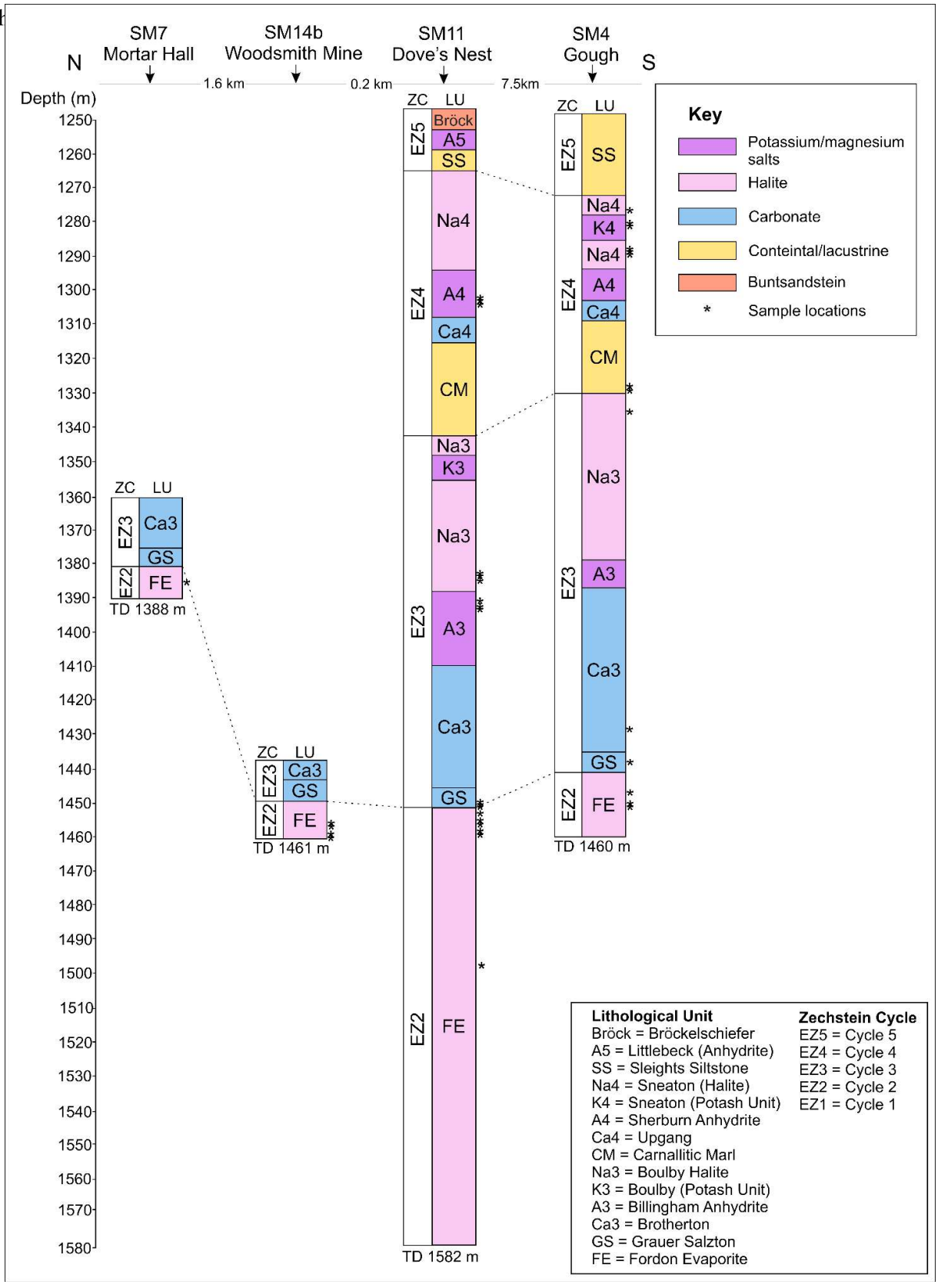

Fig. 3. Correlation of boreholes used in this study; SM4 Gough, SM7 Mortar Hall, SM11 Dove's Nest and SM14b Woodsmith Mine North Shaft. ZC, Zechstein cycle; LU, lithological unit; TD, terminal depth.

in the use of HF acid to concentrate yield irrespective of the presence of clastics in the material, enabling a smaller sample of rock salt to be used, and a resulting assemblage that is clear of sediment. In addition, this study differs from previous documentation due to the large number of samples used and how it is the most recent attempt to document the palynology of the Zechstein Group, and the only attempt to study the evaporite palynology of the Permian of the UK.

The authors recognize that different evaporite systems have inherently different yields, therefore trialling this method on different masses of source rock is recommended to ascertain the ideal weight to be used in a full palynological study.

8.5 Borehole Descriptions

The boreholes in this study were drilled by York Potash Ltd in exploration of the Zechstein Group potash salts in North Yorkshire, in the vicinity of Scarborough. This study has investigated four boreholes: SM4 Gough (SM4), SM7 Mortar Hill (SM7), SM11 Dove's Nest (SM11), and SM14b Woodsmith Mine North Shaft (SM14b). The location of the boreholes is illustrated in Fig. 2. This borehole core material covers Zechstein Group cycles EZ2-5 of the classic carbonate-evaporite structure (Smith 1989; Peryt *et al*. 2010, Smith *et al.* 2014), and sequence stratigraphic cycles ZS3-7 of the alternate evaporite-carbonate organisation (Tucker 1991), through the Yorkshire sub-basin (Smith 1989). The stratigraphic range of the boreholes is illustrated in Fig. 3.

8.5.1 SM4 Gough [NZ 94613 00188]

Borehole SM4 has a total depth of 1669.91 m bRT, passing through EZ2-5 (ZS4-7). At its base SM4 terminates in the limestone of the Kirkham Abbey Formation of EZ2. The Fordon Evaporite Formation of EZ2 is 231.2 m thick and composed of halite, polyhalite and anhydrite in the lower ~200 m, and predominantly halite in the upper ~35 m. The 0.6 m thick Grauer Salzton Formation mudstone marks EZ2/3 boundary and is topped by the Brotherton Limestone (47.8 m), the Billingham Anhydrite (11.5 m), and Boulby Halite Formation (49.3 m). The Carnallitic Marl (15.7 m) marks the EZ3/4 boundary and is topped by the dolomitic Upgang Formation (0.6 m), Sherburn Anhydrite Formation (6.53 m), Sneaton Halite Formation (14.9 m), Sneaton Potash Member (8.5 m), Sneaton Halite Formation (5.8 m). The top of the borehole passes up into the Sleights Siltstone Formation of EZ5, marking the boundary between EZ4/5. A total of 17 samples were taken from SM4 sampled in the Fordon Evaporite Formation (EZ2 Na), Boulby Halite (EZ3 Na) and the Sneaton Potash Member (EZ4 K) and Sneaton Halite Formation (EZ4 Na).

8.5.2 SM7 Mortar Hall [NZ 89989 06831]

Borehole SM7 has a total depth of 1626.84 m bRT. The 259.4 m drilled covers the upper part of the Kirkham Abbey Formation (198.3 m thick), which is overlain by the thick polyhalite succession of the Fordon Evaporite Formation (223.3 m). The EZ2/3 boundary is marked by the mudstone of the Grauer Salzton Formation (grey salt clay) (0.9 m), which is overlain by the limestone of the Brotherton Formation (16.9 m). One sample of argillaceous halite was collected from SM7, corresponding to the boundary between the Fordon Evaporite Formation (EZ2 Na) and the Grauer Salzton Formation.

8.5.3 SM11 Dove's Nest [NZ 89429 05322]

With a total depth of 1582.5 m bRT, borehole SM11 is the borehole sampled to the highest resolution in this study. At its base, SM11 terminates in the Fordon Evaporite Formation of EZ2, a 134.14 m thick sequence of halite, sulphatic halite, polyhalite, anhydrite and halite/sylvinite. At the boundary between EZ2/3, the Grauer Salzton Formation, a 0.9 m thick interval of argillaceous limestone/dolomitic mudstone, separates the Fordon Evaporite Formation from the Brotherton Formation. The Brotherton Formation represents the carbonate phase of EZ3 and comprises 46.4 m of dolomitic limestone. The evaporative phase of EZ3 is represented by a total of 66.3 m of the Billingham Anhydrite Formation (19.7 m), Boulby Halite (Units B and A) (43.3 m), Boulby Potash Member (Unit C) (2.2 m) and Boulby Halite (Unit D) (1.2 m). The Carnallitic Marl Formation, a 23.4 m thick hygroscopic reddish-brown mudstone, lies at the boundary between EZ3/4. On top of this lies the 0.7 m thick dolomite of the Upgang Formation, the Sherburn (Anhydrite) Formation (8.3 m), Sneaton (Halite) Formation (Units B and A) (16.3 m), the Sneaton Potash Member (Unit C) (2.9 m) and Sneaton (Halite) Formation (Units E and D) (20.7 m). The start of EZ5 is marked by the mudstone/siltstone of the Sleights Siltstone, which is topped by the final units of the Zechstein Group, the Littlebeck Anhydrite Formation (0.9 m), the Roxby Formation, and up into the Triassic, through to the topsoil. A total of 23 rock salt samples were taken from SM11 from the Fordon Evaporite Formation (EZ2 Na), halite within the Brotherton Formation (EZ3 Ca), the Billingham Anhydrite Formation (EZ3 A), the Boulby Halite (EZ3 Na), the Sherburn (Anhydrite) Formation (EZ4 A) and the Sneaton (Halite) Formation (EZ4 Na).

8.5.4 SM14b Woodsmith Mine North Shaft [NZ 89297 05435]

Borehole SM14b is the shortest length of borehole core sampled in this study, although originally drilled to a depth of 1627.3 m bRT. Less than 10 m of the upper part of the Fordon Evaporite Formation (EZ2), the Grauer Salzton Formation (EZ3), and the lower part of the Brotherton Formation (EZ3), fortunately capturing the EZ2/3, was available for sampling. Of the original 368.5 m of borehole core, a section 9.7 m long was sampled, from which 7 rock salt samples were collected from across the Fordon Evaporite Formation (EZ2 Na), composed of dark-coloured, organic-rich argillaceous halite.

8.6 Results

8.6.1 General comments on the palynology

Of the total 49 samples of rock salt processed 38 contained organic matter. Assemblages generally had a low yield of palynomorphs with pollen counts often under 100 palynomorphs per slide, however full counts were possible for 16 samples. The palynomorph assemblages recovered are composed of bisaccate pollen grains, of which 50-100% of them are Unidentifiable. Spores, plant tissue fragments such as tracheids and cuticle, and amorphous organic matter (AOM) were rare. The palynological composition of assemblages can be found in Appendix J.

Small bisaccates and small monosaccates are the most common type of palynomorph recovered from the evaporites, and they are also among the most common types recovered from standard Zechstein preparations, along with rare occurrences of large monosaccate pollen (Gibson and Wellman 2020). The assemblages are very typical of dispersed Euramerican palynomorph assemblages recovered from throughout the British Lopingian (Clarke 1865; Visscher 1971, 1972; Warrington and Scrivener 1988; Legler *et al*. 2005; Legler and Schneider 2008; Warrington 2005, 2008) of a dominantly gymnospermous affinity (conifer, pteridosperm). The palynomorphs are illustrated in Plate I and Plate II.

The condition of the recovered palynomorphs fall into two categories: Type I are well-preserved, transparent, and light brown in colour (50-60% PDI) (Plate I, O, Q, U), and Type II are poorly-preserved, commonly fragmented or bearing the signs of biological degradation, opaque, and a dark brown-black colour (98-100% PDI) (e.g. Plate I-M) indicative of high thermal maturity. Some assemblages contain an intermediate type which is well-preserved and intact, yet of apparent high thermal maturity (Plate I, B, P).

26 different microfossil taxa were recovered, of which 18 were pollen grain species belonging to 14 genera (Appendix J). Unidentifiable trilete spores, the palynomorph of debated fungal or algal affinity *Reduviasporonites* spp. and rare acritarchs were also recovered. *Reduviasporonites* spp. was a frequent component of assemblages, recovered from 4 samples in SM11 and one sample from SM14b. Taeniate bisaccate pollen dominate the assemblage although some non-taeniate taxa are abundant, while monosaccate pollen are typically rare.

The taxa recovered are consistent with a Lopingian age (Visscher 1971), evidenced by the presence of the characteristic Zechstein pollen grain species *Lueckisporites virkkiae* (1.1-61.4%). *Klausipollenites schaubergeri* (0.5-15.2%) was the most common non-taeniate bisaccate pollen species, with *Illinites* spp. (0.5-4.4%) also being common. *Vestigisporites minutus* (1-12%) was the most common monosaccate pollen species. A Lopingian, rather than Triassic, age is also supported by the presence of other taeniate bisaccate taxa such as the genera *Taeniaesporites* and *Protohaploxypinus* and the species *Vittatina hiltonensis*.

8.6.2 SM4 Gough

In SM4 a combination of preservation Types I and II are observed throughout the Fordon Evaporite Formation, Boulby Halite, Sneaton Potash Member, and Sneaton (Halite) Formation. Assemblages contain either a low yield of Type I palynomorphs, or a high yield of Type II palynomorphs with only a few distinct bisaccate and small monosaccate pollen grain taxa identifiable, such as *Klausipollenites schaubergeri*, *Vestigisporites minutus*, *Lueckisporites virkkiae* (Plate I, C, D), *Taeniaesporites* sp. (Plate I, K-N), *Protohaploxypinus* sp. (Plate I, G), and *Vittatina hiltonensis* (Plate I, T, U).

8.6.3 SM7 Mortar Hall

The single sample obtained from uppermost Fordon Evaporite Formation in SM7 contained a low yield of Type II preserved palynomorphs. The quality of preservation was too poor to determine the presence of individual bisaccate or monosaccate taxa.

8.6.4 SM11 Dove's Nest

SM11 yielded the best-preserved assemblages, owing to the large proportion of argillaceous halite throughout the core. Well-preserved bisaccate and small monosaccate taxa *Lueckisporites virkkiae*

(Plate I, A, B), *Klausipollenites schaubergeri* (Plate II, S), *Illinites* spp. (Plate I, P, Q), *Vestigisporites minutus* (Plate II, C, D), *Taeniaesporites* sp. (Plate I, O), and *Protohaploxypinus* spp. (Plate I, E, F, H-J) were recovered, as well as rare occurrences of the large monosaccate taxa of *Potoniesporites novicus* (Plate II, A), *Nuskoisporites dulhuntyi* (Plate II, B), and *Perisaccus granulosus* often observed in exceptional three-dimensional preservation, exhibiting minimal compression, from the Billingham Anhydrite Formation. Exceptionally well-preserved cuticles with visible stomata and guard cells in three-dimensional detail (Plate II, N) were recovered from the Sherburn (Anhydrite) Formation.

Throughout the SM11 evaporites taeniate bisaccate pollen is always more abundant than non-taeniate pollen. Monosaccate pollen is rare but is more abundant in the lower Zechstein Cycle 2 evaporites. There is an observed gradual decline in the abundance of palynomorphs up borehole, though there are several peaks in abundance which coincide with large volumes of anhydrite, especially in the Cycle 3 Billingham Anhydrite Fm.

8.6.5 SM14b Woodsmith Mine North Shaft

Assemblages from SM14b are either well-preserved, composed mostly of Type I bisaccate taxa *Lueckisporites virkkiae*, *Klausipollenites schaubergeri*, the monosaccate *Vestigisporites minutus*, and *Reduviasporonites* spp., or dominated by unidentifiable Type II palynomorphs. No large monosaccate pollen grains were recovered. SM14b was located farthest from the contemporary coastline and assemblages contain numerous examples of well-preserved taeniate bisaccate genera (*Taeniaesporites* and *Protohaploxypinus*) exhibiting transport damage along weak areas of the pollen exoexine, missing parts of the sacci (Plate I, K), or with fractured taeniae (Plate I, G).

8.6.6 Additional comments

Examples of both types of preservation were observed within samples, as well as between samples. For example, two specimens of *Vittatina hiltonensis* were recovered from SM4 1438.07 m (Plate I, T, L), both of which are well-preserved with multiple taeniae clearly visible. However, there is a noticeable difference in colour and opacity between the two. This variety is also apparent in cuticles and other palynomorphs. Cavate trilete spores, only recovered from SM11 1465.92 m, are either translucent and orange (Type I) (Plate II, E), or dark brown and relatively opaque (intermediate type) (Plate II, F).

The sacci of bisaccate and monosaccate pollen grains are lighter in colour than the corpus. This is a typical observation in saccate pollen grains due to the network of endoreticulations which form the internal structure of sacci, provide internal structure and armature, allowing for deeper penetration of macerating and oxidising reagents.

Woody material including tracheids are well-preserved, translucent and orange-brown in colour (Plate II, K-M). Cuticle-bearing stomata can be exceptionally well-preserved and very pale in colour (Plate II, N), where the stomata and guard cells are preserved in three dimensions. Possible arthropod wing cuticle (Plate II, O) was recovered from the Billingham Anhydrite Formation (Z3) of SM11; however, it may also represent a fragment of epiphyllous *Callimothallus*-type fungi (Family Microthyriae) (Dilcher 1965). Whereas it is of a different texture and pattern to confirmed plant cuticle, no other instances were recorded so it cannot be discounted as plant cuticle.

8.7 Discussion

8.7.1 Preservation potential of the Zechstein Group evaporites

The increasingly concentrated brines of the shallow Zechstein Sea margins acted as the perfect trap for organic particles, including wind-borne pollen grains. The recovery of such well-preserved palynomorphs is therefore unsurprising, especially given the prior documentation of palynomorphs in sodium chloride-rich units (Klaus 1970) as well as sulphates e.g. gypsum (Durska 2016, 2017, 2018). The preservation potential of Zechstein salts has recently been attested by the extraction of lipids from weathered evaporitic rock from Boulby Mine, UK (Cockell *et al*. 2020).

However, several factors may affect the quality of preservation observed within assemblages. The nature of evaporite crystals, the mode of transport, and the morphology of the palynomorphs must all be considered.

Halite brines are known to protect palynomorphs from microbial and inorganic decay (Durska 2016), and immediate contact with an increasingly saturated solution containing halogens is known to protect from oxidation, and bacterial and fungal activity (Klaus 1970). Salt also plays a role in mechanically protecting palynomorphs by capturing them in rapidly growing salt crystals, experimentally demonstrated by Campbell and Campbell (1994), whereby the envelopment of palynomorphs by salt crystals helped to preserve the structural integrity of large pollen grains. It is likely that mechanical stabilisation has led to preferential preservation of certain pollen grain taxa, such as large taeniate/striate bisaccates *Taeniaesporites* and *Protohaploxypinus*, large non-taeniate bisaccate *Falcisporites zapfei*, and the large monosaccate taxa *Nuskoisporites dulhuntyi* and

Perisaccus granulosus, that may otherwise have been fragmented during burial. These are still recovered despite the low assemblage yields and diluting effects of salt precipitation.

Some of the best preserved large specimens of both cuticle and monosaccate pollen grains were recovered from the anhydrites of EZ3 (Billingham Anhydrite Formation) and EZ4 (Sherburn Anhydrite Formation). Sulphate salts are the first to precipitate out of evaporating seawater (Warren 2006) indicating that the palynomorphs and cuticle that spent the least amount of time suspended in the water column had the lightest appearance as they were quickly excluded from biodegrading and oxidising factors.

Differences in preservation are strongly tied to mode of transport in evaporites. Klaus (1970) interpreted light-coloured intact palynomorphs (Type I) to be wind-borne, and dark fragmented palynomorphs (Type II) to be water-borne likely derived from clastic inclusions within the halite, especially in argillaceous halite, where they have become oxidised in the clastics prior to encapsulation in the halite. This is also responsible for the mixing of types within single assemblages.

Compaction is known to cause significant damage to pollen grain exines (Delcourt and Delcourt 1980). The Type I palynomorphs do not appear to be laterally compressed, however Type II palynomorphs do appear to be, perhaps indicative of having undergone a different mode of transport as hypothesised by Klaus (1970). In cases of argillaceous halite, it is possible that the pressure exerted on the clastic inclusions prior to being encased in the halite is greater than the pressure exerted on wind-borne palynomorphs encased within the crystalline halite, as this creates an additional source of mechanical stress. Repeated wetting-drying of pollen grains is also known to cause significant damage to pollen grains, even after one episode (Campbell 1991). Pollen may have become damaged during transportation along specific areas of exine weakness, to then incur additional damage during drying, before finally becoming encapsulated in salt.

Pollen grain morphology and the inherent structural integrity of some taxa will affect their presence or absence in the assemblages. The angle of the saccus-corpus junction of large diploxylonoid bisaccates may be an area of weakness making these grains susceptible to mechanical damage. Taeniate and striate bisaccates are characteristic of Euramerican Lopingian palynomorph assemblages (Chaloner 2013); therefore, it is important to consider the effects of taeniae on the structural integrity of pollen grains, and the saccus shape of diploxylonoid bisaccates. It is unclear whether more taeniae impact the ability of multitaeniate pollen grains to maintain integrity with greater transport distances via more turbulent water transport.

8.7.2 Taxonomic Composition

The taxonomic composition of the recovered palynoflora is typical of the Lopingian Euramerican floral province, and characteristic of the British Zechstein Group and U.K. correlatives, dominated by *Lueckisporites virkkiae* (Clarke 1865; Visscher 1971, 1972; Warrington and Scrivener 1988; Legler *et al.* 2005; Legler and Schneider 2008; Warrington 2005, 2008; Gibson and Wellman 2020). The palynomorphs were produced by a gymnospermous source vegetation dominated by conifers, peltasperms, gingkophytes, cycads, and pteridophytes (Stoneley 1958; Schweitzer 1986) indicated by the dominance of taeniate bisaccate pollen grains. See Appendix J for a list of all pollen taxa recovered.

Unlike other accounts of the Zechstein palynoflora, notably Clarke (1965), the monocolpate pollen species *Cycadopites rarus* was not recovered which may be a taphonomic effect or represent the scarcity of its parent flora in the contemporaneous vegetation. The characteristic Zechstein multisaccate pollen species *Crustaesporites globosus* and the bisaccate pollen species *Platysaccus radialis*, tetrads, or foraminiferal test linings were not recovered from the evaporites. However, this is unsurprising given their scarcity throughout the rest of the borehole material (Gibson and Wellman 2020). Given the short temporal duration of the Zechstein Sea (Menning *et al.* 2005; Menning *et al.* 2006; Szurlies *et al.* 2013) and the rapid precipitation of the salts (Kemp *et al.* 2016), any differences in composition between samples are probably not a result of evolutionary processes. Instead, they are likely to be the result of differences in environmental or depositional processes.

The factors affecting the taxonomic composition are tightly linked to those affecting the preservation of palynomorphs. The multisaccate *Crustaesporites globosus*, taeniate bisaccate *Platysaccus radialis*, the monocolpate *Cycadopites rarus*, tetrads or foraminifera test linings, are not recovered. *Illinites* spp. was not recovered from SM4 Gough despite being a common Zechstein palynomorph (Gibson and Wellman 2020); however, this is unsurprising given their extreme rarity throughout the rest of the borehole core material. No acritarchs were observed in these preparations suggesting the marine conditions were unsuitable for the organisms that produced acritarchs, or the presence of terrestrial-derived palynomorphs overwhelms marine organic matter. The cuticle preserved in these evaporites is better preserved and found in larger fragments in comparison to those extracted from standard palynological preparations of the UK Zechstein Group (Gibson and Wellman 2020). Thus, the evaporites are capturing additional aspects of the source vegetation and this allows for a more thorough interpretation of its nature.

Any minor differences between the palynomorphs recovered from this study compared to previous UK Zechstein Group and UK Lopingian correlative studies (Clarke 1865; Visscher 1971, 1972; Warrington and Scrivener 1988; Legler *et al*. 2005; Legler and Schneider 2008; Warrington 2005, 2008; Gibson and Wellman 2020) may be attributed to the diluting effects of salt precipitation meaning fewer palynomorphs are preserved per gram of source material.

Wind-dispersed assemblages are known to be affected by size sorting creating a taxonomic bias towards smaller sized bisaccate pollen (Traverse 2007). However, because rapidly growing halite crystals can mechanically stabilize large pollen grains, the size sorting effect may be mitigated to a certain degree. Large monosaccates and cuticle fragments are more abundant than expected given their rarity in standard Zechstein preparations (Clarke 1965; Gibson and Wellman 2020).

The type of preservation within samples, which is linked to transport, strongly affects the taxonomic composition of assemblages, as it determines the ability of palynomorphs to be identified. If palynomorphs are too badly damaged by transportation and opaque when viewed under transmitted light, they can be impossible to identify creating bias in analysis. Also, if certain palynomorph morphologies are more prone to damage than others, e.g., large multi-taeniate bisaccate genera such as *Taeniaesporites* and *Protohaploxypinus*, they may be underrepresented in assemblages.

Pollen of conifer and peltasperm affinity consistently dominate palynomorphs assemblages throughout the British Zechstein (Gibson and Wellman 2020). There is no evidence of major deforestation or land plant decline as pollen grains are recovered from all five evaporation-replenishment cycles and are found to persists up to the Permian-Triassic boundary. The composition of the palynoflora and its persistence of the flora may indicate that the climate during the evaporite phases may have been less severe than previously interpreted and buffered by the fluvial landscape of the upper Zechstein Cycles 4-5, supporting the existence of an semi-xerophytic adapted vegetation. However, the possibility of redeposition cannot be excluded. It is possible that climate had very little to do with evaporation, as in the Messinian Salinity Crisis, where climate only played a minor role in desiccation (Fauquette *et al.* 2006).

8.7.3 Depositional setting and mode of transport

Lithology and condition of the palynomorphs can both be used to infer depositional setting and the mode of transport. These boreholes had a marginal basin setting, located in a sabkha- or salina-type depositional environment, in an alternating arid-humid climate to predominantly humid climate during latest Zechstein Group times (EZ4-5) (Słowakiewicz *et al*. 2016). During the upper Zechstein

Group (EZ4-5) shoreline progradation and evaporative drawdown of the Zechstein Sea means these boreholes were situated in an even more marginal environment. This is reflected in the reduced presence of evaporites in the upper parts of SM4 and SM11 relative to the evaporites of the Fordon Evaporite Formation of EZ2, and the Billingham Anhydrite Formation and Boulby Halite of EZ3, and an increased terrigenous input.

Marginal Zechstein Sea water depths were generally shallow, in the range of tens of meters, particularly during the lower Zechstein Group (EZ1-3), and stratification of the water column and reduced water circulation led to heterogenetic patterns of anoxia along the western margin of the basin (Słowakiewicz *et al*. 2015). This is indicated by intermittent anoxic shales throughout the dolomitic limestones in EZ2-3 in SM4, SM7, SM11 and SM14b. The water column progressively shallowed as the sea reduced in volume and accommodation space filled with each evaporitic cycle.

The two types of preservation observed are likely a result of different modes of transport undertaken by the palynomorphs (Klaus 1970). Intact pollen grains of Type I exhibiting little to no mechanical damage are likely wind-borne, settling on the surface of the brines and becoming quickly encapsulated in the rapidly precipitating salt. Damaged Type II palynomorphs likely underwent transport via water, incurring mechanical and biological damage due to the more turbulent conditions relative to wind-borne transportation. Type II palynomorphs may also have undergone redeposition with lateral flattering of palynomorphs being a result of compression in clastics before deposition in brines. Although cuticles are of Type I appearance, their size means they are water-borne rather than wind-borne.

8.7.4 Palynomorph Darkening and the Thermal Conductivity of Salt

Alongside the noticeable variation in quality of preservation, a difference in the colour of preservation was observed. The Palynomorphs Darkness Index (PDI) of non-taeniate bisaccate pollen grains from across the material described in Gibson and Wellman (2020) identified a reverse thermal maturity profile throughout the Zechstein Group sequence, with the hyaline palynomorphs of the Marl Slate (Z1) of County Durham and Nottinghamshire being considerably lighter (<10% PDI). Pollen grains from Z2-5 were noticeably much darker with Type I palynomorphs ranging from 50-60% PDI and Type II averaging 98-100% PDI (G. Clayton pers. comm.). A lack of inertinite excludes wildfires as a cause of darkening.

Such an intense dark colour of palynomorphs is typically indicative of extreme thermal maturity. However, no sources of direct heating have been identified in the Permian strata of North

Yorkshire (G. Warrington pers. comm.), and this material has not been buried at sufficient depth to achieve such a high PDI. Furthermore, uniform darkness is a hallmark of diagenetic heating, while the darkening observed here is of a variable nature. However, there is some evidence of high thermal maturity in the Boulby Mine area (Barnard and Cooper 1983; Słowakiewicz *et al.* 2020)

Due to the high mobility of halite there is a possibility of reworking within individual halite units and therefore also of redeposition. However, the possibility of reworking between evaporite units has been discounted based upon the ability of relatively immobile anhydrite and potassium-magnesium salts to constrain layers of mobile halite. The composition of the Carnallitic Marl Formation (Z4) and Brotherton Formation (Z3) of SM11 Dove's Nest core has been examined with XRD mineralogical analysis to identify possible mineralogical causes of sporopollenin darkening. The results were inconclusive, with no evidence of unusual evaporite mineralogy (R. Goodhue pers. comm.).

The mineralogy of sample SM11 1312.24 m from the boundary between the Carnallitic Marl and Upgang (Ca4) formations shows that it is an impure evaporite. Samples SM11 1328.76 m, SM11 1332.15 m and SM11 1334.10 m contain variable halite and anhydrite, whereas sample 1406.86 m from the Brotherton Formation (Ca3) is dominated by dolomite. The results do not suggest an obvious mineralogical cause of sporopollenin darkening (R. Goodhue pers. comm.). However, the high evaporitic content of SM11 1312.24 m may explain why this sample contained exceptionally well-preserved palynomorphs (Gibson and Wellman 2020).

It may be possible that the differences in colour are simply an artefact of mode of transport. Klaus (1970) noted that assemblages from halite with clastic inclusions had a high proportion of Type II palynomorphs, whereas clear halite contained mostly Type I palynomorphs. Here, colour is dependent on whether the palynomorphs were water-borne or wind-borne. Evaporite minerals are known to give protection from sunlight, insulating from UV-B radiation (Spear *et al*. 2003; Armal *et al*. 2007; Barbieri and Stivaletta 2011), so it is less likely that the palynomorphs were being greatly affected by UV light during- and post-transport. Another cause of darkening related to transport is the reworking of clastic material into the evaporites and the frequent dissolution and crystallization of salts which would cause a combination of preservational types within samples. A combination of different transportation pathways, redeposition, and recrystallisation could explain why some lithologies, such as argillaceous halite, have a combination of the two pollen preservational types, and even some intermediate forms, but it does not explain the darkening observed throughout the material. It also does not explain the intermediate thermally mature-intact type.

A unique feature of halite is its high thermal conductivity (Warren 1999), typically 2-3 times more conductive than surrounding sedimentary rocks (Yu *et al*. 1992), with the conductivity of anhydrite ranging from 4.8-5.5 W m^{-1} K^{-1}, while the conductivity of halite typically ranges from 4.8-6.05 W m^{-1} K^{-1} (Blackwell and Steel 1989; Clauser and Huenges 1995; Allen and Allen 2005). Based on the conductive properties of salt, an alternate hypothesis for the darkening of the palynomorphs is proposed. The observed thermal maturity of some pollen grains may be a result of the high thermal conductivity of salt, with the thick evaporite units conducting heat from underlying and adjacent sediments in both vertical and horizontal planes. Differential darkening may also be related to the composition of the sporopollenin exine and how this differs between taeniate and non-taeniate taxa.

The heterogeneous flow of circulating groundwater, carrying heat from depth, may have differentially affected parts of the stratigraphy and may have contributed to the observed variability in darkening throughout the sequence. However, in the absence of evidence for significant deformation of the salt deposits from other parts of the British Zechstein basin, aside from small decimetre-scale fractures around the edges of polygons in Boulby Mine (Cockell *et al*. 2020), it seems unlikely that fluid flow is a cause of heating. Furthermore, the migration of other fluids such as hydrocarbons through evaporites is rare (Zhuo *et al*. 2014). Without evidence of substantial fluid flow, it is also most probable that the palynomorphs observed have not been reworked and were present before the crystallization of the salts, and not transported by fluids that later migrated through the evaporite deposits. However, recent evidence of oil seeping from the Brotherton Fm (EZ3) carbonate rocks in Boulby Mine (Słowakiewicz *et al.* 2020) evidences the presence of several fault systems which could create conduits for fluid migration throughout the lower Zechstein cycles. While fault systems may be a means of redeposition in the lower Zechstein, mixing of preservation types in the upper Zechstein may be the result of repeated salt dissolution and recrystallisation.

This hypothesis is supported by the reverse thermal maturity profile observed throughout the borehole material (Gibson and Wellman 2020) with the Marl Slate yielding intact hyaline pollen grains. The palynomorphs were likely suspended in the bottom stagnant anoxic portion of the water column for a long time before being covered by sediment resulting in their hyaline appearance whereas palynomorphs recovered from elsewhere in the sequence are either opaque because they have become oxidized in the carbonates, or they are opaque in the salt because of the thermal conductivity.

8.8 Conclusion

This case study highlights the preservation potential of the Zechstein evaporites. The development of a new method for evaporite palynology has enabled full biostratigraphic exploitation of the Zechstein sequence in the UK for the first time, and it demonstrates the importance of high resolution palynological sampling to help account for mixing within salts. While this method uses less source material than other approaches, it is necessary to assess the amount needed to obtain a representative palynological assemblage for quantitative analysis. This will vary between the evaporite bodies sampled for each case study.

Evaporite palynology has enabled novel insight into an otherwise undescribed vegetation, and the preservation types recovered also say something about how evaporites preserve palynomorphs. A typical Zechstein palynomorph assemblage was recovered, but the exceptional preservation potential of the evaporites provided unique insight into the Zechstein flora. While the overall composition of assemblage corroborates other reports on the Zechstein palynoflora, the evaporite samples are unique in how they preserve exceptional three-dimensional cuticle fragments and large monosaccate pollen grains, because of how rapid halite crystals grow, insulating and isolating organic matter.

Two main modes of preservation were observed which are interpreted as being tightly linked to their mode of transport. Type I palynomorphs are exceptionally well-preserved and orange-brown in colour, translucent, and likely wind-borne settling onto brines and becoming rapidly encapsulated in salt. This type was most prevalent in pure halite and anhydrite-halite samples. Type II palynomorphs are poorly-preserved, brown-black, opaque and often fragmented, reminiscent of palynomorphs of high thermal maturity. Their darker appearance may be attributed to greater oxidation in clastic samples and their fragmented nature to the more turbulent nature of water transport relative to wind transport, and as such they are more common within argillaceous halite samples. Intermediate forms were present that were apparently thermally mature but intact. Darkening of pollen grains in the absence of consistent high thermal maturity within the Zechstein sequence may be a consequence of locally-enhanced heat flux due to the relatively high thermal conductivity of salts relative to carbonate lithologies. Mixing of Type I and Type II preservation within samples was frequently observed and may be a result of redeposition of clastic material, recrystallisation of salts and reworking within halite units. Fault systems in the lower Zechstein may have created conduits for fluid migration which may have enhanced heat flux or been a means of redeposition.

This case study demonstrates the utility and possibility of extracting palynomorphs from a variety of rock salt types with efficient processing times. This method should be applicable to a wide range of evaporite bodies, applicable to exploring more recent extreme terrestrial environments including acidic hypersaline lakes. The applications extend beyond Earth as Permian evaporite systems and other saline giants are used as terrestrial analogues for parts of the Martian surface and subsurface (Benison et al. 2008; Benison 2013; Conner and Benison 2013; Benison and Karmanocky 2014; Cockell *et al.* 2020).

Acknowledgements

We thank Asher Haynes of York Potash Ltd for access to borehole material from SM4 Gough, SM7 Mortar Hall, SM11 Dove's Nest, and SM14b Woodsmith Mine North Shaft. We thank Geoff Clayton and Robbie Goodhue for their contribution of the PDI measurements and XRD analysis of sediments. We thank Geoffrey Warrington for help in interpreting the diagenetic history of the Zechstein Group sediments in the UK and Charles Wellman for comments on this manuscript. Finally, we thank the reviewers whose comments greatly improved this manuscript.

Funding

MEG was funded by a National Environment Research Council studentship through the ACCE (Adapting to the Challenges of a Changing Environment) Doctoral Training Partnership [grant number 1807541].

Plate Descriptions

Plate I – Bisaccate taeniate and non-taeniate pollen grains recovered from the Zechstein Group evaporites of the northeast Yorkshire, U.K. Scale bar (A-X) 50 μm.

A. *Lueckisporites virkkiae* 'A', SM11 1382.13 m, K31/2
B. *L. virkkiae* 'A', SM11 1382.13 m, O27
C. *L. virkkiae* 'C', SM4 1438.07 m, U25/2
D. *L. virkkiae* 'B' SM4 1438.07 m, P32
E. *Protohaploxypinus* spp., SM11 1382.13 m, U45
F. *P.* cf. *microcorpus*, SM11 1465.92 m, E42/3
G. *P. jacobii*, SM4 1438.07 m, R29
H. *P. jacobii*, SM11 1382.13 m, R44
I. *P. chaloneri*, SM11 1465.92 m, D32
J. *P. richteri,* SM11 1382.13 m, S36/2
K. *Taeniaesporites noviaulensis*, SM4 1438.07 m, U36/2
L. *T. labdacus*, SM4 1438.07 m, Q28

M. *T. novimundi*, SM4 1438.07 m, B29
N. *T. angulistriatus*, SM4 1438.07 m, P41/2
O. *T. albertae*, SM11 1458.37 m, J46/3
P. *Illinites* spp., SM11 1382.13 m, F34
Q. *I. delasaucei*, SM11 1458.37 m, J40
R. *Alisporites nuthallensis*, SM11 1458.37 m, Q38
S. *Klausipollenites schaubergeri*, SM11 1382.13 m, U27/4
T. *Vittatina hiltonensis*, SM4 1438.07 m, H32
U. *V. hiltonensis*, SM4 1438.07 m, K29
V. *Falcisporites zapfei*, SM11 1382.13 m, E39
W. *Labiisporites granulatus*, SM11 1304.14 m, K40/3
X. *Reduviasporonites* spp., SM11 1302.20 m, R29

Plate II – Monosaccate pollen grains, caveat trilete spores and assorted cuticle recovered from the Zechstein Group evaporites from northeast Yorkshire, U.K. Scale bar (A-K) 50 µm, (L, M) 25 µm.

A. *Potoniesporites novicus*, SM11 1304.14 m, E31
B. *Nuskoisporites dulhuntyi*, SM11 1382.12 m, G43/2
C. *Vestigisporites minutus*, SM11 1382.13 m, Q40/3
D. *V. minutus*, SM11 1382.14 m, L36
E. Cingulate trilete spore ?*Densosporites* spp., SM11 1465.92 m, P39
F. Cavate or camerate trilete spore, SM11 1465.92 m, C32/3
G. Hyaline tracheid, SM11 1302.20 m, L27
H. Cuticle with stomata, SM11 1302.20 m, V29
I. Plant cuticle, SM11 1382.13 m, U29/2
J. Folded tracheid, SM11 1302.20 m, V29
K. Large tracheid, SM11 1465.92 m, O30
L. Exceptional 3D preservation of cuticle with stomata, SM11 1304.14 m, D44/4
M. Possible arthropod cuticle or *Callimothallus*-type fungi, SM11 1394.88 m, E29/2

Plate I

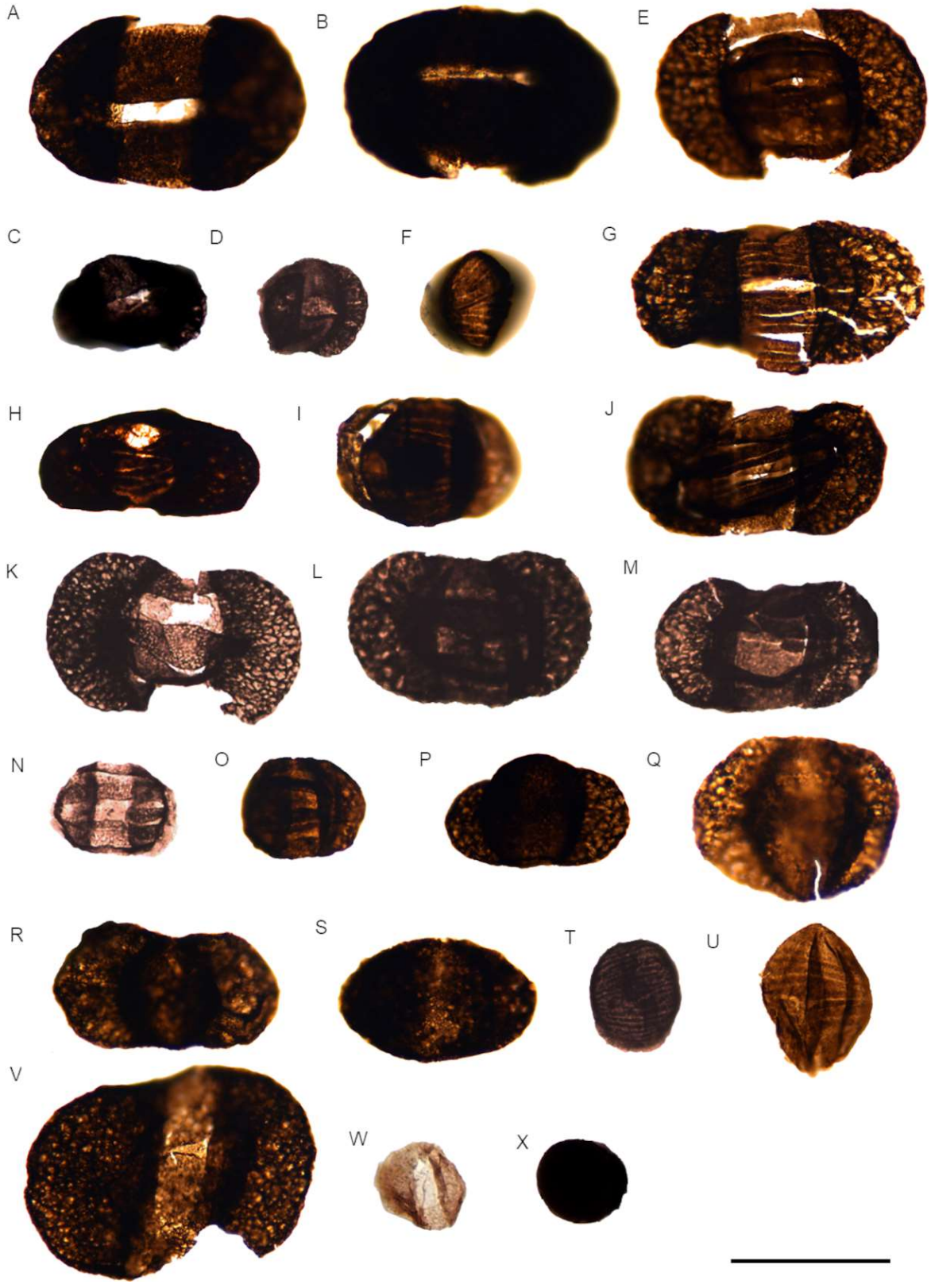

Plate II

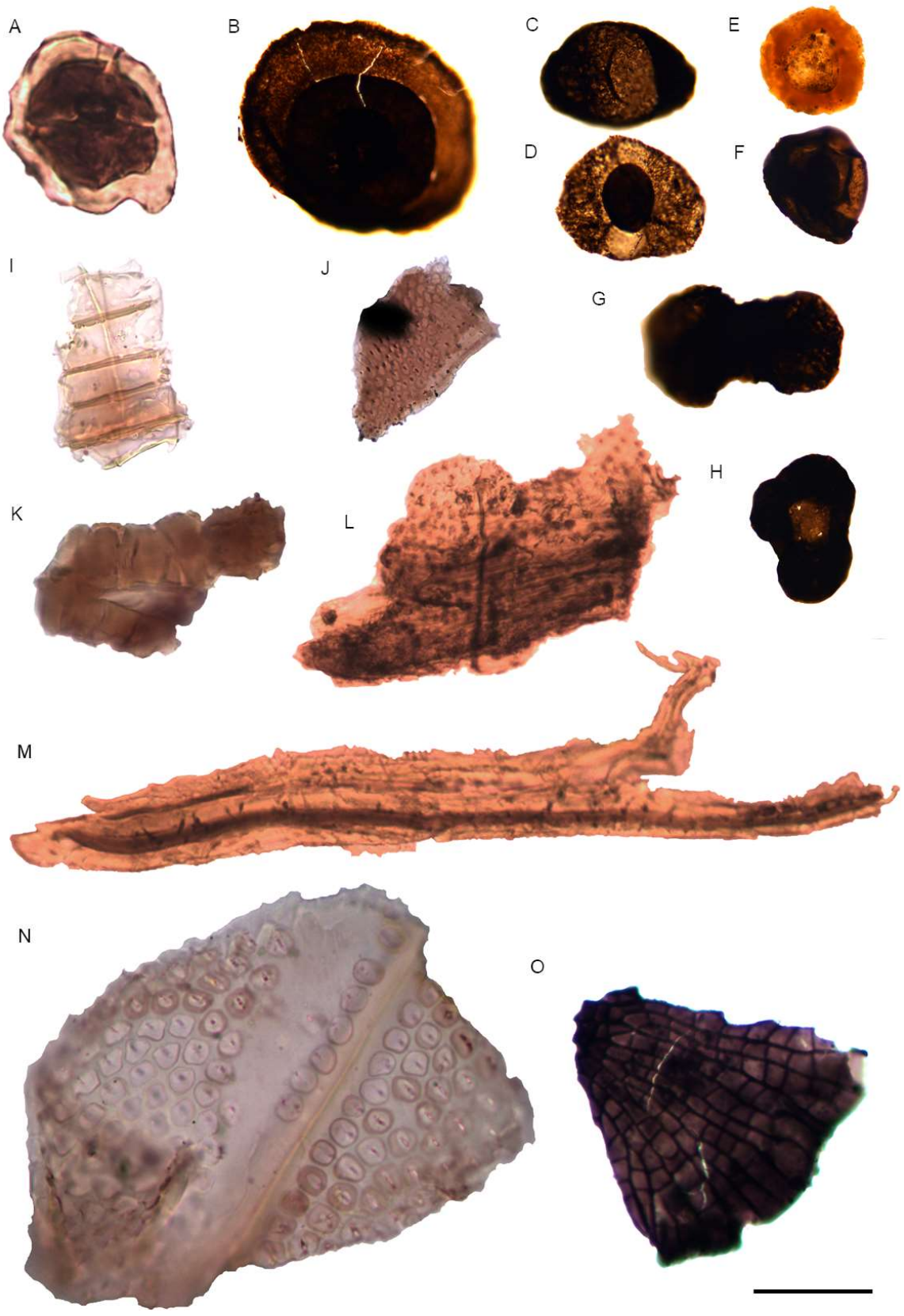

Chapter 9.

Wall ultrastructure of the Permian pollen grain *Lueckisporites virkkiae* Potonié et Klaus 1954 emend. Clarke 1965: evidence for botanical affinity

Martha E. Gibson[a*], Wilson A. Taylor[b], Charles H. Wellman[a]

[a]*Department of Animal & Plant Sciences, University of Sheffield, Alfred Denny Building, Western Bank, Sheffield S10 2TN, U.K.*

[b]*Department of Biology, University of Wisconsin-Eau Claire, 105 Garfield Avenue, Eau Claire, WI 54701, U.S.A.*

**corresponding author: marthae.gibson@gmail.com*

Status as of 11th November 2020: this manuscript is published in Review of Palaeobotany and Palynology. I picked and prepared samples for TEM. I interpreted the micrographs with help from Charles H. Wellman. Wilson A. Taylor performed the TEM sectioning and microscopy.

9.1 Abstract

Permian spore-pollen assemblages are dominated by striate bisaccate pollen grains. The botanical affinity of many of these is unknown, which limits their value in ecological reconstruction and biostratigraphy. *Lueckisporites virkkiae* Potonié et Klaus 1954 emend. Clarke 1965 is a bitaeniate bisaccate pollen grain of uncertain botanical affinity that dominates late Permian Euramerican assemblages, but also bridges phytogeographical provinces. It is classified into three 'variants', which capture a spectrum of morphological variability, but further complicates matters by questioning whether it comprises a natural taxon. Here we report on a TEM analysis of the gross structure and wall ultrastructure of *L. virkkiae* variants from the upper Permian (Lopingian) of Kimberley, Nottinghamshire, U.K. The variants have the same gross structure and wall ultrastructure. The exine consists of a three-layered ektexine composed of a thin tectum, an alveolate infratectum and a thin foot layer, subtended by a solid endexine. Alveolae are either small and rounded, columellate-like, or irregularly shaped, depending on whether the exine is viewed in transverse or longitudinal section. Sacci are protosaccate, with narrow and irregular, or large and voluminous, endoreticulations. Similarities in gross structure and wall ultrastructure suggest that the current taxonomic grouping is correct with the variants representing the range of variation within a single species. We suggest that the differences in morphology are subtle and attributable to harmomegarthy. Comparisons with fossil and modern conifer pollen grains suggest an affinity with conifers. Co-occurrence with the Zechstein conifer macrofossil *Pseudovoltzia liebeana* (Geinitz) Florin 1880 (Majonicaceae) indicates this as a possible source.

9.2 Full text

Review of Palaeobotany and Palynology 275 (2020) 104169

Contents lists available at ScienceDirect

Review of Palaeobotany and Palynology

journal homepage: www.elsevier.com/locate/revpalbo

Wall ultrastructure of the Permian pollen grain *Lueckisporites virkkiae* Potonié et Klaus 1954 emend. Clarke 1965: Evidence for botanical affinity

Martha E. Gibson [a,*], Wilson A. Taylor [b], Charles H. Wellman [a]

[a] Department of Animal & Plant Sciences, University of Sheffield, Alfred Denny Building, Western Bank, Sheffield S10 2TN, UK
[b] Department of Biology, University of Wisconsin-Eau Claire, 105 Garfield Avenue, Eau Claire, WI 54701, USA

ARTICLE INFO

Article history:
Received 22 August 2019
Received in revised form 7 January 2020
Accepted 12 January 2020
Available online 13 January 2020

Keywords:
Late Permian
Lueckisporites virkkiae
Gymnosperm
Saccate pollen
Exine ultrastructure
Alveolar infratectum

ABSTRACT

Permian spore–pollen assemblages are dominated by striate bisaccate pollen grains. The botanical affinity of many of these is unknown, which limits their value in ecological reconstruction and biostratigraphy. *Lueckisporites virkkiae* Potonié et Klaus 1954 emend. Clarke 1965 is a bitaeniate bisaccate pollen grain of uncertain botanical affinity that dominates late Permian Euramerican assemblages, but also bridges phytogeographical provinces. It is classified into three "variants," which capture a spectrum of morphological variability, but further complicates matters by questioning whether it comprises a natural taxon. Here we report on a TEM analysis of the gross structure and wall ultrastructure of *L. virkkiae* variants from the upper Permian (Lopingian) of Kimberley, Nottinghamshire, UK. The variants have the same gross structure and wall ultrastructure. The exine consists of a three-layered ektexine composed of a thin tectum, an alveolate infratectum and a thin foot layer, subtended by a solid endexine. Alveolae are either small and rounded, columellate-like, or irregularly shaped, depending on whether the exine is viewed in transverse or longitudinal section. Sacci are protosaccate, with narrow and irregular, or large and voluminous, endoreticulations. Similarities in gross structure and wall ultrastructure suggest that the current taxonomic grouping is correct with the variants representing the range of variation within a single species. We suggest that the differences in morphology are subtle and attributable to harmomegarthy. Comparisons with fossil and modern conifer pollen grains suggest an affinity with conifers. Co-occurrence with the Zechstein conifer macrofossil *Pseudovoltzia liebeana* (Geinitz) Florin 1880 (Majonicaceae) indicates this as a possible source.

1. Introduction

Late Permian spore–pollen assemblages worldwide are characterized, and often dominated, by striate bisaccate pollen. This is despite the high levels of floral provincialism shown by plant megafossils at this time and the fact that at least three distantly related plant groups are known to produce such pollen (glossopterids, peltasperms and conifers) (Chaloner, 2013). Late Permian Euramerican spore–pollen assemblages, such as those recovered from the Zechstein Basin, are often dominated by an example of this pollen type: *Lueckisporites virkkiae* Potonié et Klaus, 1954 emend. Clarke, 1965 (e.g., Clarke, 1965; Visscher, 1971). Being a "bridging taxon" that occurs across phytogeographical provinces, this taxon is not only important ecologically, but it also has biostratigraphical significance (Stephenson, 2016). However, as yet, the botanical affinity of *L. virkkiae* has not been confidently assigned. Matters are complicated because it exhibits a high degree of morphological variability that has confounded pollen taxonomists and led to questions regarding whether the taxon represents a natural grouping. The lack of understanding regarding the taxonomic status and botanical affinity of *L. virkkiae* hinders its biostratigraphical utility and use in vegetational reconstruction of the floras of Euramerica and elsewhere. In this paper we report on a detailed Transmission Electron Microscopy (TEM) analysis of the morphological variants of *L. virkkiae* in an attempt to clarify its taxonomic status and to shed light on the botanical affinities of this pollen grain.

2. Materials and methods

2.1. Locality and geology

Samples were collected from an upper Permian sequence from a railway cutting at Kimberley, Nottinghamshire, UK [NZ 503453]. This exposure has long been known (Wilson, 1876; Howard et al., 2009) and its paleobotany (Stoneley, 1958; Cleal and Thomas, 1995) and palynology (Clarke, 1965) are well documented. A 10 m sequence of the Cadeby Formation rests unconformably on Upper Carboniferous Coal Measures. It consists of a 1.5 m thick basal layer of Permian Breccia, overlain by 7 m of "Lower Marl," which is in turn overlain by several meters of "Lower Magnesian Limestone" (Howard et al., 2009). At

* Corresponding author.
E-mail address: megibson1@sheffield.ac.uk (M.E. Gibson).

https://doi.org/10.1016/j.revpalbo.2020.104169
0034-6667/

Kimberley the "Lower Marl" consists of red and yellow, medium grained, calcareous sandstone containing thin bands of pale gray shale. It is from these thin shale bands that the palynomorphs used in this study were recovered. This sequence corresponds to sample K5 of Clarke (1965). The Cadeby Formation represents marginal shallow marine deposits of the first major transgressive phase of the first depositional cycle of the Zechstein Sea (Smith et al., 1991). The precise age of the Magnesian Limestone is uncertain, but is generally considered to be late Permian (Lopingian).

2.2. Preparation and techniques

Collected rock samples were subjected to standard palynological HCl–HF–HCl acid maceration techniques. The residue was sieved using a 20 μm sieve and subjected to heavy liquid separation using zinc chloride dissolved in 10% HCl. Recovered pollen grains are extremely well preserved and of very low thermal maturity with no artificial oxidation required. The organic residue was divided with some strew mounted onto glass slides for light-microscopic (LM) analysis and some retained for picking. Three specimens of each of the three variants of Clarke (1965) were individually picked for TEM analysis. Picking was achieved by transferring the palynological residue into ethanol and strew mounting this onto glass slides. The ethanol was left to evaporate naturally before slides were examined under a light microscope attached to a micromanipulator. Selected pollen grains were then individually picked. Picked specimens were encased in agar and dehydrated in 100% ethanol, impregnated with Spurr resin, and cut into ultrathin sections using a diamond knife. Two perpendicular sections were cut; one along the transverse axis and the other along the longitudinal of the pollen grain (Fig. 2). Sections were examined and photographed under a FEI Technai Spirit TEM at 80 kV. Composite TEM images made from individual micrographs were compiled using the GIMP 2.0 software package. Materials are curated in the Centre for Palynology of the University of Sheffield (rock, remaining organic residue, LM slides) and the Department of Biology at the University of Wisconsin Eau Claire (TEM blocks and sections).

3. Taxonomic history of *Lueckisporites virkkiae*

The genus *Lueckisporites* was established by Potonié et Klaus (1954) with the type species *L. virkkiae*. The original generic concept was rather broad and allowed for multiple taeniae, although the description of the type species made it clear that it possessed only two. Subsequently numerous authors discussed the genus and some proposed formal emendations. Various authors considered the value of expanding the genus to include forms with multiple taeniae (Potonié, 1958, 1966; Grebe and Schweitzer, 1962; Mädler, 1964; Singh, 1965). However, this was eventually deemed inappropriate due to the already complex taxonomy of taeniate pollen grains and established practical applications of *L. virkkiae* in biostratigraphy. Therefore a bitaeniate concept for *Lueckisporites* was justified (Leschik, 1956a, 1956b; Jansonius, 1962; Orłowska-Zwolińska, 1962; Klaus, 1963; Hart, 1964, 1965; Ullrich, 1964, Clarke, 1965; Efremova, 1966; Mosler, 1966; Stephenson, 2008). Both Jansonius (1962) and Klaus (1963) formally emended the generic diagnosis specifying that it had only two taeniae, although Bharadwaj (1974)'s emendation allowed for more.

By this time, it had become apparent that *Lueckisporites* is characteristic of, and often dominant in, late Permian palynological assemblages of the Euramerican floral province. Many authors included all of their specimens in the type species *L. virkkiae*, whilst accepting that there was a great deal of morphological variation within this "species concept." However, some authors recognized a wider range of species (e.g., Klaus, 1963; Schaarschmidt, 1963; Singh, 1965), while others encompassed the continuum of morphological variations in the form of "variants" (Clarke, 1965) or "palynodemes" (Visscher, 1971).

Clarke (1965) used the emended diagnosis of Klaus (1963) but emended the diagnosis of the type species *Lueckisporites virkkiae*. He suggested that *L. virkkiae* showed great morphological variation with intergradation between three extremes he termed Variants A–C. According to Clarke (1965) Variant A is the largest and is described as having well-developed, distinctly separate proximal thickenings and well-developed sacci, and is most similar to the holotype and *L. microgranulatus* Klaus 1963. Variant B has sacci that are less well-developed and a small saccus offlap and is most similar to *L. parvus* Klaus 1963. Variant C has a weakly developed proximal cap that is not completely separated into two halves, and is also generally smaller with a more elongate corpus, and is most similar to *L. microgranulatus* "kleinere variante" Klaus 1963.

Visscher (1971) introduced a "palynodeme concept." He suggested the taxon could be subdivided into 11 forms (Norm A: Aa, Ab', Ab", Ac; Norm B: Ba, Bb, Bc', Bc"; Norm C; Norm D, Norm E), based on variation among four characters: (i) the structure of the sexine of the cappa; (ii) the shape of the sacci; (iii) the structure of the sexine of the sacci; (iv) the presence of teratological variations.

In both the schemes of Clarke (1965) and Visscher (1971) the variants/palynodeme norms do seem to differ in size. However, size as a means of differentiation is known to be problematic because it may reflect morphological variation, but can also be influenced by taphonomic effects (e.g., compression), ontogeny or even hydration and harmomegathic effects.

Ultimately, it is unclear whether the morphological variation observed in *Lueckisporites virkkiae* represents natural intraspecific variation or taxonomic, taphonomic, ecological, or some other factor. This lack of understanding obviously hinders our ability to use *L. virkkiae* as an interpretive tool.

This study uses the three "variants" described by Clarke (1965) rather than the palynodeme concept of Visscher (1971) for ease of discrimination. Clarke's three variants are easily recognized and provide a good starting point for assessing wall ultrastructure among the morphological variation exhibited by *L. virkkiae*.

4. Previous interpretations of the botanical affinity of *Lueckisporites*

The botanical affinity of the genus *Lueckisporites* has been considered based on association with plant megafossil remains (e.g., Visscher, 1971) or interpretation of in situ pollen (Klaus, 1966; Clement-Westerhof, 1987).

Visscher (1971) proposed an affinity with the conifer *Ullmannia bronnii* Göppert 1944 based on a strong correlation in abundance between the dispersed pollen grain *Lueckisporites virkkiae* and the plant megafossil *Hiltonia rivuli* Stoneley 1956 (a synonym of *U. bronnii*) in the Hilton Plant Beds. However, in situ pollen reported from *Ullmannia frumentaria* (Schlotheim) Göppert 1850 show extensive morphological variation and can be placed with the genera *Jugasporites* Leschik, 1956b, *Limitisporites* Leschik 1956, *Triadispora* Klaus 1964 and *Illenites* Potonié et Kremp 1954 (Florin, 1944; Potonié and Schweitzer, 1960; Potonié, 1962; Visscher, 1971; Schweitzer, 1986; Balme, 1995). Importantly, none of these taxa are striate. In situ pollen associated with *Ullmannia* cf. *bronnii* were similarly reported as belonging to the non-striate taxon *Alisporites* Daugherty 1941 emend. Nilsson 1958 (although Visscher (1971) questioned the relationship between the examined cone and *U. bronnii*).

Klaus (1966) reported (but did not illustrate) in situ pollen, which he compared to *Lueckisporites junior* Klaus 1963, from the enigmatic plant *Pramelreuthia haberfelneri* Krasser 1916 from the Triassic of Austria. Unfortunately, the biological affinity of this plant is far from clear. *Lueckisporites* has also been associated with the conifer family Majonicaceae after *Lueckisporites*-like pollen was extracted from a cone of *Majonica alpina* Clement-Westerhof 1987 from the upper Permian of Italy (Clement-Westerhof, 1987). However, only a few inconclusive light microscope images of the in situ pollen were published that

were subsequently interpreted as *Lueckisporites* by authors such as Balme (1995). Nonetheless, these pollen grains do appear to be bisaccate and bitaeniate.

5. Descriptions

LM images of all three variants of *Lueckisporites virkkiae* are provided in Plate I. TEM images and interpretive drawings are provided for each of the variants: Variant A (Plate II, 1–5); Variant B (Plate III, 1–5); Variant C (Plate IV, 1–4). Descriptive terminology is based on Osborn and Taylor (1994)'s descriptions of gymnosperm pollen ultrastructure. Sections are of unbroken pollen grains and exhibit limited compression.

5.1. Variant A

Pollen grains of Variant A possess two well-developed, distinctly separate taeniae on the proximal surface oriented parallel to the transverse axis. The corpus is elliptical in outline, with the transverse axis exceeding the longitudinal axis. The well-developed semi-circular, or more than semi-circular, sacci give grains of Variant A a diploxylonoid outline (Fig. 1, a–c).

In transmitted light the surface of the corpus and taeniae appears infrapunctate or infrabaculate. The sacci are composed of radially arranged anastomosing muri that become smaller and more frequent towards the periphery of the sacci (Plate I, 1).

Under TEM the pollen grains have a bilayered exine composed of an outer three part ektexine and an inner endexine, and varies between 1.40 and 3.55 μm in thickness (Plate II, 2, 5).

The ektexine is composed of a thin outer tectum (0.20–0.49 μm) with a contour that is smooth and gently undulating. The infratectum is the thickest layer (0.69–1.67 μm) and appears as an alveolar layer beneath the tectum. The alveolae are small and rounded, or long and elongated in transverse section (Plate II, 1) and are separated by substantial partitions. In longitudinal section (Plate II, 3) the alveolae appear more elongate and irregular. The size and density of the alveolae vary across the ektexine. Alveolae become progressively smaller and denser towards the outer edge of the ektexine. This pattern is observed in both planes of section and within individual pollen grains. The foot layer is thin (0.08–0.23 μm) and can be difficult to distinguish from the overlying infratectum. The proximal face is covered by the taeniae, however, the distal face of the corpus displays a different exine stratification. It consists only of endexine (Plate II, 3). Taeniae have an ultrastructure consistent with the ektexine.

The endexine, when visible, is a prominent homogeneous layer that varies in thickness between 0.43 and 1.16 μm, possibly due to differential compression across pollen grains. No lamellations are visible. The endexine was not present in all specimens, but this was caused by the endexine either being too compressed or specimens fractured during sectioning. The only region of the exine experiencing thinning is in the region of where the taeniae meet on the cappa (Plate II, 3). However, it is unclear whether this is a fracture in the exine or whether it represents a true aperture.

The sacci are semi-circular and well-developed, appearing protosaccate with endoreticulations that are continuous with the foot layer and span the entire width of the sacci. Endoreticulation morphology is independent of sectioning plane, appearing consistent in both transverse and longitudinal section. Alveolae vary in size and density within the saccus, with alveolae becoming smaller towards the perimeter of the sacci. Partitions between the alveolae are thick and substantial, creating column-like structures in transverse section (Plate II, 4).

5.2. Variant B

Pollen grains of Variant B have two well-developed, distinctly separate taeniae on the proximal surface. The corpus is subcircular–circular in outline, with the transverse and longitudinal axes being more-or-less equivalent relative to Variants A and C. The overall grain appears more haploxylonoid than diploxylonoid due to the small saccus offlap and smaller germinal furrow (Fig. 1, d-f).

In transmitted light the corpus and taeniae appears infrapunctate or infrabaculate. Sacci are composed of radially arranged anastomosing muri that become smaller and more frequent towards the perimeter (Plate I, 2).

In thin section the exine is bilayered consisting of a three part outer ektexine and an inner endexine (Plate III, 2, 3). It varies in thickness between 1.69 and 2.06 μm. The ektexine is composed of an outer tectum (0.18–0.50 μm) with a smooth and gently undulating contour. An intermediate infratectum (1.25–1.48 μm) has an ultrastructure that is dependent on the sectioning plane. In transverse section the infratectum appears alveolar with elongated alveolae close to the foot layer; the alveolae become progressively smaller and more rounded towards the outer edge of the infratectum. In longitudinal section the infratectum appears to be composed of larger columellate-like partitions, with smaller, more rounded alveolae towards the outer edge (Plate III, 3). The foot layer is very thin (0.06–0.12 μm) (Plate III, 3) and is present in all specimens. The distal surface of the grain is composed only of endexine, or possibly a very thin layer of ektexine (Plate III, 4). The ultrastructure of the taeniae is composed of ektexine and endexine, with alveolae resembling those of the ektexine (Plate III, 5).

The endexine forms a prominent, homogeneous, and continuous layer underneath the foot layer (0.63–1.52 μm). No lamellations are visible and in some specimens the endexine is thick (Plate III, 3, 4) while in others it is more reduced, possibly due to compression or an artifact of the sectioning process. A rough layer is present on the inside of one specimen (Plate III, 5) – this was observed in only one instance, but likely represents an artifact of the sectioning process. No thinning of the exine is observed in these sections meaning the location of the

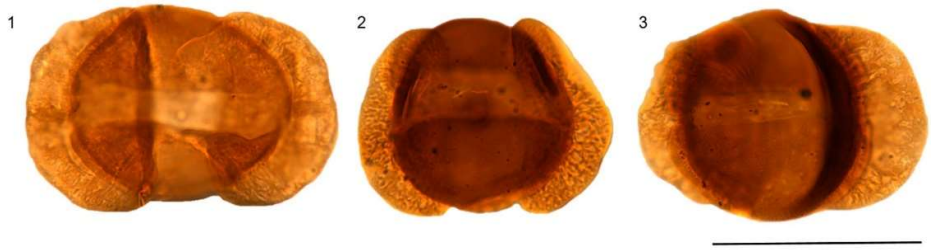

Plate I. Three variants of *Lueckisporites virkkiae* Potonié et Klaus 1954 emend. Clarke, 1965 from the Cadeby Formation, Kimberley, Nottinghamshire, U.K., LM. England Finder co-ordinates included. (1) Variant A (P45) (2) Variant B (B33/1) (3) Variant C (K48/1). Scale bar (1–3) 50 μm. Images taken using a QImaging (Model No. 01-MP3.3-RTV-R-CLR-10) camera mounted on an Olympus BH-2 transmitted light microscope in conjunction with QCapture Pro software.

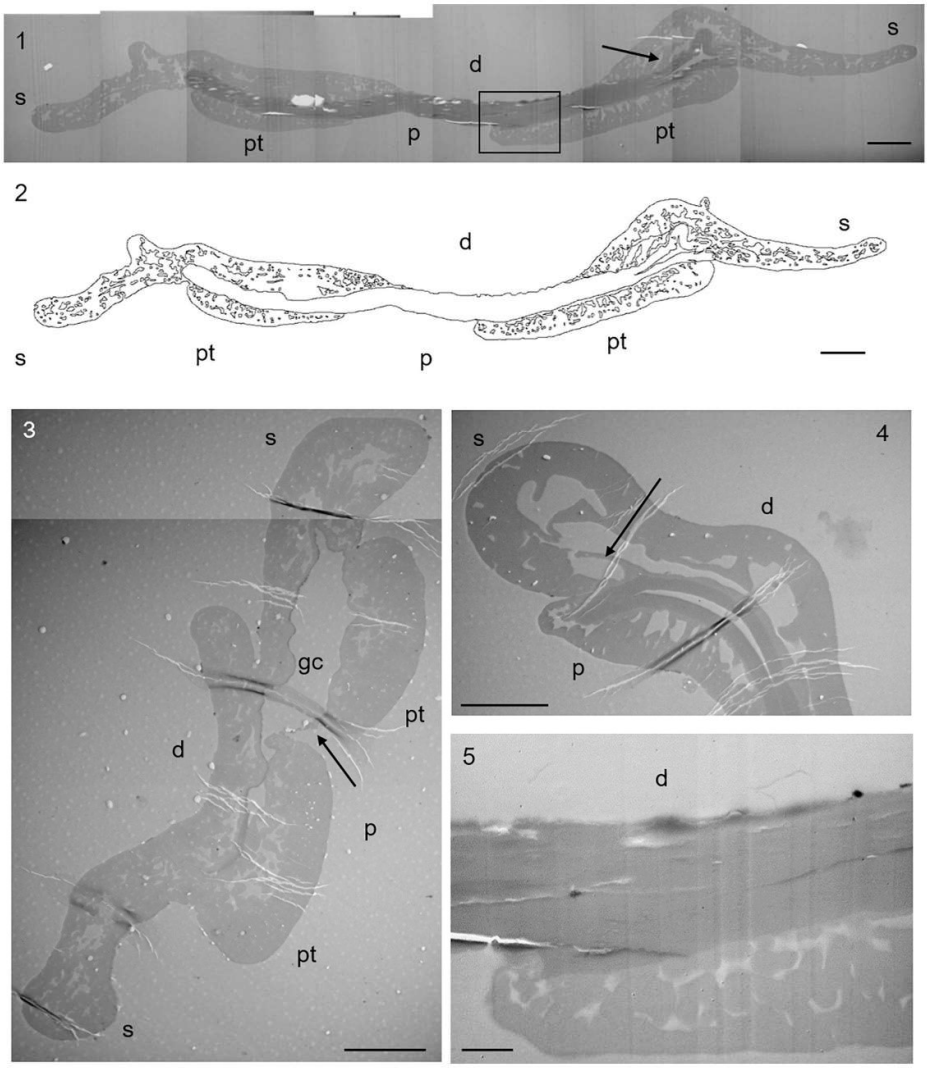

Plate II. *Lueckisporites virkkiae* Potonié et Klaus 1954 emend. Clarke, 1965. The ultrastructure of Variant A specimens. TEM.

1. A section through the transverse axis of a whole pollen grain, capturing the taeniae in transverse section. Arrow indicates saccus endoreticulations which are continuous with the foot layer. Specimen 9. TEM.
2. Variant A whole pollen grain ultrastructure schematic modeled after Specimen 9.
3. A section through the longitudinal axis of a whole pollen grain. Arrow indicates thinning of the exine between the taeniae on the proximal surface. Specimen 3. TEM.
4. Detail of the saccus region. Arrow indicates alveolar structure and protosaccate endoreticulations of the saccus. Specimen 5. TEM.
5. Enlargement of the exine of the taeniae showing alveolar infratectum of the ektexine of the proximal taeniae. Specimen 5. TEM.
d – distal, p – proximal, s – saccus, pt. – proximal taeniae, gc – germinal cavity.
Scale bars (1–4) 4 μm, (5) 800 nm.

aperture is unclear, although it could be located between the taeniae on the proximal surface as in Variants A and C.

The sacci are less well-developed than in Variant A and C, appearing greatly reduced in section (Plate III, 2). The sacci appear protosaccate but internal structure varies with the sectioning plane. In longitudinal section sacci are composed of large endoreticulations with smaller and more frequent endoreticulations towards the perimeter of the saccus (Plate III, 5). In transverse section the endoreticulations appear continuous with the foot layer, and are reduced in volume, forming a less extensive network of alveolae (Plate III, 4).

5.3. Variant C

Pollen grains of Variant C possess two taeniae on the proximal surface, that are often less distinct than in Variants A and B. The sacci are semi-circular but less so than Variant A, and the corpus is noticeably elongated along the transverse axis. The overall outline is haploxylonoid to diploxylonoid (Fig. 1, g–i).

In transmitted light pollen grains appears infrapunctate or infrabaculate, with no visible pattern on the proximal taeniae. The sacci are composed of radially arranged anastomosing muri that increase in frequency but become smaller towards the periphery of the sacci (Plate I, 3).

In section the exine is bilayered with an outer three part ektexine and an inner endexine. The exine varies in thickness between 2.48 and 5.68 μm (Plate IV, 2).

The ektexine is composed of an outer tectum (0.14–0.20 μm) with a thin and irregularly undulating contour. Some specimens display more undulation than others (Plate IV, 2b, 5). The underlying infratectum is alveolar and thick (0.64–2.40 μm). The foot layer is thin (0.90–1.54 μm), and forms a continuous layer along the base of the ektexine (Plate IV, 3).

The endexine is either relatively thick (0.87–1.54 μm), or it appears as a solid layer of constant thickness beneath the ektexine. No lamellations are observed. There is a slight thinning of the endexine center of the distal face (Plate IV, 1).

The proximal and distal surface of the exine of the corpus differ. The distal face is composed only of an endexine, while the proximal face is composed of both ektexine and endexine (Plate IV, 3). The exine between the taeniae appears to be composed only of endexine (Plate IV, 1, 2).

Saccus structure varies within single specimens, however, it is consistent between transverse and longitudinal sections. Sections taken further into the saccus reveal a longer and more differentiated, voluminous protosaccate endoreticulation pattern that is more consistent with other specimens of Variant C (Plate IV, 2a). Sections bisecting the saccus offlap show this region to be composed of many small, rounded alveolae. Towards both the inner and outer peripheries of the sacci the alveolae increase in volume forming a more complex network. Partitions between alvaolae are long and thin (Plate IV, 2b).

Taeniae were not visible in these sections of Variant C, however, they are possibly captured on the proximal surface of PP10 visible as a dramatic reduction in the thickness of the ektexine in the upper left hand quarter of the micrograph (Plate IV, 2b).

The proximal and distal exines of the corpus differ with the distal face consisting only of endexine while the proximal face also has an ektexine. The area on the proximal face where only the endexine is developed possibly represents an aperture.

6. Discussion

6.1. The bisaccate condition (phylogeny and functional morphology)

Among the extant flora bisaccate pollen occur only in gymnosperms where they are produced by some Pinaceae and Podocarpaceae (Coniferales) (see Kurmann, 1992). In the Phyllocladaceae (*Phyllocladus*) the "bisaccate" pollen grains appear to be vestigial (Tomlinson, 2000). Fossil bisaccate pollen grains have been reported in situ from various extinct and extant groups of Coniferales (extinct Voltziales and extant Pinaceae and Podocarpaceae) in addition to the extinct pteridosperm groups: Glossopteridales, Corystospermales, Peltaspermales, Caytoniales and Callistophytales (Balme, 1995; Traverse, 2007). The phylogenetic significance of bisaccate pollen is debated. For example, Tomlinson (2000) notes that saccate pollen is exclusive to gymnosperms and suggests that it may be ancestral in the conifers but with frequent losses. Others suggest that it may have arisen numerous times independently due to convergence (Leslie, 2008).

The actual function and adaptive significance of the bisaccate condition is also highly debated with suggestions that it may: (i) aid long distance wind dispersal and hence outbreeding (e.g., Schwendemann et al., 2007); (ii) aid discharge from the sporangium (e.g., Niklas, 1985); (iii) have a harmomegathic effect in limiting water loss through the sulcus (e.g., Wodehouse, 1935); (iv) facilitate pollination by orientating the pollen grain in the pollination drop (e.g., Doyle, 1945); (v) increase the likelihood of capture by pollen scavenging whilst on the pollen drop (e.g., Tomlinson et al., 1991). As noted by Tomlinson (2000) these proposed functions are not mutually exclusive.

6.2. Gross structure and wall ultrastructure of bisaccate pollen grains

Analysis of gross structure and ultrastructure of both extant and fossil bisaccate pollen grains has the potential to address some of the problems outlined above. Most importantly, the identification of homologies among wall layers may inform us of their phylogenetic significance in bisaccate pollen grains, i.e. whether their phylogenetic distribution is most likely a function of evolutionary inheritance (synapomorphy) or convergence (homoplasy). Most recently the wall ultrastructure of extant bisaccate pollen producers has been reviewed in Kurmann (1990, 1992) and Kurmann and Zavada (1994) and that of fossil producers by Taylor and Taylor (1987), Kurmann and Zavada (1994) and Osborn and Taylor (1994). Wall ultrastructure in the bisaccate pollen grains of extant coniferales (Pinaceae and Podocarpaceae) is similar and based on a four-layered wall system consisting of lamellated endexine and an ektexine comprising a foot layer, infratectum and tectum (Kurmann, 1992). Wall layering in fossil plants is similarly organized. As reviewed by Osborn and Taylor (1994) fossil gymnosperm pollen grains are composed of a four layered wall with a homogenous endexine in mature grains, and a three part ektexine composed of a perforated or undulating outer tectum, an inner alveolar or granular infratectum, and a thin foot layer. The main distinction between extant and many fossil saccate pollen is the lack of proximal taeniae that were such a prominent feature during the late Paleozoic (Chaloner, 2013).

6.3. Gross structure and wall ultrastructure of Lueckisporites virkkiae

The analysis of gross structure and wall ultrastructure in the three variants of *Lueckisporites virkkiae*, as reported in this paper, has a number of implications. Regarding ontogeny and taxonomy, the overall similarity in pollen wall ultrastructure suggests that variation in gross structure/morphology that defines the three variants most likely represents subtle structural differences due to ontogeny and developmental plasticity and/or preservation (e.g., pollen hydration prior to discharge) rather than major taxonomic differences. It seems highly likely that all

Plate III. *Lueckisporites virkkiae* Potonié et Klaus 1954 emend. Clarke, 1965. The ultrastructure of Variant B. TEM.

1. A section through the longitudinal axis of a whole pollen grain. Specimen 13. TEM.
2. Variant B whole pollen grain ultrastructure schematic modeled after Specimen 13.
3. Enlargement of the exine of the taeniae. Arrow indicates the narrow foot layer. Specimen 1. TEM.
4. Saccus detail. Endoreticulation structure visible. Specimen 1. TEM.
5. Enlargement of distal exine. Arrow indicates a protosaccate endoreticulation inside the saccus. Note how alveolae are smaller and more rounded on the distal face towards the inside of the ektexine. Specimen 13. TEM

d – distal, p – proximal, s – saccus, pt. – proximal taeniae, gc – germinal cavity.
Scale bars (1 a, b, 2 a, b) 4 μm, (3) 400 nm (4, 5) 2 μm

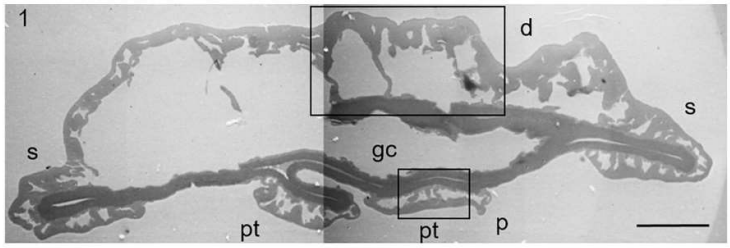
1
d
s
s
gc
pt
pt
p

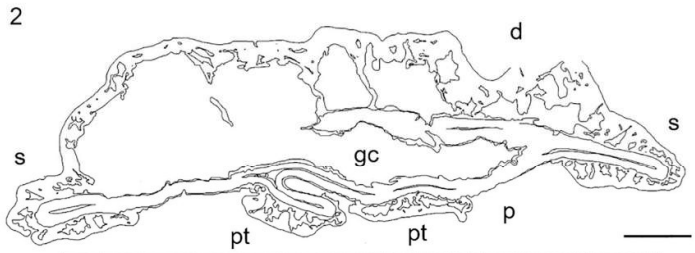
2
d
s
s
gc
p
pt
pt

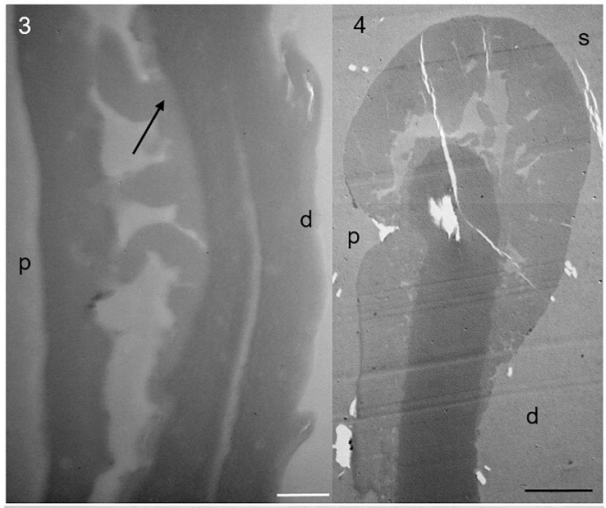
3
d
p
4
s
p
d

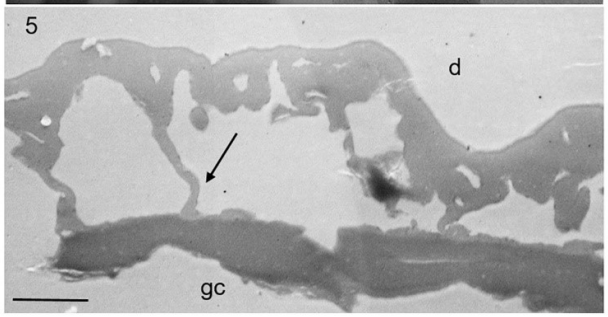
5
d
gc

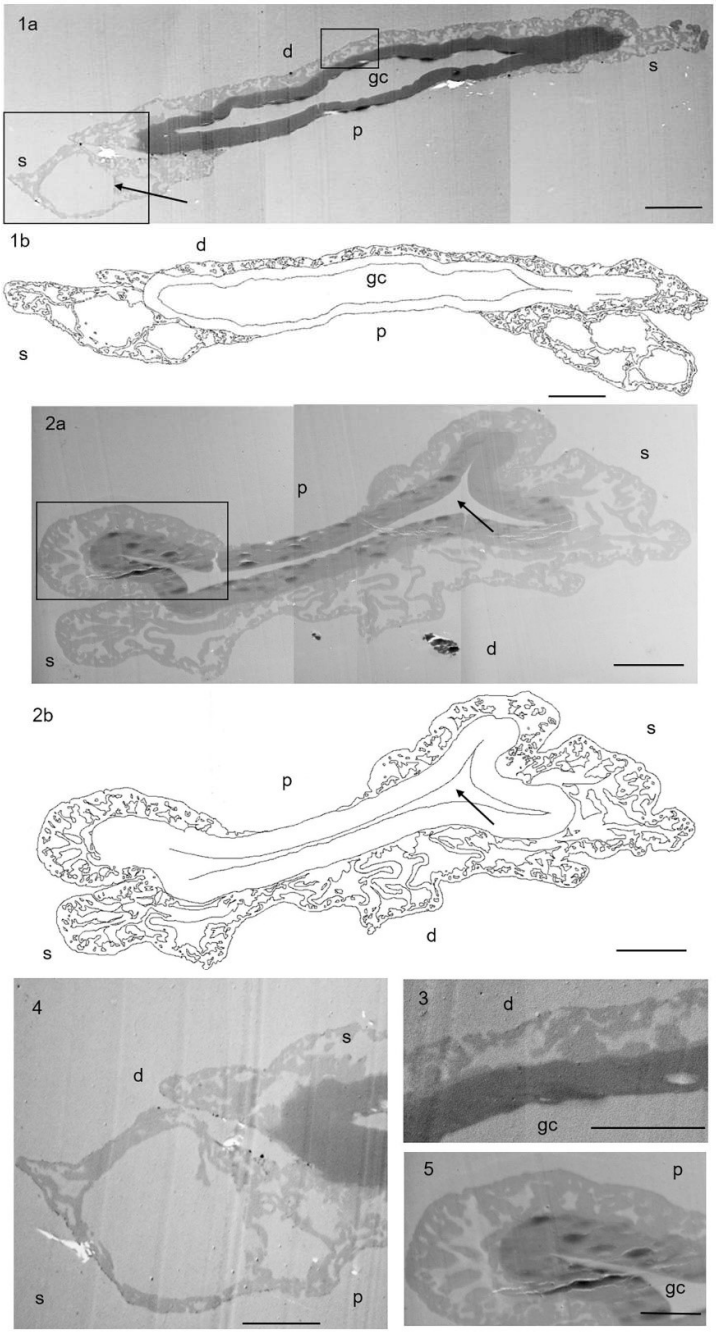
1a
d
gc
s
p
s
1b
d
gc
p
s
2a
s
p
s
d
2b
s
p
d
s
4
s
d
s
p
3
d
gc
5
p
gc

three variants examined represent mature pollen grains naturally dispersed, as suggested by their unlamellated endexine, and as would be expected from dispersed pollen assemblages. Minor variations in wall ultrastructure probably reflect deviations in the angle of sectioning that can alter the shape of the alveolae or perceived thickness of layers within the exine.

Similarly, a number of studies of in situ bisaccate pollen have demonstrated significant intraspecific morphological variation among bisaccate pollen grains both from the fossil record (e.g., Schweitzer, 1986; Lindström et al., 1997) and among extant plants (Kurmann and Zavada, 1994; Tomlinson, 1994; Owens et al., 1998; Leslie, 2008). This obviously has serious implications for the taxonomy of dispersed pollen grains and suggests there may a degree of taxon inflation. It is also relevant to the current debate concerning mutagenesis among bisaccate pollen caused by abiotic stress (Foster and Afonin, 2005; Benca et al., 2018) as it suggests that a degree of natural variation in morphology might be expected.

If the variants of *Lueckisporites virkkiae* belong to the same species then it is likely that they represent continuous, rather than discrete, forms. It is possible that the differences are a result of the relative elasticity of the exine that allows it to accommodate changing osmotic pressure of the cytoplasm, as during hydration or dehydration, causing considerable modification to the structure and appearance of the pollen grain wall. Due to the dispersed nature of this material, there can be no definitive proof of what order the variants may align regarding least to most hydrated. However, based on the appearance of modern bisaccate pollen grains in their dehydrated state, with the sacci folded over the corpus giving the pollen grains a more spherical outline (Osborn and Taylor, 1994; Pacini and Hesse, 2012), it is possible that Variant B with its large saccus overlap and reduced sacci represents a relatively dehydrated state. If pollen grains of *L. virkkiae* hydrate similarly to modern bisaccate pollen grains then it is possible that the order is Variant B–Variant C–Variant A. Variant A is also the most abundant within dispersed assemblages (e.g., Visscher, 1971), suggesting that it may be the final, most inflated, form.

6.4. The phylogenetic significance of the protosaccate versus eusaccate condition

The phylogenetic utility of saccus condition is limited because of the common compression of sacci that can make pollen grains appear superficially protosaccate. Direction of sectioning plane is also important because grains can appear protosaccate or eusaccate dependent on whether sections are longitudinal or transverse (Osborn and Taylor, 1994), as a result of sacci tapering off laterally where they attach to the corpus. Ontogenetic stage can also contribute to a protosaccate appearance. It is possible for under-developed pollen grains to appear superficially protosaccate if the sacci are not yet fully expanded (Osborn and Taylor, 1994). The robustness of endoreticulations also factors into determining whether a grain is protosaccate or eusaccate as delicate endoreticulations may be easily ruptured or separated from the underlying endexine during saccus expansion.

The pollen grains in this study are relatively uncompressed which rules out wall ultrastructure appearing superficially protosaccate. The endoreticulations observed in the specimens are not discontinuous endoreticulations that have been preservationally compressed. All variants have been sectioned both transversely and longitudinally to account for saccus tapering, and no distinct difference in saccus structure was observed. Ontogenetically, these specimens are surmised to be mature due to their unlamellated endexine (even following staining) and the endoreticulations observed in all specimens are robust and intact. All this suggests strongly that the endoreticulations in *Lueckisporites virkkiae* are protosaccate, rather than eusaccate.

Nonetheless, proving that *Lueckisporites virkkiae* is protosaccate and is not very helpful regarding determining a biological affinity for this pollen grain. This is because it is unclear which of the protosaccate or eusaccate conditions is the more primitive, as both have been described from different groups of gymnosperms creating debate about whether or not they are homologous (Crane, 1990).

6.5. Phylogenetic affinities of Lueckisporites virkkiae

Regarding the biological affinities of the parent plant of *Lueckisporites virkkiae*, pollen wall ultrastructure is again potentially more important than gross structure. Bisaccate pollen have been reported from diverse plant groups (summarized above) and is not particularly informative as the phylogenetic pattern represents either substantial losses or numerous independent origins. However, the distinctive four-layered wall and characteristic ultrastructure, coupled with the bisaccate condition, would seem to point to affinities with the conifers as this is a feature recognized in both extant and fossil conifer groups that produce bisaccate pollen.

Other pollen grains are taeniate, such as those produced by the Glossopteridales, but they display a different ultrastructure, largely in that they are eusaccate with a complete separation of the sexine and nexine in the region of the saccus. Glossopterid pollen grains, extracted from *Arberiella*-type sporangia, have a corpus exine with an infrastructural layer composed of irregular shaped rods or partitions (Zavada, 1991); a different infratectum organization than the alveolar infratectum and protosaccate sacci observed in *L. virkkiae*. Furthermore, predispersal expansion of the corpus has been observed in the sporangia of *Arbereilla* sp. cf. *A. africana* Pant and Neutiyal (Lindström et al., 1997). Predispersal expansion is another possible explanation for the differences in gross morphology observed.

Thus it seems likely that *L. virkkiae* was produced by a conifer based on a consideration of pollen morphology, gross structure and wall ultrastructure. Considering the composition of the flora described from the late Permian Zechstein Basin a possibility is *Pseudovoltzia liebeana* (Geintz), a member of the extinct conifer family Majonicaceae (Clement-Westerhof, 1987). Another member of the Majonicaceae, *Majonica alpina* Clement-Westerhof 1987, is known to produce bitaeniate bisaccate pollen that bears a distinct resemblance to *Lueckisporites* (Clement-Westerhof, 1987). An Angaran basal conifer group contemporary *Sashinia* Meyen 1968 is also known to produce the morphologically similar protobisaccate pollen grain *Scutasporites* Klaus 1963 (Gomankov et al., 1998; Gomankov, 2009). The lack of in situ reproductive material for *Pseudovoltzia* from the British Zechstein makes this association tentative and we are aware that paleobotanical/palynological co-occurrence is a

Plate IV. *Lueckisporites virkkiae* Potonié et Klaus 1954 emend. Clarke, 1965. The ultrastructure of Variant C. TEM.

1a. A section through the transverse axis of a whole pollen grain. Arrow indicates endoreticulations within the saccus. Specimen 11. TEM.
1b. Variant C whole pollen grain schematic in transverse section. Specimen 11.
2a. A section through the longitudinal axis of a whole pollen grain. Arrow indicates the germinal cavity. Specimen 10. TEM.
2b. Variant C whole pollen grain schematic in longitudinal section. Arrow indicates the germinal cavity. Specimen 10.
3. Enlargement of exine in transverse section. Arrow indicates the thin foot layer. Specimen 11. TEM.
4. Enlargement of exine in longitudinal section. Specimen 11. TEM.
5. Enlargement of saccus showing internal network of endoreticulations. Specimen 10. TEM.
d – distal, p – proximal, s – saccus, gc – germinal cavity
Scale bars (2 a, b) 4 μm (3–5) 2 μm

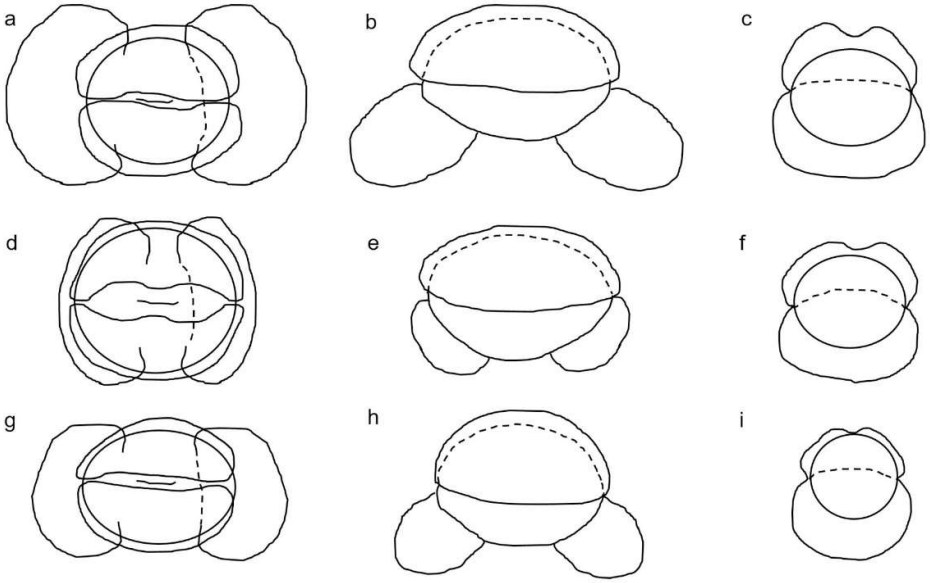

Fig. 1. Diagrammatic reconstruction of the three variants of *Lueckisporites virkkiae* Potonié et Klaus 1954 emend. Clarke, 1965. a–c Variant A, d–f Variant B, g–i Variant C. a, d, g pollen grains in proximal polar view; b, e, h pollen grains in lateral view; c, f, i pollen grains in terminal polar section. Figure modeled after text-fig. 8 in Clarke (1965).

complicated issue and basing affinities on such data may be problematic. However, the elimination of other known macroflora–pollen association from the source assemblage does provide some support for this interpretation; *Ullmannia frumentaria* (Schlotheim) Göppert 1850 is known to produce *Illenites* sp. (Schweitzer, 1986) as well as *Jugasporites, Limitisporites* and *Triadispora* (Florin, 1944; Potonié and Schweitzer, 1960; Potonié, 1962; Visscher, 1971; Schweitzer, 1986; Balme, 1995), and *Alisporites* sp. is produced by a voltziaceous conifer (Grauvogel-Stamm, 1978).

7. Conclusions

The three variants of the bisaccate pollen grain *Lueckisporites virkkiae* all exhibit similar wall ultrastructure characterized by an alveolar infratectum and homogenous endexine. We conclude that the variants belong to a single taxon and that the morphological differences between them are a result of the effects of harmomegarthy with the variants representing different levels of pollen hydration prior to discharge. A comparison with known fossil and extant bisaccate pollen has shown that the pollen grains share a number of gross structure and wall ultrastructure characteristics with coniferous pollen. However, comparisons are hindered by the absence of extant taeniate bisaccate pollen grains from which natural variation in striate features could be assessed and the development of taeniae understood. Co-occurrence data suggest *Pseudovoltzia liebeana* (family Majonicaceae) as a possible parent plant, which is supported by reports of in situ pollen in other members of Majonicaceae in the fossil record.

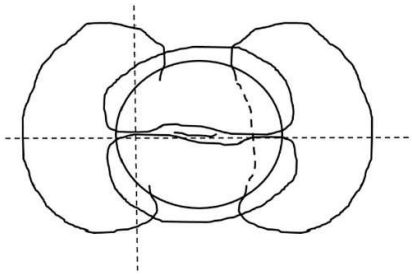

Fig. 2. Schematic for the orientation of perpendicular sections taken through *Lueckisporites virkkiae* Potonié et Klaus 1954 emend. Clarke, 1965. Longitudinal sections pass through each saccus and parts of the proximal taeniae. Transverse sections pass through a single saccus and both proximal taeniae.

Declaration of Competing Interests

The authors declare that they have no known competing financial interests or personal relationships that could have appeared to influence the work reported in this paper.

Acknowledgements

MEG was funded by a NERC studentship through the ACCE (Adapting to the Challenges of a Changing Environment) Doctoral Training Partnership (Award Reference 1807541). We thank G. Warrington for taxonomic advice.

References

Balme, B.E., 1995. Fossil in situ spores and pollen grains: An annotated catalogue. Rev. Palaeobot. Palynol. 87, 81–323.
Benca, J.P., Duijnstee, I.A.P., Looy, C.V., 2018. V-B–induced forest sterility: Implications of ozone shield failure in Earth's largest extinction. Science Advances 4 (2), e1700618. https://doi.org/10.1126/sciadv.1700618.
Bharadwaj, D.C., 1974. On the classification of gymnospermous sporae dispersae. Symposium on structure, nomenclature and classification of pollen and spores. Special Publication 4. Birbal Sahni Institute of Palaeobotany, Lucknow, pp. 7–52.
Chaloner, W.G., 2013. Three palynological puzzles. Int. J. Plant Sci. 174 (3), 602–607.
Clarke, R.F.A., 1965. British Permian saccate and monosulcate miospores. Palaeontology 8 (2), 322–354.

Cleal, C.J., Thomas, B.A., 1995. Palaeozoic Palaeobotany of Great Britain. Geological Conservation Review Series No. 9Chapman and Hall, London.
Clement-Westerhof, J.A., 1987. Aspects of Permian palaeobotany and palynology, VII. The Majonicaceae, a new family of Late Permian conifers. Rev. Palaeobot. Palynol. 52, 375–402.
Crane, P.R., 1990. The phylogenetic context of microsporogenesis. In: Blackmore, S., Knox, R.B. (Eds.), Microscopes: Evolution and Ontogeny. Academic Press, London, pp. 11–41.
Doyle, J., 1945. Development lines in pollination mechanisms in the Coniferales. Scient. Proc. R. Dublin Soc. A. 24, 43–62.
Efremova, G.D., 1966. On classification of dispersed pollen Striatiti Pant 1954. 2001. Ultrastructure of some Permian pollen grains from the Russian Platform; In. In: Zavialova, N.E., Meyer-Melikian, N.R., Gomankov, A.V., Goodman, D.K., Clarke, R.T. (Eds.), Proceedings of the IX international Palynological Congress, Houston, Texas, U.S.A., 1996. American Association of Stratigraphic Palynologists Foundation, pp. 99–114.
Florin, R., 1944. Die Koniferen des Oberkarbons und des unteren Perms. VII. Palaeontogr. B 85, 459–654.
Foster, C.B., Afonin, S., 2005. Abnormal pollen grains: An outcome of deteriorating atmospheric conditions around the Permian-Triassic boundary. J. Geol. Soc. 162, 653–659.
Gomankov, A.V., 2009. Pollen evolution in Cordaites and Early Conifers. Palaeontol. J. 43, 1245–1252.
Gomankov, A.V., Balme, B.E., Foster, C.B., 1998. Tatarian palynology of the Russian Platform: a review. Proc. R. Soc. Vict. 110, 115–135.
Grauvogel-Stamm, L., 1978. La flore du Grès a Voltzia (Bundsandstein Supérior) des Vosges du Nord (France), morphologie, anatomie, interprétations phylogénique et paléogéographique. Memoir 50Sciences Géologiques, Université Louis Paster de Strasbourg, Institute de Géologie, pp. 1–225.
Grebe, H., Schweitzer, H.J., 1962. Die Sporae dispersae des niederrheinischen Zechsteins. Fortschritte in der Geologie von *Rheinland* und *Westfalen* 12, 201–224.
Hart, G.F., 1964. A review of the classification and distribution of the Permian Miospore; Disaccate Striatiti. C.R. 5th Congr. Internat. Carbonif. Strat. Geol. 3, pp. 1171–1199.
Hart, G.F., 1965. The Systematics and Distribution of Permian Miospores. Witwatersrand University Press, p. 252.
Howard, A.S., Warrington, G., Carney, J.N., Ambrose, K., Young, S.R., Pharoah, T.C., 2009. Geology of the Country around Nottingham. Memoir of the British Geological Survey, Sheet 126 (England and Wales).
Jansonius, J., 1962. Palynology of the Permian and Triassic sediments, Peace River Area, Western Canada. Palaeontogr. B 110, 35–98.
Klaus, W., 1963. Spores aus dem südalpin Perm. Jahrb. Geol. Bundesanst. 106, 229–363.
Klaus, W., 1966. Zwei Pflanzenreste der alpinen Trias mit ihren Sporen (*Lueckisporites* und *Decussatisporites*). Verhandlungen der Geologischen Bundesanstalt 1, 172–177.
Kurmann, M.H., 1990. Exine formation in *Cunninghamia lanceolata* (Taxodiaceae). Rev. Palaeobot. Palynol. 64, 175–179.
Kurmann, M.H., 1992. Exine stratification in extant gymnosperms: a review of published transmission electron micrographs. Kew Bull. 47, 25–39.
Kurmann, M.H., Zavada, M.S., 1994. Pollen morphological diversity in extant and fossil gymnosperms. In: Kurmann, M.H., Doyle, J.A., Zavada, M.S. (Eds.), Ultrastructure of Fossil Spores and Pollen and its Bearing on Relationships among Fossil and Living Groups. The Royal Botanic Gardens, Kew, England, p. 221.
Leschik, G., 1956a. Die Keuperflora von Neuewelt bei Basel, 2. Die Iso- und Mikrosporen. Schweiz. Palaeontol. Abhandl. 72, 1–70.
Leschik, G., 1956b. Sporen aus dem Salzton des Zechsteins von Neuhof (bei Fulda). Palaeontogr. B 100, 122–142.
Leslie, A., 2008. Interpreting the function of saccate pollen in ancient conifers and other seed plants. Intl. J. Plant Sci. 169, 1038–1045.
Lindström, S., McLoughlin, S., Drinnan, A.N., 1997. Intraspecific variation of taeniate pollen within Permian glossopterid sporangia, from the Prince Charles Mountains, Antarctica. Int. J. Plant Sci. 158, 673–684.
Mädler, K., 1964. Die geologische Verbreitung von Sporen und Pollen in der deutschen Trias. Geol. Jahrb., Beih. 65, 1–147.
Mosler, H., 1966. Der Stoffbestand und Fossilinhalt des Grauen Salztones im südlichen Bereich der Deutschen Demokratischen Republik. Freiberg Forschungshefte, C 201, 95–128.
Niklas, K.J., 1985. The aerodynamics of wind pollination. Bot. Rev. 51, 328–386.
Orłowska-Zwolińska, T., 1962. A first finding of Zechstein sporomorphs in Poland. Kwart. Geol. 6, 283–297.
Osborn, J.M., Taylor, T.N., 1994. Comparative ultrastructure of fossil gymnosperm pollen and its phylogenetic implications. In: Kurmann, M.H., Doyle, J.A., Zavada, M.S. (Eds.), Ultrastructure of Fossil Spores and Pollen and its Bearing on Relationships among Fossil and Living Groups. The Royal Botanic Gardens, Kew, England, p. 221.
Owens, N.J., Takaso, T., Runions, J., 1998. Pollination in conifers. Trends Plant Sci. 3, 479–485.
Pacini, E., Hesse, M., 2012. Uncommon pollen walls: reasons and consequences. Verh. Zool. Bot. Ges. Osterr. 148–149, 291–306.
Potonié, R., 1958. Synopsis der Gattungen der Sporae Dispersae. II. Sporites (Nachträge), Saccites, Aletes, Praecolpates, Polyplicates, Monocolpates. Beihefte zum Geologischen Jahrbuch, Hefte 31, 114.
Potonié, R., 1962. Synopsis der Sporae in situ. Beihefte zum Geologischen Jahrbuch, Hefte 52, 1–204.
Potonié, R., 1966. Nachtrage zu allen Gruppen (Turmae), Pt. 4. Synopsis der Gattungen der Sporae dispersae. Hefte 72. Beihefte zum Geologischen Jahrbuch, p. 244.
Potonié, R., Klaus, W., 1954. Einige Sporengattungen des alpinen Salzgebirges. Beihefte zum Geologischen Jahrbuch 68, 517–546.
Potonié, R., Schweitzer, H.J., 1960. Der Pollen von *Ullmannia frumentaria*. Paläontol. Z. 34, 27–39.
Schaarschmidt, F., 1963. Sporen und Hystricosphaerideen aus dem Zechstein von Büdingen in der Wetterau. Palaeontogr. B 113, 38–91.
Schweitzer, H.J., 1986. The Land Flora of the English and German Zechstein Sequences. Special Publication 22Geological Society, London, pp. 31–54.
Schwendemann, A.B., Wang, G., Mertz, M.L., McWilliams, R.T., Thatcher, S.L., Osborn, J.M., 2007. Aerodynamics of saccate pollen and its implications for wind pollination. Am. J. Bot. 94, 1371–1381.
Singh, H.P., 1965. Saccate pollen grains from the lower Triassic of Hallstatt, Austria. Palaeobotanist 13, 74–81.
Smith, D.B., Taylor, J.M.C., Arthurton, R.S., Brookfield, M.E., Glennie, K.W., 1991. Permian. Memoirs 13Geological Society, London, pp. 87–96.
Stephenson, M.H., 2008. Spores and Pollen from the Middle and Upper Gharif members (Permian) of Oman. Palynology 32, 157–183.
Stephenson, M.H., 2016. Permian palynostratigraphy: A global overview. In: Lucas, S.G., Shen, S.Z. (Eds.), The Permian Timescale. Geol. Soc. Lond., Spec. Publ, pp. 1–450.
Stoneley, H.M.M., 1958. The Upper Permian flora of England. Br. Mus. Nat. Hist. Geol. Bull. 3, 295–337.
Taylor, T.N., Taylor, E.L., 1987. The ultrastructure of fossil gymnosperm pollen. Bull. Soc. Bot. Fr. 134, 121–140.
Tomlinson, P.B., 1994. Functional morphology of saccate pollen in conifers with special reference to Podocarpaceae. Int. J. Plant Sci. 155, 699–715.
Tomlinson, P.B., 2000. Structural features of saccate pollen types in relation to their functions. Pages 147–162. In: Harley, M.M., Morton, C.M., Blackwell, S. (Eds.), Pollen and Spores: Morphology and Biology. Royal Botanic Gardens, Kew, England, p. 254.
Tomlinson, P.B., Braggins, J.E., Rattanbury, J.A., 1991. Pollination drop in relation to cone morphology in Podocarpaceae: A novel reproductive mechanism. Am. J. Bot. 78, 1289–1303.
Traverse, A., 2007. Paleopalynology. Volume 28 of Topics in Geobiology, Second editionSpringer Science & Business Media, p. 813.
Ullrich, H., 1964. Zur Stratigraphie und Paläontologie der marin beeinflussten Randfazies des Zechsteinbeckens in Ostthüringen und Sachsen. Freiberger Forschungsh., C, 169 p. 163.
Visscher, H., 1971. The Permian and Triassic of the Kingscourt Outlier, Ireland. Special Paper, No. 1Geological Survey of Ireland, p. 114.
Wilson, E., 1876. Geology of Nottingham. Q. J. Geol. Soc. Lond. 32, 1–535.
Wodehouse, R.P., 1935. Pollen Grains. Their Structure, Identification and Significance in Science and Medicine. McGraw-Hill, New York, p. 574.
Zavada, M.S., 1991. The ultrastructure of pollen found in dispersed sporangia of *Arberiella* (Glossopteridaceae). Bot. Gaz. 152 (2), 248–255.

Chapter 10.

First report of spheroidal inclusions of a possible fungal nature inside pollen grains from the Permian (Lopingian) Zechstein Group

[1*]Martha E. Gibson

[1]*Department Animal and Plant Sciences, University of Sheffield, Western Bank,*

S10 2TN, Sheffield, South Yorkshire, U.K.

**corresponding author: marthae.gibson@gmail.com.*

Status as of 11th November 2020: this manuscript is in preparation for publication.

10.1 Abstract

Interesting spheroidal inclusions were observed in bisaccate and monosaccate gymnospermous pollen grains from the Lopingian Zechstein Group (258-252Ma) of northeast England, U.K. The structures are rare and occur most often singly, or in clusters of up to 20, inside the corpus of pollen grains and possibly also within the sacci. The inclusions are 10-40µm in diameter and either smooth-walled and translucent or are opaque with a fragmented circumference and are found inside the host pollen grain taxa *Lueckisporites virkkiae, Klausipollenites schaubergeri, Illinites* spp., *Taeniaesporites* spp., *Protohaploxypinus* spp., *Vestigisporites minutu*s and, on rare occasions, *Falcisporites zapfei* and *Labiisporites granulatus*. While the botanical affinities of these inclusions remain uncertain the interpretation of these structures as an endobiotic zoosporangia of a chytrid-like organism is encouraged based on the description of similar structures in other Upper Permian material, as well as the fact that pollen grains are suitable host substrates and habitats for microorganisms.

Keywords: fungi, palynology, zoosporangium, Chytridiomycota, Lopingian, Zechstein

10.2 Introduction

Pollen and spores are widely recognised as being suitable hosts for extant microfungi (Hutchison & Barron 1997; Czeczuga & Muszyńska 2004). These associations are primarily made with saprotrophic fungi, which decompose the pollen, or those which parasitize viable pollen grains (Goldstein 1960; Classen *et al.* 2000; Krauss *et al.* 2011; Phuphumirat *et al.* 2011; Wurzbacher *et al.* 2014). There is an extensive fossil record of fungal associations with vascular plants from the

Devonian to the present day. The record of vascular plant spores with fungi is more extensive than any other plant-fungal association (Taylor *et al.* 2015), suggesting there is a long record of pollen also being suitable hosts and habitats for fungi throughout the evolution of terrestrial plant life.

The earliest known example of fungi colonising spores is from the Lower Devonian Rhynie (Taylor *et al.* 1992*a*, *b*, *c*; Hass *et al.* 1994). Interactions include putative chytrid zoospores colonising the spore surface, the space between the individual layers of the spore wall, and the spore lumen as an endobiont (Kidston & Lang 1921; Illman 1984; Taylor *et al.* 1992*c*, 2004). During the Devonian the spore lumen became an available microhabitat for microfungus as seed plants evolved. It is possible that the reduction of the microgametophyte phase made the spore lumen more available as a microhabitat for microfungi. Evidence of microfungi colonising pollen grains is found from the Carboniferous onwards with many more instances of endobiotic fungus reported (e.g., Krings *et al.* 2009*a*, *b*). There is fossil evidence for microfungi colonising pollen grains as both endobionts and epibionts e.g. chytrid-like sporangia with Pennsylvanian cordite pollen grains (Millay & Taylor 1987). Degraded pollen grains from the Permian of India have been found with spherical cells attached to the pollen body, alongside the additional evidence of fungal activity of skeletonization of the exine and saccus (Strivastava *et al.* 1999).

Microfungi have been observed inside the cortex of *Biscalitheca* cf. *musata* (Zygopteridales) from the Upper Pennsylvanian Grand-Croix cherts (Saint-Etienne Basin, France) (Krings *et al.* 2009*b*). Among the morphologies described were clusters of spherical structures concluded to be saprotrophs according to the condition of the host grain and their resemblance to modern chytrid zoosporangia. However, due to the lack of further diagnostic features the systematic affinity of these structures remains tentative. Nevertheless, this finding provides a detailed insight into the types of microfungi that may have been associated with land plants ca. 300 million years ago.

Late Visean cherts from central France containing a diverse assemblage of chytrids and chytrid-like remains of uncertain affinity contribute to a more thorough understanding of the concept of biodiversity in Carboniferous non-marine ecosystems (Krings *et al.* 2009*a*). Spheroidal inclusions interpreted as endobiotic fungi have been described from the Triassic Gremout Peak peat in Antarctica, described as chytrid-like organisms with a pore inside the pollen grain corpus and sacci (Harper *et al.* 2016, Figure 2b). The spheroidal inclusions were interpreted as morphologically similar to particular extant members of the Chytridiomycota that parasitize pollen and spores. Similar morphologies have been described by Slater *et al.* (2015) from permineralized bogs of the Toploje Member (Roadian-Wordian) from the Lambert Graben, East Antarctica, with spheroidal inclusions occurring in association with pollen grains and have also been interpreted as evidence of a parasitic or saprotrophic chytrids.

Figure 1. Stratigraphy of the British Zechstein Group.

In modern communities, fungi form a major portion of total biodiversity (e.g., Baldrain *et al.* 2013; Wardle & Lindahl 2014). It is therefore expected that they were prevalent in ancient ecosystems and documented in the fossil record, however they are underrepresented in the literature. The recent effort among palaeontologists to improve the documentation of fungi in the fossil record has facilitated interpretation of the role fungi have played in ancient ecosystems.

Fungal remains are best described from cherts, providing the most valuable source of information on fungal associations with ancient organisms (Taylor & Krings 2005). Due to the nature in which cherts preserve fungi and their host organisms, interactions can be examined directly. Fungal associations that have not been preserved in chert have received considerably less attention and therefore represent an important source of new information regarding ancient fungal activity. Spheroidal inclusions from the Permian Indian coalfields show spherical cells attached to the body as well as skeletonization of the exine and saccus which is attributable to degradation of the pollen grain (Srivastava *et al.* 1999). Saccate pollen grains from the Raniganj Coalfields in India have been found to contain spheroidal inclusions in the corpus, which were interpreted as components representing stages in the development of the microgametophyte (Vijay & Meena 1996). Most recently, spheroidal inclusions inside saccate pollen grains from the Lopingian and Guadalupian of India were recovered from the Godavari Graben (Andhra Pradesh, India) (Aggarwal *et al.* 2015). These specimens were interpreted as endobiotic zoosporangia of chytrid or Hypochytridiomycota affinity.

This paper provides the first description of spheroidal inclusions of a possible microfungal nature from within saccate pollen grains from marine deposits of the Lopingian Zechstein Group of northeast England.

10.3 Materials and methods

10.3.1 Locality and geology

The Permian sediments in the northeast England were deposited along the western margin of the Zechstein Sea, a semi-isolated inland sea which occupied the Southern Permian Basin (SPB) during the Lopingian (Smith *et al.* 1989). In the U.K., the lower Zechstein Group is found either side of the Cleveland High which separates the northern Durham Sub-basin from the southern Yorkshire Sub-basin. The material described in this paper comes from drill cores from the Yorkshire Sub-Basin from both the upper and lower Zechstein.

In both sub-basins the Zechstein group can be divided into five distinct sedimentary carbonate-evaporite cycles (EZ1-5) (Figure 1) that reflect the nature of deposition within the basin. The typical Zechstein cycle starts with a transgressive siliclastic unit, followed by a limestone or dolomitic unit, which grades upwards into anhydrite/gypsum, halite, and finally K-Mg salts (potash), reflecting the progressively increasing salinity of the seawater. Due to the increasing reducing conditions within the basin, the cycles become progressively shorter in duration with thinner deposits as they were deposited in an ever-shrinking evaporite basin in combination with the progradation of terrigenous deposits towards the basin centre.

The lithostratigraphical units in each cycle can be correlated throughout the basin, starting with the anoxic shale of the Marl Slate/Kupferschiefer. In the Yorkshire Sub-basin the Marl Slate is overlain by the remaining carbonates of the Cadeby Formation, which is composed of two members, the Wetherby and Sprotbrough members, separated by the Hampole discontinuity. The EZ1 evaporites are the Hayton Anhydrites. EZ2 is composed of the carbonates of the Kirkham Abbey Formation, and the extensive evaporites of the Fordon Evaporite Formation.

The boundary between EZ2 and EZ3 is marked by the Grauer Salzton which is overlain by the limestone and dolomite of the Brotherton Formation, and evaporites of the Billingham Anhydrite, Boulby Halite, and Boulby Potash. The boundary between EZ3 and EZ4 is marked by the hygroscopic Carnallitic Marl Formation, which is overlain by the Sherburn Anhydrite, Sneaton Halite and Sneaton Potash. EZ5 starts with the deposition of the Sleights Siltstone, which is overlain by the Littlebeck Anhydrite and topped by the Bröckelschiefer. Zechstein sedimentation was ended by the final withdrawal of the Zechstein from the western margin.

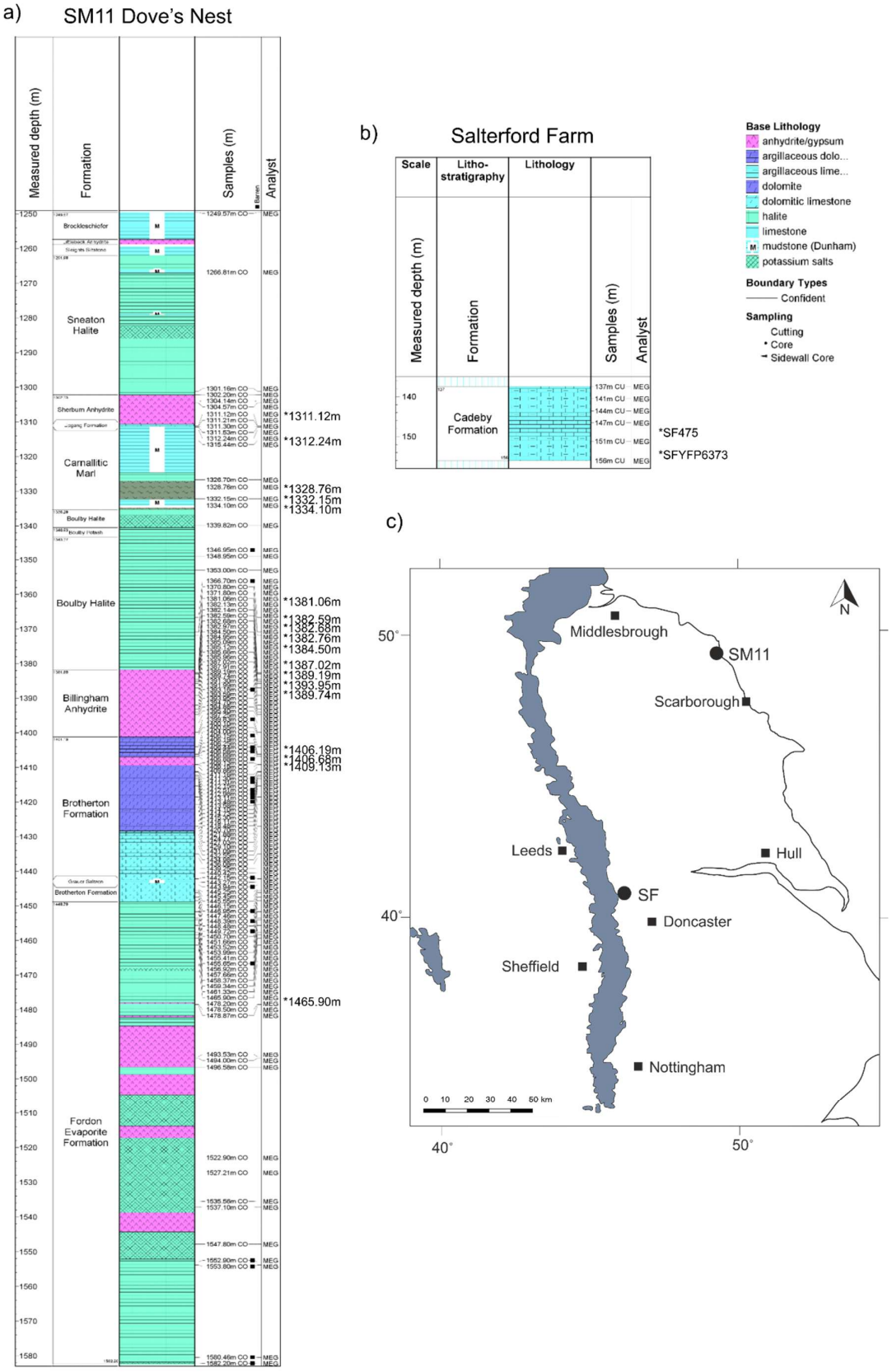

Figure 2. Litholologs for a) SM11 Doves Nest b) Salterford Farm. Samples yielding pollen grains are indicated with an asterisk (*), c) map of northeast England showing the location of the boreholes.

The precise age of the Zechstein deposits in the U.K. is unknown but is generally considered to be Lopingian in age, due to the dating of the Zechstein deposits in Central Germany to between 258-252.3Ma (Menning *et al.* 2005, 2006). Despite the lack of a complete timescale for the British Zechstein, North Sea Sr isotope data suggests the EZ2 evaporites formed at 255 ± 2 Ma (late Wuchiapingian) (Kemp *et al.*, 2016). In addition, Mawson and Tucker (2009) have suggested that the Roker Formation (EZ2Ca) was deposited within 0.3 myr, based of turbidite bed thickness at Marsden Bay, Tyne and Wear, which they correlated with Milankovitch cyclicity. The two boreholes used in this investigation come from close to Scarborough, East Yorkshire (SM11 Dove's Nest) and Nottinghamshire (Salterford Farm). For full lithological descriptions of this material see Appendix F.

10.3.2 Preparation and techniques

Samples (20g) underwent standard palynological HCl-HF-HCL acid maceration and subsequent heavy liquid treatment with zinc chloride ($ZnCl_2$) to separate organic matter. Samples were treated with a saturated aqueous solution of potassium chlorate (KOH) to remove amorphous organic material (AOM). The samples were thoroughly washed after each step and after maceration samples were thoroughly neutralised before proceeding to the next step. After KOH treatment the samples were wet-sieved through 20 µm sieves. Evaporite lithologies were handled according to the method outlined in Gibson & Bodman (2020), whereby samples are dissolved in hot water, boiled in concentrated hydrofluoric acid (40%) for 15 minutes to remove any remaining clastics, then subjected to heavy liquid separation using zinc chloride ($ZnCl_2$) to extract and further concentrate any organic residue

The residue was mounted on glass microscope slides in Petropoxy 154 medium. 200-counts, or an entire slide's worth of palynomorphs, were performed per sample, and the type and frequency of spheroidal inclusions were recorded, along with the host pollen grain species. The slides were analysed under transmitted light and photographed using a QImaging (Model No. 01-MP3.3-RTV-R-CLR-10) camera mounted on an Olympus BH-2 transmitted light microscope in conjunction with QCapturePro software. Additional lower quality, light micrographs were taken using a Meiji Techno Infinity 1-5C camera mounted on a Meiji Techno MT5300H transmitted light microscope in conjunction with InfinityAnalyze software. Light micrographs were resized in the free software GIMP2. Correlation analysis (generalised linear model (GLM)) of spheroidal inclusion abundance was carried out in PAST. Slides, rock and remaining organic residue are curated in the Centre for Palynology at the University of Sheffield, U.K. The dataset used in this chapter can be found in Appendix L and the GLM outputs can be found in Appendix O.

10.4 Results

10.4.1 General Results

Samples were taken at different depths throughout the core material and their palynological content was analysed. Special attention was paid to any pollen grains containing spheroidal inclusions. The stratigraphic range of samples yielding pollen grains with inclusions are illustrated in Figures 2a and 2b. See Table 1 for list of host taxa by sample. Host taxa are illustrated in Plates I-VI.

Between 1 and 8 spheroidal inclusions, sometimes up to 20, were observed inside multiple species of saccate gymnosperm pollen grains. The inclusions were found inside both taeniate and non-taeniate pollen grain species, inside both bisaccate and small monosaccate pollen grains. No inclusions were observed in either rare trilete spores or in the large monosaccate pollen that co-occurred with the bisaccates and small monosaccates in assemblages. Inclusions were occasionally observed within the sacci of pollen grains (Plate I Fig. A, B, G; Plate III Fig. A), but most commonly within the corpus.

The majority of spheroidal inclusions were more or less opaque, solid-looking, bodies with a grainy appearance, darker in colour than their host, with fractures around their circumference (Plate IV Fig. G, J, K, N). The remaining inclusions are comparatively translucent, larger in size, appeared hollow, and were bounded by a distinct membranous-looking wall that was slightly darker than the rest of the inclusion (Plate V Fig. A-C). One example of a chain of inclusions was observed (Plate I Fig. C), and no septate fungal hyphae or conidia were observed. Some instances of clustering were observed where 8 to 20 inclusions were observed within either the corpus (Plate I Fig. C) or sacci (Plate I Fig. B, G; Plate III Fig. A) of pollen grains.

Therefore, two types of spheroidal inclusion can be distinguished (Figure 3). Type I inclusions are small, relatively opaque, and appear as solid sphered within the hosts corpus, with an average diameter of ca. 10-20µm. Type II inclusions appear as relatively translucent, hollow-looking structures bounded by an outer dark rim with an average diameter of ca. 20-30µm. Cluster and chains appear to be of Type I morphology.

The most common pollen grain host species in this study are *Lueckisporites virkkiae* and *Klausipollenites schaubergeri,* with inclusions also present inside *Illinites* spp., *Taeniaesporites* sp., *Protohaploxypinus* sp., the monosaccate *Vestigisporites minutu*s and, on rare occasions, *Falcisporites zapfei, Labiisporites granulatus*, and *Potonieisporites novicus*. It is possible that that taeniate asaccate species *Vittatina hiltonensis* (Plate IV Fig. C) and trisaccate species *Crustaesporites globosus* (Plate II Fig. E) are also hosts but preservation of these two was poor therefore the occurrence of these taxa as hosts as inclusions is uncertain.

Depth (m)	Pollen grain taxa containing inclusions	Type
SM11 Dove's Nest		
1311.30m	*Illinites tectus* (Leschik 1956) comb. nov. Clarke 1965, *Vestigisporites minutus* Clarke 1965, Unidentifiable non-taeniate bisaccate pollen grain	Type I
1312.24m	*Lueckisporites virkkiae* Potonié et Klaus 1954 emend Clarke 1965, *Taeniaesporites novimundi* Jansonius 1962, *T. noviaulensis* Leschik 1956, *T. angulistriatus* (Klaus 1963) comb. nov. Clarke 1965, *Protohaploxypinus jacobii* Jansonius emend Hart 1954, *Klausipollenites schaubergeri* (Potonié et Klaus) Jansonius 1962, *Illinites delasaucei* (Potonié et Klaus) Grebe and Schweitzer 1962, *I. tectus* (Leschik 1956) comb. nov. Clarke 1965, Unidentified bisaccate pollen grain	Type I
1328.74m	*Klausipollenites schaubergeri* (Potonié et Klaus) Jansonius 1962, *Vestigisporites minutus* Clarke 1965	Type I
1382.76m	*Lueckisporites virkkiae* Potonié et Klaus 1954 emend Clarke 1965, Taeniaesporites novimundi Jansonius 1962, *Klausipollenites schaubergeri* (Potonié et Klaus) Jansonius 1962, *Crustaesporites* globosus/*Protohaploxypinus* spp., Unidentifiable bisaccate pollen grains	Type I Type II
1332.15m	*Lueckisporites virkkiae* Potonié et Klaus 1954 emend Clarke 1965, *Klausipollenites schaubergeri* (Potonié et Klaus) Jansonius 1962, *Taeniaesporites novimundi* Jansonius 1962, *Illinites delasaucei* (Potonié et Klaus) Grebe and Schweitzer 1962	Type I
1334.10m	*Lueckisporites virkkiae* Potonié et Klaus 1954 emend Clarke 1965, *Taeniaesporites novimundi* Jansonius 1962, *Protohaploxypinus chaloneri* Clarke 1965, *Klausipollenites schaubergeri* (Potonié et Klaus) Jansonius 1962, *Illinites delasaucei* (Potonié et Klaus) Grebe and Schweitzer 1962, *Falcisporites zapfei* (Potonié et Klaus) Leschik 1956	Type I Type II
1336.70m	*Lueckisporites virkkiae* Potonié et Klaus 1954 emend Clarke 1965	Type II
1370.80m	*Klausipollenites schaubergeri* (Potonié et Klaus) Jansonius 1962, *Vestigisporites minutus* Clarke 1965	Type II
1381.06m	*Lueckisporites virkkiae* Potonié et Klaus 1954 emend Clarke 1965, unidentified bisaccate pollen grain	Type I Type II
1382.59m	*Lueckisporites virkkiae* Potonié et Klaus 1954 emend Clarke 1965, *Klausipollenites schaubergeri* (Potonié et Klaus) Jansonius 1962, *Vestigisporites minutus* Clarke 1965, Unidentifiable bisaccate pollen grain	Type I Type II
1382.68m	*Lueckisporites virkkiae* Potonié et Klaus 1954 emend Clarke 1965	Type I
1382.76m	Detached saccus	Type I Cluster
1384.50m	*Vestigisporites minutus* Clarke 1965	Type II
1385.96m	*Lueckisporites virkkiae* Potonié et Klaus 1954 emend Clarke 1965, *Klausipollenites schaubergeri* (Potonié et Klaus) Jansonius 1962, *Vestigisporites minutus* Clarke 1965, *Falcisporites zapfei* (Potonié et Klaus) Leschik 1956, Unidentifiable bisaccate pollen grain	Type I
1387.02m	*Klausipollenites schaubergeri* (Potonié et Klaus) Jansonius 1962	Type I
1389.19m	*Lueckisporites virkkiae* Potonié et Klaus 1954 emend Clarke 1965	Type I
1389.74m	*Vestigisporites minutus* Clarke 1965	Type II
1393.95m	*Lueckisporites virkkiae* Potonié et Klaus 1954 emend Clarke 1965	Type I
1406.19m	*Lueckisporites virkkiae* Potonié et Klaus 1954 emend Clarke 1965	Type I
1406.68m	Unidentifiable trisaccate	Type I
1409.13m	*Klausipollenites schaubergeri* (Potonié et Klaus) Jansonius 1962	Type I
1465.90m	*Lueckisporites virkkiae* Potonié et Klaus 1954 emend Clarke 1965, *Vestigisporites minutus* Clarke 1965	Type I
Salterford Farm		
SF475	*Lueckisporites virkkiae* Potonié et Klaus 1954 emend Clarke 1965, *Klausipollenites schaubergeri* (Potonié et Klaus) Jansonius 1962, *Illinites delasaucei* (Potonié et Klaus) Grebe and Schweitzer 1962, *Labiisporites granulatus* Leschik 1956, *Potonieisporites novicus* Bhardwaj 1954, *Vestigisporites minutus* Clarke 1965, Unidentifiable bisaccate pollen grain	Type I
(147m)		Type II
		Cluster
		Chain
SFYFP6373 (151m)	Unidentified bisaccate pollen grain (England Finder G/36-G/35) containing a cluster of inclusions	Cluster

Table 1. List of spheroidal inclusions in pollen grains from the Lopingian of northeast England from boreholes SM11 Dove's Nest (Zechstein Cycle 2-4) and Salterford Farm (Zechstein Cycle 1).

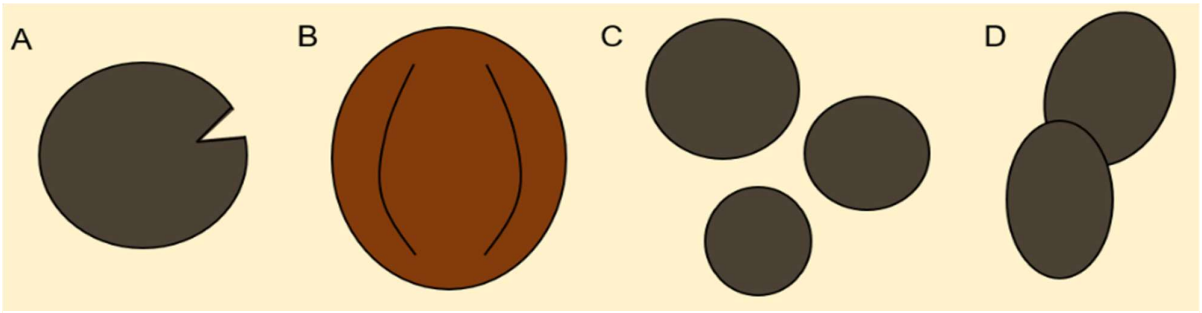

Figure 3. Diagrammatic schematic of the types of inclusions observed A) Type I, B) Type II, C) clyster, and D) chain.

Spheroidal inclusions are most often found inside the most common pollen grains encountered within assemblages, such as *Lueckisporites virkkiae* (59.0%), *Klausipollenites* schaubergeri (45.8%), *Vestigisporites minutus* (43.7%), and unidentifiable bisaccates (40.3%). *Illinites delasaucei* (16.1%), *Taeniaesporites novimundi* (14.1%) are also common hosts. These taxa are all found at high abundances through the SM11 Dove's Nest and Salterford Farm material and are typical Zechstein pollen grain species (Gibson & Wellman 2020).

Spheroidal inclusions appear to be much less common within multitaeniate bisaccate genera, as inclusions were rarely found within the genera *Protohaploxypinus* and *Taeniaesporites.* There therefore appears to be no taxonomic effect. No inclusions were observed inside the taeniate bisaccate genera *Platysaccus*, *Striatoabietites*, and *Striatopodocarpites* and were not observed inside the non-taeniate bisaccate genus *Alisporites*. Inclusions were not observed in large monosaccate genera such as *Nuskoisporites*, and *Perisaccus*, with only one occurrence of an inclusion inside *Potonieisporites novicus* (SF475).

Furthermore, spheroidal inclusions are distinct from non-organic structures inside pollen grains such as pyrite inclusions which appear as distinctly cuboidal structures (Plate I Fig. E, Plate III Fig. B), rather than the regular and spheroidal shape of the inclusions being described here.

10.4.2 SM11 Dove's Nest

In borehole SM11 spheroidal inclusions were found inside 20 of the 126 samples collected, inside the following taxa (percentages are of average host frequency); ?*Crustaesporites globosus* (6.7%), *Falcisporites zapfei* (6.5%), *Illinites delasaucei* (17.8%), *I. tectus* (7.0%), *Klausipollenites schaubergeri* (47.0%), *Lueckisporites virkkiae* (60.9%), *Taeniaesporites angulistriatus* (1.8%), *T. noviaulensis* (3.5%), *T. novimundi* (14.1%), *Protohaploxypinus chaloneri* (10.5%), *P. jacobii* (3.5%), *Vestigisporites minutus* (50.5%), and unidentifiable pollen grains (36.5%) that are either biologically

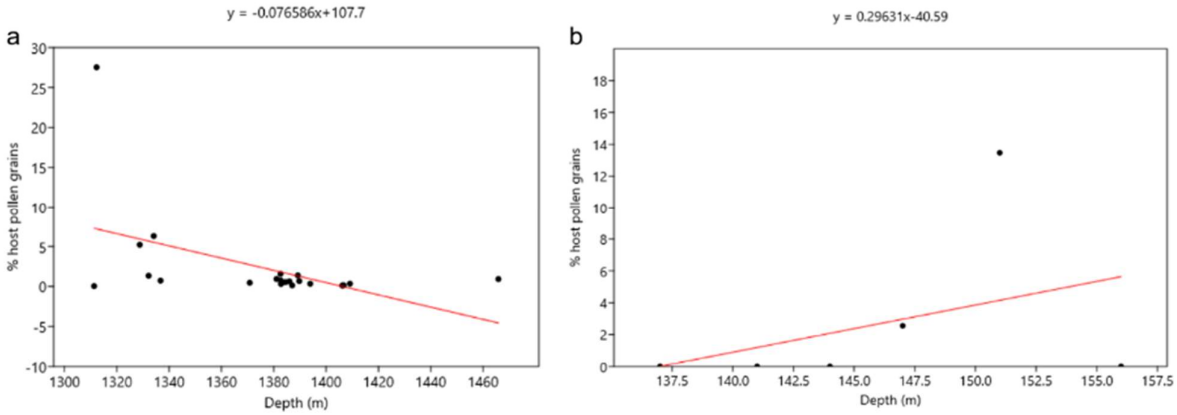

Figure 4. Correlations (GLM) of borehole depth and total percent of pollen grains within assemblages that are hosts to spheroidal inclusions a) SM11 Dove's Nest b) Salterford Farm. The red line marks the trend in abundance.

or mechanically damaged. A cluster (20 inclusions) was only observed inside sample SM11 1382.76m.

Across samples there appears to be a decline in the frequency of spheroidal inclusions with depth ($p=0.01$) (Figure 4a). Inclusions are most common in the Carnallitic Marl Formation where host frequency reaches 27.5% at its maximum in SM11 1332.15m, decreasing to 6.3% in SM11 1334.10m. Figure 5a and 5b illustrates the percentage of pollen grains within assemblages that contain spheroidal inclusions.

Frequency remains low, with minor variation, between 0.5-1.6% until SM11 1389.74m, after which frequency drops below 0.5%. There is a slight increase in frequency to 0.9% at 1465.90m which is the deepest recorded instance of inclusions within the SM11 material. However, this trend is clearly affected by the spike in inclusion abundance observed in sample SM11 1312.24m (Carnallitic Marl Formation) where Type I inclusions occupy 27.5% of pollen grains. Type I inclusions increase significantly up borehole ($p=0.03$) but there is no significant trend in Type II inclusions ($p<0.5$), nor is there a significant trend in the occurrence of clusters ($p>0.5$). Of particular interest are the samples from the Carnallitic Marl which contain the most frequently occurring spheroidal inclusions, with the sample SM11 1312.24m displaying the greatest variety in host taxa with up to 10 species being host observed. *Crustaesporites globosus* is only observed as a host in the Carnallitic Marl Formation in SM11 1328.72m.

10.4.3 Salterford Farm

In Salterford Farm spheroidal inclusions were recovered from 2 out of 6 samples, SF475 and SFYFP6373. Inclusions were observed inside the host taxa *Illinites delasaucei* (12.9%), *Klausipollenites schaubergeri* (35.5%), *Labiisporites granulatus* (3.2%), *Lueckisporites virkkiae* (32.3%), *Potonieisporites novicus* (3.2%), *Vestigisporites minutus* (9.7%), as well as unidentifiable damaged bisaccate pollen grains (3.2-100.0%). The other four samples contained rich palynological assemblages, but no inclusions were observed. Figure 5c and 5d illustrates the percentage of pollen grains within assemblages that contain inclusions. In Salterford Farm (Figure 4b) there appears to be a decline in the number of inclusions up borehole. However, this trend is not significant ($p>0.5$), neither are there significant trends in Type I ($p>0.5$) nor Type II inclusions ($p>0.5$).

Host pollen grains were found to occur at frequencies of between 2.5-13.5% of the total palynomorph assemblage, with spheroidal inclusions being more frequent in the deeper of the two samples. The types of inclusion observed differ between the two samples. In SF475 only one pollen grain was found to contain inclusions, however the inclusions occurred in the form of a cluster of up to 8 inclusions. In sample SFYFP6373, thirty-one inclusions were observed in six host species, with examples of both Type I and Type II inclusions. As in SM11, Type I inclusions were generally more frequent than Type II, with frequencies of Type I of 1.6% in SF475 and 6.5% in SFYFP6373, and 0.0% and 5.2% for Type II respectively.

Clusters were observed in SF475, where a cluster of up to eight Type I spheroidal inclusions was observed inside *Lueckisporites virkkiae* (Plate I Fig. C) and in SFYFP6373 an instance of a cluster inside *Vestigisporites minutus* (Plate I Fig. B), as well as an instance of a possible chain inside *Lueckisporites virkkiae* (Plate I Fig. D). Salterford Farm also provided the only occurrence of *Labiisporites granulatus* and *Potonieisporites novicus* as hosts.

10.4.4 Additional Evidence of Fungal Activity

Additional evidence of fungal activity may be present in the form of pitting on the surface of cuticle (Plate III Fig. B, C), and the instance of small dark opaque spherical bodies on the exterior, or possibly interior, of a detached saccus (Plate III Fig. A). There are no observed examples of septate fungal hyphae entering or extending from the pollen grains. However, it is not possible to distinguish the effects of fungal degradation from other biological degrading organisms such as bacterial.

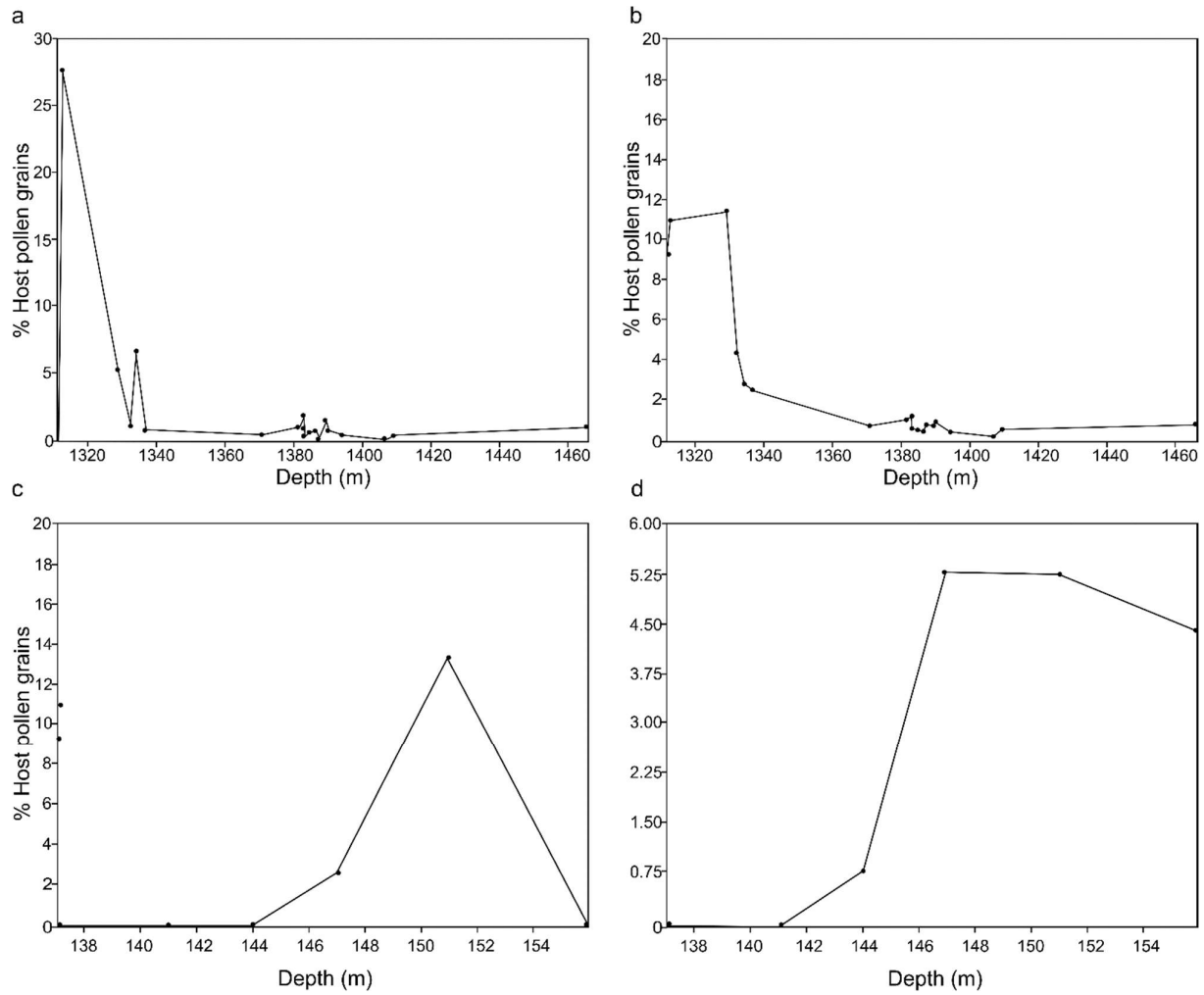

Figure 5. Proportion of host pollen grains per assemblage A) SM11 Dove's Nest absolute % b) SM11 Dove's Nest 3-sample average c) Salterford Farm absolute percent d) 3-sample average.

10.5 Discussion

10.5.1 Rarity of inclusions

The preservation of internal contents in dispersed pollen is rare, particularly in Palaeozoic material, with internal contents only being preserved during exceptional circumstances e.g., in Miocene evaporites (Durska 2016, 2017, 2018). The pollen in the assemblages described here is preserved as the exines of dispersed microspores where the innermost wall layer, the intine, is absent (Traverse 2007). Due to the dispersed nature of the assemblage little is known about the microgametophyte structure and development of the plants that produced these pollen grains, as well as about the organisms that used the pollen as a source of nutrition or habitat. Most of this documentation comes from permineralised pollen grains preserved in chert or coal ball matrix (e.g., Millay & Eggert 1974; Nishada *et al.* 2003). Dispersed pollen grains containing any sort of internal structures are therefore

important for enriching our understanding of the biology of ancient pollen, the reproduction of ancient plants, and the relationships with any organisms that inhabited them. This is important for the Euramerican vegetation which is understudied in comparison to the neighbouring Gondwanan vegetation during the Lopingian.

The abundance of spheroidal inclusions varies per assemblage. Inclusions are most abundant in the Marl Slate and Cadeby Formation in Salterford Farm and in the Carnallitic Marl Formation of SM11. These strata contain well-preserved, speciose, palynomorph assemblages (Gibson & Wellman 2020) with pollen grains preserved with minimal lateral compression. Therefore, the high abundance of spheroidal inclusions observed within these samples is likely a preservational effect. It may also be a reflection on the suitability of the contemporary environment for fungal activity as the upper Zechstein climate was more humid (Słowakiewicz *et al.* 2009), compared to the arid-humid cyclotherm climate of the lower Zechstein. The environment of the Marl Slate was similarly humid, being deposited during the initial transgression of the Zechstein Sea, conditions ideal for fungal proliferation (Harrison *et al.* 1994).

Variation in the abundance of spheroidal inclusions may well be an effect of preservation bias related to changes in depositional setting resulting in greater or fewer pollen grains being colonised by microorganisms. Both Marl Slate and Carnallitic Marl Formations are transgressive units known to have high preservation potentials. The Marl Slate is a bituminous black shale deposited in an anoxic environment and the Carnallitic Marl Formation is a hygroscopic saline marl also deposited under anoxic conditions. These are ideal conditions for preserving palynomorph assemblages well.

10.5.2 Potential host preference

Although it appears that spheroidal inclusions are correlated with the most frequent palynomorphs within assemblages and influenced by preservational effects, there does appear to be some bias against the multitaeniate pollen host taxa *Striatoabietites*, *Striatopodocarpites*, *Platysaccus*, and *Protohaploxypinus*, with one recorded instance of an inclusion inside *P. chaloneri* in SM11 1334.10m and one inside *P. jacobii* in SM11 1312.24m. In addition, *Vittatina hiltonensis*, a distinct Euramerican palynomorph of glossopterid affinity was not confidently recorded as a host.

These multitaeniate pollen grain taxa have a botanical affinity with the Pteridosperms e.g., *Protohaxploxypinus* s.str. which is closely associated with *Glossopteris* (Potonié & Schweitzer 1960; Pant & Nautiyal 1960), and *P. cancellatus* and *Striatopodocarpites cancellatus* have been recovered from an *Arberiella* sporangium (Lindström *et al.* 1997). Perhaps the inclusions do not find glossopterid pollen grains suitable hosts, instead preferring the pollen grains of conifers such as

Illinites, *Lueckisporites* (Clement-Westerhof 1987; Gibson *et al.* 2020), and *Taeniaesporites*. The multiple anastomosing taeniae may present a sufficient barrier to corpus occupation while pollen grains with fewer or no taeniae may be easier to colonise when damaged or accessed through their aperture. *Alisporites* was not observed to host inclusions and has been associated with peltasperms, podocarp, and voltzian conifer cones (Balme 1995), but may also be aligned with glossopterids (Lindström & McLoughlin 2007). Meanwhile, the possible host taxon *Potonieisporites* has been linked to coniferophytes (Balme 1995; Taylor *et al.* 2009).

Unfortunately, certain frequent host taxa have yet to be assigned to a macroflora taxa, such as *Klausipollenites schaubergeri* and *Vestigisporites minutus*. Therefore, a preference solely for coniferous pollen grains cannot be confidently determined. Furthermore, the absence of modern analogues for glossopterid flora and multitaeniate pollen grains means the viability of multitaeniate pollen grains cannot be directly assessed.

The absence of spheroidal inclusions inside large monosaccate genera such as *Nuskoisporites* and *Perisaccus* may suggest that corpus volume is not the most significant factor for host preference. If corpus volume was a significant factor, a higher frequency of these genera as hosts would be expected. However, as these are dispersed assemblages there is likely a transport and/or preservational size sorting against large monosaccate. Thus, without this large size fraction of the population present for analyses they cannot be disregarded as potential hosts and corpus volume cannot be excluded as a significant factor.

10.5.3 Discounting a non-fungal affinity

The spheroidal inclusions described in this study are morphologically similar to those described from the Permian coalfields of India (Jha 1985; Vijaya & Meena 1996; Meena 1999; Tiwari & Kumar 2002; Aggarwal *et al.* 2015). Out of these studies only Vijay & Meena (1996) and Aggarwal *et al.* (2015) attempt to address the nature of these structures. Vijay & Meena (1996) described inclusions occurring inside taeniate and non-taeniate bisaccate gymnosperm pollen grains from the Upper Permian of the East Raniganj Coalfield. They termed the inclusions ‘bodies’ or ‘corpuscles’ and they were observed to occur in clusters of up to seven. They are opaque, circular to oval in shape, and range from 15-40µm in diameter exhibiting irregular cracks at their circumference. It was suggested that the inclusions represent coagulated cytoplasm, fungi, or stages in the development of the microgametophyte. Coagulated cytoplasm was disregarded based on the occurrence of inclusions as clusters and a fungal affinity was disregarded due to the lack of associated hyphae. The authors

concluded therefore that the inclusions represent components or stages in the development of the microgametophyte.

Aggarwal *et al.* (2015) studied saccate pollen grains from the Lopingian and Guadalupian of India from the Godavari Graben (Andhra Pradesh, India). The authors also ruled out coagulated cytoplasm as their spheroidal inclusions were too regular and clustered. However, their inclusions occurred infrequently throughout their section, were not evenly distributed throughout, and their inclusions were hollow and bounded by a wall. Their interpretation was that the inclusions did not represent a stage in the development of the microgametophyte. Instead, the authors concluded spheroidal inclusions represented pollen-colonising microorganisms, possibly a chytrid or member of the Hypochytridiomycota.

The inclusions observed here are of comparable dimensions and morphology to the fungal bodies frequently observed inside pollen grains from cherts in Antarctica (S. McLoughlin pers. comm.). Published examples of fungus from the Permian and Triassic of Antarctica have focused on cherts preserving fungal bodies inside cells, and a few examples of inclusions inside the pollen corpus have been recorded (Slater *et al.* 2015; Harper *et al.* 2016). These inclusions also occurred infrequently throughout the section at varying abundances.

No circular openings in the wall of the inclusions have been observed, as in Aggarwal *et al.* (2015) who reported that 30% of inclusions possessed such an opening, only what may be a tear in the inclusion wall (Plate 5 Fig. Ai). The circular openings were interpreted as either pre-formed discharged pores of saprotrophic or parasitic Chytridiomycota microfungi, or as the attachments site of a discharge tube or subtending hyphae. The absence of such features within the samples of this study could reflect the development stage of the fungal inclusion or a taxonomic feature of the inclusions or could be evidence against a fungal affinity. Based on the morphological evidence the spheroidal inclusions are interpreted as representing the remains of a pollen-colonising organism, a member of the Chytridiomycota or Hypochytridiomycota.

10.5.4 Effects of processing

This study contains a mix of spheroidal inclusion types as observed in other studies. As in Vijay & Meena (1996), this study is dominated by more opaque Type I spheroidal inclusions which suggest they represent solid bodies. As in Aggarwall *et al.* (2015) a second translucent type is present (Type II). Aggarwall *et al.* (2015) interpreted all the inclusions as being hollow structures bounded by a distinct wall and that the differences in opacity of the inclusions are artefacts of the maceration process. It is possible that small spheres bounded by a distinct wall that occur within pollen grains

are not normally reached by the macerating chemicals which have not penetrated deep enough into the pollen grain. As different host species will macerate differently, especially taeniate compared to non-taeniate pollen grains, the degree of opacity following maceration will vary depending on the developmental stage of the inclusion, the integrity of the inclusion wall, and consistency of any organic material within the inclusion.

There is some variation in the colour of pollen grains and the spheroidal inclusions which is likely an effect of diagenesis, original quality of the pollen grains, and taxonomic differences in the penetration of macerating chemicals. For example, in Plate III a variety of pollen grain colour can be seen from almost hyaline (Plate III Fig. D) to a dark brown-black colour (Plate III Fig. M). Some of the opaque inclusions may also be biomimetic structures (e.g., the fuzzy material inside pollen grains in Plate I Fig. A-G), the result of authigenic minerals such as carbonates that have accumulated within hollow inclusions. Aggarwall et al. (2015) suggested that authigenic precipitation may be initiated by anaerobic sulphate reducing bacteria (Klymuik *et al.* 2013), which aligns with the heterogeneric anoxic conditions and chemical signatures of sulphate reducing bacteria along the western margin of the Zechstein Sea (Słowakiewicz *et al.* 2015, 2016).

10.5.5 The PTB "fungal-spike"

A fungal spike has been associated with the End Permian Mass Extinction (EPME), based on the controversial biological proxy for environmental crisis; *Reduviasporonites*. Proliferation of this species coincides with mass extinction and a number of geochemical disturbances. *Reduviasporonites* is controversial because it was originally assigned to fungi (Elsik 1999; Foster *et al.* 2002; Sephton *et al.* 2009) and proposed to have opportunistically exploited the vegetation die off at the end of the Permian causing a proliferation in wood-decaying fungi (Visscher *et al.* 2011; Hochuli *et al.* 2016). However, geochemical data has been used to suggest it is algal in origin with algal blooming possibly being indicative of widespread ponding and the swamping of rivers during end-Permian times (Afonin *et al.* 2001). Yet, the resounding consensus is that it is fungal rather than algal.

A "fungal spike" is typically expressed as mass occurrences of *Reduviasporonites* (sometimes up to 95% of assemblages) (Vajda & McLoughlin 2004; Lei *et al.* 2013). However, in this material the abundance of *Reduviasporonites* never surpassed 8.5% of the assemblage. While it does not appear that the "fungal spike" is observed in this material other kinds of fungal activity may be present if the spheroidal inclusions are indeed of a fungal nature. Evidence of fungal activity near the PTB, that is not associated with Reduviasporonites, has important implications for ecosystem

reconstructions. The infrequent occurrence of spheroidal inclusions, if of a fungal affinity, would not support a PTB "fungal spike".

10.5.6 Implications for the Zechstein environment

In modern ecosystems fungi routinely use pollen grains as a substrate, many of which are known to produce globose sporangia within their host, especially members of the Chytridiomycota, including *Entophylyctis variabilis* (Aggarwall *et al.* 2015), *Olipidium longicollum* (Sekimoto *et al.* 2011), and the Hypochytridiomycota e.g., *Hypochytrium catenoides* (Barr 1970). The presence of fungi as part of the Zechstein ecosystem is not surprising, yet it begs further questioning of the details of ecosystem function.

The association of these inclusions with putative chytrids is difficult to resolve due to the absence of evidence of host responses e.g., responses in vegetative tissues such as local necroses, not recognisable due to the fragmented nature of plant cuticle and tracheids preserved alongside the palynomorphs, and the dispersed nature of the assemblages, and no *in situ* examples. It is not possible in this instance to distinguish host responses from post-mortem decay or transport damage and in pollen grains it is not possible to distinguish any possible damage caused by the fungus from disintegration during pollen grain transport to the site of deposition or from other types of biological degradational.

If the putative chytrids occurring inside the corpus of pollen grains colonized their hosts while the pollen grains were still viable, then these associations would represent degrees of parasitism. This seems to be a reasonable interpretation as viable pollen grains are habitats for parasitic microfungi and were available in great abundance during the Lopingian. However, in the lack of conclusive evidence of any host responses of structural alterations or modification, which would be indicative of a parasitic relationship, it is impossible to distinguish fossil parasites from saprotrophs, which would have colonised and used the dead organic matter within pollen grains as a carbon source (Dix & Webster 1994). It is plausible that these inclusions represent saprotrophic microfungi, however there is no evidence of callosities, which would be evidence of a specific response of a viable host to parasitism (Hass *et al.* 1994).

Unfortunately, in the absence of cherts, greater insights on the morphology, life history, spatio-temporal distribution, and diversity of microfungi cannot be consistently discerned, as has been possible with the Rhynie palaeoecosystem.

10.6 Conclusions

The ability to track microbial diversity and interactions with other organisms through time based on already well-studied and documented terrestrial biotas represents an important database that needs completing in order to reflect properly on changes in ecosystem functioning. This contribution focusing on British Lopingian material is an initial step towards a comparison with other contemporaneous ecosystems e.g., other parts of the Zechstein basin, and modern analogues.

The Lopingian in particular is important to understanding fungal dynamics during an Icehouse-Hothouse climate transition as well as dynamics preceding the PTME. Fungal dynamics across the P-T boundary are heavily debated due to the controversial nature of the "fungal spike" palynomorph *Reduviasporonites*. The evidence presented here is independent of this controversy, yet the low abundances of the spheroidal inclusions does not necessarily support the "fungal spike" hypothesis.

Nevertheless, this contribution adds dimensionality to environmental reconstructions of the Lopingian of the U.K. It shows how it is imperative to expand the targets within palynological analysis beyond logging the abundance of spores and pollen grains. It highlights the need to re-log historical slide collections to identify spheroidal inclusions to compensate for previous biases in the literature. This study shows that standard palynological preparations, not just non-chert, coal, and evaporative lithologies, still have value when it comes to the study of internal spore-pollen grain structures.

Based on previous reports these spheroidal inclusions are interpreted as representing a pollen-colonising organism of possibly chytrid affinity. If the interpretation of these inclusions as fungus is correct, then the shifting proportions of inclusions in fossil pollen grains that has been observed in the Zechstein Group may be related to shifts in depositional environment resulting in varying proportions of pollen grains being colonised by microorganisms. Furthermore, the observed bias towards small, non-taeniate pollen grains may be related to the taxonomic nature of pollen grains and their botanical affinity to conifers. To the best of the author's knowledge, endobiotic fungus has not been documented from British Euramerican Lopingian pollen grains before. Therefore, this study provides new insights into Euramerican ecosystems. As the majority of reports focus on Gondwanan occurrences, this study helps correct bias within the publication record.

Acknowledgements

MEG was funded by a NERC studentship through the ACCE (Adapting to the Challenges of a Changing Environment) Doctoral Training Partnership [Award Reference 1807541].

Plate Descriptions

Plate I. Spheroidal Inclusions from Salterford Farm samples SF475 and SFYFP6373. P=pyrite crystal, Ch=chain. Images taken at x100 magnification. Scale bar 50µm.

A. Type I spheroidal inclusions possible within the corpus or right sacci of a bisaccate pollen grain (possibly *Labiisporites granulatus*), the folding and three-dimensional preservation makes it hard to determine (SF475 T47/3)
B. Cluster of Type I spheroidal inclusions inside the sacci of *Vestigisporites minutus* (SF475 Q34/4)
C. Cluster of Type I spheroidal inclusions inside the corpus of *Lueckisporites virkkiae*, note how different the non-organic material trapped inside the left saccus looks compared to the round inclusions (SF475 H30/4)
D. Possible chain of Type I spheroidal inclusions inside the corpus of a taeniate bisaccate (possibly *Lueckisporites virkkiae*) (SF475 R29/3)
E. Possible spheroidal inclusions alongside cuboidal pyrite crystals inside an unidentifiable, possibly taeniate, bisaccate pollen grain (SF475 O39/1)
F. Cluster, or possible chain, of spheroidal inclusions inside the corpus of a bisaccate pollen grain (SFYFP6373 G36)
G. Possible Type I spheroidal inclusion cluster, combined with biogenic or non-organic material inside the corpus and sacci of a bisaccate pollen grain (SF475 T47/3)

Plate II. Well-preserved examples from SM11 Dove's Nest. Figures A-D taken at x100 magnification. Figure E taken at x40 magnification. Scale bar (1-4) 50µm, (5) 100µm.

A. Type I spheroidal inclusion inside *Illinites delasaucei* (SM11 1312.24m U33/2)
B. Type I spheroidal inclusion inside *Lueckisporites virkkiae* (SM11 1312.24m S33/2)
C. Type I spheroidal inclusion inside *Labiisporites granulatus* (SM11 1382.14m L39)
D. Type I spheroidal inclusion inside *Taeniaesporites noviaulensis* (1312.24m ox2 D44/3)
E. Possible inclusion inside Crustaesporites globosus (SM11 1334.10m ox #90 x40)

Plate III. Evidence of spheroidal inclusions associated with sacci and vascular plant cuticle. P=pyrite crystal. Figures A & C taken at x100 magnification. Figure B taken at x40 magnification. Scale bar (1) 50µm, (2,3) 100µm.

A. Detached saccus of a bisaccate pollen grain containing ~20 Type I spheroidal structures of varying size (SM11 1328.76m J35/2)
    i. Focusing on the central spheroidal inclusions
    ii. Focusing on the marginal spheroidal inclusions
B. Possible Type I spheroidal inclusions on gymnospermous vascular plant cuticle (SF475 W34/1)
C. Cuticle with spheroidal inclusions (SF475 coordinate unknown)

Plate IV. Spheroidal inclusions observed within SM11 Dove's Nest. Taken at x40 magnification (while logging slides for quantitative analysis). Scale bar (1-5, 7-9, 12-15) 50µm, (6, 11) 75µm, and (10) 30µm.

A. Type I spheroidal inclusion inside *Illinites* spp. (SM11 1334.10m #44 x40)
B. Type II spheroidal inclusion inside *Illinites delasaucei* (SM11 1334.10m ox2 #8 x40)
C. Type I spheroidal inclusion inside *Vittatina hiltonensis* (SM11 1334.10m ox4 #11 x40)

D. Type I spheroidal inclusion inside ?*Cycadopites* (SM11 1328.76m ox2 #7 x40)
E. Type II spheroidal inclusions inside *Labiisporites granulatus* (SM11 1334.10m #67 x40)
F. Type I spheroidal inclusion inside *Taeniaesporites noviaulensis* (SM11 1334.10m ox2 #91 x40)
G. Type I spheroidal inclusion inside *Klausipollenites schaubergeri.* Arrow indicates the fractured right margin (SM11 1334.10m ox2 #72 x40)
H. Type II spheroidal inclusion inside Illinites spp. (SM11 1334.10m ox2 #68 x40)
I. Type II spheroidal inclusions inside Illinites spp. (SM11 1334.10m ox3 #65 x40)
J. Possible Type I inclusion inside taeniate bisaccate. Arrow indicates a marginal fracture (SM11 1334.10m ox4 #90 x40)
K. Possible Type II inclusion inside taeniate bisaccate. Arrow indicates a marginal fracture (SM11 1334.10m ox3 #53 x40)
L. Possible Type II inclusion inside *Vestigisporites minutus*. Arrow indicates a marginal fracture (SM11 1334.10m ox #61 x40)
M. Type I inclusion inside ?*Lueckisporites* virkkiae (SM11 1389.74m #5 x40)
N. Type I inclusion inside *Taeniaesporites* spp. (SM11 1465.90m ox #7 x40)
O. Type II inclusion inside *Lueckisporites virkkiae* (SM11 1381.06m ox #1 x40)

Plate V. Enlarged examples of well-preserved spheroidal inclusions. Figures a) for each example focuses on the proximal surface of the pollen grain to show that the inclusion is underneath the exine, while figures b) focus on the actual spheroidal inclusion surface. Taken at x100. Scale bar 25µm.

A. Type II inclusions inside *Lueckisporites virkkiae* (SM11 1328.76m Q45/1).
    i. Focusing on the surface of the pollen corpus showing how the inclusion is beneath the proximal face of the exine.
    ii. Focusing on the folded Type II spheroidal inclusion. Arrow points to a possible fracture or opening on its surface.
B. Type II inclusion inside *L. virkkiae* (SM11 1328.76m U45/1).
    i. Focusing on the proximal taeniae on the pollen grain corpus.
    ii. Focusing on the surface of the Type II spheroidal inclusion. Arrow points to a fold on the inclusion.
C. Type II inclusion inside *L. virkkiae* (SM11 1328.76m V43).
    i. Focusing on the surface of the pollen corpus.
    ii. Focusing on the Type II spheroidal inclusion.

Plate VI. Enlarged examples of well-preserved spheroidal inclusions from SM11 Dove's Nest. Figures a) for each example focuses on the proximal surface of the pollen grain to show that the inclusion is underneath the exine, while figures b) focus on the actual spheroidal inclusion surface. Figure A & B taken at x100 magnification. Figure C taken at x100 magnification. Scale bar (1) 25µm, (2) 30µm and (3) 10µm.

A. Type I inclusion inside *Illinites* spp. (SM11 1332.15m ox V42/2)
    i. Focusing on the sacci and proximal face of the pollen grain corpus
    ii. Focusing on the Type I spheroidal inclusion within the pollen grain corpus
B. Type II inclusion inside *Taeniaesporites* spp. (SM11 1328.76m R44/3)
    i. Focusing on the taeniae on the proximal surface of the corpus
    ii. Focusing on the folded Type II spheroidal inclusion within the corpus. Arrow points towards a longitudinal fold in the inclusion.
C. *Lueckisporites virkkiae* with 4 large and 2 smaller Type I inclusions. The 2 left-most inclusions (indicated by arrows) can be seen to push up against the exine creating a bulge.

Plate I

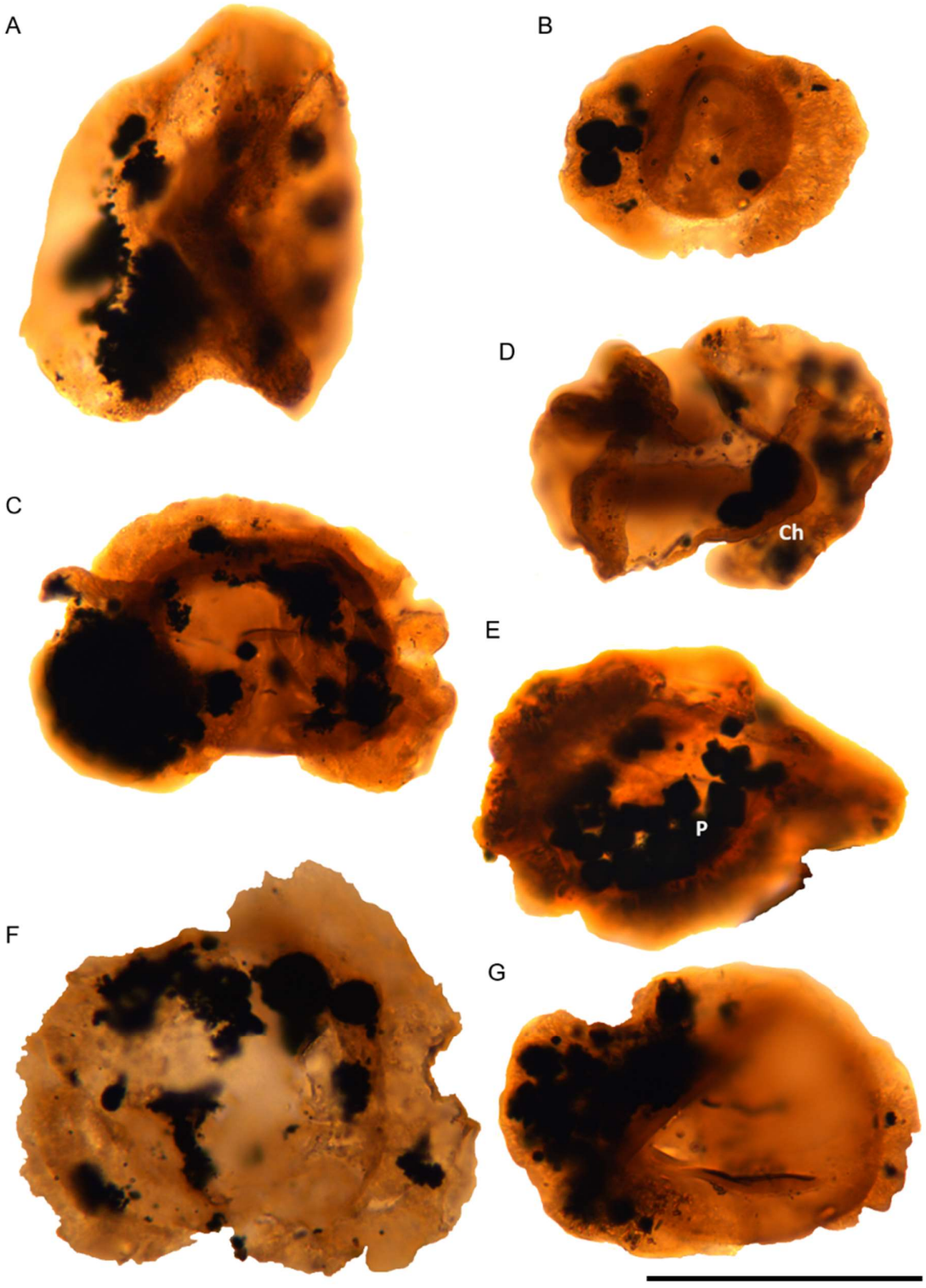

Plate II

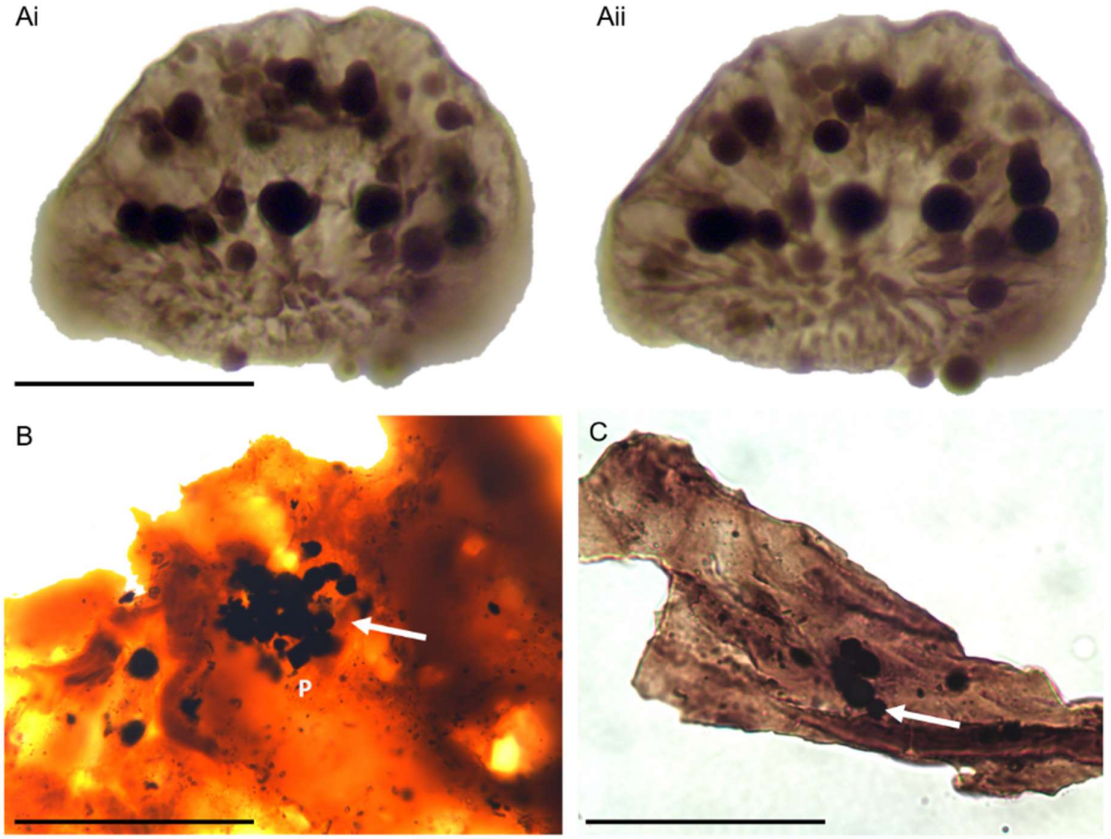

Plate III

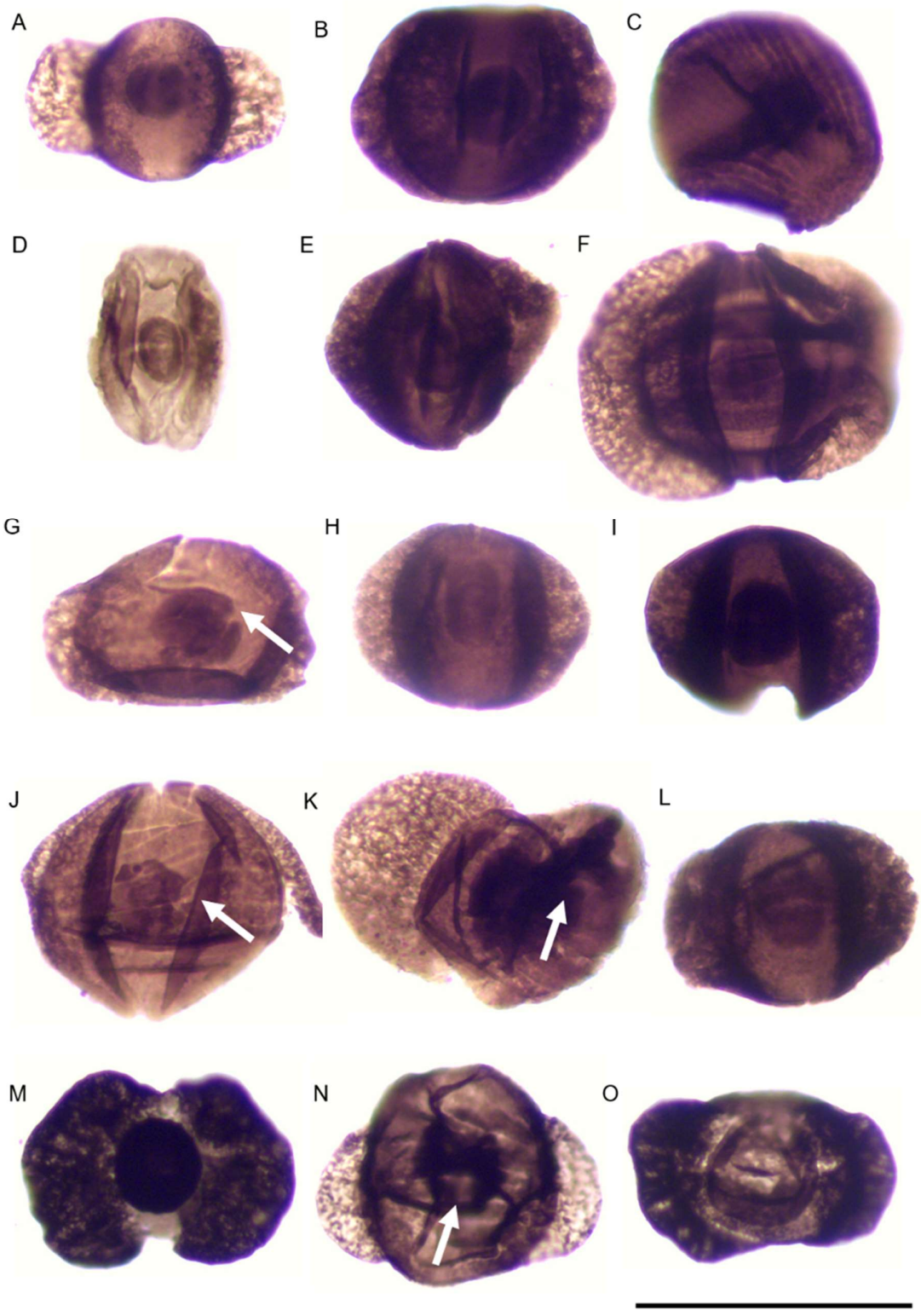

Plate IV

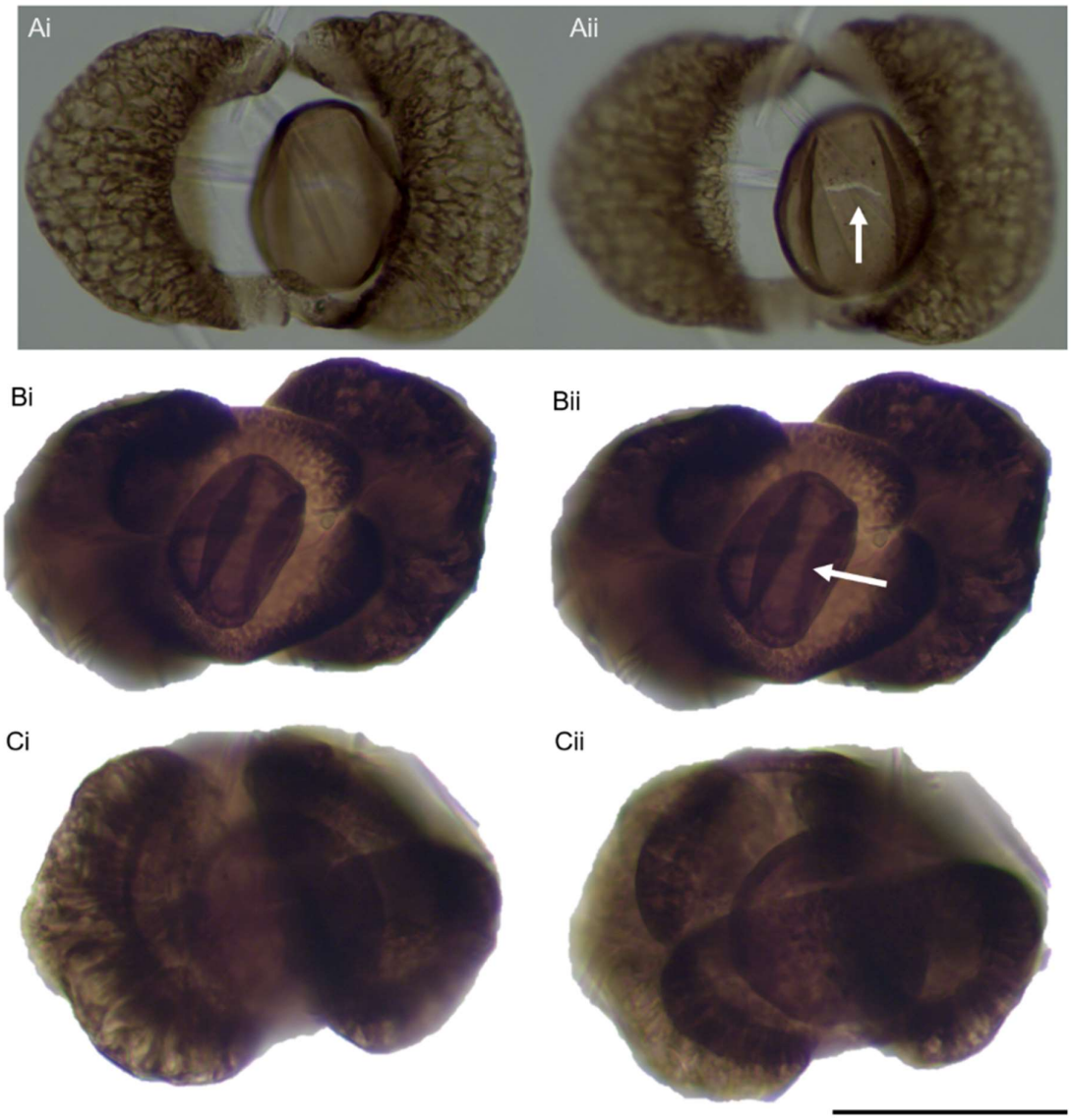

Plate V

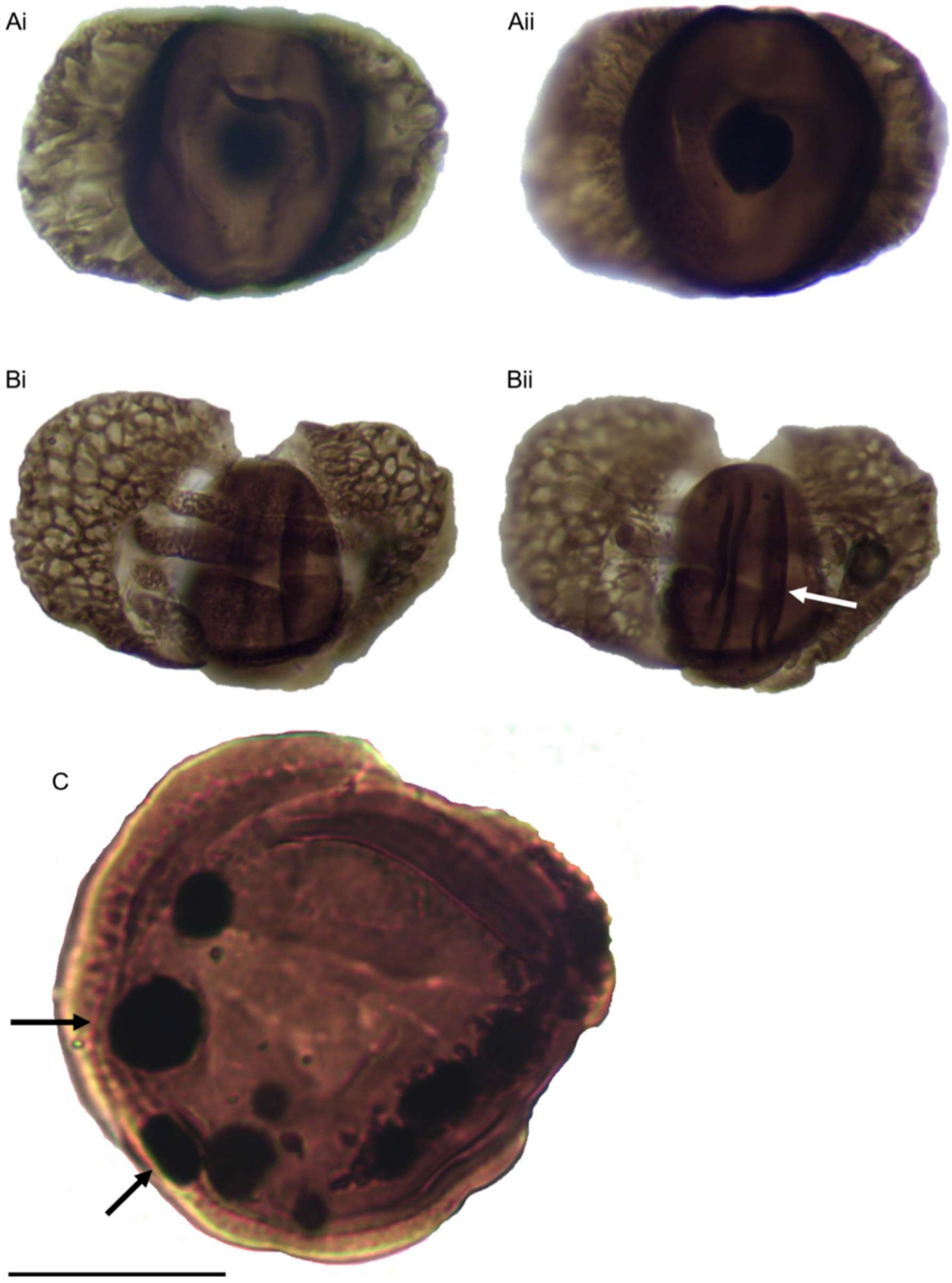

Chapter 11. Conclusion

Chapter 5: Palynological results

- Pollen-dominated assemblages were recovered from the entire Zechstein Group, from all five cycles. They were previously not recovered past Cycle 2, making this the highest resolution analysis of Zechstein Group palynology.
- Assemblages are dominated by the taeniate bisaccate pollen of conifer and pteridosperm affinity e.g., *Lueckisporites virkkiae*, *Protohaploxypinus, Striatoabietites, Striatopodocarpites, Taeniaesporites* representing inland conifer-pteridosperm forests.
- Non-taeniate bisaccates were also common e.g., *Alisporites, Illinites, Klausipollenites*, *Labiisporites* etc. as well as the small monosaccate *Vestigisporites minutus*, while large monosaccate pollen e.g., *Nuskoisporites* and *Perisaccus* were scarce.
- Spores of lycopsids and bryophytes, the fungi *Reduviasporonites*, acritarchs and foraminiferal test linings were rare, scattered intermittently throughout the sequence.
- The dominance of an inland conifer-pteridosperm flora throughout assemblages may reflect the true nature of the flora as the macrofossil record suggests. However, distinguishing an inland or coastal vegetation presence is hampered by the paucity of known pollen grain-parent plant associations, a poor understanding of their reproductive strategies and outputs, as well as the poor preservation potential of certain coastal pollen grain taxa e.g., horsetails.
- Throughout the sequence conifer and peltasperm pollen dominate both high- and low-productivity assemblages.
- The only observed difference between the Yorkshire and Durham Sub-basin assemblages are differences in the relative abundance of taxa.
- The composition of assemblages remains relatively unchanged throughout the sequence confirming the suspected uniformity of the flora across the Zechstein Basin.
- With no evidence of reworking the Zechstein falls within one palynomorph biozone.
- The abundance of Unidentifiable pollen grains is evidence of a vegetated landscape in the absence of any other evidence. Omitting this class may have led to the inappropriate designation of a barren landscape.
- The assemblages from the Carnallitic Marl Formation of the Cycle 3-Cycle 4 boundary were exceptionally well-preserved illustrating the diversity and abundance of the flora in the fluvial landscape of upper Zechstein.
- The palynological data was interpreted at two temporal scales: a long-term trend of impoverishment both in terms of abundance and species richness throughout the entire

Zechstein sequence, and short-term changes within cycles that may reveal the responses of vegetation to the patterns of drastic climate and environmental changes that accompanied the cycles.

- Long-term changes are likely to be a reflection on climate and environmental changes during the Lopingian. No significant trend were observed other than the impoverished assemblages of highly degraded pollen in Cycle 5 which are likely a result of aqueous transport from upland areas to the site of deposition via the fluvial system of the Upper Zechstein.
- Minor changes in abundance are difficult to disentangle from taphonomic effects which are prominent both in the carbonate and evaporite phases, evidenced by the varying abundance of "Unidentifiable" pollen grains throughout the sequence.
- The temporal extent of the palynomorph assemblages suggests that the gymnospermous flora persisted throughout the course of Zechstein deposition, implying a more productive landscape that experienced more precipitation and less harsh environmental conditions than previously assumed.

Chapter 6: Environmental interpretation

- The uniformity of assemblages suggests there was no significant vegetation turnover, implying the vegetation did not undergo a gradual decline preceding the Permian-Triassic mass extinction and vegetation loss was instead rapid and catastrophic.
- Vegetation inhabited the hinterlands despite extreme global climate changes. Perhaps the shift to a humid depositional system after Cycle 3 acted as a buffer, allowing the inland conifer-pteridosperm vegetation to persist.
- The persistence of the gymnospermous flora may reflect their suitability to semi-arid conditions via xerophytic adaptations as well as their regeneration and recovery capabilities following disturbance and deforestation.
- The lycopsid "spore spike" observed in PTB studies, as well as during other environmental catastrophes, is absent here suggesting pteridophytes did not achieve the short-term high abundances characteristic of PTB floristic changes during Zechstein times and is further evidence for a lack of severe environmental or climatic change.
- *Reduviasporonites* was not observed in mass occurrences which are typical of local changes in depositional setting such as "ponding", yet there is no evidence of this in the Zechstein landscape. Their association with brackish environments and continual recovery throughout the sequence concurs with the interpretation of the Zechstein environment presented here.

- The lack of significant composition changes in the Zechstein flora suggests that the change to a pteridophyte dominated flora occurred following the PTME.
- The Zechstein flora may be used as a realistic model for future change especially for low diversity gymnospermous flora of semi-arid climate such as those in the Mediterranean.

Chapter 7: Evaporite palynology

- Development of a method for extracting palynomorphs from Zechstein evaporites facilitated the sequence-wide palynological analysis of the British Zechstein Group.
- Processing the evaporites emphasized the importance of high-resolution sampling through evaporites to combat the high mobility of salt which causes mixing within halite units.
- An apparent reverse thermal maturity profile through the sequence was observed following Palynomorph Darkness Index (PDI) analysis of non-taeniate bisaccate pollen grains.
- Two types of preservation were observed yet XRD analysis revealing no obvious mineralogical causes of darkening. The two types are most likely a result of intact hyaline pollen grains being suspended in bottom stagnant anoxic waters for a long time before being encapsulated in salt, with dark intact pollen grains becoming oxidized in the carbonates or darkened because of the thermal conductivity through the surrounding evaporites.
- This method will be applicable to other ancient saline giant, other evaporite systems, and the more recent extreme terrestrial environments such as acidic hypersaline lakes which are used as terrestrial analogues for the Martian surface and subsurface.

Chapter 8: Wall-ultrastructure and development in *Lueckisporites virkkiae*

- *Lueckisporites virkkiae* is a typical Zechstein palynomorph and a "bridging taxon" that is found across phytogeographical provinces, is a protosaccate bitaeniate bisaccate occurring in three variants in British Zechstein material.
- *L. virkkiae* has as not been assigned a botanical affinity which hinders its biostratigraphic utility and use in reconstructions of the Euramerican flora. It is not known whether the Variants represent a natural grouping or whether they are examples of convergent evolution among conifer and pteridosperm pollen grains.
- All three of Clarke's *L. virkkiae* variants exhibit similar wall ultrastructure which is characterized by an alveolar infratectum and homogenous endexine. This similarity in basic morphology suggests all variants belong to a single taxon likely being produced by the same parent plant group

- Morphological differences are attributed to the effects of harmomegarthy with different variants representing different levels of pollen hydration prior to discharge, with the tentative progression from Variant B – Variant C – Variant A based on the saccus overlap-offlap ratio
- Comparisons with known fossil and extant bisaccate pollen shows how *L. virkkiae* shares gross structural and wall ultrastructural features with modern coniferous pollen.
- Such comparisons are hindered by the absence of extant taeniate bisaccate pollen grains which could form the basis for comparing natural variation and the development of taeniae.
- Co-occurrence data suggests that *Pseudovoltzia liebeana* (Majonicaceae) may be a possible parent plant, supported by reports of other members of Majonicaceae in the fossil record.
- *L. virkkiae* has previously been used to erect biozones for the Lopingian of Europe, being adopted in the subsequent literature without questioning the ecology of the species or the ontogeny of the pollen grain.
- With the variants of *L. virkkiae* concluded to be harmomegarthic morphs and not naturally distinct, biostratigraphical zonation derived from *L. virkkiae* palynodemes or variants is strongly discouraged.

Chapter 9: Endobiotic fungus

- This is the first report of endobiotic fungus from the British Euramerican Lopingian, providing new insights into ecosystem functioning and nutrient cycling, countering some of the bias for Gondwana in the literature.
- Spheroidal inclusions were observed within the corpus and sacci of bisaccate pollen grains and may have an affinity with the Chytridiomycota or Hypochytridiomycota based on comparisons with similar structures previously described from the Permian of India and Antarctica.
- An affinity based solely on morphological observations is difficult to resolve in the absence of evidence of host responses which are not possible to distinguish from postmortem decay or transport damage. However, it is unlikely that they represent a component or stage in the development of the microgametophyte, or a biomimetic structure due to their regular spheroidal appearance.
- Two types of inclusions were observed 1) small and opaque, often with a fragmented circumference, and 2) larger and translucent, with the appearance of being a hollow membrane-bound.

- Corpus volume does not appear to be a contributing factor in host occupancy, and a possible bias towards small non-taeniate pollen grains may reflect a preference for coniferous pollen grain hosts
- Spheroidal inclusions were most common inside pollen grains from the Carnallitic Marl Formation (Cycle 4), likely a preservational effect considering the abundance and well-preserved quality of all palynomorphs recovered from the Carnallitic Marl Formation or an effect of regional deforestation enhancing run-off and erosion leading to the accumulation of woody debris which would have encouraged microbial and fungal activity – however there is no evidence of large-scale deforestation. It may be that the fluvial depositional environment of Cycle 4 broadened the taphonomic window allowing for this unique facet of the environment to be preserved.
- Fungal dynamics are across the Permian-Triassic boundary are heavily debated due to the controversial nature of the "fungal spike" palynomorph *Reduviasporonites* which may be either fungal or algal in affinity, and if these inclusions are indeed fungal they provide evidence in support of this hypothesis independent of this controversy. Regardless, the abundance and distribution of the spheroidal inclusions in this material does not indicate a "fungal spike".
- This study contributes to the growing literature on fungi in the late Palaeozoic and adds dimensionality to the Zechstein ecosystem, as well as highlighting how important it is to expand the targets of palynological analysis beyond the logging of spore-pollen abundances.
- As a result of the research limitations imposed by the COVID-19 pandemic it was not possible to undertake scanning electron microscopy (SEM) analysis to prove the spheroidal inclusions are endobiotic rather than epibiotic – this should be the focus of further study.

Bibliography

Afonin, S.A., Barinova, S.S., Krassilov, V.A. 2001. A bloom of *Tympanicysta* Balme 1980 (green algae of zygnematalean affinities) at the Permian–Triassic boundary. *Geodiversitas* 23, 481–487.

Aggarwall, N., Krings, M., Jha, N., Taylor, T.N. 2015. Unusual spheroidal inclusions in Late Permian gymnosperm pollen grains from southern India revisited: evidence of a fungal nature. *Grana* 54(3), 174-183.

Alderton, D., Selby, D., Kucha, H., Blundell, D.J. 2016. A multistage origin for Kupferschiefer mineralization. *Ore Geology Reviews* 79, 535-543.

Allen, M. R., Ingram, W. J. 2002. Constraints on future changes in climate and the hydrologic cycle. *Nature* 419, 224-232.

Allen, P.A., Allen, J.R. 2005. Basin Analysis: Principles and Applications, 2nd ed., Blackwell Publishing, Malden, Massachusetts, 549 pp.

Anderson, J.M., Anderson, H.M. 1983. Palaeoflora of southern Africa, Molteno Formation (Triassic) 1. (Part 1. Introduction; Part 2. Dicroidium). Balkema, Rotterdam.

Archangelsky, S., Wagner, R.H. 1983. *Glosspteris anatolica* sp. nov. from uppermost Permian strata in south east Turkey. Bulletin of the British Museum (Natural History). *Geology* 37, 81–91.

Armal, G., Martinez-Frias, J., Vásquez, L. 2007. UV shielding properties of jarosite vs. gypsum: astrobiological implications for Mars. *World Applied Sciences Journal* 2, 112-116.

Arthurton, R.S., Burgess, I.C., Holliday, D.W. 1978. Permian and Triassic. In: Moseley, F. (editor) The geology of the Lake District. *Yorkshire Geological Society Occasional Publication* 3, 565-592.

Bachmann, G.H., Kozur, H.W. 2004. The Germanic Triassic: Correlation with the international chronostratigraphic scale, numerical ages, Milankovitch cyclicity. *Hallesches Jahrbuch für Geowissenschaften B* 26, 17–62.

Baldrian, P., Větrovský, T., Cajthaml, T., Dobiášová, P., Petránková, M., Šnajdr, J., Eichlerová, I. 2013. Estimation of fungal biomass in forest litter and soil. *Fungal Ecology* 6,1–11.

Balme, B. 1995. Fossil in situ spores and pollen grains: an annotated catalogue. *Review of Palaeobotany and Palynology* 87(2-4), 81-323.

— Segroves, K. 1966. *Peltacystia* gen. nov.: a microfossil of uncertain affinities from the Permian of Western Australia. *Journal of the Royal Society of Western Australia* 49, 26–31.

Balteş, N. 1967. Microflora from Miocene salt-bearing formations of the pre-Carpathian depression (Rumania). *Review of Palaeobotany and Palynology* 2, 183-194.

Barbeiri, R., Stivaletta, N. 2011. Continental evaporites and the search for life on Mars. *Geological Journal* 46, 513-524.

Barnard, P.C., Cooper, B.S. 1983. A review of geochemical data related to the Northwest European Gas Province. *Geological Society, London, Special Publications* 12, 19–33.

Barr, D.J.S. 1970. *Hyphochytrium catenoides*: a morphological and physiological study of North American isolates. *Mycologia* 62, 492–503.

— Kustatscher, E., Krings, M. 2013. The ginkgophytes from the German Kupferschiefer (Permian), with considerations on the taxonomic history and use of *Baiera* and *Sphenobaeria*. *Bulletin of Geosciences* 88, 539–556.

Bauer, K., Kustatscher, E., Butzmann, R., Fischer, T.C., van Konijnburg-van Cittert, J.H.A., Krings, M., 2014. Ginkgophytes from the Upper Permian of the Bletterbach Gorge (Northern Italy). *Rivisita Italiana di Paleontologia e Stratigrafia* 120(3), 271-279.

Beauchamp, B. 1994. Permian climatic cooling in the Canadian Arctic. In: Klein, G.D. (Ed.), Pangea: Paleoclimate, Tectonics and Sedimentation during Accretion, Zenith and Breakup of a Supercontinent. *Geological Society of America Special Paper* 228, 229–246.

Bechtel, A., Püttmann, W. 1997. Palaeoceanography of the early Zechstein Sea during Kupferschiefer deposition in the Lower Rhine Basin (Germany): A reappraisal from stable isotope and organic geochemical investigations. *Palaeogeography, Palaeoclimatology, Palaeoecology* 136(1-4), 331-358.

Bell, P.R., Hemsley, A.R. 2011. Green Plants: Their Origin and Diversity (2nd eds). 330 pp.

Benison, K. 2013. Acid saline fluid inclusions: examples from modern and Permian extreme lake systems. *Geofluids* 13, 579–593.

— Karmanocky, F.J., III. 2014. Could microorganisms be preserved in Mars gypsum? Insights from terrestrial examples. *Geology* 42, 615-618.

— Jagniecki, E.A., Edwards, T.B., Mormile, M.R., Storrie-Lombardi, M.A. 2008. Hairy blobs: microbial suspects preserved in modern and ancient extremely acid lake evaporites. *Astrobiology* 8(4), 807–821.

Benninghoff, W.S. 1962. Calculation of pollen and spores density in sediments by addition of exotic pollen in known quantities. *Pollen et Spores* 4, 332–333.

Benton, M.J., Twitchett, R.J. 2003. How to Kill (Almost) All Life: The End-Permian Extinction Event. *Trends in Ecology and Evolution* 18(7), 358–365.

— Newell, A.J. 2014. Impacts of global warming on Permo-Triassic terrestrial ecosystems. *Gondwana Research* 25, 1308-1337.

— Cook, E., Turner, P. 2002. Permian and Triassic Red Beds and the Penarth Group of Great Britain. Geological Conservation Review Series 24. Joint Nature Conservation Committee, Peterborough.

Bercovici, A., Diez, J.B., Broutin, J., Bourquin, S., Linol, B., Villanueva-Amadoz, U., López-Gómez, J., Durand, M. 2009. A palaeoenvironmental analysis of Permian sediments in Minorca (Balearic Islands, Spain) with new palynological and megafloral data. *Review of Palaeobotany and Palynology* 158, 14–28.

Berner, R.A. 2006. GEOCARBSULF: A combined model for Phanerozoic atmospheric O2 and CO2. *Geochimica et Cosmochimica Acta* 70(23 SPEC.ISS.), 5653–5664.

Berridge, N.G., Pattison, J., Samuel, M.D.A., Brandon, A., Howard, A.S., Pharaoh, T. C., Riley, N.J. 1999. Geology of the Grantham district. *Memoir of the British Geological Survey* 127, 1-133.

Best, G. 1989. Die Grenze Zechstein/Buntsandstein in Nordwest-Deutschland nach Bohrlochmessungen. *Zeitschrift der Deutschen Geologischen Gesellschaft* 140, 73-85.

Bharadwaj, D.C., Tiwari, R.S. 1964. On two monosaccate genera from Barakar Stage of India. *Palaeobotanist* 12(2), 139-146.

Birks, H.J.B., Felde, V.A., Bjune, A.E., Grytnes, J.-A., Seppä, H., Giesecke, T. 2016. Does pollen-assemblage richness reflect floristic richness? A review of recent developments and future challenges. *Review of Palaeobotany and Palynology* 228, 1-25.

Black, B.A., Neely, R.R., Lamarque, J-F., Elkins-Tanton, L., Kiehl, J.T., Sheilds, C.A., Mills, M., Bardeen, C. 2019. Systemic swings in end-Permian climate from Siberian Traps carbon and sulfur outgassing. *Nature Geoscience* 11(12), 949-954.

Blackwell, D.D., Steel, J.L. 1989. Thermal conductivity of sedimentary rocks: Measurement and significance, in Thermal History of Sedimentary Basins, pp. 13–36, Springer-Verlag, London.

Bödige, H. 2007. Kutikularanalyse der Flora des Zechsteins bei Gera-Trebnitz. Unpublished MSc Thesis, University Münster, 110 pp.

Bomfleur, B., Serbet, R., Taylor, E.L., Taylor, T.N. 2011. The possible pollen cone of the Late Triassic conifer Heidiphyllum/Telemachus (Voltziales) from Antarctica. *Antarctic Science* 23, 379–385.

Botha, J., Smith, R.M. 2007. Lystrosaurus species composition across the Permo-Triassic boundary in the Karoo Basin of South Africa. *Lethaia* 40, 125-137.

Bourquin, S., Durand, M., Diez, J., Broutin, J., Fluteau, F. 2007. The Permian-Triassic boundary and Early Triassic sedimentation in Western European basins: an overview. *Journal of Iberian Geology* 33, 221-236.

Bowring, S.A., Erwin, D.H., Jin, Y.G., Martin, M.G., Davidek, K., Wang, W. 1998. U/Pb zircon geochronology and tempo of the end-Permian mass extinction. *Science* 280, 1039–1045.

Brauns, C.M., Pätzold, T., Haack, U. 2003. A Re-Os study bearing on the age of the Kupferschiefer at Sangerhausen (Germany). International Congress on Carboniferous and Permian Stratigraphy, Utrecht, August 2003, 66 pp.

Bronn, H. 1828. Untersuchung der versteinerten Kornähren und anderer Pfanzentheile, zu Cupressus Ullmanni gehörig, aus den Frankenberger Erz-Flözzen. *Zeitschrift Mineral* 2, 509-531.

Came, R.E., Eiler, J.M., Veizer, J., Azmy, K., Brand, U., Weidman, C.R. 2007. Coupling of surface temperatures and atmospheric CO2 concentrations during the Palaeozoic era. *Nature* 449(7159), 198-201.

Campbell, I.D., Campbell, C. 1994. Pollen preservation: Experimental wet-dry cycles in saline and desalinated sediments. *Palynology* 15: 5-10.

Cao, W., Flament, N., Zahirovic, S., Williams, S., Dietmar Müller, R. 2019 The interplay of dynamic topography and eustasy on continental flooding in the late Paleozoic. *Tectonophysics* 761, 108-121.

Chaloner, W.G. 2013. Three Palynological Puzzles. *International Journal of Plant Sciences* 174(3), 602-607.

Chen, J., Shen, S.-Z., Li, X.-H., Xu, Y.-G., Joachimski, M.M., Bowring, S.A., Erwin, D.H., Yuan, D.-X., Chen, B., Zhang, H. et al. 2015. High-resolution SIMS oxygen isotope analysis on conodont apatite from South China and implications for the end-Permian mass extinction. *Palaeogeography, Palaeoclimatology, Palaeoecology* 448, 26–38.

Schlotheim, E. F. von. 1820. Die Petrefactenkunde auf ihrem jetztigen Standpunkte durch die Beschreibung seiner Sammlung versteinerter und fossiler Überreste des Thierund Pflanzenreichs der Vorwelt. Becker, Gotha. 437 pp.

Chu, D.L., Yu, J.X., Tong, J.N., Benton, M.J., Song, H.J., Huang, Y.F., Song, T., Tian, L. 2017. Biostratigraphic correlation and mass extinction during the Permian-Triassic transition in continental-marine siliciclastic settings of South China. *Global Planetary Change* 146, 67-88.

Chuvashov, B.I. 1995. Permian Deposits of the Urals and Preduralye. In: Scholle P.A., Peryt T.M., Ulmer-Scholle D.S. (eds) The Permian of Northern Pangea. Springer, Berlin, Heidelberg.

Clapham, M.E., Bottjer, D.J. 2007. Permian marine paleoecology and its implications for large-scale decoupling of brachiopod and bivalve abundance and diversity during the Lopingian. *Palaeogeography, Palaeoclimatology, Palaeoecology* 249, 283–301.

Clapham, W.B. 1970. Permian miospores from the Flowerpot Formation of Western Oklahoma. *Micropaleontology* 16, 15–36.

Clarke, R.F.A. 1965a. British Permian saccate and monosulcates miospores. *Palaeontology* 8(2), 322-354.

— 1965b. Keuper Miospores from Worcestershire England. *Palaeontology* 8(2), 294-321.

Classen, B., Amelunxen, F., Blaschek, W. 2000. Concentric bodies in a parasitic fungus of *Malva sylvestris* (Malvaceae) pollen. *Journal of Phytopathology* 148, 313–317.

Clauser, C., Huenges, E. 1995. Thermal conductivity of rocks and minerals, in Rock Physics and Phase Relations—A Handbook of Physical Constants, edited by T. J. Ahrens, AGU Reference Shelf, vol. 3, 105–126, American Geophysical Union, Washington, D. C.

Clayton, G. Goodhue, R., Adelbagi, S. T., Vecoli, M., 2017. Correlation of Palynomorph Darkness Index and vitrinite reflectance in a submature Carboniferous well section in northern Saudi Arabia. *Revue de Micropaléontologie* 60, 411–416 ARAMCO-CIMP.

Cleal, C.J. 2016. A global review of Permian macrofloral biostratigraphical schemes. In: Lucas, S.G. and Shen, S.Z. (eds) The Permian Timescale. Geological Society, London, Special Publications, 450 pp.

— Thomas, B.A. 1991. Carboniferous and Permian palaeogeography. In: Cleal, C.J. (ed.) Plant Fossils in Geological Investigation: The Palaeozoic. Ellis Horwood, Chichester, 154–181.

— Thomas, B.A. 1995. Palaeozoic Palaeobotany of Great Britain, Geological Conservation Review Series, No. 9, Chapman and Hall, London, 295 pp.

Clement-Westerhof, J.A. 1984. Aspects of Permian palaeobotany and palynology. IV. The conifer Ortiseia Florin from the Val Gardena Formation of the Dolomites and the Vicentinian Alps (Italy) with special reference to a revised concept of the Walchiaceae (Göppert) Schimper. Review of Palaeobotany and Palynology 41, 51-166.

— 1987. Aspects of Permian palaeobotany and palynology. VII. The Majonicaceae, a new family of Late Permian conifers. *Review of Palaeobotany and Palynology* 52, 375–402.

— 1988. Morphology and phylogeny of Paleozoic conifers. 298-337. In: Beck, C. (Ed.), Origin and Evolution of Gymnosperms. Columbia University Press, New York, 504 pp.

Cockell, C.S., Wilhelm, M.B., Perl, S., Wadsworth, J., Payler, S. McMahon, S., Paling, S., Edwards, T. 2020. 0.25 Ga salt deposits preserve signatures of habitable conditions and ancient lipids. *Astrobiology* 20(7), 864-877.

Cocks, L. & Torsvik, T. 2006. European geography in a global context from the Vendian to the end of the Palaeozoic. *European Lithosphere Dynamics* 32, 83-95.

Conner, A.J., Benison, K.C. 2013. Acidophilic halophilic microorganisms in fluid inclusions in halite from Lake Magic, Western Australia. *Astrobiology* 13, 850–860.

Conrad, C.P. 2013. The solid Earth's influence on sea level. *GSA Bulletin* 125 (708), 1027-1052.

Cui, Y., Kump, L.R., Ridgwell, A. 2013. Initial assessment of the carbon emission rate and climatic consequences during the end-Permian mass extinction. *Palaeogeography, Palaeoclimatology, Palaeoecoogy* 389, 128-136.

Cuneo, C.R. 1996. Permian phytogeography in Gondwana. *Palaeogeography, Palaeoclimatology, Palaeoecology* 125, 75-104.

Czapowski, G. 1990. Kontynentalne osady chlorkowe w górnym cechsztynie Polski [in Polish]. In: García-Veigas, J., Cendón, D.I., Pueyo, J.J., Peryt, T.M. 2011. Zechstein saline brines in Poland, evidence of overturned anoxic ocean during the Late Permian mass extinction event. *Chemical Geology* 290, 189-201.

Czarnocki, J. 1965. Stratigraphy of the Swiety Krzyz Mountains, 4. Carboniferous and Permian. In: Visscher, H. 1971. The Permian and Triassic of the Kingscourt Outlier, Ireland: A palynological investigation related to regional stratigraphical problems in the Permian and Triassic of Western Europe. Geological Survey of Ireland Special Paper No. 1. 114 pp.

Czeczuga, B., Muszyńska, E. 2004. Aquatic zoosporic fungi from baited spores of cryptogams. *Fungal Diversity* 16, 11-22.

Déak, M.H. 1959. Experimental palynological investigations of gypsum from the Messek Mountain Range. *Bulletin of the Hungarian Geological Society 89*, 170-173 [in Hungarian with German summary].

Denison, R.E., Peryt, T.M. 2009. Strontium isotopes in the Zechstein anhydrites of Poland: evidence of varied meteoric contributions to marine brines. Geological Quarterly 53(2), 159–166.

Diedrich, C.G. 2009. A coelacanthid-rich site at Hasbergen (NW Germany): taphonomy and palaeoenvironment of a first systematic excavation in the Kupferschiefer (Upper Permian, Lopingian). *Palaeobiodiversity and Palaeoenvironments* 89, 67-94.

Dijkstra, S.J. 1972. Some megaspores from South Africa and Australia. *Palaeontologica Africa* 14, 1–13.

Dilcher, D.L. 1965. Epiphyllous fungi from Eocene deposits in Western Tennessee, U.S.A. *Palaeontographica Abteilung B* 116(1-4), 1-54.

DiMichele, W.A., Hook, R.W. 1992. Palaeozoic terrestrial ecosystems. In: Labandeira, C. 2006. Silurian to Triassic Plant and Hexapod Clades and their Associations: New Data, a Review and Interpretations. *Arthropod Systematics and Phylogeny* 64(1), 53-94.

Dineley, D., Metcalf, S. 2007. Chapter 10: British Permian fossil fish sites Site: Middridge (GCR ID: 9022). Volume 16: Fossil Fishes of Great Britain. *Geological Conservation Review* 16, 1-9.

Dix, N.J., Webster, J. 1994. Fungal Ecology. Chapman & Hall, London. 394 pp.

Donovan, S.K., Hollingworth, N.T., Veltcamp, C. 1986. The British Permian crinoid *Cyathocrinites ramosus* (Sclotheim). *Palaeontology* 29, 809-25.

Doornenbal, J.C., Stevenson, A.G. (Eds.) 2010. Petroleum Geological Atlas of the Southern Permian Basin Area. EAGE Publications b.v., Houten, 342 pp.

Dunbar, C.O. 1940. The type Permian: its classification and correlation. *American Association of Petroleum Geologists Bulletin* 24(2), 237-281.

Dunham, K.C. 1961. Black shale and sulphide ore. *Advancement of Science* 18, 284-299.

Durska, E. 2016. Exceptional preservation of Miocene pollen: plasmolysis captured in salt. *Geologica acta* 14(1), 25-34.

— 2017. The Badenian Salinity Crisis in the palynological record: vegetation during the evaporative event (Carpathian Foredeep, southern Poland. *Annales Sociatatis Geologrum Poloniae* 87, 213-228.

— 2018. Pollen in a perfect trap: the palynological record in Miocene gypsum. Grana 57(4), 260-272.

Dybová-Jachowicz, S. 1974. Analyse palynologique des sédiments rouges salifères du Zechstein supérieur ("Zouber" rouge) à Kłodawa, Pologne. *Review of Palaeobotany and Palynology* 17, 57-61. [French with English summary].

Dypvik, H., Hankel, O., Nilsen, O., Kaaya, C., Kilembe, E. 2001. The lithostratigraphy of the Karoo supergroup in the Kilombero Rift Valley, Tanzania. *Journal of African Earth Sciences* 32, 451–470.

Eden, R.A., Stevenson, J.P., Edwards, W. 1957. Geology of the Country around Sheffield. *Memoir of the Geological Survey of Great Britain*, Sheet 100.

Edwards, R.A., Warrington, G., Scrivener, P.C., Jones, N.S., Waslam, H.W., Ault, L. 1997. The Exeter Group, south Devon, England: A contribution to the early post-Variscan stratigraphy of northwest Europe. *Geological Magazine* 134(2), 177-197.

Elsik, W.C. 1999. Reduviasporonites Wilson 1962: Synonymy of the Fungal Organism Involved in the Late Permian Crisis. *American Association of Stratigraphic Palynologists* 23, 27-41.

Enos, P. 1993. The Permian in China, in Permian of Northern Continents. Springer-Verlag, New York.

Erwin, D.H., 1993. The Great Paleozoic Crisis: Life and Death in the Permian. Columbia University Press, New York. 327 pp.

— 2006. Extinction: How Life on Earth Nearly Ended 250 Million Years Ago. Princeton University Press, Princeton, New Jersey. 296 pp.

Eshet, Y. 1990. Paleozoic–Mesozoic palynology of Israel, I. Palynological aspects of the Permo-Triassic succession in the subsurface. *Geological Survey of Israel Bulletin* 81, 1–20.

Eshet, Y., Rampino, M.R., Visscher, H. 1995. Fungal event and palynological record of ecological crisis and recovery across the Permian-Triassic boundary. *Geology* 23(11), 967-970.

Faddeeva, I.Z. 1980. Regularities in the changes of miospore complexes in stratotype sections of the East European platform and the Urals. In: Proceedings of the Fourth International Palynological Conference, 1976–1977, Lucknow, Volume 2. Birbal Sahni Institute of Palaeobotany, Lucknow, India, pp. 844–848.

Farabee, M.J., Taylor, E.L., Taylor, T.N. 1991. Late Permian palynomorphs from the Buckley Formation in the central Transantarctic Mountains. *Review of Palaeobotany and Palynology* 69, 353–368

Fauquette, S., Suc, J-P., Bertini, A., Popescu, S-M., Warny, S., Bachiri Taoufiq, N., Perez Villa, M-J., Chikhi, H., Feddi, N., Subally, D. et al. 2006. How much did climate force the Messinian salinity crisis? Quantified climatic conditions from pollen records in the Mediterranean region. *Palaeogeography, Palaeoclimatology, Palaeoecology* 238, 281–301.

Fielding, C.R. & McLoughlin, S. 1992. Sedimentology and palynostratigraphy of Permian rocks exposed at Fairbairn Dam, central Queensland. *Australian Journal of Earth Science* 39, 631–649.

Fielding, C.R., Frank, T.D. & Isbell, J.L. 2008. The late Paleozoic ice age—a review of current understanding and synthesis of global climate patterns. In: Fielding, C.R., Frank, T.D., Isbell, J.L. (Eds.), Resolving the Late Paleozoic Ice Age in Time and Space. *Geological Society of America*, pp. 343–354.

Fielding, C.R., Frank, T.D., McLoughlin, S., Vajda, V., Mays, C., Tevyaw, A.P., Winguth, A., Winguth, C., Nicoll, R.S., Bocking, M. et al. 2019. Age and pattern of the southern high-latitude continental end-Permian extinction constrained by multi proxyanalysis. *Nature Communications* 10,1–12.

Florin, R. 1944. Die Koniferen des Oberkarbons und des Unteren Perms. *Palaeontographica Abteilung B* 85, 365–456.

Florin, R. 1954. Note on Ullmannia from the Upper Permian formation of north-eastern Belgium. In Visscher, H. 1971. The Permian and Triassic of the Kingscourt Outlier, Ireland: A palynological investigation related to regional stratigraphical problems in the Permian and Triassic of Western Europe. Geological Survey of Ireland Special Paper No. 1. 114 pp.

Fluteau, F., Besse, J., Broutin, J., Ramstein, G. 2001. The Late Permian climate. What can be inferred from climate modelling concerning Pangea scenarios and Hercynian range altitude? *Palaeogeography, Palaeoclimatology, Palaeoecology* 167, 39-71.

Foster, C.B., Afonin, S.A. 2005. Abnormal pollen grains: an outcome of deteriorating atmospheric conditions around the Permian-Triassic boundary. *Journal of the Geological Society of London* 162, 653-659.

Foster, C.B., Stephenson, M.H., Marshall, C., Logan, G.A., Greenwood, P. F. 2002. A Revision of Reduviasporonites Wilson 1962: Description, Illustration, Comparison and Biological Affinities. *American Association of Stratigraphic Palynologists* 26, 35-58.

Freudenthal, T. 1964. Palaeobotany of the mesophytic I palynology of lower Triassic rock salt, Hengelo, the Netherlands. *Acta Botanica Neerlandica* 13, 209–236.

Galfetti, T., Bucher, H., Ovtcharova, M., Schaltegger, U., Brayard, A., Brühwiler, T., Goudeman, N. Weissert, H., Hochuli, P.A., Cordey, F. et al. 2007. Timing of the Early Triassic carbon cycle perturbations inferred from new U/Pb ages and ammonoid biochronozones. *Earth and Planetary Science Letters* 258, 593–604.

García-veigas, J., Cendón, D.I., Pueyo, J.J., Peryt, T. M. 2011. Zechstein saline brines in Poland, evidence of overturned anoxic ocean during the Late Permian mass extinction event. *Chemical Geology* 290, 189-201.

Garofalo, P.S., Fricker, M.B., Günther, D., Forti, P., Mercuri, A-M., Loreti, M., Capaccioni, B. 2010. Climatic control on the growth of gigantic gypsum crystals within hypogenic caves (Naica mine, Mexico)? *Earth and Planetary Science Letters* 289: 560–569.

Gasiewicz, A., Peryt, T.M. 1994. Biolaminites at the Zechstein (Upper Permian) Platy Dolomite (Ca3)-Main Anhydrite (A3) boundary: implications for evolution of an evaporite basin. *Beiträge zur Paläontologie Österreich-Ungarns und des Orients* 19, 91-101.

Gastaldo, R.A. 2019. Plants escaped an ancient mass extinction. *Nature Research Reviews* 567, 38-39.

Geinitz, H.B. 1861. Dyas, oder die Zechstein formation und das Rotliegend, Leipzig, 130 pp.

Geinitz, H.B. 1869. Über fossile Pflanzenreste aus der Dyas von Val Trompia. *Neues Jahrbuch für Mineralogie, Geologie and Paliontologie* 456-461.

Geluk, M. 2005. Stratigraphy and tectonics of Permo-Triassic basins in the Netherlands and surrounding areas. Unpublished PhD Thesis, Utrecht University.

Geluk, M.C. 1999. Late Permian (Zechstein) rifting in the Netherlands: models and implications for petroleum geology. *Petroleum Geoscience* 5(2), 189-199.

Geluk, M. 2005. Stratigraphy and tectonics of Permo-Triassic basins in the Netherlands and surrounding areas. Unpublished PhD Thesis, Utrecht University.

Geluk, M.C. 2007. Permian. In: Wong, T.E., Batjes, D.A.J. & de Jager, J. (eds.): Geology of the Netherlands. (Royal Netherlands Academy of Arts and Sciences), pp. 63-83.

Gibson, M.E., Wellman, C.H. 2020 The use of spore-pollen assemblages to reconstruct vegetation changes in the Late Permian Zechstein deposits of northeast England. *Review of Palaeobotany and Palynology*. Accepted subject to minor revision.

— Bodman, D.J. 2020. Evaporite Palynology: a case study on the Permian (Lopingian) Zechstein Sea. *Journal of the Geological Society*. Accepted pending minor revision.

— Taylor, W.A. & Wellman, C.H. 2020. Wall ultrastructure of the Permian pollen grain Lueckisporites virkkiae Potonié et Klaus 1954 emend. Clarke: Evidence for botanical affinity. Review of Palaeobotany and Palynology 275, 104169.

Glennie, K.W. 1972. Permian Rotliegendes of N.W. Europe interpreted in light of modern desert sedimentation studies. *Bulletin of the American Association of Petroleum Geologists* 56, 1048-1071.

— 1983. Lower Permian sedimentation in the North Sea area. pp. 521-541. In: Brookfield, M. E. & Ahlbrandt, T. S. (editors) Eolian sediments and processes. Developments in Sedimentology 38. Elsevier, Amsterdam. pp. 660.

Glennie, K.W. 1984. Early Permian (Rotliegendes) Palaeowinds of the North Sea. *Sedimentary Geology* 34, 245–265.

— 1989. Some effects of the Late Permian Zechstein transgression in Northern Europe. In: Boyle, R.W., Brown, A.C., Jefferson, C.W., Jowett, E.C. & Kirkham, R.V. (Eds.), Sediment-hosted Stratiform Copper Deposits. Geological Association of Canada Special Papers Volume 36, pp. 557–565.

— Buller, A. 1983. The Permian Weissliegend of N.W. Europe: the partial deformation of aeolian sand caused by the Zechstein transgression. *Sedimentary Geology* 35, 43-81.

— Higham, J., Stemmerik, L. 2003. Permian. In: Evans, D., Graham, C., Armour, A., Bathurst, P. (Eds.): The Millennium Atlas: petroleum geology of the central and northern North Sea, The Geological Society, 91-103.

Goldstein, S. 1960. Degradation of pollen by phycomycetes. *Ecology* 41, 543–545.

Golonka, J., Ford, D. 2000. Pangean (Late Carboniferous-Middle Jurassic) paleoenvironment and lithofacies, *Palaeogeography, Palaeoclimatology, Palaeoecology* 161(1–2), 1–34.

— Meyen, S.V., 1986. Tatarian flora (composition and distribution in the Late Permian of Eurasia). Nauka, Moscow. 175 (in Russian).

— Balme, B.E., Foster, C.B. 1998. Tatarian palynology of the Russian Platform: a review. *Proceedings of the Royal Society of Victoria* 110, 115-135.

Goodall, I.G. 1987. Sedimentology and diagenesis of the Edlington Formation (Upper Permian) of Teesside. Unpublished Ph.D. thesis, University of Reading.

Goodhue, R. and Clayton, G. 2010. Palynomorph darkness index (PDI) - A new technique for assessing thermal maturity. *Palynology* 34(2), 147-156.

Göppert, H.R. 1850. Monographie der fossilen Coniferen, mit Berücksichtigung der Lebenden. Arnz, Leiden, 286 pp.

Gothan, W., Nagalhard, K. 1921. Kupferschieferpflanzen aus dem niederrheinischen Zechstein. *Jahrbuch der Königlich Preussischen Geologischen Landesanstalt und Bergakademie* 42, 440–460.

Gothan, W., Gimm, O. 1930. Neuere Beobachtungen und Betrachtungen über die Flora des Rotliegenden in Thüringen. *Arb. Inst. Palaeobot. Petrograph. Brennsteile* 2, 39–74.

Götz, A.E., Ruckwied, K., Wheeler, A. 2018. Marine flooding surfaces recorded in Permian black shales and coal deposits of the Main Karoo Basin (South Africa): Implications for basin dynamics and cross-basin correlation. *International Journal of Coal Geology* 190, 178–190.

Gould, R.E., Delevoryas, T. 1977. The biology of Glossopteris: evidence from petrified seed- bearing and pollen-bearing organs. *Alcheringia* 1, 387–399.

Gradstein, S.R., Kerp, H. 2012. A brief history of plants on Earth. In: Gradstein, F.M., Ogg, J.G., Schmitz, M., Ogg, G. (eds) The Geologic Time Scale 2012. Elsevier, Amsterdam, 233–237.

Grasby, S. E., Beauchamp, B., Bond, D.P.G., Wignall, P.B., Talavera, C., Galloway, J.M., Piepjohn, K., Reinhardt, L., Blomeier, D. 2015. Progressive environmental deterioration in northwestern Pangea leading to the latest Permian extinction. *Bulletin of the Geological Society of America* 127(9–10), 1331–1347.

Grauvogel-Stamm, L., 1978. La flore du Grès à Voltzia (Buntsandstein súperieur) des Vosges du Nord (France). Morphologie, anatomie, interprétations phylogénique et paléogéographique. Université Louis-Pasteur de Strasbourg Institut de Géologie 50, 1-225.

— Grauvogel, L., 1973. Masculostrobus acuminatus nom. nov., un nouvel organe reproducteur mâle de Gymnosperme de Grès à Voltzia (Trias inférieur) des Vosges (France). *Geobios* 6, 101–114.

— Doubinger, J. 1975. Deux fougères fertiles du Stéphanien du Massif Central (France). *Geobios* 6, 409–421.

— Ash, S.R. 2005. Recovery of the Triassic land flora from the end-Permian crisis. *General Palaeontology (Palaeoecology)* 4, 593-608.

Grebe, H. 1957. Zur Mikroflora der Niederrheinischen Zechsteins. *Geologisches Jahrbuch* 73, 51–74.

— Schweitzer, H.J. 1962. Sie Sporae dispersae des niederrheinschen Zechsteins. *Fortschritte in der Geologie von Rheinland und Westfalen* 12, 201-224.

Griffith, J.D., Willcox, A., Powers, D.W., Nelson, R., Baxter, B.K. 2008. Discovery of abundant cellulose microfibers encased in 250 Ma Permian halite: a macromolecular target in the search for life on other planets. *Astrobiology* 8(2), 215-228.

Guillaume, B., Pochat, S., Monteaux, J., Husson, L., Choblet, G. 2016. Can eustatic charts go beyond first order? Insights from the Permian-Triassic. *Lithosphere* 8, 505-518.

Halbritter, H., Ulrich, S., Grímsson, F., Weber, M., Zetter, R., Hesse, M., Buchner, R., Svojtka, M., Frosch-Radivo, A. 2018. Illustrated Pollen Terminology (2nd eds.) Springer Open. 487 pp.

Hallam, A., Wignall, P. B. 1997. *Mass Extinctions and their Aftermath*. Oxford University Press, Oxford, 320 pp.

Hankel, O. 1992. Late Permian to Early Triassic microfloral assemblages from the Maji ya Chumvi Formation, Kenya. *Review of Palaeobotany and Palynology* 72, 129–147.

Haq, B.U., Schutter, S.R., 2008. A chronology of Paleozoic sea-level changes. *Science* 322(5898), 64–68.

Harland, W.B., Armstrong, R.L., Cox, A.V., Craig, L.E., Smith, A.G., Smith, D.G. 1990. *A Geologic Time Scale 1989*. Cambridge University Press, Cambridge, 263. pp.

Harper, C., Taylor, T., Krings, M., Taylor, E.L. 2016. Structurally preserved fungi from Antarctica: diversity and interactions in late Palaeozoic and Mesozoic polar forest ecosystems. *Antarctic Science* 28(3), 153-173.

Harrington, M.G., Sackett, S.S. 1992. Past and present fire influences on southwestern ponderosa pine old growth. In: Kaufmann, M.R., Moir, W.H., Bassett, R.L. (Eds.), Proceedings of a Workshop: Old-growth Forests in the South- west and Rocky Mountain Regions, March 9-13, Portal, AZ. Gen. Tech. Rep. RM-213, U.S. Dept. of Agriculture, Forest Service, Rocky Mountain Forest and Range Experiment Station, Fort Collins, CO, pp. 44-50.

Harrison, J.G., Lowe, R., Williams, N.A. 1994. Humidity and fungal diseases of plants – problems. In: J.P. Blakeman, B. Williamson (eds.). *Ecology of plant pathogens*. Wallingford: CAB International, pp. 79–97.

Hart, G.F. 1964. A review of the classification and distribution of the Permian miospore: Disaccate Striatiti. Cinqième Congrès International de Stratigraphie et de Géologie du Carbonifère, Paris 1963. C. R. 3, 1171–1199.

— 1969. Palynology of the Permian Period. In: Tschudy, R.H., Scott, R.A. (Eds.), Aspects of Palynology. Wiley-Interscience, New York, pp. 271–289.

— 1970. The biostratigraphy of Permian palynofloras. In Warrington, G. (1996) Chapter 18E. Permian spores and pollen. In Jansonius J. and McGregor, D.C. (ed.), Palynology: principles and applications. *American Association of Stratigraphic Palynologists Foundation* 2, 607-619.

Harwood, G. M. 1981. Controls of mineralization in the Cadeby Formation (Lower Magnesian Limestone). Unpublished Ph.D. thesis, Open University. In: Smith, D.B. 1989. The late Permian palaeogeography of north-east England. *Proceedings of the Yorkshire Geological Society* 47, 285-312.

Hass, H., Taylor, T.N., Remy, W. 1994. Fungi from the Lower Devonian Rhynie chert: mycoparasitism. *American Journal of Botany* 81, 29–37.

Haubold, H., Schaumberg, G. 1985. Die Fossilien des Kupferschiefer: Pflanzen-und Tierwelt zu Beginn des Zechsteins; eine Erzlagerstatte und ihre Palaontologie. Wittenberg Lutherstadt. 223 pp.

Hauke, R.L., 1963. A taxonomic monograph of the genus Equisetum subgenus Hippochaete. *Nova Hedwigia* 8, 1-123.

Henderson, C.M. 2016. Permian conodont biostratigraphy. In: Lucas, S.G. & Shen, S.Z. (eds) The Permian Timescale. *Geological Society, London, Special Publications* 450.

Henderson, C.M., Davydov, V.I., Wardlaw, B.R., Gradstein, F.M., Hammer, O., 2012. The Permian Period. In: Gradstein, F.M., Ogg, J.G., Schmitz, M.D., Ogg, G.M. (Eds.) *The Geologic Time Scale* 2012. vol. 2. Elsevier, Amsterdam, pp. 653–679.

Hermann, A. 1964. Gips- und Anhydritvorkommen in Norclwestdeutschland. Silikat Journal 3(6), 442-466.

— Hochuli, P.A., Bucher, H., Roohi, G. 2012. Uppermost Permian to Middle Triassic palynology of the Salt Range and Surghar Range, Pakistan. *Review of Palaeobotany and Palynology* 169, 61-95.

— Hochili, P.A., Bucher, H., Brühwiler, T., Hautmann, M., Ware, D., Roohi, G. 2011. Terrestrial ecosystems on North Gondwana following the end-Permian mass extinction. *Gondwana Research* 20, 630–637 (2011).

Hernandez-Castillo, G.R., Rothwell, G.W., Mapes, G. 2001. Thucydiaceae fam. nov., with a review and reevaluation of Paleozoic walchian conifers. *International Journal of Plant Sciences* 162, 1155–1185.

Hirst, D.M., Dunham, K.C. 1963. Chemistry and Petrology of the Marl Slate of SE Durham, England. *Economic Geology* 58, 912 - 940.

Hjelle, K.L., Sugita, S. 2012. Estimating pollen productivity and relevant source area of pollen using late sediments in Norway: how does lake size variation affect the estimates? *The Holocene* 22, 313-324.

Hochuli, P.A., 2016. Interpretation of “fungal spikes” in Permian-Triassic boundary sections. *Global and Planetary Change* 144, 48-50.

— Hermann, E., Vigran, J.O., Bucher, H., Weissert, H. 2010. Rapid demise and recovery of plant ecosystems across the end Permian extinction event. *Global and Planetary Change* 74, 144–155.

Hofmann, R., Goudemand, N., Wasmer, M., Bucher, H., Hautmann, M. 2011. New trace fossil evidence for an early recovery signal in the aftermath of the end-Permian mass extinction. *Palaeogeography, Palaeoclimatology, Palaeoecology* 310, 216–226.

Hollingworth, N.T. 1987. Palaeoecology of the Upper Permian Zechstein Cycle 1 reef of NE England. Unpublished Ph.D. Thesis, University of Durham.

— Pettigrew, T.H. 1988. Zechstein reef fossils and their palaeoecology. Palaeontological Association Field Guides to Fossils 3, London. 75 pp.

— Baker, M.J. 1991. Gastropods from the Upper Permian Zechstein (Cycle 1) reef of north-east England. *Proceedings of the Yorkshire Geological Society* 48, 347- 365.

Horowitz, A. 1973. Late Permian palynomorphs from southern Israel. In: Lei, Y., Servais, T. & Feng, Q. 2013. The diversity of the Permian phytoplankton. *Review of Palaeobotany and Palynology* 198, 145-161.

— 1974. Especes du genre Veryhachium du Permo-Trias du Sud d'Israel. In: Lei, Y., Servais, T. and Feng, Q. 2013. The diversity of the Permian phytoplankton. Review of *Palaeobotany and Palynology* 198, 145- 161.

— 1990. Palynology and paleoenvironment of uranium deposits in the Permian Beaufort Group, South Africa. *Ore Geology Reviews* 5, 537–540.

Hounslow, M., Balabanov, Y.P. 2016. A geomagnetic polarity timescale for the Permian, calibrated to stage boundaries. In: Lucas, S.G. and Shen, S.Z. (eds) The Permian Timescale. Geological Society, London, Special Publications, pp. 450.

Howse, R. 1848. A catalogue of the fossils of the Permian System of the counties of Northumberland and Durham. *Transactions of the Tyneside Naturalists' Field Club* 1, 219-64.

— 1858. Notes on the Permian System of the counties of Northumberland and Durham. *Annals and Magazine of Natural History* 19, 304-12.

Hug, N. 2004. Sedimentgenese und Paläogeographie des höheren Zechsteins bis zur Basis des Buntsandsteins in der Hessischen Senke. *Geologische Abhandlungen Hessen* 113, 1–238.

— Gaupp, R. 2006. Palaeogeographic reconstruction in red beds by means of genetically related correlation: results from the upper part of the German Zechstein (Late Permian). *Zeitschrift der Deutschen Gesellschaft für Geowissenschaften* 157, 107–120.

Hughes, N.F., De Jekhowsky, B., Smith, A.H.V. 1964. Extraction of spores and other organic microfossils from Palaeozoic clastic sediments and coals. In: Visscher, H. 1971. The Permian and Triassic of the Kingscourt Outlier, Ireland: A palynological investigation related to regional stratigraphical problems in the Permian and Triassic of Western Europe. Geological Survey of Ireland Special Paper No. 1. 114. pp.

Husby, C. 2013. Biology and functional morphology of Equisetum with emphasis on the giant horsetails. *Botanical Review* 79(2), 147-177.

Hutchison, J.L., Barron, G.L. 1997. Parasitism of pollen as a nutritional source for lignicolous Basidiomycota and other fungi. *Mycological Research* 101(2), 191-194.

Illman, W.I. 1984. Zoosporic fungal bodies in the spores of the Devonian fossil vascular plant, †Horneophyton. *Mycologia* 76, 545–547.

Inosova, K.I., Krusina, A.K., Shvartsman, E.G. 1975. The scheme of distribution of characteristic genera and species of microspores and pollen in Carboniferous and Lower Permian deposits. In: Field Excursion Guide-book for the Donets Basin, Ministry of Geology of the Ukrainian SSR. Nauka, Moscow [in Russian and English].

Jackson, D.I., Johnson, H. 1996. Lithostratigraphic nomenclature of the Triassic, Permian and Carboniferous of the U.K. offshore East Irish Sea Basin. British Geological Survey, Nottingham. In: Warrington, G. 2008. Palynology of the Permian succession in the Hilton Borehole, Vale of Eden, Cumbria, U.K. *Proceedings of the Yorkshire Geological Society* 57(2), 123-130.

— Mulholland, P., Jones, S.M., Warrington, G. 1987. The geological framework of the East Irish Sea Basin, in Petroleum Geology of North West Europe (eds]. Brooks and KW. Glennie), Graham & Trotman, London, pp. 191-203.

Jekhowsky, de B. 1961. Sur quelques hystrichospheres Permo-Triassiques d'Europe et d'Afrique. *Revue de Micropaleontologie* 3, 207–212.

Jha, N. 1985. Palynology of the Gondwana sediments in Godavari Valley. PhD Thesis, Birbal Sahni Institute of Palaeobotany, University of Lucknow, India.

Jizba, K.M.M. 1962. Late Palaeozoic bisaccate pollen from the United States midcontinent area. *Journal of Paleontology* 36, 871–887.

Joachimski, M.M., Lai, X., Shen, S., Jiang, H., Luo, G., Chen, B., Chen, J., Sun, Y. 2012. Climate warming in the latest Permian and the Permian–Triassic mass extinction. *Geology* 40, 195–198.

Jowett, E.C., Pearce, G.W., Rydzewski, A. 1987. A mid-Triassic age of the Kupferschiefer mineralisation in Poland, based on a revised apparent polar wander path for Europe and Russia. *Journal of Geophysical Research* 92, 581–598.

Jux, U. 1961. The palynological age of diapiric and bedded salt in the Gulf Coastal Province. *Louisiana Department of Conservation Geological Bulletin* 38, 1–46.

Käding, K.C. 2000. Die Aller-, Ohre-, Friesland- und Fulda-Folge (vormals Bröckelschiefer-Folge). *Kali und Steinsalz* 13, 760–770.

Kaiho, K., Chen, Z.Q., Ohashi, T., Arinobu, T., Sawada, K., Cramer, B.S. 2005. A negative carbon isotope anomaly associated with the earliest Lopingian (Late Permian) mass extinction. *Palaeogeography, Palaeoclimatology, Palaeoecology* 223, 172–180.

Kaiser, H. 1976. Die permische Mikroflora der Cathaysiaschichten von nordwest-Schansi, China. *Palaeontographica Abteilung B* 159, 83–157.

Kaldi, J. 1986. Diagenesis of nearshore carbonate rocks in the Sprotbrough Member of the Cadeby (Magnesian Limestone) Formation (Upper Permian) of eastern England. 87- 102. In: Harwood, G M and Smith, D B (Editors). The English Zechstein and related topics. Geological Society of London, Special Publication, No. 22, pp. 244.

Kar, R.K., Jain, K.P. 1975. Libya, a probable part of Gondwanaland. *Geophytology* 5, 72–80.

— Ghosh, A.K. 2018. First record of Reduviasporonites from the Permian– Triassic transition (Gondwana Supergroup) of India. *Alcheringa: An Australasian Journal of Palaeontology* 43, 373-382.

Kemp, S.J., Smith, F.W., Wagner, D., Mounteney, I., Bell, C.P., Milne, C.J., Gowing, C.J.B., Pottas, T.L. 2016. An improved approach to characterise potash-bearing evaporite deposits, evidenced in North Yorkshire, U.K. *Economic Geology* 111, 719–742.

— Rushton, J.C., Horstwood, M.S.A., Nénert, G. 2018. Kalistronite, its occurrence, structure, genesis and significance for the evolution of potash deposits in North Yorkshire, UK. *American Mineralogist* 103(7), 1136-1150.

Kerp 2000

Kidder, D.L., Worsley, T.R. 2004. Causes and consequences of extreme Permo-Triassic warming to globally equable climate and relation to the Permo-Triassic extinction and recovery. *Palaeogeography, Palaeoclimatology, Palaeoecology* 203, 207–237.

Kidston, R., Lang, W.H. 1921. On Old Red Sandstone plants showing structure, from the Rhynie Chert bed, Aberdeenshire. Part V. The Thallophyta occurring in the peat-bed; the succession of the plants throughout a vertical section of the bed, and the conditions of accumulation and preservation of the deposit. *Transactions of the Royal Society of Edinburgh* 52, 855–902.

Kiehl, J.T., Shields, C.A. 2005. Climate simulation of the latest Permian: implications for mass extinction. *Geology* 33, 757–760.

Kirchheimer, F. 1950. Mikrofossilien aus Salzablagerungen des Tertiärs. *Palaeontographica Abteilung B* 90, 127–160.

Kirkby, J.W. 1857. On some Permian fossils from Durham. *Quarterly Journal of the Geological Society of London* 8, 213-8.

— 1858. On Permian Entomostraca from the Shell-Limestone of Durham. *Transactions of the Tyneside Naturalists' Field Club* 4, 122-71.

— 1859. On the Permian Chitonidae. *Quarterly Journal of the Geological Society of London* 15, 607-26.

— 1860. On the occurrence of 'sandpipes' in the Magnesian Limestone of Durham. *The Geologist* 3(9), 329-336.

— 1861. On the Permian rocks of South Yorkshire; and on their palaeontological relations. *Quarterly Journal of the Geological Society of London* 7, 287-325.

— 1863. Fossil fish in Magnesian Limestone at Fulwell Hill. *Transactions of the Tyneside Naturalists' Field Club* 5, pp. 248.

— 1864. On some remains of fish and plants from the 'Upper Limestone' of the Permian series of Durham. *Quarterly Journal of the Geological Society of London* 20, 345-58 (reprinted 1867 in the Transactions of the Natural History Society of Northumberland, Durham and Newcastle upon Tyne 1, 64-83).

— 1867. On the fossils of the Marl Slate and Lower Magnesian Limestone. *Transactions of the Natural History Society of Northumbria* 1, 184-200.

— 1870. Notes on the 'Geology' of Messrs Baker and Tate's New Flora of Northumberland and Durham. *Transactions of the Natural History Society of Northumberland, Durham and Newcastle upon Tyne* 3, 357-60.

Kiuntzel, M.K. 1965. Palynological characteristics of the Upper Permian and Lower Triassic strata in the basin of the Vetluga River and the Volga-Unsha interfluve, with borders of the Kostroma area. In Visscher, H. 1971. The Permian and Triassic of the Kingscourt Outlier, Ireland: A palynological investigation related to regional stratigraphical problems in the Permian and Triassic of Western Europe. Geological Survey of Ireland Special Paper No. 1. 114 pp.

Klaus, W. 1953a. Alpine Salzmikropaläontologie (Sporen- diagnose). *Paläontologische Zeitschrift* 27, 52–56.

— 1953b. Mikrosporen-Stratigraphie der ost-alpinen Salzberge. *Verhandlungen der Geologischen Bundesanstalt* 3, 161–175.

— 1955a. Alpinen Salzsporendiagnose. *Deutsche Geologische Gesellschaft Zeitschrift* 105, 234–236.

— 1955b. Über die Sporendiagnose des deutschen Zechsteinsalze in des alpinen Salzgebirges. *Deutsche Geologische Gesellschaft Zeitschrift* 105, 776–788.

— 1955. Über die Sporendiagnose des deutschen Zechsteinsalze in des alpinen Salzgebirges. *Deutsche Geologische Gesellschaft Zeitschrift* 105, 776–788.

— 1963. Sporen aus dem südalpinen Perm. *Jahrbuch der Geologischen Bundesanstalt* 106, 229–361.

— 1964. Zur sporenstratigraphischen Einstufung von gipsführenden Schichten in Bohrungen. *Erdöl-Zeitschrift* 4, 119–132.

— 1970. Utilization of spores in evaporite studies. In: Rau JL, Dellwig LF, eds. Third Symposium on Salt, 30–33. Cleveland, OH: Northern Ohio Geological Society.

— 1972. State of preservation of fossil spores as an aid to saline stratigraphy. In: Geology of saline deposits (Earth Sciences 7), Proceedings of the Hanover Symposium, Hanover, Germany, 129–130. Paris: UNESCO

Kłosowska, T., Dowgiałło, J. 1964. Sporomorphs in the Zechstein salts from bore holes Lebork IG I. In Visscher, H. 1971. The Permian and Triassic of the Kingscourt Outlier, Ireland: A palynological investigation related to regional stratigraphical problems in the Permian and Triassic of Western Europe. Geological Survey of Ireland Special Paper No. 1. 114 pp.

Kluska, B., Rospondek, M.J., Marynowski, L., Schaeffer, P. 2013. The Werra cyclotheme (Upper Permian, Fore-Sudetic Monocline, Poland): insights into fluctuations of the sedimentary environment from organic geochemical studies. *Applied Geochemistry* 29, 73–91.

Klymuik, A.A., Harper, C.J., Moore, D.S., Taylor, E.L., Taylor, T.N., Krings, M. 2013. Reinvestigating Carboniferous "Actinomycetes": Authigenic formation of biomimetic carbonates provides insight into early diagenesis of permineralized plants. *Palaios* 28, 80–92.

Korte, C., Jasper, T., Kozur, H.W., Veizer, J. 2006. 87Sr/86Sr record of Permian seawater. *Palaeogeography, Palaeoclimatology, Palaeoecology* 224, 89–107.

Korte, C., Kozur, H.W., Bruckschen, P., Veizer, J. 2003. Strontium isotope evolution of Late Permian and Triassic seawater. *Geochimica et Cosmochimica* Acta 67, 47–62.

Korwowksi, L., Klapcinski, J. 1986. Macrofauna of the Polish Zechstein: its occurrence and stratigraphy. In: Harwood, G.M. and Smith, D.B. (eds). 1986. The English Zechstein and Related Topics, Geological Society Special Publication No. 22, pp. 211-216.

Kosanke, R.M. 1995. Palynology of Part of the Paradox and Honaker Trail Formations, Paradox Basin, Utah. Washington, DC: US Geological Survey Bulletin 2000-L.

Kotanska, H., Krason, J. 1966 New sites of sporomorphs in the Zechstein deposits of Poland. In Visscher, H. 1971. The Permian and Triassic of the Kingscourt Outlier, Ireland: A palynological investigation related to regional stratigraphical problems in the Permian and Triassic of Western Europe. Geological Survey of Ireland Special Paper No. 1. 114 pp.

Kozur, H. 1994. The correlation of the Zechstein with the marine standard. *Jahrbuch der Geologischen Bundesanstalt* 137, 85–103.

Kozur, H.W., Weems, R.E. 2010. The biostratigraphic importance of conchostracans in the continental Triassic of the northern hemisphere. In: Lucas, S.G. (Ed.), The Triassic Timescale. Geological Society of London Special Publications 334, 315–417.

Kozur, H.W. 1989. The Permian-Triassic boundary in marine and continental sediments. *Zentralblatt für Geologie und Paläontologie* I(11-12), 1245-1277.

— 1998. Some aspects of the Permian-Triassic boundary (PTB) and of the possible causes for the biotic crisis around this boundary. *Palaeogeography, Palaeoclimatology, Palaeoecology* 143, 227-272.

— 1999. The correlation of the Germanic Buntsandstein and Muschelkalk with the Tethyan scale. In: Bachmann, G.H. and Lerche, I. (eds) The Epicontinental Triassic, Volume 1. *Zentralblatt für Geologie und Paläontologie* 7–8(7–12), 701–725.

Krauss, G.J., Solé, M., Krauss, G., Schlosser, D., Wesenberg, D., Bärlocher, F. 2011. Fungi in freshwaters: Ecology, physiology and biochemical potential. *FEMS Microbiology Reviews* 35, 620–651.

Krings, M., Dotzler, N., Galtier, J., Taylor, T.N. 2009a. Microfungi from the upper Visean (Mississippian) of central France: Chytridiomycota and chytrid-like remains of uncertain affinity. *Review of Palaeobotany and Palynology* 156, 319–328.

— Galtier, J., Taylor, T.N., Dotzler, N. 2009b. Chytrid-like microfungi in Biscalitheca cf. mU.S.A.ta (Zygopteridales) from the upper Pennsylvanian Grand- Croix cherts (Saint-Etienne basin, France). *Review of Palaeobotany and Palynology* 157, 209-316.

Kuhn, R., Schwerdtner. W. 1959. Nachweis deszendentner Vorgänge während der Entstehung der Leine-Serie des deutschen Zechstein-salzes. *Kali Steinsalz* 2, 380–383.

Kump, L.R., Pavlov, A. & Arthur, M.A. 2005. Massive release of hydrogen sulfide to the surface ocean and atmosphere during intervals of oceanic anoxia. *Geology* 33(5), 397-400.

Kustatscher, E., Wachtler, M. & Van Konijnburg-van Cittert, J.H.A. 2007. Horsetails and seed ferns from the Middle Triassic (Anisian) locality Kühwiesenkopf (Monte Prà della Vacca), dolomites, northern Italy. *Palaeontology* 50(5), 1277-1298.

— Bernardi, M., Petti, F.M., Franz, M., van Konijnenburg-van Cittert, J.H.A., Kerp, H. 2017. Sea-level changes in the Lopingian (late Permian) of the northwestern Tethys and their effects on the terrestrial palaeoenvironments, biota and fossil preservation. *Global and Planetary Change* 148, 166–180.

— Konijnenburg-van Cittert, J.H.A. van, Bauer, K., Butzmann, R., Meller, B., Fischer, T.C. 2012. A new flora from the upper Permian of Bletterbach (Dolomites, N-Italy). *Review of Palaeobotany and Palynology* 182, 1–13.

— Bauer, K., Butzmann, R., Fischer, T.C., Meller, B., Konijnenburg-van Cittert, J.H.A. van, Kerp, H., 2014. Sphenophytes, pteridosperms and possible cycads from the Wuchiapingian (Lopingian, Permian) of Bletterbach (Dolomites, Northern Italy). *Review of Palaeobotany and Palynology* 208, 65-82.

Labandiera, C.C., Kustatscher, E., Wappler, T. 2016. Floral assemblages and patterns of insect herbivory during the Permian to Triassic of Northeastern Italy. *PLoS ONE* 11(11), e0165205.

Langereis, C. G., Krijgsman, W., Muttoni, G., Menning, M. 2010. Magnetostratigraphy – concepts, definitions, and applications. *Newsletters on Stratigraphy* 43, 207–233.

Legler, B., Schneider, J. 2008. Marine ingressions into the Middle/Late Permian saline lake of the Southern Permian Basin (Rotliegend, Northern Germany) possibly linked to sea-level highstands in the Arctic rift system. *Palaeogeography, Palaeoclimatology, Palaeoecology* 267(1-2), 102-114.

— Gebhardt, U., Schneider, J.W. 2005. Late Permian non-marine-marine transitional profiles in the central Southern Permian Basin, northern Germany. *International Journal of Earth Sciences* 94(5–6), 851–862.

Lei, Y., Servais, T., Feng, Q. 2013. The diversity of the Permian phytoplankton. *Review of Palaeobotany and Palynology* 198, 145–161.

Leonova, T.B. 2016. Permian ammonoid biostratigraphy. In: Lucas, S.G. and Shen, S.Z. (eds) The Permian Time- scale. Geological Society, London, Special Publications, 450 pp.

Leschik, G. 1956. Sporen aus dem Salzton des Zechsteins von Neuhof (Fulda). *Palaeontographica Abteilung B* 100, 122– 142.

Leslie, A. 2011. Shifting functional roles and the evolution of conifer pollen-producing and seed-producing cones. *Paleobiology* 37(4), 587-602.

Lewis, R.J., Szava-Kovats, R., Pärtel, M. 2016. Estimating dark diversity and species pools: an empirical assessment of two methods. *Methods in Ecology and Evolution* 7, 104–113.

Lignum, J., Jarvis, I., Pearce, M.A. 2008. A critical assessment of standard processing methods for the preparation of palynological samples. *Review of Palaeobotany and Palynology* 149 (3–4), 133–149.

Lindström, S. 1996. Late Permian palynology of Fossilryggen, Vestfjella, Dronning Maud Land, Antarctica. *Palynology* 20(1), 15–48.

— McLoughlin, S. 2007. Synchronous palynofloristic extinction and recovery after the end-Permian event in the Prince Charles Mountains, Antarctica: implications for palynofloristic turnover across Gondwana. *Review of Palaeobotany and Palynology* 145, 89–122.

Lindström, S., McLoughlin, S., Drinnan, A.N. 1997. Intraspecific variation of taeniate bisaccate pollen within Permian glossopterid sporangia, from the Prince Charles Mountains, Antarctica. *International Journal of Plant Sciences* 158, 673–684.

Lo, C.H., Chung, S.L., Lee, T.Y., Wu, G. 2002. Age of the Emeishan flood magmatism and relations to Permian–Triassic boundary events. *Earth and Planetary Science Letters* 198, 449–458.

Loffler, J., Schulze, G. 1962. Die Kali- und Steinsalzlagerstätten des Zechsteins in der deutschen demokratischen Republik, 3. Sachsen-Anhalt. *Freiberger Forschungshefte C* 97(3), 347 pp.

Logan, A. 1962. A revision of the palaeontology of the Permian limestones of County Durham. Unpublished Ph.D. Thesis, University of Newcastle upon Tyne.

— 1967. The Permian Bivalvia of Northern England. Monograph of the Palaeontographical Society, London, 72 pp.

Looy, C.V., Twitchett, R.J., Dilcher, D.L., Van Konijnenburg-Van Cittert, J.H.A., Visscher, H. 2001. Life in the end-Permian dead zone. *Proceedings of the National Academy of Sciences of the United States of America* 98, 7879–7883.

Lucas, S.G. 2006. Global Permian tetrapod biostratigraphy and biochronology. In: Lucas, S.G., Cassinis, G. and Schneider, J.W. (eds) Non-marine Permian Biostratigraphy and Biochronology. Geological Society, London, Special Publications 265, 65–93.

— Shen, S.Z. 2016. (eds) The Permian Timescale. Geological Society, London, Special Publications, 450 pp.

Madler, K. 1957. Ullmannia-Blatter und andere Koniferenrests aus dem Zechstein der Bohrung Friedrich Henrich 57. *Geologisches Jahrbuch* 73, 75-90.

Magraw, D., Clarke, A.M., Smith, D.B. 1963. The stratigraphy and structure of part of the south-east Durham coalfield. *Proceedings of the Yorkshire Geological Society* 34,153-208.

Malzahn, E., Rabitz, A. 1962. Ain Aufschluss in Zechstein-Randfazies im Hunxer Graben bei Bottrop und seine Fauna. In: Visscher, H. 1971. The Permian and Triassic of the Kingscourt Outlier, Ireland: A palynological investigation related to regional stratigraphical problems in the Permian and Triassic of Western Europe. Geological Survey of Ireland Special Paper No. 1. 114 pp.

Malzahn, E. 1968. Uber neue Funde von *Janassa bituminosa* (Schloth.) im neiderrheinisschen Zechstein. *Geologisch Jarhbuch* 85, 67–96.

Marie, J.P.P. 1975. Rotliegendes stratigraphy and diagenesis. In: Woodland, A.W. (editor) Petroleum and the continental shelf of north-west Europe. Vol. 1, Geology. Applied Science Publishers Ltd: Institute of Petroleum, Great Britain.

Marmottant, P., Ponomarenko, A., Bienaimé, D. 2013. The walk and jump of Equisetum spores. *Proceedings of the Biological Society* 280(1770), 20131465.

Massari, F., Conti, M.A., Fontana, D., Helmold, K., Mariotti, N., Neri, C., Nicosia, U., Ori, G.G., Pasini, M. et al. 1988. The Val Gardena Sandstone and BellerophonFormation in the Bletterbach gorge (Alto Adige, Italy): biostratigraphy and sedimentology. *Memorie di Scienze Geologiche* 40, 229–273.

Massari, F., Neri, C., Fontana, D., Manni, R., Mariotti, N., Nicosia, U., Pittau, P., Spezzamonte, M., Stefani, C., 1999. Excursion 3: The Bletterbach section (Val Gardena Sandstone and Bellerophon Formation), in: Stratigraphy and Facies of the Permian Deposits between Eastern Lombardy and Western Dolomites - Field Trip Guidebook. Presented at the International Fiel Conference on "The Continental Permian of the Southern Alps and Sardinia (Italy). Regional Reports and General Correlations," Brescia, Italy, pp. 111–134.

Massari, F., Neri, C., Pittau, P., Fontana, D., Stefani, C. 1994. Sedimentology, palynostratigraphy and sequence stratigraphy of a continental to shallow-marine rift-related succession: Upper Permian of the eastern Southern Alps (Italy). *Geological Sciences Memoirs* 46, 119–243.

Mawson, M., Tucker, M. 2009. High-frequency cyclicity (Milankovitch and millennial-scale) in slope-apron carbonates: Zechstein (Upper Permian), North-east England. *Sedimentology* 56, 1095-1936.

McCann, T., Kiersnowski, H., Krainer, K., Vozárová, A., Peryt, T.M., Oplustil, S., Stollhofen, H., Schneider, J., Wetzel, A., Boulvain, F. et al. 2008. Permian. In: The Geology of Central Europe, McCann, T. (ed.), Volume 1: Precambrian and Palaeozoic. The Geological Society of London: London; pp. 531–597.

McKay, J. 2019. *Trilobites, Dinosaurs and Mammoths: An Introduction to the Prehistory of the British Isles.* Published by The Palaeontological Association, Distributed by GSL. pp. 96.

McKie, T. 2017. Chapter 7 - Paleogeographic Evolution of Latest Permian and Triassic Salt Basins in Northwest Europe, Editor(s): Soto, J.I., Flinch, F.J., Tari, G. 2017. Permo-Triassic Salt Provinces of Europe, North Africa and the Atlantic Margins, Elsevier. pp. 159-173.

McLoughlin, S., Lindström, S., Drinnan, A.N. 1997. Gondwanan floristic and sedimentological trends during the Permian–Triassic transition: new evidence from the Amery Group, northern Prince Charles Mountains, East Antarctica. *Antarctic Science* 9, 281–298.

McMinn, A. 1982. Late Permian acritarchs from the northern Sydney Basin. *Journal and Proceedings of the Royal Society of New South Wales* 115, 79–86.

Meier, R. 1977. Turbidite und Olisthostrome- sedimentationsphanomene des Werra-Sulfats (Zechstein 1) am Osthang der Eiehsfeld-Schwelle im Gebiet des Siidharzes [in German]. In: Smith, D.B. 1989. The late Permian palaeogeography of north-east England. *Proceedings of the Yorkshire Geological Society* 47, 285-312.

Menning, M., Alekseev, A.S. et al. 2006. Global time scale and regional stratigraphic reference scales of central and west Europe, east Europe, Tethys, south China, and North America as used in the Devonian-Carboniferous-Permian Correlation Chart 2003 (DCP 2003*). Palaeogeography, Palaeoclimatology, Palaeoecology* 240, 318–372.

Menning, M., Gast, R., Hagdorn, H., Käding, K.-C., Szurlies, M., Nitsch, E. 2005. Die Zeitskala für die höhere Dyas und die Germanische Trias der Stratigraphischen Tabelle von Deutschland 2002. *Newsletters on Stratigraphy* 41, 173–210.

Mertmann, D. 2003. Evolution of the marine Permian carbonate platform in the Salt Range (Pakistan). *Palaeogeography, Palaeoclimatology, Palaeoecology* 191, 373–384.

Metcalfe, I., Foster, C.B., Afonin, S.A., Nicoll, R.S., Mundil, R., Xiaofeng, W., Lucas, S.G. 2009. Stratigraphy, biostratigraphy and C-isotopes of the Permian–Triassic non-marine sequence at Dalongkou and Luaogou, Xinjiang Province, China. *Journal of Asian Earth Sciences* 36, 503–520.

Meyen, S.V. 1984. Basic features of gymnosperm systematics and phylogeny as shown in the fossil record. *The Botanical Review* 50, 1–111.

— 1997. Permian conifers of western Anagaraland. *Review of Palaeobotany and Palynology* 96, 351–447.

Millay, M.A., Eggert, D.A. 1974. Microgametophyte development in the Paleozoic seed fern family Callistophytaceae. *American Journal of Botany* 61, 1067–1075.

— Taylor, T.N. 1978. Chytrid-like fossils of Pennsylvanian age. *Science* 200, 1147–1149.

Mondal, S., Harries, P.J. 2016. Phanerozoic trends in ecospace utilization: the bivalve perspective. *Earth Science Reviews* 152, 106–118.

Montañez, I.P., Tabor, N.J., Niemeier, D., DiMichele, W.A., Frank, T.D., Fielding, C.R., Isbell, J.L., Birgenheier, L.P., Rygel, M.C. 2007. CO2-forced climate and vegetation instability during Late Paleozoic deglaciation. *Science* 315, 87–91

Mosler, H. 1966. Der Stoffbestand und Fossilinhalt des grauen Salztones im sudlichen Bereich der Deutschen Demokratischen Republik. In Visscher, H. 1971. The Permian and Triassic of the Kingscourt Outlier, Ireland: A palynological investigation related to regional stratigraphical problems in the Permian and Triassic of Western Europe. Geological Survey of Ireland Special Paper No. 1. 114 pp.

Moss, M. 1986. The geochemistry and environmental evolution of the Hampole Beds at the type area of the Cadeby Formation (Lower Magnesian Limestone). *American Geologist* 10, 115-125.

Mulholland, P., Esestime, P., Rodriguez, K., Hargreaves, P.J. 2018. The role of palaeo-relief in the control of Permian facies distribution over the Mid North Sea High, U.K.CS. *Geological Society Special Publications* 471(1), 155

Mundil, R., Ludwig, K.R., Metcalfe, I., & Renne, P.R. 2004. Age and timing of the Permian mass extinctions: U/Pb dating of closed-system zircons. Science 305, 1760-1763.

Murchison, R.I. 1841. First sketch of some of the principal results of a second geological survey of Russia. *The Philosophical Magazine* 19, 417–422.

Nader, A.D., Khalaf, F.H. & Hadid, A.A. 1993a. Palynology of the Permo-Triassic boundary in Borehole Mityah-1, south west Mosul City, Iraq. *Mu'tah Journal Research and Studies* 8, 223–280.

— Khalaf, F.H. & Yousif, R.A. 1993b. Palynology of the upper part of the Ga'ara Formation in the western Iraqi desert. *Mu'tah Journal Research and Studies* 8, 77–137.

Naugolnykh, S.V. 2014. A new genus of male cones of voltzialean affinity, *Uralostrobus voltzioides* nov. gen., nov. sp., from the Lower Permian of the Urals (Russia). *Geobios* 47, 315-324.

Nawrocki, J. 1997. Permian to Early Triassic magnetostratigraphy from the Central European Basin in Poland: Implications on regional and worldwide correlations. *Earth and Planetary Science Letters* 152, 37–58.

— 2004. The Permian-Triassic boundary in the Central European Basin: magnetostratigraphic constraints. *Terra Nova* 16, 139–145.

— Kuleta, M., Zbroja, S. 2003. Buntsandstein magnetostratigraphy from the northern part of the Holy Cross Mountains. *Geological Quarterly* 47, 253–260.

Nishida, H., Pigg, K.B., Rigby, J.F. 2003. Swimming sperm in an extinct Gondwanan plant. *Nature* 422, 396–397.

Nowak, H., Schneebeli-Hermann, E., Kutatscher, E. 2019. No mass extinction for land plants at the Permian-Triassic transition. *Nature Communications* 10, 385.

Ogg, J.G., Ogg, G., Gradstein, F.M. 2008. The Concise Geologic Time Scale. Cambridge University Press, New York. 177 pp.

Orłowska-Zwolinska, T. 1962. A first finding of Zechstein sporomorphs in Poland [in Polish, English summary]. *Kwartalnik Geologiczny* 6, 283-298.

Osborn, J.M., Taylor, T.N.,1993. Pollen morphology and ultrastructure of the Corystospermales: permineralized in situ grains from the Triassic of Antarctica. *Review of Palaeobotany and Palynology* 79, 205–219.

Oszczepalski, S., Rydzewski, A. 1987. Paleogeography and sedimentary model of the Kupferschiefer in Poland. In: The Zechstein Facies in Europe, Peryt, T.M. (ed.), Lecture Notes in Earth Sciences 10,189–205.

Ouyang, S. 1982. Upper Permian and Lower Triassic palynomorphs from eastern Yunnan, China. *Canadian Journal of Earth Sciences* 19(1), 68-80.

— 1986. Palynology of Upper Permian and Lower Triassic strata of Fuyuan district, Eastern Yunnan. *Acta Palaeontologica Sinica* 169, 1-122 [in Chinese, English summary].

— Utting, J. 1990. Palynology of upper Permian and lower Triassic rocks, Meishan, Changxing County, Zhejiang Province, China. *Review of Palaeobotany and Palynology* 66(102), 65-103.

Pancost, R.D., Crawford, N., Maxwell, J.R. 2002. Molecular evidence for basin-scale photic zone euxinia in the Permian Zechstein Sea. *Chemical Geology* 188, 217–227.

Pant, D.D., Nautiyal, D.D. 1960. Some seeds and sporangia of Glossopteris flora from Raniganj coalfield, India. *Palaeontographica* 107B, 41-64.

— Mishra, S.N. 1986. On Lower Gondwana megaspores from India. *Palaeontographica* 198, 13–73.

Pattison, J. 1981. Permian, in Stratigraphical Atlas of Fossil Foraminifera, 2nd eds (eds D.G. Jenkins and J.W. Murray), Ellis Harwood, Chichester, pp. 70-7.

— Smith, D.B. & Warrington, G. 1973. A review of Late Permian and Early Triassic biostratigraphy in the British Isles. 220-260. In: Logan, A., Howse, L.V. (eds), 1973. The Permian and Triassic Systems and their Mutual Boundary. Memoir (Canadian Society of Petroleum Geologists) 2, 766 pp.

Paul, J. 1982. Environmental analysis of basin and schwellen facies in the lower Zechstein of Germany. *Geological Society of London Special Publications* 22, 143-147.

— 1986. Stratigraphy of the Lower Werra Cycle (Zl) in West Germany (preliminary results). In: Harwood, G. M. & Smith, D. B. (editors) q.v.

— 1987. Der Zechstein am Harzrand: Querprofil über eine permische Schwelle. In: Internationales Symposium Zechstein 1987, Exkursionsführer I.I., Kulick, J., Paul, J. (eds). Hessisches Landesamt für Bodenforschung und Industriedienst: Wiesbaden. pp.193–293

— 2006. Der Kupferschiefer: Lithologie, Stratigraphie, Fazies and Metallogenese eines Schwarzschiefers. *Zeitschrift der Deutschen Gesellschaft für Geowissenschaften* 157, 57–76.

Paysen, T.E., Ansley, R.J., Brown, J.K., Gottfried, G.J., Haase, S.M., Harrington, M.G., Narog, M.G., Sackett, S.S., Wilson, R.C. 2000. Fire in western shrubland, woodland, and grassland ecosystems. In: Wildland Fire in Ecosystems: Effects of Fire on Flora. USDA Forest Service General Technical Reports RMRS-GTR-42 2, 121-158.

Pertescu, I., Bican-Brişan, N. 2005. First palynological submitted on the salt deposit from Praid (NE Transylvania). Contribuţii Botanice 40, 301–306.

— Bican-Brişan, N., Mera, O. 1999. Paleoclimatic and environmental conditions during genesis of evaporitic formation from Truda-Cheia area (Western Transylvanian Basin, Romania) based on palynological investigations. *Acta Palaeontologica Romaniae* 2, 361–368.

Peryt, T.M. 1984. Sedymentacja i wczesna diageneza utworów wapienia cechsztyńskiego w Polsce Zachodniej [in polish, English summary and figure captions*]. Prace Państwowego Instytutu Geologicznego* 109, 1–70.

— 1992. Debris-flow deposits in the Zechstein (Upper Permian) Main Dolomite of Poland, significance for the evolution of the basin. *Neues Jahrbuch für Geologie und Paläontologie Abhandlungen* 185, 1–19.

— Piathowski, T.S. 1976. Osady caliche w wapieniu cechsztynskim zachodniej czesci syneklizny perybaltyciej [in Polish]. *Kwartalnik Geologiczny* 20, 525-537.

— Peryt, D. 1977. Zechstein foraminifera from the Fore-Sudetic monocline area (West Poland) and their paleoecology. *Annales Societatis Geologorum Poloniae* 47, 301–326. [In Polish with English summary]

— Dyjaczyński, K. 1991. An isolated carbonate bank in the Zechstein Main Dolomite Basin, western Poland. *Journal of Petroleum Geology* 14, 445-458.

— Peryt, D. 2012. Geochemical and foraminiferal records of environmental changes during Zechstein Limestone (Lopingian) deposition in Northern Poland. *Geological Quarterly* 56(1), 187-198.

— Kasprzyk, A., Czapowski, G. 1996. Basal Anhydrite and Screening Anhydrite (Zechstein, Upper Permian) in Poland. *Bulletin of the Polish Academy of Sciences, Earth Sciences* 44, 131-140.

— Hałas, S., Peryt, D. 2015. Carbon and oxygen isotopic composition and foraminifers of condensed basal Zechstein (Upper Permian) strata in western Poland: environmental and stratigraphic implications. *Journal of Geology* 50, 446–464

— Antoniowicz, L., Gasieqicz, A., Roman, S. 1989. O fazach sedymentacji dolomite glownego w Polsce polnocno-zachodniej [in Polish]. *Przeglad Geologiczny* 37, 187-193.

— Raczyński, P., Peryt, D., Chłódek, K. 2012. Upper Permian reef complex in the basinal facies of the Zechstein Limestone (Ca1), western Poland. *Geological Quarterly* 47, 537-533.

— Geluk, M. C., Mathiesen, A., Paul, J., Smith, K. 2010. Zechstein. In: Doornenbal, J.C. and Stevenson, A. G. (eds) Petroleum Geological Atlas of the Southern Permian Basin Area. European Association of Geoscientists and Engineers, Houten. pp. 123–147.

Pettigrew, T.H., Athersuch, J. & Wilkinson, I. (eds) 1980. Biostratigraphical Atlas of British Ostracods, Chapman and Hall, London. pp. 350.

Phuphumirat, W., Gleason, F.H., Phongpaichit, S., Mildenhall, D.C. 2011. The infection of pollen by zoosporic fungi in tropical soils and its impact on pollen preservation: A preliminary study. *Nova Hedwigia* 92, 233–244.

Pittau, P. 1999. Excursion 3: the Bletterbach section (Val Gardena Sandstone and Bellerophon Formation). 3. Palynology. Stratigraphy and facies of the Permian deposits between Eastern Lombardy and the Western Dolomites. Field trip guidebook 23–25.

— Kerp, H., Kustatscher, E., 2005. "Let us meet across the P/T boundary"—workshop on Permian and Triassic Palaeobotany and Palynology, Bozen. The Bletterbach canyon. Naturmuseum Südtirol/Museo Scienze Naturali Alto Adige/Museum Natöra Südtirol, 26 pp.

Podoba, B.G. 1975. Spores and pollen. In: Suveizdis, P. (ed.), Permian deposits of the Baltic area (stratigraphy and gauna); Lietuvos Geologijos Mokslinio Tyrimo Institutas, Darbai, Mintis, Vilnius 29, 184-192 (In Russian; English summary p. 196-207).

Poort, R.J. & Kerp, H. 1990. Aspects of Permian palaeobotany and palynology XI. On the recognition of true peltasperms in the Upper Permian of western and central Europe and a reclassification of species formerly included in Peltaspermum Harris. *Review of Palaeobotany and Palynology* 63, 197-225.

Poort, R. J., Clement-Westerhof, J.A., Looy, C.V., Visscher, H., 1997. Aspects of Permian palaeobotany and palynology XVII. Conifer extinction in Europe at the Permian-Triassic junction: Morphology, ultrastructure and geographic/stratigraphic distribution of Nuskoisporites dulhuntyi (prepollen of Ortiseia, Walchiaceae). *Review of Palaeobotany and Palynology* 97(1-2), 9-39.

Potonié, R., 1962. Synopsis der Sporae in situ. *Beiheste zum Geologische Jahrbuch* 52, 1–204.

— Schweitzer, H.-J. 1960. Der Pollen von Ullmannia frumentaria. *Paleontologicheskii Zhurnal* 34, 27-39.

Prentice, I.C. 1985. Pollen analysis theory: pollen deposition and source area in model basins. *Quaternary Research* 23, 76-86.

Prevec, R., Gastaldo, R.A., Neveling, J., Reid, S.B., Looy, C.V. 2010. An autochthonous glossopterid flora with latest Permian palynomorphs and its depositional setting in the Dicynodon Assemblage Zone of the southern Karoo Basin, South Africa. *Paleogeography, Palaeoclimate, Palaeoecology* 292, 391–408.

Pryor, W.A. 1971. Petrology of the Permian Yellow Sands of northeastern England and their North Sea Basin equivalents. *Sedimentary Geology* 6, 221-254.

Qiu, Y.-L., A.B. Taylor, & H.A. McManus. 2012. Evolution of the life cycle in land plants. *Journal of Systematics and Evolution* 50, 171–194.

Raine, J.I., Mildenhall, D.C., Kennedy, E.M. 2011. New Zealand Fossil Spores and Pollen: An Illustrated Catalogue, 4th edition. GNS Science miscellaneous series no. 4.

Ramanathan, V., Crutzen, P.J., Kiehl, J.T., Rosenfeld, D. 2001. Aerosols, climate, and the hydrological cycle. *Science* 294, 2119-2124.

Ramezani, J., Bowring, S.A. 2017. Advances in numerical calibration of the Permian timescale based on radioisotopic geochronology. In: Lucas, S.G. & Shen, S.Z. (eds) The Permian Timescale. Geological Society, London, Special Publications, 450.

Rampino, M., Eshet, Y. 2018. The fungal and acritarch events as time markers for the latest Permian mass extinction: an update. *Geoscience Frontiers* 9, 147–154.

Raymond, L.R. 1953. Some geological results from the exploration for potash in north-east Yorkshire. *Quarterly Journal of the Geological Society of London* 108, 383-310.

Rees, P. M. 2002. Land-plant diversity and the end-Permian mass extinction. *Geology* 30(9), 827-830.

— Gibbs, M.T., Ziegler, A.M., Kutzbach, J.E., Behling, P.J. 1999. Permian climates: Evaluating model predictions using global paleobotanical data. *Geology* 27, 891–894

— Ziegler, A.M., Gibbs, M.T., Kutzbach, J.E., Behling, P.T., Rowley, D.B. 2002. Permian Phytogeographic Patterns and Climate Data/Model Comparisons. *The Journal of Geology* 110(10), 1-31.

Reissinger, A. 1938. Die Pollenanalyse ausgedehnt auf alle Sedimentgesteine der geologischen Vergangenheit. *Palaeontographica Abteilung B* 84, 1–20.

Retallack, G.J. 1995. Permian-Triassic life crisis on land. *Science* 267, 77-80.

— 2002. Lepidopteris callipteroides, an early Triassic seedfern of the Sydney Basin, southeastern Australia. *Alcheringa* 1, 475–500.

— 2013. Global Cooling by Grassland Soils of the Geological Past and Near Future. *Annual Review of Earth and Planetary Sciences* 41, 69-86.

Richter-Bernburg, G. 1955. Stratigraphische Gliederung des deutschen Zechstein. *Zeitschrift für Geologische Wissenschaften* 105, 843–854.

— 1982. Stratogenese des Zechsteinkalkes am Westharz. Zeitschrift der Deutschen Geologischen Gesellschaft 133,381-401.

— 1985. Zechstein-Anhydrite - Fazies und Genese. Geologisches Jahrbuch Reihe A 85, 3-82.

Riding, J.B., Kyffin-Hughes, J.E. 2010. The use of pre-treatments in palynological processing. *Review of Palaeobotany and Palynology* 158(3–4), 281–290.

Robinson, J.E. 1978. Permian. In: A Stratigraphical Index of British Ostracoda (eds R.H. Bate and J.E. Robinson), Seel House Press, Liverpool, pp. 47-96.

Röhling, H.-G., 1993. Der Untere Buntsandstein in Nordwest- und Nordostdeutschland – Ein Beitrag zur Vereinheitlichung der stratigraphischen Nomenklatur. *Geologisches Jahrbuch A* 142, 149–183.

Roscher, M. 2009. Environmental reconstruction of the Late Palaeozoic – numeric modelling and geological evidences. PhD thesis, University of Freiberg.

— Schneider, J.W. 2006. Permo-Carboniferous climate: early Pennsylvanian to Late Permian climate development of central Europe in a regional and global context. In: Lucas, S. G., Cassinis, G. & Schneider, J.W. (eds) Non-Marine Permian Biostratigraphy and Biochronology. Geological Society, London, Special Publications 265, 95–136.

— Berner, U., Schneider, J.W. 2008. A tool for the assessment of the Paleodistribution of source and reservoir rocks. *OIL GAS European Magazine* 34, 131–137.

— Stordal, F., Svensen, H. 2011. The effect of global warming and global cooling on the distribution of the latest Permian climate zones. *Palaeogeography, Palaeoclimatology, Palaeoecology* 309, 186–200.

Rothman, D.J. 2002. Atmospheric carbon dioxide levels for the last 500 million years. *Proceedings of the National Academy of Sciences* 99(7), 4167-4171.

Rothwell, G. W., Mapes, G., Hernandez-Castillo, G. R., 2005. *Hanskerpia* gen. nov. and phylogenetic relationships among the most ancient conifers (Voltziales). *Taxon* 54, 733–750.

Rowan, M.G. 2017. Chapter 4 - An Overview of Allochthonous Salt Tectonics, Editor(s): Soto, J.I., Flinch, F.J. & Tari, G. 2017. Permo-Triassic Salt Provinces of Europe, North Africa and the Atlantic Margins, Elsevier. pp. 97-114.

Royer, D. L. 2006. CO2-forced climate thresholds during the Phanerozoic. *Geochimica et Cosmochimica Acta* 70(23 SPEC. ISS.), 5665–5675.

— Berner, R.A., Beerling, D.J. 2001. Phanerozoic CO2 change: evaluating geochemical and paleobiological approaches. *Earth Science Reviews* 54, 349–392.

Sarjeant, W.A.S. 1970. Acritarchs and tasmanitids form the Chhidru Formation, uppermost Permian of West Pakistan, Stratigraphic Boundary Problems. *Permian and Triassic of West Pakistan, Special Publication* 4, 277–304.

Sauer, E. 1964. Das Perm am Schiefergebirgsrand zwischen Gilsserberg und Lollar. Diss Univ Marburg, pp. 115. In: Poort, R.J., Kerp, H.H.F. 1990. Aspects of Permian palaeobotany and palynology. XI. On the recognition of true peltasperms in the Upper Permian of Western and Central Europe and a reclassification of species formerly included in Peltaspermum Harris. *Review of Palaeobotany and Palynology* 63, 197-225.

Schaarschmidt, F. 1963. Spores und Hystrichosphaerideen ays dem Sechstein von Budingen in der Wetterae. *Palaeontographica Abteilung B* 113, 38-91.

Schaumberg, G. 1996. Über wenig bekannt Acrolepiden aus dem oberpermischen Kupferschiefer und Marl-Slate von Deutschland und England. *Philippia* 7(5), 325–354

— 1978. Neuebeschriebung von Coelacanthus granulus Agassiz (Actinistia, Pisces) aus dem Kupferschiefer von Richelsdorf (Perm, W-Deutschland). *Paläontologische Zeitschrift* 52, 169–267.

Schlager, W., Bolz, H. 1977. Clastic accumulation of sulphates in deep water. *Journal of Sedimentary Petrology* 42, 600-609.

Schneebeli-Herman, E., Hochuli, A., Bucher, H. 2017. Palynofloral associations before and after the Permian – Triassic mass extinction, Kap Stosch, East Greenland. *Global and Planetary Change* 155, 178-195.

— Kürschner, W.M., Kerp, H., Bomfleur, B., Hochuli, P.A., Bucher, H., Ware, D., Roohi, G. 2015. Vegetation history across the Permian-Triassic boundary in Pakistan (Amb section, Salt Range). *Gondwana Research* 24, 911–924.

Schneider, J.W., Scholze, F. 2016. Late Pennsylvanian–Early Triassic conchostracan biostratigraphy: a preliminary approach. In: Lucas, S.G. & Shen, S.Z. (eds) The Permian Timescale. Geological Society, London, Special Publications. 450 pp.

Schulze, E. 1966. Erlauterungen zur Tabelle der stratigraphischen Verbreitund der Sporen und Pollen von oberen Perm bis untersten Lias. *Abhandlungen des Zentralen Geologischen Instituts* 8, 3-10.

Schuster, A. 1933. OberRotliegends und Zechstein in Sachsen. *Abhandlung des Sächsischen Geologischen Landesamtes* 13, 85 pp.

Schweitzer, H.-J. 1960. Die Makroflora des niederrheinischen Zechsteins. Fortschritte in der Geologie von Rheinland und Westfalen 6, 1–46.

— 1962. Die Makroflora des niederrheinischen Zechsteins. *Fortschritte in der Geologie von Rheinland und Westfalen* 6, 331–376.

— 1963. Der weibliche Zapfen von Pseudovoltzia liebeana and seine Bedeutung für die Phylogenie der Koniferen. *Palaeontographica Abteilung B* 113, 1–29

— 1968. Die Flora des Ober Perms in Mitteleuropa. *Naturwissenschaften Rundschau* 21, 93–102.

— 1986. The land flora of the English and German Zechstein sequences. In: Harwood, G.M., Smith, D.B. (eds) The English Zechstein and Related Topics. Geological Society, London, Special Publications 22, 31–54.

Scotese, C.R., Lanford, R.P. 1995. Pangea and the paleogeography of the Permian. In Golonka, J., and Ford, D. 2000. Pangean (Late Carboniferous-Middle Jurassic) paleoenvironment and lithofacies. *Palaeogeography, Palaeoclimatology, Palaeoecology* 161(1–2), 1–34.

Sedgwick, A. 1829. On the geological relations and internal structure of the Magnesian Limestone, and the lower portions of the New Red Sandstone in their range through Nottinghamshire, Derbyshire, Yorkshire, and Durham, to the southern extremity of Northumberland. *Transactions of the Geological Society of London* 3, 37-124.

Sekimoto, S., Rochon, D., Long, J.E., Dee, J.M., Berbee, M.L. 2011. A multigene phylogeny of Olpidium and its implications for early fungal evolution. *BMC Evolutionary Biology* 11, 331.

Şengor, A.M.C., Atayman, S. 2009. The Permian extinction and the Tethys: an exercise in global geology. *Geological Society of America Special Papers* 448, 1–85.

Sephton, M., Visscher, H., Looy, C.V., Verchovsky, A.B., Watson, J.W. 2009. Chemical constitution of a Permian-Triassic disaster species. *Geology* 37(10), 875-878.

Shaffer, B.L. 1964. Stratigraphic and paleoecologic significance of plant microfossils in Permian evaporites of Kansas. In: Cross AT, ed. Palynology in oil exploration, 97–115. Society of Economic Paleontologist and Mineralogist Special Publication 11. Tulsa, OK: Society of Economic Paleontologist and Mineralogist.

Sheilds, C., Kiehl, T. 2018. Monsoonal precipitation in the Paleo-Tethys warm pool during the latest Permian. *Palaeogeography, Palaeoclimatology, Palaeoecology* 291, 123-136.

Sherlock, R.L. 1911. The relationship of the Permian to the Trias in Nottinghamshire. Quarterly *Journal of the Geological Society of London* 67,75-117.

Shouxin, Z., Yongyi, Z., 1991. The geology of China. In: Moullade, M., Nairn, A.E.M. (Eds.), The Phanerozoic Geology of the World. The Paleozoic Elsevier, Amsterdam, pp. 219-274.

Slater, B.J., McLoughlin, S., Hilton, J. 2015. A high-latitude Gondwanan lagerstätte: the Permian permineralised peat biota of the Prince Charles Mountains, Antarctica. *Gondwana Research* 27, 1446–1473.

Słowakiewicz, M., Kiersnowski, H., Wagner, R. 2009. Correlation of the Middle and Upper Permian marine and terrestrial sedimentary sequences in Polish, German, and U.S.A. Western Interior Basins with reference to global timemarkers. *Palaeoworld* 18, 193–211.

— Tucker, M., Perri, E., Pancost, R. 2015. Nearshore euxinia in the photic zone of an ancient sea. *Palaeogeography, Palaeoclimatology, Palaeoecology* 426, 242-259.

— Tucker, M., Hindenberg, K., Mawson, M., Idiz, E., Pancost, R. 2016. Nearshore euxinia in the photic zone of an ancient sea: Part II – The bigger picture and implications for understanding ocean anoxia. *Palaeogeography, Palaeoclimatology, Palaeoecology* 461. 432-448.

Smith, D.B. 1958. Some observations on the Magnesian Limestone reefs of north-eastern Durham. Geological Survey of Great Britain Bulletin 15,71-84.

— 1970a. Permian and Trias. pp. 66-91. In: Hickling, G. (editor) *The geology of Durham County. Transactions of the Natural History Society of Northumberland, Durham and Newcastle upon Tyne* 41.

— 1970b. The palaeogeography of the English Zechstein. pp. 20-23. In: Dellwig, L. F. and Rau, J. L. (editors) Third symposium on salt. Northern Ohio Geological Society, Cleveland.

— 1970c. Submarine slumping and sliding in the Lower Magnesian Limestone of Northumberland and Durham. Proceedings of the Yorkshire Geological Society 38,1-36.

— 1971. Possible displacive halite in the Permian Upper Evaporite Group of northeast Yorkshire. *Sedimentology* 17, 221-232.

— 1973. The origin of the Permian Middle and Upper Potash deposits of Yorkshire: an alternative hypothesis. *Proceedings of the Yorkshire Geological Society* 39, 237-246.

— 1974a. The stratigraphy and sedimentology of Permian rocks at outcrop in north Yorkshire. *Journal of Earth Sciences* 8, 365-386.

— 1974b. Permian. pp. 115-144. In: Rayner, D. H. and Hemingway, J. E. (editors) The geology and mineral resources of Yorkshire. Yorkshire Geological Society Occasional Publication 2.

— 1980. The evolution of the English Zechstein Basin. pp. 7-34. In: Fuchtbauer, H. & Peryt, T.M. (editors) q.v.

— 1981. The Magnesian Limestone (Upper Permian) reef complex of north-eastern England. pp. 161-186. In: Toomey, D. F. (editor) European fossil reef models. Society of Economic Paleontologists and Mineralogists Special Publication 30.

— 1985. Gravitational movements in Zechstein carbonate rocks in north-east England. Pp. F1-F12. In: Taylor, J. C. M. (editor) The role of evaporites in hydrocarbon exploration (JAPEC Course Notes No. 39). Geological Society, London.

— 1986. The Trow Point Bed - a deposit of Upper Permian marine oncoids, peloids and columnar stromatolites in the Zechstein of north-east England. pp. 113-125.

— 1989. The late Permian palaeogeography of north-east England. *Proceedings of the Yorkshire Geological Society* 47, 285-312.

— Francis, E.A. 1967. The geology of the country between Durham and Hartlepool. Memoir of the Geological Survey of Great Britain, Sheet 27.

— Crosby, A. 1979. The regional and stratigraphical context of Zechstein 3 and 4 potash deposits in the British sector of the southern North Sea and adjoining land areas. *Economic Geology* 74, 397-408.

— Taylor, J.C.M. 1992. Permian. In: Cope, J.C.W., Ingham, I.K., Rawson, P.F. (Eds.), Atlas of Palaeogeography and Lithofacies. Geological Society, London, Memoirs Vol. 13, 87–95.

— Brunstrom, R.G.W., Manning, P.I., Simpson, S., Shotton, F.W., 1974. A Correlation of the Permian Rocks of the British Isles. Geological Society, London, Special Reports 5, 45 pp.

Smith, F.W., Dearlove, J.P.L., Kemp, S.J., Bell, C.P., Milne, C.J., Pottas, T.L. 2014. Potash - Recent exploration developments in North Yorkshire. pp. 45-50 in Hunger, E., Brown, T.J., Lucas, G. (Eds.) Proceedings of the 17th Extractive Industry Geology Conference, EIG Conferences Ltd. 202 pp.

Soffel, H.C., Wippern, J. 1998. Magnetostratigraphy of Upper Permian and Lower Triassic Rocks from the Drill Site Obernsees near Bayreuth, Germany. *Geologica Bavarica* 103, 275–294.

Solms-Laubach, H. Graf Von 1884. Die Coniferenformen des deutschen Kupferschiefers und Zechsteins. *Palaeontologische Abhandlungen* 2(2), 81–116.

Sørensen, A.M., Håkansson, E., Stemmerik, L. 2007, Faunal migration into the Late Permian Zechstein Basin - Evidence from bryozoan palaeobiogeography. *Palaeogeography, Palaeoclimatology, Palaeoecology* 251(2), 198-209.

Soto, J.I., Flinch, J.F., Tari, G. 2017. 1 - Permo-Triassic Basins and Tectonics in Europe, North Africa and the Atlantic Margins: A Synthesis, Editor(s): Juan I. Soto, Joan F. Flinch, Gabor Tari, Permo-Triassic Salt Provinces of Europe, North Africa and the Atlantic Margins, Elsevier, pp. 3-41.

Southwood, D.A. 1985. The taxonomy and palaeoecology of bryozoa from the Upper Permian Zechstein reef of NE England. Unpublished Ph.D. Thesis, University of Durham.

Spear, J.R., Ley, R.E., Berger, A.B., Pace, N.R. 2003. Complexity in natural microbial ecosystems: the Guerrero Negro. *The Biological Bulletin* 204, 168–173.

Spina, A., Cirilli, S., Utting, J., Jansonius, J. 2015. Palynology of the Permian and Triassic of the Tesero and Bulla sections (Western Dolomites, Italy) and consideration about the enigmatic species Reduviasporonites chalastus. *Review of Palaeobotany and Palynology* 218, 3–14.

— Vecoli, M, Riboulleau, A., Clayton, G., Cirilli, S., Di Michele, A., Marcoguiseppe, A., Rettori, R., Sassi, P., Servais, T. et al. 2018. Application of Palynomorph Darkness Index (PDI) to assess the thermal maturity of palynomorphs: A case study from North Africa. *International Journal of Coal Geology* 188, 64-78.

Srivastava, S.C., Srivastava, A.K., Bhattacharyya, A.P., Tewari, R. 1999. Degraded Permian palynomorphs from North-East Himalaya, India. *Permophiles* 33, 32–36.

Steele, R.P. 1981. Aeolian sands and sandstones. Unpublished Ph.D. thesis, University of Durham.

— 1983. Longitudinal draa in the Permian Yellow Sands of north-east England. pp. 543-550. In: Brookfield, M. E. & Ahlbrandt, T. S. (editors) Eolian sediments and processes. Developments in Sedimentology 38. Elsevier, Amsterdam.

Steemans, P., Breuer, P., Petus, E., Prestianni, C., de Ville de Goyet, F., Gerrienne, P. 2011. Diverse assemblages of Mid Devonian megaspores from Libya. *Review of Palaeobotany and Palynology* 165 (3–4), 154-174.

Stephenson, M.H. 2018. Permian palynostratigraphy: a global overview. *Geological Society Special Publication* 450(1), 321-347.

Stewart, F. H. 1949-1951. The petrology of the evaporites of the Eskdale No. 2 boring, east Yorkshire. Part III 1951b. The Upper Evaporite Bed. *Mineralogical Magazine* 29, 557-572.

Stewart, W.N., Rothwell, G.W. 1993. Paleobotany and the evolution of plants, second edition. Cambridge University Press, Cambridge. pp. 521.

Stockmans, F., Willière, Y. 1960. Hystrichosphères du Dévonien belge (Sondage de l'Asile d'aliénés à Tournai). Senckenbergiana. *Lethaea* 41, 1–11.

Stockmarr, J. 1971. Tablets with spores used in absolute pollen analysis. *Pollen et Spores* 13(January), 615–621.

Stollhofen, H., Bachmann,G. H. et al. 2008. Upper Rotliegend to Early Cretaceous basin development. In: Littke, R., Bayer, U., Gajewski,D.& Nelskamp, S. (eds) Dynamics ofcomplex intracontinental Basins: the Central European Basin System. Springer, Berlin, 181–210

Stone, P., Milward, D., Young, B., Merritt, J.W., Clarke, S.M., McCormac, M., Lawrence, D.J.D., 2010. British regional geology: Northern England. Fifth edition. Keworth, Nottingham: British Geological Survey. 307 pp.

Stoneley, H.M.M. 1958. The Upper Permian flora of England. Bulletin of the British Museum *Geology* 3(9), 293-337.

Strohmenger, C., Rockenbauch, K. & Waldmann, R. 1998. Fazies, Diagenesis und Reservoirentwicklung des Zechstein-2 Karbonate (Ober Perm) in Nordostdeutschland. *Geologisches Jahrbuch A* 149, 81–113.

Stuhl, A. 1962. Results of spore investigations of Permian sediments of the Balaton Upland. *Bulletin of the Hungarian Geological Society* 91, 405–412 (in Hungarian with German summary).

Sugita, S. 1994. Pollen representation of vegetation in quaternary sediments: theory and method in patchy vegetation. *Journal of Ecology* 82, 881–97.

Sugita, S. 2007a. Theory of quantitative reconstruction of vegetation. I. Pollen from large sites REVEALS regional vegetation composition. *Holocene* 17, 229–241

— 2007b. Theory of quantitative reconstruction of vegetation. II. All you need is LOVE. *Holocene* 17, 243–257

Sun, Y., Joachimski, M.M., Wignall, P.B., Yan, C., Chen, Y., Jiang, H., Wang, L., Lia, W. 2012. Lethally hot temperatures during the Early Triassic greenhouse. *Science* 338, 366-370.

Suveizdis, P.I., ed. 1975 – Permskaya sistema Pribaltiki (Fauna i stratigrafiya). Trudy, 29, Mintis, Vilnius.

Swift, A. 1986. The conodont Merrillina divergens (Bender and Stoppel) from the Upper Permian of England, in The English Zechstein and Related Topics (eds G.M. Harwood and D.B. Smith), Geological Society of London. Special Publication No. 22, pp. 55-62.

Szaniawski, H. 1969. Conodonts of the Upper Permian of Polan. *Acta Palaeontologica Polonica* 14, 325-341.

Szaniawski, H. 2001. Typ Incertae Sedis, gromada Conodonta. In: Pajchlowa, M.,Wagner, R. (Eds.), Budowa Geologiczna Polski 3. Warszawa, pp. 85–86 (in Polish).

Szurlies, M. 2004. Magnetostratigraphy: the key to a global correlation of the classic Germanic Trias – case study Volpriehausen Formation (Middle Buntsandstein), Central Germany. *Earth and Planetary Science Letters* 227, 395–410.

— 2007. Latest Permian to Middle Triassic cyclo-magnetostratigraphy from the Central European Basin, Germany: implications for the geomagnetic polarity timescale. *Earth and Planetary Science Letters* 261, 602–619.

— 2013. Late Permian (Zechstein) magnetostratigraphy in Western and Central Europe. Geological Society Special Publication 376, 73-85.

— Bachmann, G.H., Menning, M., Nowaczyk, N.R., Käding, K.-C. 2003. Magnetostratigraphy and high-resolution lithostratigraphy of the Permian-Triassic boundary interval in Central Germany. *Earth and Planetary Science Letters* 212, 263–278.

— Geluk, M.C., Krijgsman, W., Kürschner, W.M. 2012. The continental Permian-Triassic boundary in the Netherlands: Implications for the geomagnetic polarity time scale. Earth and Planetary Science Letters 317–318, 165–176.

Talbot, C.J., Tully, C.P., Woods, P.J.E. 1982. The structural geology of Boulby (potash) mine, Cleveland, United Kingdom. *Tectonophysics* 85, 167– 204.

Tauber, H. 1965. Differential pollen dispersion and the interpretation of pollen diagrams, Danmarks Geol. Unders. II Række 89

Taylor, F.M. 1968. Permian and Triassic formations. pp. 149-173. In: Sylvester-Bradley, P.C. & Ford, T. D. (editors) The geology of the East Midlands. Leicester University Press, Leicester.

Taylor T.N., Taylor, E.L., Krings, M. 2009. Paleobotany. 2nd ed. Elsevier, Amsterdam.

— 1974. Permian and Lower Triassic landscapes of the East Midlands. *American Geologist* 5, 89-100.

— Krings, M. 2005. Fossil microorganisms and land plants: associations and interactions. *Symbiosis* 40(3), 119-135.

— Hass, H., Remy, W. 1992a. Devonian fungi: interactions with the green alga *Palaeonitella*. *Mycologia* 84, 901–10.

— Remy, W., Hass, H. 1992b. Parasitism in a 400-million-year-old green alga. *Nature* 357, 493–4.

— Remy, W., Hass, H. 1992c. Fungi from the Lower Devonian Rhynie chert: chytridiomycetes. *American Journal of Botany* 79, 1233–41.

— Krings, M., Taylor, E.L. 2015. Fossil fungi. London, San Diego CA, Waltham MA, Oxford: Elsevier/Academic Press Inc.

— Klavins, S.D., Krings, M., Taylor, E.L., Kerp, H., Hass, H. 2004. Fungi from the Rhynie chert: A view from the dark side. *Transactions of the Royal Society of Edinburgh, Earth Sciences* 94, 457–473.

Taylor, J.C.M. & Colter, V.S. 1975. Zechstein of the English sector of the Southern North Sea Basin. pp. 249-263. In: Woodland, A. W. (editor) Petroleum and the continental shelf of north-west Europe. Vol. I, Geology. Applied Science Publishers Ltd: Institute of Petroleum, Great Britain

— 1980. Origin of the Werraanhydrit in the Southern North Sea - a reappraisal. pp. 91-113. In: Fuchtbauer, H. & Peryt, T.M. (editors), q.v. (London) 224,173-175.

Theuerkauf, M., Kuparinen, A., Joosten, H. 2012. Pollen productivity estimates strongly depend on assumed pollen dispersal. *The Holocene* 23(1), 14-24.

Tiwari, R.S., Kumar, R. 2002. Indian Gondwana palynochronology: Relationship and chronocalibration. *The Palaeobotanist* 51, 13–30.

Traverse, A. 2007. Paleopalynology. (N. H. Landman & D. S. Jones, Eds.) (2nd ed.). Topics in Geobiology. pp. 613.

Trechmann, C.T. 1945. On some new Permian fossils from the Magnesian Limestone near Sunderland. *Quarterly Journal of the Geological Society of London* 100, 333-54.

Tripathi, A. 2001. Permian, Jurassic and Early Cretaceous palynofloral assemblages from subsurface sedimentary rocks in Chuperbhita Coalfield, Rajmahal Basin, India. *Review of Palaeobotany and Palynology* 113, 237–259.

Trusheim, F. 1964. uber den Untergrund Frankens-Ergebnisse von Tiefbohrungen in Franken und Nachbargebieten, 1953-1960.

Truswell, E.M. 1980. Permo-Carboniferous palynology of Gondwanaland: progress and problems in the decade of 1980. Bureau of Mines and Mineral Resources. *Journal of Australian Geology and Geophysics* 5, 95–111.

Tschudy, R.H., Kosanke, R.M. 1966. Early Permian vesiculate pollen from Texas, U.S.A. *Palaeobotanist* 15, 59–71.

Tucker, M. 1991. Sequence stratigraphy of carbonate-evaporite basins; models and application to the Upper Permian (Zechstein) of Northeast England and adjoining North Sea. *Journal of the Geological Society of London* 148, 1019-1036.

— Hollingworth N.T.J. 1986. The Upper Permian Reef Complex (EZ1) of North East England: Diagenesis in a Marine to Evaporitic Setting. In: Schroeder J.H., Purser B.H. (eds) Reef Diagenesis. Springer, Berlin, Heidelberg.

Tyroff, H. 1966. Die Algen und Koniferen des Zechsteins von Budingen. In: Uhl, D. and Kerp, H. 2002. Preservation of fossil plants from the Zechstein (Upper Permian) of Central Europe. *Freiberger Forschungshefte C* 497, 29-43.

Uhl, D., Kerp, H. 2003. Wildfires in the Late Palaeozoic of Central Europe - The Zechstein (Upper Permian) of NW-Hesse (Germany). *Palaeogeography, Palaeoclimatology, Palaeoecology* 109(102), 1-15.

Ulh, D., Kerp, H. 2002. Preservation of fossil plants from the Zechstein (Upper Permian) of Central Europe. *Freiberger Forschungshefte* 497(January), 29-43.

Ullrich, H. 1964. On the stratigraphy and paleontology of the marine marginal transgression of the Zechstein Basin of East Thunguria and Saxony. Freiberger Forschungshefte, Geologie, 163 pp.

Utting, J. 1978. Lower Karroo pollen and spore assemblages from the coal measures and underlying sediments of the Siankondobo Coalfield, Mid-Zambezi valley, Zambia. *Palynology* 2, 53-68.

— 1994. Palynostratigraphy of Permian and lower Triassic rocks, Sverdrup Basin, Canadian Arctic Archipelago. Geological Survey Canada. 73 pp.

— Piasecki, S. 1995. Palynology of the Permian of northern Continents: a review. In: Scholle, P.A., Peryt, T.M. and Ulmer-Scholle, P.A. (eds) The Permian of Northern Pangea, Volume 1. Palaeogeography, Palaeoclimates, Stratigraphy. Springer, Berlin, pp. 236–261.

— Esaulova, N.K., Silantiev, V.V., Makarova, O.V. 1997. Late Permian palynomorph assemblages from Ufimian and Kazanian type sequences in Russia and comparison with Roadian and Wordian assemblages from the Canadian Arctic. *Canadian Journal of Earth Sciences* 34, 1–16.

Vachard, D. 2016. Permian smaller foraminifers: taxonomy, biostratigraphy, biogeography. In: Lucas, S.G. and Shen, S.Z. (eds) The Permian Timescale. Geological Society, London, Special Publications, 450 pp.

Vajda, V., McLoughlin, S. 2004. Extinction and recovery patterns of the vegetation across the Cretaceous-Palaeogene boundary – a tool for unravelling the causes of the end-Permian mass-extinction. *Review of Palaeobotany and Palynology* 144, 99-112.

— Mcloughlin, S, Mays, C., Frank, T.D., Fielding, R. Tevyaw, A, Lehsten, V, Bocking, M., Nicoll, R.S. 2020. End-Permian (252 Mya) deforestation, wildfires and flooding – An ancient biotic crisis with lessons for the present. *Earth and Planetary Science Letters* 529, 11587.

Van Adrichem Boogaert, H.A., Kouwe, W.F.P., 1994. Stratigraphic nomenclature of The Netherlands: revision and update by RGD and NOGEMPA – Section D, Permian. Mededelingen Rijks Geologische Dienst 50.

Van Wees, J.-D., Stephenson, R.A., Ziegler, P.A., Bayer, U., Mccann, T., Dadlex, R., Gaupp, R., Narkiewicz, M., Bitzer, F., Scheck, M. 2000. On the origin of the Southern Permian Basin, Central Europe. *Marine and Petroleum Geology* 17, 43-59.

Varencov, M.I., Ditmar, V.I., Li, A.B., Schmakova, Y.I. 1964. Age du sel gemme dans les structure de diaper de la depression de Chu-Sarysu. *Doklady Academii Nauk SSSR* 159: 327–329 [in Russian with French summary].

Variakhuna, L.M. 1971. Spores and pollen of the red beds and coal deposits of the Permian and Triassic of the northeastern region of the USSR (in Russian). In: Warrington, G. 1996. Chapter 18E. Permian spores and pollen. *American Association of Stratigraphic Palynologists Foundation* 2, 607-619.

Variakhuna, L.M. 1971. Spores and pollen of the red beds and coal deposits of the Permian and Triassic of the northeastern region of the USSR; Akademiia Nauk SSSR, Komi Filial, Institut Geologii, Nauka, Leningrad, 158 pp. (in Russian).

Venable, J. H., Coggeshall, R. 1965. A simplified lead citrate stain for use in electron microscopy. *Journal of Cell Biology* 25(2), 407–408.

Versey, H.C. 1925. The beds underlying the Magnesian Limestone in Yorkshire. *Proceedings of the Yorkshire Geological Society* 20, 200-214.

Vijay, A., Meena, K.L. 1996. Corpuscules in the Permian pollen from India. *Journal of the Palaeontological Society of India* 41, 52–61.

Visscher, H. 1966. Plant microfossils from the Upper Bunter of Hengelo, The Nederlands. *Acta Botanica Neerlandica* 15, 316–375.

— 1967. Permian and Triassic palynology and the concept of "tethys twist." Palaeogeography, Palaeoclimatology, Palaeoecology 3, 151–166.

— 1971. The Permian and Triassic of the Kingscourt Outlier, Ireland. A palynological investigation related to regional stratigraphical problems in the Permian and Triassic of Western Europe. Geological Society of Ireland Special Paper No. 1. 114 pp.

— 1972. The Upper Permian of Western Europe – a palynological approach to chronostratigraphy. In: Logan, A. and Hills, L.V. (eds) The Permian and Triassic Systems and their Mutual Boundary. *Canadian Society of Petroleum Geologists Memoirs* 2, 200–219.

— Sephton, M.A. & Looy, C.V. 2011. Fungal virulence at the time of the end-Permian biosphere crisis? *Geology* 39(9), 883-886.

— Looy, C.V., Collinson, M.E., Brinkhuis, H., Konijnenburg-van Cittert, J.H.A. van, Kürschner, W.M., Sephton, M.A. 2004. Environmental mutagenesis during the end-Permian ecological crisis. Proceedings of the National Academy of Sciences of the United States of America 101, 12952–12956.

— Brinkhuis, H., Dilcher, D.L., Elsik, W.C., Eshet, Y., Looy, C.V., Rampino, M. R., Traverse, A. 1996. The terminal Paleozoic fungal event: Evidence of terrestrial ecosystem destabilization and collapse. *National Academy of Sciences Proceedings* 93, 2155–2158.

Wade, D.C., Abraham, N.L., Farnsworth, A.L., Valdes, P.J., Bragg, F., Archibald, A.T. 2019. Simulating the climate response to atmospheric oxygen variability in the Phanerozoic: a focus on the Holocene, Cretaceous and Permian. *Climate Pas*t 15, 1463–1483.

Wagner, R., Peryt T.M. 1997. Possibility of sequence stratigraphic sub-division of the Zechstein in the Polish Basin. *Geological Quarterly* 41, 457–474.

Wagner, R. (Ed.) 2009. Suplement doTabeli Stratygraficznej Polski [in Polish]. Państwowy Instytut Geologiczny, Warszawa, 96 pp.

Wagner, R. 1994. Stratigraphy and development of the Zechstein Basin in Poland. Prace *Państwowego Instytutu Geologicznego* 146, 1–71.

— Peryt, T.M., 1997. Possibility of sequence stratigraphic subdivision of the Zechstein in the Polish Basin. *Geological Quarterly* 41, 457–474.

Waldin, J.G. 1778. Die Frankenberger Versteinerungen, nebst ihrem Ursprunge. Universitäts-Buchhandlung, Marburg.

Wall, D., Downie, C. 1963. Permian hystrichospheres from Britain. *Palaeontology* 5, 770-784.

Wang, D.-M., J.F. Basinger, P. Huang, L. Liu, J.-Z. Xue, M.-C. Meng, Y.-Y. Zhang, Z.-Z. Deng. 2015. Latisemenia longshania, gen. et sp. nov., a new Late Devonian seed plant from China. *Proceedings of the Royal Society B, Biological Sciences* 282, 20151613.

Wardlaw, B.R., Collinson, J.W. 1986. Paleontology and deposition of the Phosphoria Formation. *Rocky Mountain Geology* 24, 107-142.

Wardle, D.A., Lindahl, B.D. 2014. Disentangling global soil fungal diversity. *Science* 346, 1052–1053.

Ware, D., Bucher, H. Brayard, A. Schneebeli-Hermann, E., Brühwiler, T. 2015. High-resolution biochronology and diversity dynamics of the Early Triassic ammonoid recovery: The Dienerian faunas of the Northern Indian Margin. *Palaeogeography, Palaeoclimatology, Palaeoecology* 440, 363–373.

Warren, J.K. 1999. Evaporites: Their Evolution and Economics. Blackwell Science, Oxford. pp. 1-438.

— 2006. Evaporites: Sediments, Resources and Hydrocarbons. Springer. pp. 1042.

Warrington, G. 1996. Palaeozoic spores and pollen (Chapter 18E) Permian. In: Jansonius, J. and McGregor, D.C. (eds) Palynology: Principles and Applications, Volume 3. American Association of Stratigraphical Palynologists Foundation, Dallas, TX, pp. 607–619.

— 2005. The chronology of the Permian and Triassic of Devon and south-east Cornwall (U.K.): a review of methods and results. *Geoscience in south-west England* 11, 117-122.

— 2008. Palynology of the Permian succession in the Hilton Borehole, Vale of Eden, Cumbria, U.K. *Proceedings of the Yorkshire Geological Society* 57(2), 123-130.

— Scrivener, R.C. 1988. Late Permian fossils from Devon: regional geological implications. *Proceedings of the Usher Society* 7, 95-96.

Weigelt, J. 1928. Die Pflanzenreste des mitteldeutschen Kupferschiefers und ihre Einschaltung ins Sediment – Eine palökologische Studie. *Fortschritte der Geologie und Paläontologie* 19, 395–592.

— 1930. Über die vermutliche Nahrung von Protorosaurus und über einen körperlich erhaltenen Fruchtstand von Archaeopodocarpus germanicus aut. *Leopoldina* 6, 269-280.

Westoll, T.S. 1934. On the structures of the dermal ecthioid shield of Osteolepis. *Geological Magazine* 73, 157–71.

Whitaker, D.L., Edwards, J. 2010. Sphagnum moss disperses spores with vortex rings. Science 329, 406.

Wignall, P. B., Hallam, A. 1992. Anoxia as a cause of the Permian/Triassic mass extinction: facies evidence from northern Italy and the western United States. *Palaeogeography, Palaeoclimaology, Palaeoecology* 93, 21-46.

Wilson, L.R. 1962a. Permian Plant Microfossils from the Flowerpot Formation, Greer County, *Oklahoma. Oklahoma Geological Survey, Circular* 49. pp. 49.

Wilson, L.R. 1962b. A Permian fungus spore type from the Flowerpot Formation of Oklahoma. *Oklahoma Geology Notes* 22, 91e96.

Winch, N.J. 1817. Observations on the geology of Northumberland and Durham. *Transactions of the Geological Society of London* 4, 1-101.

Winguth, A.M.E., Shields, C.A., Winguth, C. 2015. Transition into a Hothouse World at the Permian-Triassic boundary-A model study'. *Palaeogeography, Palaeoclimatology, Palaeoecology* 440, 316–327.

Wurzbacher, C., Rösel, S., Rychła, A., Grossart, H.P. 2014. Importance of saprotrophic freshwater fungi for pollen degradation. *PloS ONE* 9, e94643.

Yardley, M.J. 1984. Cross-bedding in the Permian Yellow Sands of County Durham. *Proceedings of the Yorkshire Geological Society* 45, 11-18.

Yeh, M-W., Shellnut, J.G. 2016. The initial break-up of Pangaea elicited by Late Palaeozoic deglaciation. *Nature Scientific Reports* 6, 31442.

Yu, J., Broutin, J., Chen, Z.-Q., Shi, X., Li, H., Chu, D., Huang, Q. 2015. Vegetation changeover across the Permian-Triassic boundary in southwest China: extinction, survival, recovery and palaeoclimate: a critical review. *Earth Science Reviews* 149, 203e224.

Yu, Z., Lerche, I., Lowrie, A. 1992. Thermal impact of salt: Simulation of thermal anomalies in the Gulf of Mexico. *Pure and Applied Geophysics* 138, 181–192.

Zhang, Y., Wang, Y. 2017. Permian fusiline biostratigraphy. *Geological Society London Special Publications* 450(1), SP450.14.

Zavada, M.S. 1991. The ultrastructure of pollen found in dispersed sporangia of Arberiella (Glossopteridaceae). *Botanical Gazette* 152, 248–255.

Zavada, M.S., Crepet, W.L. 1985. Pollen wall ultrastructure of the type material of *Pteruchus africanus*, *P. dubius* and *P. papillatus*. *Pollen et Spores* 27, 271–276.

Zavialova, V., Nosova, N., Gavrilova, O. 2016. Pollen grains associated with gymnospermous mesofossils from the Jurassic of Uzbekistan. *Review of Palaeobotany and Palynology* 233, 125-145.

Zhang, L., Feng, Q.L., He, W.H. 2017. Permian radiolarian biostratigraphy. In: Lucas, S.G., Shen, S.Z. (eds) The Permian Timescale. Geological Society, London, Special Publcations, 450 pp.

Zhang, Y., Krause, M., Mutti, M. 2013. The Formation and Structure Evolution of Zechstein (Upper Permian) Salt in Northeast German Basin: A Review. *Open Journal of Geology* 3, 411-426.

Zhuo, Q.G., Meng, F.W., Yang, H.J., Li, Y., Ni, P. 2014. Hydrocarbon migration through salt: evidence from Kelasu tectonic zone of Kuqa foreland basin in China. *Carbonate Evaporite* 29, 219-297.

Ziegler, A.M. 1990. Phytogeographic patterns and continental configurations during the Permian period. Palaeozoic Palaeogeography and Biogeography, McKerrow, W.S., Scotese, C.R. (Eds.). Memoirs of the Geological Society 12, 363-379.

— Hulver, M.L. and Rowley, D.B. 1997. Permian world topography and climate. In: Martini, I.P. (Ed.), Late Glacial and Post-glacial Environmental Changes: Quaternary. Carboniferous-Permian and Proterozoic. Oxford University Press, Oxford, pp. 111–146.

— Eshel. G., McAllister Rees, P., Rothfus, T.A., Rowley, D.B. & Sunderlin, D. 2003. Tracing the tropics across land and sea: Permian to present. *Lethaia* 36, 227-254.

Zirngast, M. 1991. Die Entwicklungsgeschichte des Salzstocks Gorleben — Ergebnis einer strukurgeologischen Bearbeitung. Geologisches Jahrbuch A 32: 3–31. In: Peryt, T. M., Geluk, M. C., Mathiesen, A., Paul, J. & Smith, K. 2010. Zechstein. In: Doornenbal, J.C. & Stevenson, A. G. (eds) Petroleum Geological Atlas of the Southern Permian Basin Area. European Association of Geoscientists and Engineers, Houten. pp. 123–147.